THE JOURNAL
OF
CHEMICAL PHYSICS

VOLUME 19, NUMBER 2 FEBRUARY, 1951

The Kinetics of the Forward and Reverse Reactions for the Vapor Phase Thermal Bromination of Chloroform*

JOHN H. SULLIVAN† AND NORMAN DAVIDSON
Gates and Crellin Laboratories of Chemistry,‡ California Institute of Technology, Pasadena, California
(Received October 16, 1950)

The rates of the forward and reverse reactions for the homogeneous vapor phase thermal bromination of chloroform, $CHCl_3+Br_2=CBrCl_3+HBr(A)$, have been measured in the range 420–455°K and are given by $-d(Br_2)/dt=k_f(CHCl_3)(Br_2)^{\frac{1}{2}}[1+k_2(HBr)/k_3(Br_2)]^{-1}-k_r(CBrCl_3)(Br_2)^{\frac{1}{2}}[1+k_3(Br_2)/k_2(HBr)]^{-1}$; where $\log_{10}k_f$ (liter/mole)$^{\frac{1}{2}}$ sec$^{-1}=(-32{,}030/4.575T)+11.15$, $\log_{10}k_r=(-32{,}930/4.575T)+12.70$. The mechanism of the reaction is,

$$M+Br_2=2Br+M$$
$$Cl_3CH+Br=Cl_3C-+HBr \quad \rightarrow(1) \quad \leftarrow(2)$$
$$Cl_3C-+Br_2=CCl_3Br+Br \quad \rightarrow(3) \quad \leftarrow(4)$$

where $\log_{10}k_1=(-9300/4.575T)+9.36$, $\log_{10}k_4=(-10{,}200/4.575T)+10.91$, $(k_2/k_3)=0.040$. The activation energies imply that the CH bond in $CHCl_3$ is weaker than that in CH_4 by $6+E_2$ kcal and the Cl_3C-Br bond is weaker than the H_3C-Br bond by $11+E_2$ kcal, where E_2, the activation energy of reactions (2) and (3), is estimated to be ≤ 7 kcal.

The directly determined equilibrium constant for (A) agrees well with the kinetic value, $K_e=k_1k_3/k_2k_4$; $\log_{10}K_e=(900/4.575T)-0.15$. From these data, for CCl_3Br, $\Delta H°_{f,298°}=-9.4$ kcal, $S°_{298°}=80$ eu $S°$ was calculated as 80 eu from electron diffraction and spectroscopic data.

The equation for k_4 is identical with that obtained in a previous study of the exchange of radioactive bromine between Br_2 and $CBrCl_3$, thus proving this free radical mechanism for the exchange reaction.

INTRODUCTION

MILLER and Willard[1] and the authors[2] have shown that the exchange of bromine between trichlorobromomethane and elementary bromine proceeds by the following mechanism. Bromine atoms formed by the dissociation of Br_2 attack CCl_3Br molecules to give exchange. This attack of bromine atoms could either be a Walden inversion type of reaction, $Br^*+Cl_3CBr\rightarrow Br^*CCl_3+Br$; or it could involve the reaction, $Br+BrCCl_3\rightarrow Br_2+-CCl_3$ (4) and then the reverse of (4). Evidence for the formation of $-CCl_3$ radicals by (4) was obtained,[2] in that, in systems containing HBr, Br_2, and CCl_3Br, chloroform was formed, presumably according to the equation,

$$Cl_3C-+HBr\rightarrow Cl_3CH+Br. \qquad (2)$$

The present quantitative investigation of the rates of the reactions

$$Cl_3CH+Br_2\rightleftarrows CCl_3Br+HBr \qquad (A)$$

confirms the proposed mechanism of the exchange reaction (via 4) and provides information about the equilibrium constant for (A) and about the rates of some elementary reactions of bromine atoms and of trichloromethyl radicals.

EXPERIMENTAL

The rates of (A) were determined by measurement of the initial and final amounts of bromine in each reaction system.

Eastman Kodak white label chloroform was washed with concentrated sulfuric acid, dilute sodium hydroxide, and several portions of distilled water.[3] After drying in the dark over potassium carbonate it was fractionally distilled in the dark in an all-glass apparatus to give a middle fraction of 300 ml from a total of 700 ml.

* From the Ph.D. thesis by J. H. S., March, 1950; presented at the meeting of the American Chemical Society, Detroit, April, 1950.

† Present address, Los Alamos Scientific Laboratories.

‡ Contribution No. 1478 from the Gates and Crellin Laboratories.

[1] A. A. Miller and J. E. Willard, J. Chem. Phys. **17**, 168 (1949).

[2] N. Davidson and J. H. Sullivan, J. Chem. Phys. **17**, 176 (1949).

[3] A. Weissberger and E. Proskauer, *Organic Solvents* (The Clarendon Press, Oxford, 1935), p. 153.

TABLE I. Rate of the uninhibited forward reaction.

$(Br_2)_0$ $\times 10^3$	$(Br_2)_t$ (mole/liter) $\times 10^3$	$(CHCl_3)_0$ $\times 10^3$	T °K	k_f (mole/liter)$^{-\frac{1}{2}}$ sec^{-1} $\times 10^6$	k_f (Av)
0.452	0.238	38.4	442.03	20.61	20.76
0.366	0.203	31.15		20.92	
0.746	0.379	32.15	441.81	19.70	19.88
1.752	1.161	30.15		20.85	
1.815	1.211	31.25		20.20	
1.200	0.829	15.39		19.50	
1.087	0.770	13.97		19.23	
2.102	1.653	13.73		19.87	
1.351	0.598	29.00	442.05	20.23	20.09
2.098	1.127	29.12		20.03	
2.082	1.120	28.90		20.08	
2.165	1.151	30.07		20.03	
2.070	1.462	28.65	419.98	2.972	3.015
1.977	1.403	27.40		2.995	
1.448	0.901	30.92		3.040	
1.411	0.882	30.10		3.040	
1.358	0.861	29.00		3.025	
1.994	1.174	27.70	455.06	57.7	57.8
1.425	0.689	30.40		58.2	
1.363	0.672	29.10		58.2	
2.092	1.240	28.60		57.8	
2.028	1.476	17.77		58.4	
2.200	1.285	30.10		57.8	
1.407	0.707	29.63		57.8	
1.471	0.734	30.95		57.3	

Merck reagent grade bromine was dried over phosphorus pentoxide. Hydrogen bromide and trichlorobromomethane were prepared as described previously.[2]

The reactants, after degassing, were distilled into storage vessels attached to a vacuum line and kept in the dark at the temperature of dry ice. Apiezon grease was used as a stopcock lubricant. To prepare a reaction mixture, chloroform or trichlorobromomethane was distilled through a tube containing potassium hydroxide pellets and phosphorus pentoxide. Portions of the condensate were tested for oxidizing matter with starch iodide solution, and in the case of chloroform, for phosgene with barium hydroxide solution. The tests were always negative. Using a micropipet (50–300 microliters) that had been calibrated to deliver with chloroform, a measured volume of the liquid was then added to a glass tube that could be attached to the vacuum apparatus with a ground joint. The chloroform or trichlorobromomethane was distilled through P_2O_5 and condensed at liquid air temperature in a U-tube with constant pumping, and then distilled in a closed system into the evacuated reaction cell. Bromine was measured as a gas at the vapor pressure of the liquid at 0°C in vessels of known volume. Hydrogen bromide was measured in a system of known volume using a mercury manometer. For each substance, some of the stored material was always pumped out before taking the sample to be used. After the reactants were condensed in the reaction vessel, it was sealed at a pressure of 10^{-4}–10^{-5} mm of mercury while under constant pumping. The cleaning of the reaction vessels (*ca.* 80 ml) and details of the temperature measurements have already been described.[2]

At the end of a reaction, the vessels were chilled in liquid air and cracked open; the bromine content was measured by addition of excess aqueous potassiuin iodide and titration with standard 0.02N thiosulfate solution. The bromine content of unreacted samples was (to ±1 percent) that expected from the amount of bromine taken as a gas, and there was no change in the amount of bromine in a sample stored at liquid air temperature for 24 hours.

RESULTS

The rate law for the forward reaction of (A) has been found to be

$$-d(Br_2)/dt = k_f(CHCl_3)(Br_2)^{\frac{1}{2}} \times [1+k_2(HBr)/k_3(Br_2)]^{-1}. \quad (R1)$$

For the reverse reaction, the rate law is

$$d(Br_2)/dt = k_r(CCl_3Br)(Br_2)^{\frac{1}{2}} \times [1+k_3(Br_2)/k_2(HBr)]^{-1}. \quad (R2)$$

Equation (R1), for example, shows that the forward reaction is inhibited by hydrogen bromide. The term $[1+k_2(HBr)/k_3(Br_2)]^{-1}$ and the similar term in (R2) will be referred to as "inhibition terms." The evidence for these expressions is given in the following sections.

(a) The Uninhibited Forward Reaction

For runs in which the initial concentrations of hydrogen bromide and trichlorobromomethane were zero and $(CHCl_3) \gg (Br_2)$, Eq. (R1) has been integrated assuming the concentrations of chloroform, and of bromine and hydrogen bromide in the inhibition term, to be constant at the average values defined by equations like $(CHCl_3)_a = [(CHCl_3)_0 + (CHCl_3)_t]/2$. Subscripts 0, t, and a on the reactants refer to initial, final, and average concentrations. The integral of (R1) then is

$$k_f = 2\frac{(Br_2)_0^{\frac{1}{2}} - (Br_2)_t^{\frac{1}{2}}}{(CHCl_3)_a t}[1+k_2(HBr)_a/k_3(Br_2)_a]. \quad (R3)$$

For these runs, the change in $(CHCl_3)$ was only about two percent; the fractional changes in (HBr) and (Br_2) are of course larger, but since $k_2/k_3 = 0.040$ (see later) and for all these runs $(HBr)_t/(Br_2)_t < 0.5$, the use of average values in the inhibition term produces errors in k_f which are small compared to experimental error.

As shown in Table I, fourfold variations in $(Br_2)_0$ and twofold variations in $(CHCl_3)_0$ have no effect on the calculated values of k_f. The inhibition term was close to 0.98 for all the runs.

(b) The Reverse Reaction

For the measurements of the rate of (A) in the reverse direction, the initial concentrations of hydrogen bromide and of trichlorobromomethane were large compared to

that of bromine. However it was not possible to achieve the condition $[k_3(Br_2)/k_2(HBr)] \ll 1$; it was therefore necessary to evaluate simultaneously k_r and k_2/k_3 from the results of several runs at a fixed temperature. Assuming (CCl_3Br) and (HBr) to be constant at their average values, an integrated form of (R2) is

$$k_r = \frac{(2/3)(k_3/k_2)[(Br_2)_t^{\frac{3}{2}} - (Br_2)_0^{\frac{3}{2}}] + 2(HBr)_a[(Br_2)_t^{\frac{1}{2}} - (Br_2)_0^{\frac{1}{2}}]}{(HBr)_a(CCl_3Br)_a t}. \quad \text{(R4)}$$

The results are given in Table II. For a series of runs at a given temperature, trial and error numerical methods were used to select that value of k_2/k_3 which gave the most consistent set of values of k_r, that is, which minimized the mean square deviation of the calculated k_r's from their average value.

(c) The Inhibited Forward Reaction

The constant, k_2/k_3, can be evaluated from measurements of the inhibition of the forward reaction by hydrogen bromide as well as from the rate of the reverse reaction. First we note that the rate laws (R1) and (R2) are mutually consistent in that they predict an equilibrium constant for reaction (A) of the correct functional form.

$$K_e = \frac{k_f k_3}{k_2 k_r} = \frac{(CCl_3Br)(HBr)}{(CCl_3H)(Br_2)}. \quad \text{(R5)}$$

For the experiments of this section, there was no added trichlorobromomethane, and the initial concentrations of chloroform and hydrogen bromide were large compared to that of bromine. Because k_r is larger than k_f by a factor of about 10 and because the concentrations of hydrogen bromide were large, the small amounts of trichlorobromomethane ($\sim 1\times10^{-3}$ mole/liter) produced by the forward reaction were enough to make the average rate of the reverse reaction about 10 percent of the forward reaction. By using (R5) and the total rate law obtained by combining (R1) and (R2), and by treating (HBr) and ($CHCl_3$) as constant during the course of the reactions, one obtains

$$\frac{k_2}{k_3} = \frac{M}{(HBr)_a}\left\{\frac{k_f N t - 2[(Br_2)_0^{\frac{1}{2}} - (Br_2)_t^{\frac{1}{2}}]}{M^{\frac{1}{2}} \log\left[\frac{(Br_2)_0^{\frac{1}{2}} - M^{\frac{1}{2}}}{(Br_2)_0^{\frac{1}{2}} + M^{\frac{1}{2}}}\right]\left[\frac{(Br_2)_t^{\frac{1}{2}} + M^{\frac{1}{2}}}{(Br_2)_t^{\frac{1}{2}} - M^{\frac{1}{2}}}\right]} - 1\right\} \quad \text{(R6)}$$

where

$$M \equiv (Br_2)_a + K_e(CHCl_3)_a(Br_2)_a/(HBr)_a,$$
$$N \equiv (CHCl_3)_a + (HBr)_a/K_e.$$

This relation and values of K_e and k_f from Tables I and II were used to calculate the values of k_2/k_3 given in Table III. In (R6), k_2/k_3 is sensitively dependent on k_f (a one percent error in k_f gives a three percent error in k_2/k_3) and insensitively dependent on K_e (a one percent error in K_e gives a 0.2 percent error in k_2/k_3); therefore this determination of k_2/k_3 from the forward reaction is reasonably independent of the determination of k_2/k_3 from the reverse reaction. It is seen that the values of k_2/k_3 obtained in this study of the inhibited forward reaction are in good agreement with those calculated from the reverse reaction.

TABLE II. Rate of the reverse reaction.

$(Br_2)_0$ $\times10^3$	$(Br_2)_t$ (mole/liter) $\times10^3$	$(CBrCl_3)_0$ $\times10^3$	$(HBr)_0$ $\times10^3$	T °K	k_r $\times10^5$	k_r (Av) (mole/liter)$^{-\frac{1}{2}}$ sec^{-1} $\times10^5$	k_2/k_3
0.552	2.030	15.06	33.55	420.10	3.64	3.64	0.0408
0.541	2.067	14.75	37.30		3.66		
0.570	3.105	24.30	39.10		3.64		
0.576	1.822	15.72	21.40		3.675		
1.350	3.630	22.79	36.90		3.64		
0.532	1.843	11.48	35.90	442.07	25.50	25.48	0.0403
0.567	2.012	12.25	38.45		25.50		
1.240	3.295	20.90	28.85		25.55		
1.395	3.825	23.50	33.05		25.20		
1.315	3.585	22.13	31.20		25.65		
1.482	4.068	24.90	36.10	455.06	75.6	75.7	0.0392
0.567	3.155	23.50	37.65		75.8		
0.598	2.640	24.78	22.27		75.6		
1.360	2.810	14.42	32.45		75.7		
0.540	1.669	13.99	19.94		76.2		
0.587	3.003	23.68	34.20		75.0		

(d) The Equilibrium Constant, K_e

Table IV summarizes the average values of k_f and k_r; and of the equilibrium constant, K_e, calculated from (R5) using $k_2/k_3 = 0.040$, independent of temperature.

TABLE III. The ratio of k_2/k_3 from the inhibited forward reaction.

$(Br_2)_0$	$(Br_2)_t$ (mole/liter) $\times10^3$	$(CHCl_3)_0$	$(HBr)_0$	T °K	k_f (Av) $\times10^6$	k_2/k_3	k_2/k_3 (Av)
1.962	1.372	27.23	14.65	442.07	20.1	0.0425	0.0428
2.317	1.577	32.15	17.34			0.0435	
2.265	1.550	31.45	17.10			0.0444	
2.023	1.498	27.80	24.70			0.0422	
2.247	1.638	30.90	27.45			0.0416	
1.252	0.915	26.96	33.35	419.98	3.015	0.0385	0.0390
2.168	1.566	30.10	37.25			0.0393	
2.064	1.365	28.67	19.25			0.0394	
2.041	1.459	28.35	31.20			0.0387	
1.933	1.395	26.82	29.67			0.0391	

TABLE IV. Values of k_f, k_r, and K_e.

T °K	k_f ×10⁶ (mole/liter)$^{-\frac{1}{2}}$ sec^{-1}	k_r ×10⁵ sec^{-1}	K_e
420.0	3.015	3.65	2.06
422.07	20.1	25.48	1.97
445.06	57.8	75.7	1.91

An attempt was made to check the "kinetic" equilibrium constant by a direct measurement of the equilibrium at 442°K. Systems close to equilibrium change their composition very slowly and these studies served only to indicate limits for K_e. A representative selection of the data is given in Table V. The quantities K_0 and K_t are the initial and final values of the function, $K=(\mathrm{HBr})(\mathrm{CBrCl_3})/(\mathrm{Br_2})(\mathrm{CHCl_3})$.

It is evident that the K's are tending towards a value close to 1.97, the value of K_e indicated by the kinetic data. (A defect in the experiments is that there was only one case in which K_0 was chosen substantially smaller than 1.97, so that an increase in the K function was observed.) The K_e column in Table V lists values of the equilibrium constant calculated from the change in K (from K_0 to K_t) in time t. To do this, the rate equation was integrated, assuming a constant value for the term $[1+k_2(\mathrm{HBr})/k_3(\mathrm{Br_2})]$, and K_e evaluated in terms of K_0, K_t, t, k_f, and k_2/k_3. The rather complicated expressions used are given elsewhere.* It may be said that the value of K_e obtained by observing small changes in systems close to equilibrium is in satisfactory agreement with the K_e obtained by rate measurements on systems far from equilibrium.

(e) Side Reactions and Surface Effects

Experiments on both the forward and reverse reactions in vessels packed with glass beads with a total surface area of *ca.* six times that in unpacked vessels established that the rates were independent of the surface area.

It is to be recalled that we previously reported[2] the formation of $CHCl_3$, but of no CCl_4, C_2Cl_6, CCl_2Br_2, or other products when a mixture of Br_2, HBr, and CCl_3Br was heated to 460°K for a time somewhat longer than that used typically in the present measurements. This and the general consistency of the kinetic results indicate that only reaction (A) was of importance for the present study.

(f) Numerical Results

The parameters of the equations

$$\log_{10}k_f\ (\mathrm{liter/mole})^{\frac{1}{2}}\ \mathrm{sec}^{-1} = \frac{-32{,}030(\pm 300)}{4.575T}+11.15(\pm 0.15), \quad (R7)$$

$$\log_{10}k_r = \frac{-32{,}930(\pm 300)}{4.575T}+12.70(\pm 0.15) \quad (R8)$$

TABLE V. Measurement of the equilibrium constant at 442.07°K.

t sec ×10⁻⁴	(CHCl₃)₀	(CBrCl₃)₀	(HBr)₀	(Br₂)₀	(Br₂)$_t$	K_0	K_t	K_e
	(mole/liter) ×10³							
2.31	30.0	12.06	8.72	1.404	1.478	2.50	2.33	2.05
2.31	28.8	11.60	7.09	1.350	1.378	2.10	2.06	1.96
3.858	17.77	7.00	5.97	1.246	1.249	1.89	1.885	1.87
3.858	18.07	7.12	5.02	1.267	1.203	1.57	1.68	1.89
							Average	1.94

were determined graphically from plots of $\log k_f$ (Av) and $\log k_r$ (Av) against $1/T$. Probable errors r, of k_f (Av) and k_r (Av) at the extreme temperatures, were calculated from the individual value of k_f and k_r at these temperatures. The errors in the parameters are those resulting from the assumption of errors of 0.1°C in each of the extreme temperatures and errors of $2r$ in k_f (Av) and k_r (Av)—the errors taken so as to give a maximum error in the activation energies.

The data in Tables II and III indicate that over the temperature range 420–455°K, $k_2/k_3=0.040\pm0.002$. The corresponding, kinetically derived equation for the equilibrium constant, K_e, of the reaction (A) is

$$\log_{10}K_e=\frac{900(\pm 600)}{4.575T}-0.15(\pm 0.30). \quad (R9)$$

DISCUSSION

(a) The Thermodynamics of Reaction (A)

Equation (R9) implies that, for (A), $\Delta H^\circ_{440^\circ}=-0.90(\pm 0.6)$ kcal, and $\Delta S^\circ_{440^\circ}=-0.70(\pm 1.4)$ eu. From tabulated values of heat capacities,[4] $\Delta C^\circ_{p,\,298^\circ}=3.23$. Assuming this as an average value of ΔC_p over the temperature range 298°–440°, $\Delta H^\circ_{298^\circ}=-1.4$ kcal, $\Delta S^\circ_{298^\circ}=-2.0$ eu. For the hitherto unreported quantities, the heat of formation and entropy of trichlorobromomethane one calculates, $\Delta H^\circ_{f,\,298^\circ}=-9.4$ kcal, and $S^\circ_{298^\circ}=80.1(\pm 1.4)$ eu. Comparison of various thermochemical compilations[4,5] suggests that an uncertainty in the heat of formation of chloroform (taken as -24.0 in the above calculations) as well as the uncertainty of ΔH for (A) contributes to the uncertainty for the heat of formation of CCl_3Br. Using the molecular structure given by Pfeiffer[6] from electron diffraction measurements (C−Cl=1.76A, C−Br=1.91A,

[4] *Selected Values of Chemical Thermodynamic Properties* (Natl. Bur. of Standards, Washington, D. C.):
Br₂ and Br, Series I, Table 11-1, June 30, 1948; Series III, June 30, 1948.
HBr, Series I, Table 11-2, June 30, 1948.
$CHCl_3$, Series I, Table 23-7, June 30, 1949.
CCl_4, Series I, Table 23-7, June 30, 1949.
CCl_3Br, Series I, Table 23-10, March 31, 1948.
Cl, Series I, Table 10-1, June 30, 1948.
H, Series I, Table 8-1, June 30, 1947.

[5] F. R. Bichowsky and F. D. Rossini, *The Thermochemistry of the Chemical Substances* (Rheinhold Publishing Corporation, New York, 1936), p. 241.

[6] H. G. Pfeiffer, Ph.D. thesis, California Institute of Technology, 1948.

$\measuredangle$Cl−C−Br=110°), and the vibrational frequency assignment made by Simanouti[7] (A_1, 710, 418, 243 cm^{-1}; E, 765, 289, 187 cm^{-1}), one computes for the entropy of CCl_3Br, $S_{ROT}=27.1$, $S_{VIB}=10.9$, and $S°_{298°}=79.8$ eu. The vibrational entropy was calculated using the harmonic oscillator approximation. The agreement with the measured entropy is excellent.

(b) The Mechanism of the Reaction

A mechanism for reaction (A) that is consistent with the rate laws is similar to the one proposed by Braunwarth and Schumacher[8] for the photo-bromination of chloroform.

$$Br_2+M\rightarrow 2Br+M, \qquad (d)$$

$$2Br+M\rightarrow Br_2+M, \qquad (r_1)$$

$$Cl_3CH+Br\rightarrow Cl_3C-+HBr, \qquad (1)$$

$$Cl_3C-+HBr\rightarrow Cl_3CH+Br, \qquad (2)$$

$$Cl_3C-+Br_2\rightarrow Cl_3CBr+Br, \qquad (3)$$

$$Cl_3CBr+Br\rightarrow Cl_3C-+Br_2. \qquad (4)$$

Apart from (4) which is the elementary reaction responsible for the reversal of (A), the mechanism is like that involved in the bromination of hydrogen or methane. So long as (r_1) is the only important chain terminating reaction, the equilibrium concentration of bromine atoms is maintained,

$$(Br)=[K_c(Br_2)]^{\frac{1}{2}} \qquad (R10)$$

where $K_c(=k_d/k_{r1})$ is the equilibrium constant, in concentration units, for the dissociation of bromine.

The rate laws derived from this mechanism are (R1) and (R2), and the rate constants for the elementary reactions (1) and (4) are given by $k_1=k_fK_c^{-\frac{1}{2}}$ and $k_4=k_rK_c^{-\frac{1}{2}}$. In a small temperature range around 440°K,

$$K_c=(RT)^{-1}K_p$$
$$=(RT)^{-1}\exp[(\Delta S-R)/R]\exp(-\Delta E/RT).$$

Using the thermodynamic data for bromine,[4] one obtains

$$\log_{10}k_1\ (\text{liter/mole sec})=\frac{-9300(\pm 300)}{4.575T}+9.36, \qquad (R11)$$

$$\log_{10}k_4=\frac{-10{,}200(\pm 300)}{4.575T}+10.91. \qquad (R12)$$

As previously remarked,[3] the frequency factor for (4) (8.1×10^{10} liter/mole sec) is of the order of magnitude of the collision number. The ratio of the frequency factors of (4) and (1) is 35. The ratio of the frequency factors of (3) and (2) is 25. In general the frequency factor for a reaction in which a radical picks off a bromine atom from a molecule will be greater than the frequency factor for removal of a hydrogen atom because of the greater dimensions of the activated complex in the former case.

Reactions (3) and (4) provide a mechanism for the exchange of labelled bromine between trichlorobromomethane and bromine. The equations (R8) and (R12) are, within experimental error, identical with the corresponding results, obtained by us,[2] for the exchange rate constants, thus demonstrating that reactions (3) and (4) are indeed the path for the exchange.

Braunwarth and Schumacher, on the basis of their study[8] of the photo-bromination of chloroform at 110° to 130°, report that the activation energy for (1) is 10 kcal and that $k_2/k_3=0.14$, independent of temperature. The value of the activation energy for (1) agrees with the result obtained by us, but the values of k_2/k_3 are not in good agreement. Activation energies for both (4) and (3) were assigned as 6 kcal on the basis of a study of the bromine sensitized photo-chemical oxidation of trichlorobromomethane. We have already pointed out[2] that these assignments imply the implausible value of ΔH for (A) of 4 kcal.

(c) Activation Energies and Bond Strengths

If we let the positive number E_2 be the activation energy for reactions (2) and (3),[9] then at 440°, $\Delta H(1)=9.3-E_2$, and $\Delta H(4)=10.2-E_2$ kcal. The difference in ΔC_p's for (1) and (4) is taken as 3.2 cal mole deg^{-1}, but the individual values are not known. Purely for the sake of numerical consistency with the thermochemical calculations of Sec. (a), we revise these ΔH's slightly and take at 298°, $\Delta H°(1)=9.0-E_2$, and $\Delta H°(4)=10.4-E_2$ kcal. The heat of formation of the $-CCl_3$ radical is then $20.4-E_2$. Then:

$$CCl_3H\rightarrow -CCl_3+H, \quad \Delta H=96.5-E_2,$$
$$CCl_3Br\rightarrow -CCl_3+Br, \quad \Delta H=56.5-E_2,$$
$$CCl_4\rightarrow -CCl_3+Cl, \quad \Delta H=74.9-E_2.$$

It is indicated in the next section that probably $E_2<7$ kcal. For comparison, these values and the values of some bond dissociation energies, $D(RY)$ (that is, ΔH_{298} for the reaction, $RY\rightarrow R+Y$), as compiled by Roberts and Skinner[10] are exhibited in Table VI.

It is seen that the Cl_3C-Br bond is at least 11 kcal weaker than the H_3C-Br bond, that the Cl_3C-H bond is at least 6 kcal weaker than the H_3C-H bond, and that the Cl_3C-Cl bond is at least 6 kcal weaker than H_3C-Cl bond. The situation is just the reverse for the comparison of the $t-Bu-$radical with the $-CH_3$

[7] T. Simanouti, J. Chem. Phys. **17**, 245 (1949).

[8] V. V. Braunwarth and H. J. Schumacher, Kolloid Z. **89**, 184 (1939).

[9] From the relation $k_2/k_3=0.040\pm 0.002$ over the temperature range 420° to 455°, it follows that $E_2-E_3=0\pm 1$ kcal. It may be recalled that, for the corresponding reactions of the methyl radical, Kistiakowsky and Van Artsdalen (reference 12) give $E_2-E_3=2$ kcal, and for the corresponding hydrogen atom reactions, $E_2-E_3=0.06$ kcal, and $E_2=1.0$ kcal [M. Bodenstein and S. C. Lind, Z. physik. Chem. **119**, 123 (1926); M. Bodenstein and G. Jung., *ibid.* **121**, 127 (1926)].

[10] J. S. Roberts and H. A. Skinner, Trans Faraday Soc. **45**, 339 (1949).

TABLE VI. $D(R-Y)$ values (kcal).

R	Y	H	Cl	Br
$-CH_3$		102	80.7	67.4
$-t-Bu$		86.5	74.7	60.8
$-CCl_3$		$96.5-E_2$	$74.9-E_2$	$56.5-E_2$

radical; in this case there is a marked weakening of the C−H bond and a less marked weakening of the C−Br bond.

One would expect that by introducing free radicals into a mixture of isobutane and trichlorobromomethane one could initiate the chain reaction,

$$Cl_3C-+t-BuH\rightarrow Cl_3CH+t-Bu-,$$
$$t-Bu-+BrCCl_3\rightarrow t-BuBr+-CCl_3,$$

in which each step is exothermic, resulting in an exchange of hydrogen and bromine between the two radicals. West and Schmerling[11] have observed the corresponding exchange of chlorine and hydrogen atoms between carbontetrachloride and various hydrocarbons.

It should be noted that many of the comparisons of bond strengths that can be made using Table VI or an extension thereof are dependent on the rather uncertain values of the heats of formation of the organic halides. The comparison of the Cl_3C-H and H_3C-H bond strengths is not subject to this difficulty but is essentially a comparison of the energy of activation of (1) with the activation energy for the corresponding reaction

$$CH_4+Br\rightarrow H_3C-+HBr.^{12}$$

(d) The Activation Energies of Reactions (2) and (3)

It is of interest to investigate what information about the rates of reactions (2) and (3) or about E_2, the activation energy for both of these reactions, is given by the present research. For simplicity, consider the uninhibited forward reaction

$$Br_2+M\rightarrow 2Br+M, \quad (d)$$
$$Cl_3CH+Br\rightarrow Cl_3C-+HBr, \quad (1)$$
$$Cl_3C-+Br_2\rightarrow Cl_3CBr+Br \quad (3)$$

and the conceivable chain terminating reactions

$$2Br+M\rightarrow Br_2+M, \quad (r_1)$$
$$Cl_3C-+Br+M(?)\rightarrow Cl_3CBr+M, \quad (r_2)$$
$$Cl_3C-+Cl_3C-+M(?)\rightarrow C_2Cl_6+M. \quad (r_3)$$

Rabinowitch and Wood have measured the rates of (r_1).[13] From their data we estimate that for $M=$ chloroform, $k_{r1}=1.5\times10^{10}$ (liter^2/mole^2 sec) at room temperature. (The quantity k_{r1} is one-half the rate constant of Rabinowitch and Wood.) Knowing the equilibrium constant for the dissociation of bromine, one can then calculate $k_d=K_ck_{r1}$. Assuming[14] that k_{r1} is independent of temperature, k_d (liter/mole sec)$=7\times10^{13}\times\exp(-45{,}300/RT)$.

The rate of homogeneous dissociation of bromine at 440° when $(Br_2)=0.001$ mole/liter and $(M)=(CHCl_3)=0.03$ is calculated to be 6×10^{-14} mole/liter sec. The rate of formation of CCl_3Br according to Table I is 2×10^{-8} mole/liter sec. There is probably also some heterogeneous dissociation of bromine molecules, but the above calculation strongly suggests that every bromine atom created by (d) initiates a large number of cycles of the chain reactions (1) and (3) before one of the radical recombinations (r) occurs. Under these conditions of long chain length, if (r_2) or (r_3) were the important chain terminating reactions, the rate equation would be $d(CCl_3Br)/dt=(k_1k_3k_d/k_{r2})^{\frac{1}{2}}(Cl_3CH)^{\frac{1}{2}}(Br_2)$ or $k_3(k_d/k_{r2})^{\frac{1}{2}}(Br_2)^{\frac{1}{2}}$ respectively (assuming that $M=CHCl_3$), rather than (R1).

Since these equations do not fit the facts, (r_2) and (r_3) are not important and (r_1) is. However, it is probable that k_{r2} and k_{r3} are as large as k_{r1}; or, if these reactions are not subject to three body restrictions, effectively larger. Therefore the steady-state concentration of trichloromethyl radicals must be less than the steady-state concentration of bromine atoms; otherwise (r_2) or (r_3) would contribute to the kinetics. When the chain length is large, $(Cl_3C-)/(Br)=k_1(Cl_3CH)/k_3(Br_2)$. We suppose that this ratio, $(Cl_3C-)/(Br)$, ≤0.1. Then using the typical conditions, $(Br_2)=0.001$, $(Cl_3CH)=0.03$, $k_3/k_1\geq300$. However, as noted previously, the frequency factor for (3) may well be *ca.* 30 times the frequency factor for (1). Therefore, $\exp(E_1-E_2/RT)\geq10$; $E_2\leq7$ kcal.

[11] J. P. West and L. Schmerling, J. Am. Chem. Soc. **72**, 3525 (1950).

[12] G. B. Kistiakowsky and E. R. Van Artsdalen, J. Chem. Phys. **12**, 474 (1944).

[13] E. Rabinowitch and W. C. Wood, Trans. Faraday Soc. **32**, 907 (1936).

[14] O. K. Rice, J. Chem. Phys. **9**, 258 (1941), has pointed out the possibility of this calculation and interpreted the high value of the frequency factor for this bimolecular reaction.

Solid Solutions of the Alkali Halides. II. The Theoretical Calculation of Lattice Constants, Heats of Mixing, and Distributions between Solid and Aqueous Phases*

GEORGE S. DURHAM AND JANET A. HAWKINS
Department of Chemistry, Smith College, Northampton, Massachusetts
(Received September 11, 1950)

In all previous attempts to calculate interionic distances and heats of mixing for alkali-halide solid solutions, uniform anion-cation distances throughout a given solution have been postulated. In the present paper, the more logical assumption is made that the ions are not at a constant nearest-neighbor distance, but take up positions of minimum potential energy relative to one another. A method making use of the Born-Mayer-Huggins equation for the lattice energies of the alkali halides is developed for the determination of these positions in a simplified model and for the calculation of the potential energy associated with the resultant lattice. From these values, the average lattice constant, the heat of mixing, and the activity-coefficient ratio in the solid solution are calculated; from the latter is obtained the theoretical distribution ratio between solid and aqueous solutions. Values of the listed properties have been calculated at various mole fractions for the solid solutions KBr—KCl, RbBr—RbCl, RbCl—KCl, RbBr—KBr at 25° and have been found to be in good agreement with the experimental data available.

INTRODUCTION

In the past a number of attempts have been made to calculate heats of mixing for alkali-halide solid solutions from the relationship

$$\Delta H_{ss} = -U_{ss} + (N_1 U_1^{\circ} + N_2 U_2^{\circ}), \qquad (1)$$

where ΔH_{ss} and U_{ss} are the heat of mixing and the lattice energy per mole of solid solution, N_1 and N_2 are mole fractions, and U_1° and U_2° are the lattice energies of the pure components. For alkali-halide pairs which are completely isomorphous at room temperature, the heats of mixing for equimolal solid solutions average only about 250 calories per mole as compared to lattice energies of the order of magnitude of 160,000 calories; however, provided the lattice energy equation used is of the correct form and the assumptions made concerning the solid solution structure are reasonably exact, there is no reason why Eq. (1) should not yield acceptable results, since the relative and not the absolute accuracy of the lattice energies is involved.

Such calculations were first made by Grimm and Herzfeld[1] for many of the alkali-halide systems, the lattice energies being obtained by means of the original Born equation, which for these salts is

$$-U = -(Ae^2/r) + (B/r^9). \qquad (2)$$

Here A is the Madelung constant, e is the charge on the electron, r is the distance between nearest neighbors, and B is the specific repulsive constant.

Wallace[2] has made similar calculations using the Born-Mayer equation with the omission of the dipole-quadrupole attraction term. In both of these cases, values calculated under the assumption that the specific repulsion constants remain the same in the solution as in the pure crystals are approximately twice as large as the experimental, and it must be concluded that the refinements of the more recent equation do not bring any appreciable improvement to the calculation.

The factor which previous work has shown to have the greatest effect on the values of ΔH_{ss} is the treatment of the specific repulsive constant. The form of the Born equation usually written for the alkali halides is

$$U = (Ae^2/r)(1 - 1/9), \qquad (3)$$

in which the repulsive constant B of Eq. (2) has been substituted for in terms of r and other constants; it applies only when the potential energy is a minimum. If this equation is used at various values of r, it follows that the constant B must assume a new value for each case such that this restriction is satisfied mathematically. Thus, when Grimm and Herzfeld and Tobolsky[3] used arbitrary lattice parameters obtained from the substitution of different values of n in the mixing rule

$$r_{ss}^{n} = N_1 (r_1^{\circ})^n + N_2 (r_2^{\circ})^n, \qquad (4)$$

they were effectively changing the specific repulsive constants in the lattice energy equations. Only for $n = 8$, the value consistent with lattice theory, do these constants retain the same values as in the pure crystals. The effect of change in n upon the value of ΔH_{ss} can be seen from the results calculated by Grimm and Herzfeld for an equimolal KBr—KCl solution using values of n of 8 and 3; the corresponding decrease in r_{ss} is only 0.004 A.U., but ΔH_{ss} goes from 400 calories to 190 calories. If the repulsive constants are kept the same, a change in r_{ss} of this amount raises ΔH_{ss} by about 20 calories; thus, the former large decrease is due to the change in repulsive constants.

It would seem highly improbable in view of the successful assignment of specific repulsive radii to the ions of the alkali halides by Huggins and Mayer, and of the uniformly consistent results so obtained, that the repulsive constants in these solid solutions are appreciably different from those in the pure components.

* This research has been made possible through support by the ONR, under contract N9onr-84400.
[1] H. G. Grimm and K. F. Herzfeld, Z. Physik **16**, 77 (1923).
[2] W. E. Wallace, J. Chem. Phys. **17**, 1095 (1949).
[3] A. V. Tobolsky, J. Chem. Phys. **10**, 187 (1942).

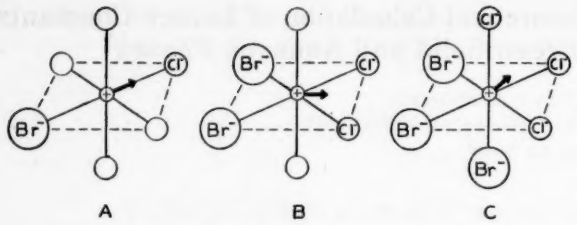

FIG. 1. Directions of ion displacement in the solid solution MBr–MCl for different basic-group configurations. (A) 5 Br^-, 1 Cl^-; 5 Cl^-, 1 Br^-; 3 Br^-, 3 Cl^-; (B) 4 Br^-, 2 Cl^-; 4 Cl^-, 2 Br^-; (C) 3 Br^-, 3 Cl^-.

Hence, the semi-empirical method making use of Eq. (3) with arbitrary lattice constants, used by Grimm and Herzfeld and by Tobolsky, besides being inconsistent with lattice theory, would seem to be ruled out on this score.

Wallace[2] has suggested that the poor agreement between calculated and observed values of lattice constants and heats of mixing is probably due to uncertainties concerning the repulsion potential. In view of the general success of the Born-Mayer-Huggins equation and also because of the magnitude of the changes in the repulsion potential necessary to bring agreement, this explanation seems questionable.

Grimm and Herzfeld, Tobolsky, Wallace, and indeed, almost all workers in the field of solid solutions, have taken for granted that in a given solid solution of the binary unordered type, the nearest-neighbor distance for any particular composition does not vary with the ions involved.[4] This assumption, which is based upon the results of x-ray diffraction measurements carried out on many solid solutions, must be incorrect at least to some degree, for it does not correspond to an equilibrium state of minimum potential energy in the solution. Therefore, in the present paper it is discarded.

Instead, we assume that, consistent with random distribution of the substituting ions, the particles are in positions of minimum potential energy with respect to each other. Simplifying assumptions are made to allow the calculation of the equilibrium positions of the ions within a suitable frame of reference. Through use of the hypotheses of Born, Mayer, and Huggins concerning the interionic forces involved, additional terms are added to the Born-Mayer-Huggins equation so as to obtain a corrected lattice energy of the solid solution in terms of an average anion-cation distance $\bar{r}_{aa}$. After values of this parameter are found in the usual way, they are substituted in this equation, and lattice energies and heats of mixing are determined.

A knowledge of how isomorphous substances distribute themselves between their solid solution and a liquid solvent is of interest from the theoretical standpoint, and also practically, since the calculation of such distribution values from known properties of the pure components would be advantageous in the separation of isomorphous substances by fractional crystallization. In 1923 an attempt by Herzfeld[5] to use lattice energies for the calculation of distribution data proved unsuccessful. In the present paper, a method is developed for the calculation of such distributions in the case of regular ionic solid solutions from a knowledge of the activity-coefficient ratio in the solid, the latter being obtained from lattice energies through the heat of mixing.

POSITIONS OF MINIMUM POTENTIAL ENERGY

The general procedure followed is that of evaluating the positions of minimum energy of the ions in terms of displacements from the normal lattice. From x-ray studies, as well as from geometric considerations, it is evident that the alkali-halide solid solution lattice is not appreciably distorted, and hence that any movement of the ions from normal lattice positions is limited to small noncumulative displacements. To approximate such a situation we have chosen to regard the substituting ions as fixed at normal lattice points, with the common ions moving to positions of least potential energy in the resulting framework. Although it is obvious that this is not a true physical representation, and that all species of ions must occupy positions of minimum potential energy, we feel that such a simplification is a reasonable one for purposes of calculation; it fulfills the experimental requirements mentioned above and allows for considerable stabilization over the previously postulated normal lattice.

The basic group which we consider is made up of a common ion and its six surrounding nearest neighbors of opposite charge. The movements of the common ion from the normal lattice positions under the influence of different configurations (combinations) of the surrounding ions are found to be limited to only a few directions. The displacement necessary to give a position of minimum potential energy for the central ion is calculated for each case, and after the probabilities (P) for the various configurations have been evaluated at different compositions, the total energy of displacement, $\Sigma(P\Delta B)$, is found for each composition. In order to make these calculations, it is necessary to assume a value for $\bar{r}_{aa}$, a quantity which depends upon $\Sigma(P\Delta B)$; hence, successive approximations must be made until $\bar{r}_{aa}$ and $\Sigma(P\Delta B)$ are found to remain constant.

Consideration of the basic group shows that only three types of displacement are possible; this is illustrated in Fig. 1 for a bromide-chloride solid solution. In case A, the cation moves between the two opposite unlike anions along their common axis. The other four anions may be of any species as long as like ions oppose each other. In case B, in which the two unmarked ions must be the same, the cation moves away from the bromide ions to a point equidistant from each of the two opposing chloride ions. In the last case, C, the cat-

[4] See J. A. Ketelaar, Chem. Weekblad **35**, 858 (1939), for a discussion of the work of Grimm and Herzfeld, in which this hypothesis is questioned.

[5] K. F. Herzfeld, Z. Physik **16**, 84 (1923).

ion is displaced to a position equidistant from each of three like anions.

It has been shown experimentally[6] that silver chloride and silver bromide form a "regular" solution in Hildebrand's sense, i.e., a solution for which the entropy of mixing is ideal and hence in which there is a random distribution of the substituting ions. If the reasonable assumption is made that the alkali halides form regular solid solutions, the probability of a basic-group configuration of specific energy at a given composition is given by

$$P=XN_1^{w_1}N_2^{w_2}. \quad (5)$$

Here w_1 and w_2 represent the numbers of each kind of substituting ion surrounding the common ion in the basic group ($w_1+w_2=6$), and X is the number of possible configurations which have the same energy. Probabilities calculated for the common-cation system MBr−MCl are listed in Table I.

In the evaluation of the energy of displacement, $\Sigma(P\Delta B)$, the repulsive forces were considered first, since they vary much more rapidly with distance than do the Coulomb and dipole-dipole forces, and are very much larger than the dipole-quadrupole forces. The potential energy due to the repulsive forces is best represented by the exponential function of Born, Mayer, and Huggins.[7–9] For the case at hand, where only forces between nearest neighbors are considered, the potential energy per basic group can be expressed as

$$B_{(x,y,z)}=b\sum_{n_1^2+n_2^2+n_3^2=1}\exp a\{r_++r_--[(n_1\bar{r}_{ss}-x)^2+(n_2\bar{r}_{ss}-y)^2+(n_3\bar{r}_{ss}-z)^2]^{\frac{1}{2}}\}, \quad (6)$$

in which x, y, and z are displacements in these directions from the center of the basic group, the n's take the values $+1$, -1, and 0, and only the positive root of the bracketed expression is used. The values of the repulsive radii r_+ and r_- must be varied with each term in the summation, depending upon which ion pair the term represents. Values for the various constants involved were chosen as described in a later section of this paper. The repulsive energy was calculated using combinations of values of x, y, and z corresponding to various positions of displacement in the allowable directions; it was found for all three types of displacement and for all systems studied that the position of minimum energy was reached with displacements of between 0.025 $\bar{r}_{ss}$ and 0.030 $\bar{r}_{ss}$ along the particular orthogonal axes involved. Since energy variations near this minimum were found to be small, and not to depend markedly upon $\bar{r}_{ss}$, it was possible to use the displacements calculated for an equimolal solution in a given system for all other compositions as well.

The energy of displacement due to the van der Waals forces proved to be always less than 10 calories per mole when calculated for nearest neighbors only, at and near the displacement positions found from consideration of the repulsive forces. The contribution of these forces to the position of minimum energy and to the energy of displacement was therefore shown to be negligible, and they were not taken into account.

TABLE I. Probabilities for specific basic-group configurations in the solid-solution system $MBr_{(1)}-MCl_{(2)}$.

	$P=XN_1^{w_1}N_2^{w_2}$ (Eq. 5)					
	(A) configurations			(B) configurations		(C) configuration
N_1 (MBr)	5 Cl^- 1 Br^- ($X=6$)	5 Br^- 1 Cl^- ($X=6$)	3 Br^- 3 Cl^- ($X=12$)	4 Cl^- 2 Br^- ($X=12$)	4 Br^- 2 Cl^- ($X=12$)	3 Br^- 3 Cl^- ($X=8$)
0.1	0.354	0.000	0.009	0.079	0.001	0.006
0.3	0.303	0.010	0.111	0.259	0.047	0.074
0.5	0.094	0.094	0.188	0.188	0.188	0.125
0.7	0.010	0.303	0.111	0.047	0.259	0.074
0.9	0.000	0.354	0.009	0.001	0.079	0.006

Calculations concerning the effect of the Coulomb forces were made by means of the expression derived by Ewald[10] for the electrostatic potential at any point within a lattice. If from the potential calculated in this way is subtracted the potential due to the displaced ion in its normal lattice position, the value resulting is the potential at the position of the displaced ion. This method assumes that the remaining ions of the lattice are in normal positions, which in the case of a solid solution is not so. However, their displacements will be random, and since the Coulomb summation converges so slowly, such a treatment seems reasonable. Our calculations show that at displacements of the magnitude of those found from consideration of the repulsive forces, the rate of change of the Coulomb potential is insufficient to affect the position of displacement, and that the contribution of the Coulomb energy to the energy of displacement is always less than 10 calories per mole and hence can be neglected.

Of the repulsion, van der Waals, and Coulomb energies, then, only the first need be considered in arriving at the position of minimum potential energy of the displaced ion and in evaluating the energy of displacement, $\Sigma(P\Delta B)$. ΔB for each configuration of specific energy was calculated from Eq. (6) by means of the relationship.

$$\Delta B=B_{(x,y,z)}-B_{(x=y=z=0)}. \quad (7)$$

The contributions of the three types of configurations to the total energy change, $\Sigma(P\Delta B)$, together with values of $\Sigma(P\Delta B)$, are listed at various compositions for the four systems studied in Table II.

LATTICE CONSTANTS

Making the assumption that the change in thermal energy with respect to volume can be neglected, Born

[6] E. D. Eastman and R. T. Milner, J. Chem. Phys. **1**, 444 (1933).
[7] M. Born and J. E. Mayer, Z. Physik, **75**, 1 (1932).
[8] M. L. Huggins and J. E. Mayer, J. Chem. Phys. **1**, 643 (1933).
[9] M. L. Huggins, J. Chem. Phys. **5**, 143 (1937).
[10] P. P. Ewald, Ann. Physik **64**, 253 (1921). See also G. J. Dienes, J. Chem. Phys. **16**, 620 (1948), and M. Born, *Problems in Atomic Dynamics*, (Massachusetts Institute of Technology, Cambridge, 1926), pages 158–164.

TABLE II. Lattice constants, displacement energies, heats of mixing, and distributions between aqueous and solid solutions for alkali-halide systems at 25°.

System	N_1 solid	$\bar{r}_{ss}$ A.U. (calc) (Eq. 9)	ΔH_{ss} cal/mole (neglecting displacements) (Eq. 1)	config. (A)	$P\Delta B$ config. (B)	config. (C)	$\Sigma(P\Delta B)$ cal/mole	ΔH_{ss} cal/mole including $\Sigma(P\Delta B)$ (Eq. 10)	ΔH_{ss} cal/mole (exp)	$\log\left(\frac{\gamma_{\pm 1}}{\gamma_{\pm 3}}\right)^2_L$	$\log\left(\frac{f_{\pm 1}}{f_{\pm 2}}\right)_s$ (Eq. 23)	N_1 liquid (calc)	N_1 liquid (exp)
	0.1	3.1557[a]	185	−71	−29	−3	−103	82	85[b]	0.043	0.266	0.37	0.32[c]
	0.3	3.1880	402	−72	−105	−38	−215	187	200	0.041	0.111	0.54	0.52
$KBr_{(1)}-KCl_{(2)}$	0.5	3.2191	446	−60	−119	−61	−240	206	232	0.037	−0.022	0.60	0.59
	0.7	3.2494	352	−62	−88	−31	−181	171	190	0.034	−0.136	0.68	0.67
	0.9	3.2786	142	−50	−21	−2	−73	69	40	0.032	−0.232	0.84	0.82
	0.1	3.3108	181	−65	−28	−3	−96	85		−0.032	0.284	0.22	0.18[c]
	0.3	3.3416	402	−69	−104	−37	−208	194		−0.031	0.118	0.34	0.30
$RbBr_{(1)}-RbCl_{(2)}$	0.5	3.3722	451	−57	−115	−57	−229	222		−0.031	−0.022	0.39	0.38
	0.7	3.4018	355	−61	−86	−31	−178	177		−0.030	−0.140	0.47	0.51
	0.9	3.4304	139	−48	−20	−2	−70	69		−0.029	−0.239	0.68	0.74
	0.1	3.1611	180	−84	−36	−4	−124	56		−0.036	0.174	0.40	0.44[d]
	0.3	3.1916	400	−95	−139	−49	−283	117		−0.042	0.072	0.62	0.63
$RbCl_{(1)}-KCl_{(2)}$	0.5	3.2216	454	−79	−157	−77	−313	141	203[b]	−0.046	−0.014	0.72	0.72
	0.7	3.2508	353	−83	−118	−41	−242	111		−0.050	−0.088	0.82	0.79
	0.9	3.2791	139	−71	−28	−3	−102	37		−0.056	−0.149	0.93	0.87
	0.1	3.3146	150	−76	−34	−4	−114	36		−0.103	0.128	0.19	0.22[c]
	0.3	3.3442	340	−97	−116	−43	−256	84		−0.102	0.055	0.39	0.42
$RbBr_{(1)}-KBr_{(2)}$	0.5	3.3735	377	−64	−137	−67	−268	109		−0.101	−0.010	0.52	0.53
	0.7	3.4019	295	−73	−104	−36	−213	82		−0.100	−0.067	0.66	0.63
	0.9	3.4298	117	−59	−25	−3	−87	30		−0.099	−0.111	0.86	0.82

[a] Lattice constants for the KBr−KCl system were calculated using r's expressed in K.X. units and are so expressed here; to convert to A.U., these values should be multiplied by 1.00202.
[b] N. Fontell, Soc. Sci. Fennica, Commentationes Phys.-Math. 10, No. 6 (1939). Values for the KBr−KCl solutions are interpolated.
[c] Durham, Rock, and Frayn, "Solid solutions of the alkali halides. I. The systems KBr−KCl−H_2O, RbBr−RbCl−H_2O, and RbBr−KBr−H_2O at 25°," to appear in J. Am. Chem. Soc.
[d] J. d'Ans and F. Busch, Z. anorg. allgem. Chem. 232, 337 (1937).

and Mayer,[7] have shown thermodynamically that for an equilibrium state with respect to the lattice distance r in a crystal, the following relationship must hold:

$$rd\phi_{(r)}/dr=(3T/\mathbf{N}\beta)(\partial V/\partial T)_P. \quad (8)$$

Here $\phi_{(r)}$ is the potential energy per ion pair in the normal lattice, $\mathbf{N}$ is Avogadro's number, and β is the compressibility. For the solid solution model involving ionic displacements, this equation becomes

$$\bar{r}_{ss}\left[\frac{d\phi_{(\bar{r}ss)}}{d\bar{r}_{ss}}+\frac{d\Sigma(P\Delta B)}{d\bar{r}_{ss}}\right]=\frac{3T}{\mathbf{N}\beta_{ss}}\left(\frac{\partial V}{\partial T}\right)_{P(ss)}, \quad (9)$$

where $\bar{r}_{ss}$ is the average nearest-neighbor distance in the solid solution (rigorously, it is one-half the distance between the centers of two substituting ions of similar charge measured across the intervening normal lattice point in the basic group), $\Sigma(P\Delta B)$ is the total energy of displacement per ion pair, and β_{ss} and $(\partial V/\partial T)_{P(ss)}$ are calculated from values for the pure salts on the assumption that they vary linearly with composition. An expression for $\phi_{(\bar{r}ss)}$ is given in the next section of this paper. Values of β and $(1/V)(\partial V/\partial T)_P$ are listed by Huggins and Mayer.[8] Since Eq. (9) could not be solved directly for $\bar{r}_{ss}$, Newton's method of approximations was used. Resulting values of lattice constants at 25° for the systems KBr−KCl, RbBr−RbCl, RbCl−KCl, RbBr−KBr at mole fractions of 0.1, 0.3, 0.5, 0.7, 0.9, are listed in Table II.

HEATS OF SOLID SOLUTION

The heat of formation of a solid solution of the two alkali-halide components 1–3 and 2–3, where 3 represents the common ion, may now be written as follows:

$$\Delta H_{ss}=-U_{ss}+\mathbf{N}\Sigma(P\Delta B)+(N_1U_{13}^{o}+N_2U_{23}^{o}), \quad (10)$$

where U_{ss}, the lattice energy of the solid solution calculated for the normal lattice points, is equal to $-\mathbf{N}\phi_{(\bar{r}ss)}$, $\mathbf{N}$ is Avogadro's number, and N_1 and N_2 are mole fractions of components 1–3 and 2–3, respectively.

Following Huggins and Mayer,[8] we write for $\phi_{(\bar{r}ss)}$, the energy per ion pair in normal lattice positions,

$$\phi_{(\bar{r}ss)}=-\frac{Ae^2}{\bar{r}_{ss}}-\frac{C_{ss}}{\bar{r}_{ss}^{6}}-\frac{D_{ss}}{\bar{r}_{ss}^{8}}+bMe^{-a\bar{r}_{ss}}[N_1c_{13}e^{a(r_1+r_3)}+N_2c_{23}e^{a(r_2+r_3)}]+bM'e^{-a\sqrt{2}\bar{r}_{ss}}\left[\frac{N_1N_1}{2}c_{11}e^{2ar_1}+\frac{N_2N_2}{2}c_{22}e^{2ar_2}+\tfrac{1}{2}c_{33}e^{2ar_3}+N_1N_2c_{12}e^{a(r_1+r_2)}\right]. \quad (11)$$

Van der Waals Terms[11]

$$C_{ss}=S_6'[N_1c_{13}+N_2c_{23}]+\tfrac{1}{2}S_6''[2N_1N_2c_{12}+N_1N_1c_{11}+N_2N_2c_{22}+c_{33}] \quad (12)$$

$$D_{ss}=S_8'[N_1d_{13}+N_2d_{23}]+\tfrac{1}{2}S_8''[2N_1N_2d_{12}+N_1N_1d_{11}+N_2N_2d_{22}+d_{33}]. \quad (13)$$

[11] J. E. Mayer, J. Chem. Phys. 1, 270 (1933).

C_{ss} is the dipole-dipole interaction constant per average ion pair in a solid solution of given composition, c_{13} is the specific interaction constant for ions 1 and 3, and S_6' and S_6'' are summations over odd and even lattice points, respectively. D_{ss} is the corresponding constant for the dipole-quadripole forces, with d_{13} the interaction constant for ions 1 and 3 and S_8' and S_8'' summations over odd and even lattice points. Both equations assume random distribution of the substituting ions in the lattice. Values used in determining C_{ss} and D_{ss} were those of Mayer,[11] and constants for the rubidium-potassium and the bromide-chloride interactions, which were not available, were calculated according to his method.

Repulsion Terms

The terms for the repulsion energy take into account interactions between both nearest and next-nearest neighbors. The constant b is chosen arbitrarily for convenience as 10^{-12}. The constants c_{13}, c_{23}, etc., which weight the repulsion according to the charges on the ions concerned, have been evaluated by Pauling. M and M' are the numbers of unlike and like neighbors of each ion, in this case 6 and 12, respectively.

Instead of the average value of 3.00 being used for the repulsive constant a, found by Huggins[9] to give the most consistent over-all results for the alkali halides, separate values of a were calculated by the method of Born and Mayer[7] for each pure component of a given solid solution, and the average was used in all calculations involving that system. Values of r_1, r_2, and r_3, the specific repulsive radii of the ions, which would be consistent with the average a used, were then calculated for each system following the method of Huggins and Mayer.[8] In each case the common ion was assigned a value such as to leave the differences between the anion and cation radii for a given salt pair as near as possible to the values used by Huggins. As a check on the consistency of the constants a, r_1, r_2, and r_3, they were substituted into Eq. (4) for each pure solid and the equation was solved for r_0; in all cases the values obtained were within 0.0002 A.U. of the r_0's originally used in obtaining the values of a and the repulsive radii. Values of the constants used in this and the other calculations of this paper are listed in Table III.

Values of U_{ss} were calculated for each system at various mole fractions, together with lattice energies for the pure components. From these values and $\Sigma(P\Delta B)$, ΔH_{ss} was determined by means of Eq. (5). Values of the latter quantity are listed in Table II, together with available experimental data.

Table III. Values of constants.

Charge on electron	$e=4.8022\times10^{-10}$ absolute esu
Avogadro's number	$N=6.0227\times10^{23}$
Gas constant	$R=1.9871$ cal/deg
Madelung constant	$A=1.7476$
Repulsion-weighting constants (Eq. 11)	$c_{+-}=1.00$
	$c_{--}=0.75$
	$c_{++}=1.25$

(Temp. 25°)	KBr	KCl	RbBr	RbCl
Solubilities, moles/1000 g H_2O	5.73[a]	4.84[a]	6.80[a]	7.80[a]
Mean ionic activity coefficients at saturation; $\gamma_\pm$	0.655	0.573	0.522	0.565
Lattice constants; r_0, A.U.	3.300	3.146	3.4446[c]	3.2935[c]
K.X. units	3.293[b]	3.139[b]		
Repulsive constants; a, 10^8 cm^{-1} (Eq. 11)	3.0687	3.1434	3.0507	3.1815

	KBr–KCl	RbBr–RbCl	RbCl–KCl	RbBr–KBr
Repulsive radii (Eq. 11)				
r_{K^+} A.U.	1.2437		1.2475	1.2448
r_{Rb^+}		1.3830	1.3860	1.3832
r_{Br^-}	1.5660	1.5731		1.5689
r_{Cl^-}	1.4464	1.4482	1.4481	
k (Eq. 21) cal/mole	838	883	551	414
log$K$ (Eq. 16)	0.261	−0.188	0.402	−0.048

[a] Reference c, Table II, this paper.
[b] P. P. Ewald and C. Hermann, *Strukturbericht* 1913–1928 (Akad. Verlagsgesellschaft, Leipzig, 1931).
[c] Reference 15, this paper.

DISTRIBUTION OF THE ALKALI HALIDES BETWEEN THEIR SOLID AND AQUEOUS SOLUTIONS

If equilibrium is to be maintained in a system consisting of a solid and a liquid phase, the relationship

$$a_L = ka_S \qquad (14)$$

must be true for each component, where a_L and a_S are the activities in the liquid and solid solutions, respectively. Both the standard and reference states for the solid phase are taken as the pure salt, whereas the standard state for the liquid phase is chosen as a one-molal solution and the reference state as an infinitely dilute solution. If activities are expressed as products of concentrations and activity coefficients, it follows, for a system consisting of the two uniunivalent salts 1–3 and 2–3 in water, that

$$\left(\frac{m_1m_3}{m_2m_3}\right)_L\left(\frac{\gamma_{\pm13}}{\gamma_{\pm23}}\right)^2_L = K\left(\frac{N_1N_3}{N_2N_3}\right)_S\left(\frac{f_{\pm13}}{f_{\pm23}}\right)^2_S, \qquad (15)$$

where $K=k_{13}/k_{23}$ and m and N are the concentrations and $\gamma_\pm$ and $f_\pm$ the mean ionic activity coefficients in molal and mole fraction units respectively. After the logarithms of both sides are taken and cancellations made where possible, this equation can be written in the following convenient form:

$$\log\left(\frac{m_1}{m_2}\right)_L = \log K - \log\left(\frac{\gamma_{\pm13}}{\gamma_{\pm23}}\right)^2_L + \log\left(\frac{N_1}{N_2}\right)_S + \log\left(\frac{f_{\pm13}}{f_{\pm23}}\right)^2_S. \qquad (16)$$

If Eq. (14) is applied to saturated solutions of each pure component, k_{13} and k_{23} may be evaluated, since

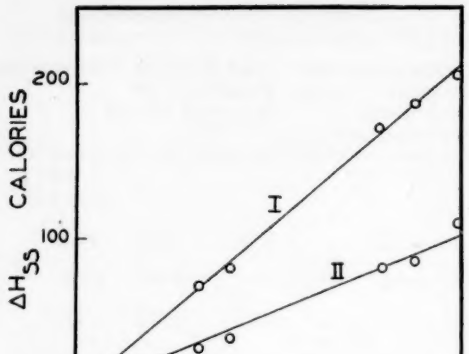

FIG. 2. The theoretical heat of solid solution as a function of volume fractions. I: KBr—KCl, II: RbBr—KBr.

the activities for the solids are then unity. Mean ionic activity coefficients for saturated aqueous solutions have not been determined for all of the alkali halides. Therefore, the semi-empirical relationship of Van Rysselberghe and Eisenberg[12] was used to obtain extrapolated values at concentrations corresponding to saturation. For the sake of consistency, this equation was used for all of the salts, whether or not direct determinations were available. From the solubilities and the corresponding activity coefficients, the distribution constant K for each of the four systems was calculated.

The ratio $(\gamma_{\pm 13}/\gamma_{\pm 23})_L$ for any saturated aqueous solution containing both of the completely isomorphous alkali halides 1–3 and 2–3 is close to unity, since the two salts concerned are so closely alike and are present in the same solution. An approximate evaluation of it was made by means of the easily applicable theory of specific ion-interaction in solutions of mixed electrolytes of Guggenheim,[13] according to which the logarithm of the ratio of the mean ionic activity coefficients of two salts present together at a constant total molality m is equal to one-half the logarithm of the ratio of the activity coefficients of the salts when in their pure solutions at the concentration m. At a value of m equal to the solubility of the more soluble salt, Van Rysselberghe's equation (see above) was used to determine a hypothetical value of $\gamma_\pm$ for the less soluble salt. By means of Guggenheim's theory and with the necessary values of $\gamma_\pm$, the desired ratio was calculated at the two limiting values of m equal to the solubilities of the pure salts. The activity-coefficient ratio in any specific mixed solution was assumed to vary linearly with composition between the two limiting values, and was so calculated. The values used are given in Table II.

The following general thermodynamic relationships are true for either component of a solid solution:

$$\Delta\bar{F}=RT\ln a=RT\ln N+RT\ln f=\Delta\bar{H}-T\Delta\bar{S}. \quad (17)$$

With the assumption of regularity already made, and neglecting any entropy corrections due to unequal molar volumes, we may write

$$-T\Delta\bar{S}=RT\ln N. \quad (18)$$

It then follows from Eqs. (17) and (18) that for either salt

$$\Delta\bar{H}=RT\ln f=RT\ln f_\pm^2, \quad (19)$$

and for both components

$$\Delta\bar{H}_{13}-\Delta\bar{H}_{23}=RT\ln(f_{13}/f_{23})=RT\ln(f_{\pm 13}/f_{\pm 23})^2. \quad (20)$$

The partial molal heats may be obtained from the integral heats of mixing graphically by the method of tangents, or better, analytically, if the relationship between ΔH_{ss} and composition can be expressed mathematically with sufficient accuracy. Scatchard and his co-workers[14] have found for a number of nonpolar binary liquid solutions that the experimental heat of mixing is a simple function of volume fractions. We have found a similar relationship to hold with respect to the calculated heats of mixing for all of the binary solid solutions considered here. Within the accuracy of our calculations (±10 calories)

$$\Delta H_{ss}=kV_1^fV_2^f, \quad (21)$$

where V_1^f and V_2^f are the volume fractions of components 1–3 and 2–3, respectively, and V_1^f is defined in terms of mole fractions and molar volumes of the pure components as follows:

$$V_1^f=N_1V_{13}^0/(N_1V_{13}^0+N_2V_{23}^0). \quad (22)$$

Figures 2 and 3 illustrate how closely this relationship is followed.

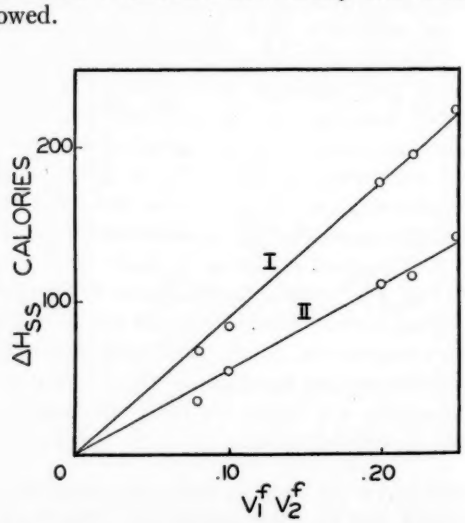

FIG. 3. The theoretical heat of solid solution as a function of volume fractions. I: RbBr—RbCl, II: RbCl—KCl.

[12] P. Van Rysselberghe and S. Eisenberg, J. Am. Chem. Soc., **61**, 3030 (1939).

[13] See H. S. Harned and B. B. Owen, *The Physical Chemistry of Electrolytic Solutions* (Reinhold Publishing Corporation, New York, 1943), pages 464–466.

[14] Scatchard, Wood, and Mochel, J. Am. Chem. Soc. **62**, 712 (1940).

The ratio of activity coefficients in the solid was calculated (for a temperature of 25°) by means of the following relationship, obtained through Eqs. (20) and (21), and thermodynamic considerations:

$$RT \ln(f_{\pm 13}/f_{\pm 23})_s^2 = \Delta\bar{H}_{13} - \Delta\bar{H}_{23} = \partial\Delta H_{ss}/\partial N_1 = kV_1'V_2'(V_2' - V_1')/N_1N_2. \quad (23)$$

Values of k were obtained for use in Eq. (23) by the method of least squares.

By means of Eq. (16) the distribution of the salts between solid and aqueous phases was determined. The calculated distribution values, together with the experimental, are listed in Table II. Roozeboom distribution curves, in which N_1 in the liquid (disregarding the water) is plotted against N_1 in the solid, are shown in Figs. 4 and 5 for both calculated and observed data.

DISCUSSION

The calculated heats of mixing can be compared with experimental values only in the cases of the KBr–KCl and the RbCl–KCl solid solutions; for both systems the calculated heats are a little lower than the experimental. For solutions of KBr–KCl the agreement is probably within the experimental and calculatory errors. In the case of the RbCl–KCl solutions, the deviation is larger, with a calculated value for an equimolal solution of 141 calories per mole, as compared with 203 calories for the only available experimental value. In general, the agreement seems very good; this is especially true when it is remembered that theoretical values calculated without consideration of ionic displacements are approximately twice too large.

The few experimental lattice constants now available for the four systems here studied are of insufficient accuracy for any very quantitative comparison. However, the present calculated values, which are in rather close agreement with those given by Retgers' law of additive volumes, appear to be reasonable, whereas all previous theoretical lattice constants have been without question too high. X-ray diffraction studies of several of the above systems are now being carried out by Alexander, Pitman, and Klug; publication of their results is planned for the near future.[15]

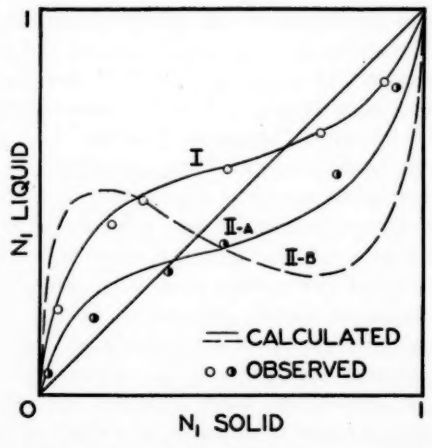

FIG. 4. Distribution between aqueous and solid solution. I: $KBr_{(1)}-KCl_{(2)}$; IIA: $RbBr_{(1)}-RbCl_{(2)}$; IIB: theoretical curve for $RbBr_{(1)}-RbCl_{(2)}$ obtained without considering displacements of ions from normal lattice positions.

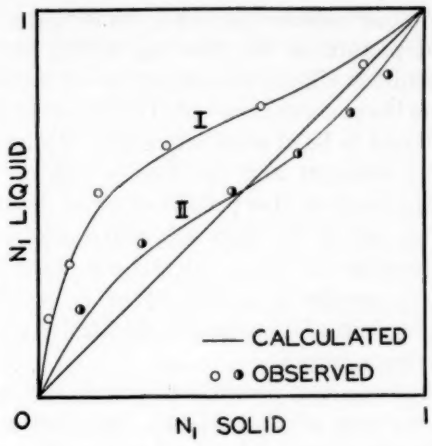

FIG. 5. Distribution between aqueous and solid solution. I: $RbCl_{(1)}-KCl_{(2)}$; II: $RbBr_{(1)}-KBr_{(2)}$.

The calculated and observed distributions between aqueous and solid solutions are compared in Figs. 4 and 5; good over-all agreement is obtained for the four systems. To indicate the effect of the size of ΔH_{ss} upon distributions, in Fig. 4 there is plotted, as a broken line, the distribution curve for the system RbBr–RbCl calculated from values of ΔH_{ss} obtained without taking into account displacements from the normal lattice. The resulting distribution bears little resemblance to the observed, since it corresponds to incomplete solid solution over the greater portion of the concentration range.

Comparison of the extent of the displacement of the ions in solid solution from normal lattice positions as calculated here, with their movement due to thermal vibrations, shows that the former is small compared with the latter. Consequently one would not expect such irregularities in the positions of the ions to appear in x-ray diffraction studies at usual temperatures. However, x-ray measurements of alkali-halide solid solutions at very low temperatures would be expected to indicate such a condition, and for this reason, might be of some interest.

The over-all agreement of the heats of mixing, lattice constants, and distributions as calculated in this paper with observed values would seem to confirm the postulate that in an ionic solid solution, the ions are not present at a uniform nearest-neighbor distance, but instead occupy positions of minimum potential energy

[15] See Alexander, Pitman, Klug, and Durham, "Solid solutions of the alkali halides. III. Experimental and theoretical lattice constants in RbBr–RbCl and RbBr–KBr solid solutions," to appear in J. Am. Chem. Soc.

relative to one another, as well as to indicate that the simplified picture of the resulting lattice here introduced furnishes a good approximation of the displacements and the energies involved. The energy of displacement is found to be of great importance in determining the lattice constant and the heat of mixing in solid solutions, as well as other properties which depend upon these. That use of the Born-Mayer-Huggins repulsion-energy function in these calculations leads to such satisfactory results is evidence that it describes the repulsion-energy relationships in the alkali halides with high relative accuracy.

Calculations are at present being made in this laboratory for the case of alkali halides which are known to form discontinuous solid solutions at some compositions. Such systems will provide a further check on the methods set forth in this paper.

Note added in proof:—After the completion of this paper, abstracts of three pertinent articles have come to the attention of the authors. Two are by J. A. Wasastjerna [Acta Soc. Sci. Fennicae **3**, No. 8 (1944); Soc. Sci. Fennica, Commentationes Phys.-Math. **15**, No. 3 (1950). See Chem. Abstracts **42**, 14^{i} (1948); **44**, 398^{c} (1950).] In the first, experimental evidence is presented that the ions in alkali-halide solid solutions are displaced from normal lattice positions; in the second a theory of geometrical displacements of ions in such solutions is developed. The third paper, by V. Hovi [Soc. Sci. Fennica, Commentationes Phys.-Math. **15**, No. 12 (1950); see Chem. Abstracts **44**, 10481^{a} (1950)] makes use of this theory to calculate heats of formation for KBr−KCl and RbCl−KCl solid solutions. Since it has not yet been possible to obtain copies of these publications, a comparison of the methods and results of Wasastjerna and Hovi with those presented in the present paper could not be included here.

THE JOURNAL OF CHEMICAL PHYSICS VOLUME 19, NUMBER 2 FEBRUARY, 1951

The Electronic Energy Levels of Molecular Crystals

HARVEY WINSTON
Department of Chemistry, University of California, Berkeley, California
(Received October 2, 1950)

The electronic energy levels of a molecular crystal are classified according to representations of the space group of the crystal. When the ground state of the free molecule is totally symmetric, the number of crystal levels active in the absorption of light can be determined by a simple rule. Applications to rare earth crystal spectra and to the crystalline benzene spectrum are discussed.

IN molecular crystals, the electronic wave functions must be quite similar to the wave functions for the free molecules, since the visible and ultraviolet spectra are but little changed by crystallization. There are, however, a number of small but significant effects depending on the crystal structure. One of these is the splitting by the crystal fields of levels degenerate in the free molecules; this has been discussed by Bethe[1] and applied[2] extensively in the case of rare earth crystal spectra. These R. E. spectra, since they arise from inner electrons of the ions, are similar to the spectra of molecular crystals. The crystal fields may also cause the appearance of transitions altogether forbidden in the vapor. Another effect of crystallization is implicit in the work of Frenkel[3] and Peierls[4] on the theory of excitons; it has been treated more recently by Davydov.[5] Briefly, their work shows that there are bands of energy levels in the crystal associated with each excited level of the free molecule, and, what is less well known, that there may be several optical transitions in the crystal for each one of the free molecule, even when the original free molecule levels are nondegenerate. Davydov has carried out a very full treatment for monoclinic crystals with the naphthalene or anthracene structure. While his method leads to expressions for the resulting splitting of the free molecule energy levels in terms of intermolecular forces, it is not well adapted to situations where the crystal symmetry is more complicated, nor is the importance of the crystal symmetry in the general case made clear. This paper shows how an application of the theory of representations of space groups[6–8] makes possible in many cases an extremely simple discussion of this effect, which will be called "Davydov splitting" to distinguish it from the better-known "Bethe splitting."

Our method of attack is application of the principle that stationary states of the crystal belong to irreducible representations of the crystal symmetry. In what follows, we shall also assume that the ground state of the free molecule is totally symmetric in the molecular symmetry, unless the contrary is explicitly stated. When the constituent molecules of a crystal interact only weakly, a zero-order wave function for the whole system can be made by forming a product of molecular

[1] H. Bethe, Ann. Physik **3**, 133 (1929).
[2] S. Freed, Revs. Modern Phys. **14**, 105 (1942).
[3] J. Frenkel, Phys. Rev. **37**, 17, 1276 (1931); Physik. Z. Sowjetunion **9**, 158 (1936).
[4] R. Peierls, Ann. Physik **13**, 905 (1932).
[5] A. Davydov, J. Exptl. Theoret. Phys. (U.S.S.R.) **18**, 210 (1948); translated by M. Kasha and distributed under ONR Contract N6-ori-211, T.O. 3.
[6] F. Seitz, Ann. Math. **37**, 17 (1936).
[7] Bouckaert, Smoluchowski, and Wigner, Phys. Rev. **50**, 58 (1936).
[8] H. Winston and R. S. Halford, J. Chem. Phys. **17**, 607 (1949).

functions, one for each molecule. For example, a state of the crystal in which the jth molecule is excited and the rest are in their ground states would have the wave function

$$\Psi_j' = \psi_j' \prod_{i \neq j} \psi_i, \qquad (1)$$

where ψ' and ψ are excited and ground-state free molecule functions, respectively. Ψ_j', however, is deficient in three respects: (1) it does not satisfy the Pauli principle; (2) when intermolecular forces are considered, it does not represent a stationary state; and (3) it does not belong to an irreducible representation of crystal symmetry. It has in many ways a status similar to that of one of several resonance structures for a molecule. The first objection can be easily met by antisymmetrizing the function in the electron coordinates in the usual manner; the antisymmetry in the electrons has no qualitative importance in the effect we are considering and will not be mentioned again. Objections (2) and (3), which are related, deserve closer consideration. Ψ_j', as defined above, is degenerate with all Ψ_k', functions which place the excitation on the kth molecule, as long as intermolecular interactions are neglected. If we imagine that by some means a state corresponding to localization of the excitation on the jth molecule has been set up in the crystal, application of time-dependent perturbation theory shows us that it can persist only about $\hbar/\Delta E$ seconds, where ΔE is the nearest-neighbor interaction, or, in a standard notation, $\int \psi_1' \psi_2 H_{12} \psi_1 \psi_2' d\tau_1 d\tau_2$. At the end of this interval, there is a good chance that the excitation will appear on a neighboring molecule. Stationary states of the crystal must belong to irreducible representations of the crystal symmetry group, so the linear combinations of Ψ_k' which do belong to such irreducible representations are better approximations to the true wave functions than the Ψ_k' themselves. Such combinations are formed when we reduce the representation of crystal symmetry for which the Ψ_k' form a basis. The ground state of the crystal, $\prod_i \psi_i$, however, is satisfactory as soon as it is antisymmetrized; only one state of the crystal, the totally symmetric one, can be formed by placing each molecule in its totally symmetric ground state.

Whether the Ψ_k' or their linear combinations are better suited for the description in a given approximation of a process in the crystal is a question determined in part by the time scale of the process. Let us consider a case for which ΔE is 100 cm^{-1}, an order of magnitude which, according to Davydov,[5] may often occur. The quantity $\hbar/\Delta E$ is then about 10^{-12} sec. Internal vibrations of the molecules, with periods less than about 10^{-13} sec, could best be treated in an early approximation by assuming the excitation localized on one molecule. We might say that in this case the vibrations couple strongly with the free molecule electronic levels, and the composite electronic-vibrational levels of different molecules then combine with each other. The situation is reminiscent of the problem of atomic energy levels, where the strength of coupling among the various angular momentum vectors determines which of them is most influential in fixing the energy. Light absorption and emission, with half-lives of 10^{-8} sec or more, would be better described with the aid of wave functions which distribute the excitation over a large part of the crystal. In intermediate cases (lattice modes or low lying internal modes) where the period of the process is of the same order as the period of energy transfer between molecules, we would expect to find appreciable interaction between the process and the energy transfer.

In this section we shall treat the pure electronic problem, deferring until later the additional complication of vibrations. Our aim is to predict with a minimum of calculation and for any particular case what effects on the spectrum are to be expected when a crystal is formed from molecules. We imagine that we know the wave functions appropriate to a molecule in the time average potential of its site. The site functions rather than the free molecule functions are employed because the molecular symmetry has no strict significance when the molecule is embedded in the crystal. These site functions belong to irreducible representations of the site symmetry, and their relation to the free molecule wave functions can be determined by Bethe's method. Now we take into account the interactions due to the instantaneous deviations of the potentials around the sites from their time averages. These interactions will cause a spreading out of the crystal energy levels related to particular site levels, and we will follow in detail the crystal levels which arise in this way from a site level. We assume that cyclic boundary conditions[8,9] hold.

Employing at first just the translation subgroup of the space group, we find that linear combinations of products of molecular wave functions appropriate to the translation symmetry are

$$^j\Phi_p{}^\alpha(\kappa) = \sum_k \exp[-2\pi i(\kappa \cdot \mathbf{r}_{k\alpha})]\, ^j\Psi_{k\alpha}{}^{p'}. \qquad (2)$$

$^j\Phi_p{}^\alpha(\kappa)$ is a function belonging to the κ-representation of translational symmetry in which the excitation is to be found on the αth site of each unit cell, where it resides in the pth partner of a set of functions belonging to the jth site representation. $^j\Psi_{k\alpha}{}^{p'}$ is a generalization of the previous Ψ_k', where k now enumerates unit cells rather than molecules. There should also be an index to specify which energy level of the jth site representation is involved; but since in this approximation we consider just one such level at a time, we omit the extra index for simplicity.

For most values of κ, the stars§ of κ will be non-

[9] M. Born, Proc. Phys. Soc. (London) **54**, 362 (1942).

§ The term *star* was introduced by the authors of reference 7 in order to simplify the discussion of the space-group representations derived in reference 6. Those vectors in three-dimensional space (actually vectors of the reciprocal lattice) which are transformed into each other by operations of the point group underlying the space group are collectively called a *star*. Stars which contain vectors equal in number to the order of the point group are *nondegenerate;* certain stars, containing vectors lying on symmetry elements, contain only submultiples of this number, and are

degenerate, and symmetry considerations will give us no further aid in reducing the order of the secular equations which determine the coefficients of the ${}^{i}\Phi_{p}{}^{\alpha}(\kappa)$ (for fixed κ and running α and p) in the linear combination which approximates the wave function for the particular intermolecular potential. At certain points in the reciprocal lattice, however, the star degenerates; and a still finer symmetry classification, which reduces the order of the secular equations, is possible. It has been shown[10] for metals how this circumstance makes much more feasible the approximate determination of energy bands. For our purposes the most important region in the reciprocal space is near the origin, at which the functions belonging to the $\kappa=0$ representation can be subjected to a finer classification according to the representations of the factor group of the space group. A simple relation between the character systems of the factor and site groups, to be described in the next paragraphs, suffices to determine which factor group representations are populated when the site group representation of the excited level is known. This in turn enables us to predict optical selection rules, as the following argument shows. If the selection rule based on the translational symmetry were really $\Delta\kappa=0$, it is clear that the active representations in the factor group will correspond to the only representations of the whole space group to which optical transitions from a totally symmetric ground state could be permitted. On account of the finite wavelength of the radiation, however, the translation group selection rule is not so simple, though it still exists and is responsible for the sharpness of pure electronic transitions. Still, we know that for each wave function belonging to a factor group representation, there will be wave functions with only very slightly different energies which belong to representations for which κ is small. That is, there will be a band of energies near each factor group energy, and it seems reasonable that the chief transitions will be to levels in those bands which contain levels with active factor group representations. Thus, the factor grqup representation retains to a considerable extent its role in determining whether or not a transition is permitted to some level of the band.

For this reason, it is useful to consider all the functions ${}^{i}\Phi_{p}{}^{\alpha}(0)$ for all values of α and p. These belong to the totally symmetric representation of the translation subgroup, but in general they must be subjected to a linear transformation to produce functions belonging to the various factor group representations. We shall determine what reducible factor group representation is induced by this set of functions. On reducing this representation, we will have the irreducible representations of the factor group, the $\Gamma_{i}{}^{f.g.}$, which are desired, and the transformation which effects the reduction will be just the one which provides suitable linear combinations of the ${}^{i}\Phi_{p}{}^{\alpha}(0)$. The n molecules per unit cell are distributed on sites of order h, and the factor group is of order $H=nh$.

Any symmetry operation R of the factor group not in the αth site group will change ${}^{i}\Phi_{p}{}^{\alpha}(0)$ into some other ${}^{i}\Phi_{q}{}^{\beta}(0)$, where $\alpha\neq\beta$, so there are in this case no diagonal elements. If R is in the site group, the sum over p of diagonal elements associated with ${}^{i}\Phi_{p}{}^{\alpha}(0)$ is just $\chi_{j}{}^{s.g.}(R)$. An expression for the character of R in the reducible factor group representation is therefore

$$
\begin{aligned}
{}^{(i)}\chi^{f.g.}(R)&=\textstyle\sum_{\alpha}\delta_{\alpha}(R)\chi_{j}{}^{s.g.}(R)\\
&\qquad \delta_{\alpha}=1 \text{ if } R \text{ is in } \alpha\text{th site group}\\
&\qquad =0 \text{ otherwise.}
\end{aligned}
\tag{3}
$$

This may be reduced. The number of times $\Gamma_{i}{}^{f.g.}$ appears is

$${}^{i}n_{i}=(1/H)\textstyle\sum_{R}\chi_{i}{}^{f.g.*}(R)\,{}^{(i)}\chi^{f.g.}(R). \tag{4}$$

We now substitute for ${}^{(i)}\chi^{f.g.}(R)$ from Eq. (3), use the relation

$$\chi_{i}{}^{f.g.}(R)=\textstyle\sum_{k}a_{ik}\chi_{k}{}^{s.g.}(R) \tag{5}$$

and rearrange. The last equation holds because the site group is a subgroup of the factor group. The coefficients a_{ik}, which are independent of R, are readily determined from the character tables.

$${}^{i}n_{i}=(1/H)\textstyle\sum_{\alpha}\sum_{k}\sum_{R}a_{ik}\chi_{k}{}^{s.g.*}(R)\chi_{j}{}^{s.g.}(R)\delta_{m}(R). \tag{6}$$

We use the orthogonality relations of group characters to reduce this to

$${}^{i}n_{i}=a_{ij}. \tag{7}$$

This result is equivalent to one of Winston and Halford,[8] their Eq. 11; but since the argument leading to that equation was couched in the language of vibrations, this more general derivation has been given.

Equation (7) contains all the information we need for a qualitative discussion of the energy levels and spectrum. It tells us how many energy levels belonging to the ith factor group representation in the crystal arise from one level belonging to the jth site group representation. As discussed above, the selection rules for the factor group representations may then be used to find the number of crystalline transitions corresponding to a transition to this level of the site. For actual calculations of energies, we would also need the coefficients of the ${}^{i}\Phi_{p}{}^{\alpha}(\kappa)$ in the linear combinations. For the factor group representations which contain only one energy level, the coefficients are entirely determined by symmetry.

Equation (7) also shows that unless a transition between the ground state and an excited state is permitted in the symmetry of the site, it is not permitted between the crystalline levels related to these site states, because the coefficients a_{ij} will not connect an optically active factor group representation with an inactive site group representation. Furthermore, it is worth pointing out that perturbations which preserve the crystalline sym-

degenerate. The representations associated with nondegenerate stars are all of similar form and dimensionality; the representations associated with degenerate stars are of smaller dimensionality and hence functions belonging to them can be subjected to a finer symmetry classification than can functions associated with nondegenerate stars.

[10] M. Chodorov and M. Manning, Phys. Rev. **52**, 731 (1937).

metry can cause mixing only of levels belonging to the same space-group representation. This last circumstance is of particular interest when vibrations are excited as well as electrons, where the significant representations are those of the combined electronic-vibrational states.

Our first example will be the crystal of EuF_3. The space group[11] is V_h^{16} and the Eu^{+++} ions occupy sites of symmetry C_s, four per unit cell. The ground state of the ion has a J of zero, and all the states concerned have even parity;[12] thus, the ground state is totally symmetric, and the theory is applicable. Table I shows the correlations among the representations of spherical symmetry (for the free ion), the site group, and the factor group.

The first line of Table I was obtained in the following way. An even atomic state with $J=0$ will go over, in site symmetry C_s, to a state belonging to the representation A'. There will be q states of the whole crystal belonging to the factor group representation Γ and related to the original ionic level if $a_{\Gamma A'}$ is q. In Table II we have the correlation between V_h and C_s. When Γ_i is A_g, B_{1g}, B_{2u}, B_{3u}, $a_{\Gamma A'}$ is 1, and for other Γ_i, it is 0.

In Table III are summarized the numbers of different transitions which can occur by different mechanisms of absorption from the ground state. It appears that there are, for example, 8 different electric dipole transitions to crystal levels corresponding to the level $J=2$ in the free ion. Five levels, $2J+1$, would be expected in Bethe splitting. There are in all twenty (5 levels per molecule X4 molecules per unit cell) levels of the totally symmetric representation of the translation group corresponding to the $J=2$ level of the ion, of which the eight mentioned belong to factor group representations active in electric dipole absorption. In addition, seven transitions are possible by the magnetic dipole mechanism, and there are ten electric quadrupole transitions, of which all but three are also magnetic dipole transitions. As Van Vleck[13] has pointed out, all three mechanisms of transition may be important in rare earth spectra.

Freed and Weissman[14] found splittings into five and seven lines respectively for two Eu^{+++} absorptions in this crystal, and accordingly assigned values of J of 2 and 3 to the corresponding upper levels. However, a great deal of evidence from other Eu^{+++} crystals, summarized by Hellwege,[15] points to an assignment of 1 and 2 for the same levels. It is seen that Davydov splitting can account for the number of lines found in EuF_3 if the Hellwege assignment is used. Whether the magnitude of the splittings can be accounted for on this basis is another question. Davydov has pointed out that the weaker the transition in the free molecule, the smaller the crystal splitting is likely to be. Also, of course, the wave functions of different Eu^{+++} ions overlap only very slightly. Still, if the effect is to occur at all, one would expect to find it in a nonhydrated crystal like the fluoride.

Dr. Freed[16] has pointed out that this explanation cannot account for all the anomalies of Eu^{+++} ion spectra. As an example typical of a number of cases, he cited certain chelated compounds, containing definitely only one Eu^{+++} per molecule, the lines of which are split into more than $2J+1$ components if J is assigned according to Hellwege. There is, however, another phenomenon in a number of Eu^{+++} crystals which may find a proper explanation in the notion of Davydov splitting. This is a doubling of the spectral lines which, if only Bethe splitting were operative, would be single, and to which Hellwege[15,17] refers as "hyperfine structure." According to the present explanation, these doublings would correspond to the slight energy differences to be expected between levels which correspond to different representations of the factor group, even though they arise from the same site representation. It is suggested that the considerations outlined here for Eu^{+++} may provide at least a partial explanation for "extra levels" (those in excess of $2J+1$) for other rare earth crystals, although Eq. (7) cannot be applied directly to other rare earth ions, because the ground states are usually not totally symmetric.

A more typically molecular crystal is benzene. The

TABLE I. Correlations among representations of spherical, C_s, and V_h symmetry.

J	C_s	V_h
0^+	A'	$A_g, B_{1g}, B_{2u}, B_{3u}$
1^+	$A'+A''$	$A_g, B_{1g}, B_{2u}, B_{3u}$ $2(A_u, B_{1u}, B_{2g}, B_{3g})$
2^+	$3A'+2A''$	$3(A_g, B_{1g}, B_{2u}, B_{3u})$ $2(A_u, B_{1u}, B_{2g}, B_{3g})$

TABLE II. Correlation between V_h and C_s symmetry.

Activity	V_h	C_s
$2Q$	A_g	A'
	A_u	A''
Q R_z	B_{1g}	A'
T_z	B_{1u}	A''
Q R_y	B_{2g}	A''
T_y	B_{2u}	A'
Q R_x	B_{3g}	A''
T_x	B_{3u}	A'

TABLE III. Numbers of transitions by various mechanisms.

J	Dipole (T)	Magnetic dipole (R)	Quadrupole (Q)
0	2	1	2
1	4	5	6
2	8	7	10

[11] A. Zalkin and D. H. Templeton, private communication.
[12] G. Herzberg, *Atomic Spectra and Atomic Structure* (Dover Publications, New York, 1944).
[13] J. Van Vleck, J. Phys. Chem. **41**, 67 (1937).
[14] S. Freed and S. Weissman, J. Chem. Phys. **8**, 878 (1940).
[15] K. Hellwege, Gött. Nachr. **1947**, 58.
[16] S. Freed, comments at Am. Phys. Soc. meeting, New York, February, 1950.
[17] A. Hellwege, Ann. Physik **37**, 1226 (1940).

lowest excited singlet state of the free molecule is B_{2u}, or possibly B_{1u}, in D_{6h} symmetry.[18] In the crystal, with a space group[19] V_h^{15}, the four molecules per unit cell occupy sites of symmetry C_i, in which the excited state in question belongs to the ungerade representation. The 0−0 transition from the ground state is forbidden in the free molecule; in the site there is no symmetry prohibition on this transition, and the 0−0 band does indeed appear weakly. There are four levels with $\kappa=0$ associated with an ungerade site representation, corresponding to the representations A_u, B_{1u}, B_{2u}, and B_{3u} of the factor group V_h. No electric dipole transition is allowed to the first; and the transitions to the other three are polarized in the x, y, and z directions, respectively. It should be possible to demonstrate the existence of these levels by studying single crystals with polarized radiation. The situation is somewhat complicated by the possibility of accompanying vibrational transitions to levels related to internal vibrations of the molecule and to lattice vibrational modes. This is considered in later paragraphs. The spectrum by Kronenberger[20] shows an amount of fine structure in excess of that which could reasonably be accounted for without some crystal effect, either Davydov splitting or combination with lattice modes. In all probability both are operative.

It was remarked earlier that events which lasted less than $\hbar/\Delta E$ seconds would occur as if the excitation were localized on one particular molecule. Intramolecular vibrations have periods shorter than this time in many cases, and we therefore expect that the vibrational frequencies observed in the absorption spectrum of a molecular crystal will be quite similar to the vibrational frequencies of the excited electronic state of the free molecule. In this case the excited molecule wave functions which are used in building up the crystalline product wave functions should include a vibrational factor. The treatment by symmetry will be much the same as when vibration is neglected, but for the fact that the site representations will now be those of a vibrational-electronic rather than pure electronic state.

So far the discussion has been confined to molecules with totally symmetric ground states. We shall now investigate the effects which might be expected when the ground state is not totally symmetric, particularly when the ground state in the site is either degenerate or separated from the next highest level by energies small compared with kT. In these cases, the ground electronic state of the crystal will no longer be the only low lying electronic level; there may be a large number of low levels, arising from the possibility of a molecule in a site being assigned to any of a number of states. Linear combinations of the resulting crystal states can be formed, characterized by different values of κ. Even if there is only little difference in energy among these levels, it is evident that optical transitions may be permitted by symmetry from some of these to any excited level, regardless of its κ, with the result that the absorption line will be broadened to the order of the width of the excited band. In general, we would expect that when totally symmetric ground states occur well below any other states in the site approximation, the absorption lines will be sharper than otherwise.

The vibrational motions of a crystal offer the possibility of a large number of values of κ, and vibrational broadening is a well-recognized phenomenon. Even at liquid hydrogen temperatures, we would expect in certain cases to find many vibrational levels of the acoustic branches excited, leading to the possibility of many initial values of κ and therefore, according to the considerations of the last paragraph, a broad band. In spite of this, there often occurs an appreciable sharpening of absorption bands between liquid nitrogen and liquid hydrogen temperatures, which may be interpreted as due to a difference in the effects of the acoustic modes (the only ones appreciably excited at the lower temperature) and those of higher frequency. Broadening from vibration depends upon the magnitude of interaction between vibrational and electronic motions. It is to be expected that the acoustic modes, in which near neighbors move more or less in phase, would interact less with electronic motion than modes in which near neighbors move in opposition. Bands which sharpen at low temperatures do so not because of a symmetry prohibition on the transitions responsible for broadening, but rather because these broadening transitions are very weak on account of the small interaction with electronic motion of the vibrational modes which may be excited at low temperature.

ACKNOWLEDGMENT

The author is indebted to Bell Telephone Laboratories, Inc., for the grant of a Frank B. Jewett Fellowship under which this work was carried out, and to Dr. Donald S. McClure for many helpful discussions.

[18] Sponer, Nordheim, Sklar, and Teller, J. Chem. Phys. **7**, 207 (1939).
[19] E. Cox, Proc. Roy. Soc. (London) **A135**, 491 (1932).
[20] A. Kronenberger, Z. Physik **63**, 494 (1930).

Interpretation of the Vibration Spectrum of Mix-Crystals

FRANK MATOSSI
Naval Ordnance Laboratory, White Oak, Silver Spring, Maryland
(Received August 28, 1950)

The vibration frequencies of a linear chain of the type $\ldots XZYZXZYZ\ldots$ are calculated and discussed. The chain is considered to be a model for a mix-crystal of the components XZ and YZ. Only one vibration is strongly active enough to give a reflection band, its frequency being intermediate between those of the components, in agreement with observation. Another vibration, at lower frequencies, is very weak or inactive, depending on the exact nature of the mix-crystal structure—whether the ions X and Y are distributed regularly or statistically.

INTRODUCTION

IT is well known that crystals of the alkali-halide type have one eigenfrequency, which is observable as a strong reflection band in the infrared. Of course, the frequency is dependent on the masses of the constituents of the lattice. For many years, it has also been equally well known[1] that the infrared spectrum of mix-crystals[2] (or solid solutions) of alkali-halides contains only one reflection maximum, although the number of different atoms is greater than in the single components. The vibration frequency of a mix-crystal varies with the concentration of the components, as is to be seen from Table I which refers to NaCl−KCl mix-crystals.[1]

Obviously, this means that the lattice of a mix-crystal is not a mixture of the lattice of the components, but is a unique lattice of its own.

Similar observations were made recently[3] with mix-crystals of $NaNO_3$ and KNO_3. The Raman lines of the inner vibrations of the NO_3-ion are not doubled in the mix-crystal. Only one line appeared in the mix-crystal for every line of the pure components, its frequency being an intermediate one. In a real mixture, however, the two lines appeared which had been expected.

These facts can be interpreted in the same manner as above, but the conclusions are not as direct as from the infrared observations. Here, the influence of neighboring K-ions or Na-ions on the inner vibrations of the NO_3-ion (which do not depend directly on the anions) is involved; there, the frequencies of the lattices themselves.

The statement that mix-crystals build a unique lattice is in itself almost self-evident, but it involves another problem. The lattice of the mix-crystal is certainly more complicated than that of its components and, therefore, the spectrum should show more frequencies. Perhaps they are inactive, but this has never been investigated.

The purpose of this paper is to give a simple explanation of the facts mentioned above, utilizing calculations with a linear model of a mix-crystal of the alkali-halide type. The model is idealized in several respects; but, nevertheless, it is suitable to show the essential features of the interpretation to be suggested.

VIBRATIONS OF A LINEAR MODEL OF MIX-CRYSTALS

As a model of a mix-crystal of the components XZ and YZ with 50 percent concentration, we choose the following linear equidistant chain:

$$\begin{array}{cccccccc} \cdots X & Z & Y & Z & X & Z & Y & Z\cdots \\ \cdots 4i & 4i+1 & 4i+2 & 4i+3 & 4(i+1)\cdots. & & & \end{array}$$

i is a running index indicating the "cell" of this linear crystal. Homologous ions have the index $4i+k$ with $k=\text{const}=0, 1, 2$ or 3. The masses of the ions shall be designated by M, M', m for X, Y, Z, respectively. The (harmonic) forces shall be described by the force constants f (between X and Z) and f' (between Y and Z); x_n shall be the deviation of point n from its equilibrium position. Then the equations of motion are:

$$\begin{aligned} M\ddot{x}_{4i} &= f(x_{4i+1}-x_{4i})-f(x_{4i}-x_{4i+3}), \\ M'\ddot{x}_{4i+2} &= f'(x_{4i+3}-x_{4i+2})-f'(x_{4i+2}-x_{4i+1}), \\ m\ddot{x}_{4i+1} &= f'(x_{4i+2}-x_{4i+1})-f(x_{4i+1}-x_{4i}), \\ m\ddot{x}_{4i+3} &= f(x_{4i}-x_{4i+3})-f'(x_{4i+3}-x_{4i+2}). \end{aligned} \tag{1}$$

This model is idealized in the following points:

(1) It is a linear model, and forces are assumed only between neighbors. This is no serious defect in view of the success of this kind of treatment in well-known classical cases.

(2) It is a periodic structure with a regular distribution of X-ions and Y-ions, whereas the true distribution of X-ions among Y-ions is supposed to be at random.

(3) We consider only those frequencies of the different branches of the entire spectrum in which homologous points oscillate with equal phases. This is equivalent to infinite wavelength. Only these frequencies need be considered, in a first approximation, as funda-

TABLE I.

Molar conc. of NaCl:	0	30	50	70	85	100 percent
ω of refl. maximum:	165	171	180	188	191	195 cm^{-1}

[1] F. Krueger, O. Reinkober a.E. Koch-Holm, Ann. Physik **85**, 110 (1928).

[2] The term "mix-crystal," instead of "mixed-crystal," is used according to a proposal by W. P. Davey, *A Study of Crystal Structure and its Application* (McGraw-Hill Book Company, Inc., New York, 1934), p. 536.

[3] M. K. Raju, Proc. Indian Acad. Sci. (A) **22**, 150 (1945).

mental vibrations according to Born's theory of lattice dynamics. The modification of the system (1) for the smallest wavelength is shown below.

(4) It takes care of the 50–50 mixture only. We shall consider the possible limitations caused by these idealizations later.

To solve Eqs. (1), we put, in the usual manner,

$$\begin{aligned} &x_{4i}=A\exp(-j\omega t),\ x_{4i+2}=B\exp(-j\omega t),\\ &x_{4i+1}=C\exp(-j\omega t),\ x_{4i+3}=C'\exp(-j\omega t),\ j^2=-1, \end{aligned} \tag{2}$$

in which the amplitudes A, B, C, C' shall be independent of the cell index. With these assumptions, the following vibrations are obtained:

(a) ω_1 and ω_2 are given by

$$\begin{aligned} \omega_1^2+\omega_2^2&=(\tfrac{1}{2})[\omega_0^2(1+m/(M+m))\\ &\quad+\omega_0'^2(1+m/(M'+m))],\\ \omega_1^2\omega_2^2&=(\tfrac{1}{2})\omega_0^2\omega_0'^2Mm\\ &\quad\times(1+2m/M+M'/M)/(M+m)(M'+m), \end{aligned} \tag{3}$$

in which

$$\omega_0=[2f(1/M+1/m)]^{\frac{1}{2}}$$

and

$$\omega_0'=[2f'(1/M'+1/m)]^{\frac{1}{2}}$$

are the frequencies of the pure components. The amplitudes of ω_1 and ω_2 are given by

$$\begin{aligned} B/A&=\omega_0'^2[m\omega_0^2-(M+m)\omega_{1,2}^2]/\\ &\quad\omega_0^2[m\omega_0'^2-(M'+m)\omega_{1,2}^2],\\ C/A&=1-(M+m)\omega_{1,2}^2/m\omega_0^2,\quad C'=C. \end{aligned} \tag{4}$$

(b) $\omega_3^2=(f+f')/m$ with $A=B=0,\ C'=-C$

(c) $\omega_4^2=0$ with $A=B=C=C'$ (translation).

It is easy to calculate also the frequencies for the smallest possible wavelength. In the equations (1), we have to change the signs of the factors of x_{4i+3} in the first equation and of x_{4i} in the last one. The signs in equations (2) are retained. The solution yields four frequencies satisfying the equations

$$\begin{aligned} &\omega^4-[(f+f')/m+2f/M]\omega^2+2ff'/Mm=0\\ \text{and}\qquad &\qquad\qquad\qquad\qquad\qquad\qquad\qquad\qquad (5)\\ &\omega^4-[(f+f')/m+2f'/M']\omega^2+2ff'/M'm=0. \end{aligned}$$

These frequencies are irrelevant as fundamentals, but might play a role in the second-order spectra.

It is not worth while, although not difficult, to calculate the frequencies for the whole set of the quasi-continuous spectrum for the different optical and acoustical branches; the quantitative details are not important for our considerations, and the linear model would not give them accurately enough anyway.

For $M=M'$ and $f=f'$, ω_1 becomes ω_0, as is expected; ω_2 and ω_3 become the frequencies for the minimum wavelength of the XZ crystal with $B=-A,\ C'=-C$ for ω_2. (The expressions (4) cannot be utilized for this particular case.)

NUMERICAL EVALUATION AND DISCUSSION

We evaluate the results for NaCl–KCl mix-crystals with X=Na, Y=K, Z=Cl. At first, we take as values of ω_0 and ω_0' those of the observed reflection maxima ($\omega_0=195$, $\omega_0'=165$ cm^{-1}). Then $f/f'=1.06$; $\omega_1=176$, $\omega_2=132$, $\omega_3=120$ cm^{-1}. $\omega_1=176$ agrees well with the observed value 180 cm^{-1}. The amplitude ratios in this case are

$$\begin{aligned} B/A&=\ 0.25,\ C/A=-0.34 &&\text{for}\ \ \omega_1;\\ B/A&=-0.68,\ C/A=\ 0.25 &&\text{for}\ \ \omega_2. \end{aligned}$$

If we choose, as the fundamental frequencies, ω_0 and ω_0', the values of the absorption maxima (which are nearer to the true values of the lattice frequencies than the reflection maxima), i.e., $\omega_0=164$, $\omega_0'=141$ cm^{-1}; then $f/f'=1.02$; $\omega_1=155$, $\omega_2=110$, $\omega_3=103$ cm^{-1}. The amplitudes are given by

$$\begin{aligned} B/A&=\ 0.43,\ C/A=-0.97 &&\text{for}\ \ \omega_1;\\ B/A&=-0.93,\ C/A\cong\ 0 &&\text{for}\ \ \omega_2. \end{aligned}$$

No observations on the absorption of mix-crystals exist; but if the shift from reflection to absorption corresponds to that of the pure crystals, we should expect ω_1=about 153 cm^{-1} from the observed reflection maximum at 180 cm^{-1}.

We see that one frequency, ω_1, falls into the interval between ω_0 and ω_0'. As the amplitude ratios indicate, this frequency has the normal properties of an active vibration, the oscillation phases of the ions X and Y being opposite to those of the Z-ions. It can be shown (by somewhat lengthy but elementary calculations) that this is so for any ratio of the masses: One of the solutions of equations (3) is within the interval $\omega_0\cdots\omega_0'$; the other one, outside. The former one has equal signs for A and B opposite to the sign of C. The latter one has not.

For the reflection bands, ω_1 is about 8.5 times more intense than ω_2, as calculated from the theoretical amplitude ratios. The absorption data would yield a practically inactive ω_2 in our particular case, but the intensity ratios are very sensitive to small changes in the data.

From the foregoing, we infer that we have to expect only one strong band with a frequency between those of the pure crystals. The other frequency, outside the interval at the lower frequency side, should have at least smaller intensity, unless it is not rigorously inactive because of other reasons. ω_3 corresponds to an oscillation which indeed is exactly inactive and we need not consider it as far as fundamentals are concerned. However, the frequencies ω_2 and ω_3, together with the solutions of (5) and the complete sets of branch frequencies, should have a certain influence on the spectrum of the harmonics which appears in the Raman effect and, as "secondary maxima," also in the infrared spectrum of the alkali-halides. Therefore, an investigation of the Raman effect of alkali-halide mix-crystals would be of particular interest. ω_4, as the rigid translation, is irrelevant in any case.

It has not yet been investigated, experimentally, whether ω_2 is really inactive in the infrared or whether there might be a weak reflection or absorption band at lower frequencies. If there is indeed no such band (as

probably is the case), the reason for this might be the irregular distribution of X-ions and Y-ions. Because then, after cells with the order $XZYZ$, a cell $YZXZ$, or sometimes $XZXZ$ or $YZYZ$, might follow. But such an arrangement would destroy the phase relations between homologous points, which are a necessary condition for the excitation of an oscillation by the long wavelengths of the incident radiation. This disturbance would affect mainly ω_2, for which X and Y vibrate in opposite phases. For ω_1, the influence of the disturbance would be much smaller (though possibly not nonexistent).

From these considerations, it appears that, in principle, an infrared-spectroscopical proof of the usually assumed irregular, statistical, distribution of the ions in a mix-crystal would be possible; but it would depend on intensity measurements of the additional band at the low frequency side of the main band, which cannot be done easily with the required accuracy.

RAMAN EFFECT

In the periodic model, ω_1 and ω_2 would be Raman inactive because they are antisymmetric with respect to the inversion centers, just as ω_0 is Raman inactive in the pure components. They might become active in the statistical structure, but probably with a small intensity only.

With ω_3 it is different. It would be Raman-active for the periodic structure and perhaps very strongly so. It should remain active also for the unperiodic structure, because in a structure without symmetry, all fundamental vibrations are active, unless some other reason prevents the appearance of the lines, for instance, the ionic character of the bonds.

But even if we would not find a change in the first-order Raman spectra, at least we should expect that the second-order spectrum is sensitive to changes of the structure, because it is regulated by the entire set of frequencies of the several branches of the spectrum, and these can certainly be supposed to be strongly independent on the details of the structure. A quantitative treatment of this problem seems to be impossible.

From all these considerations, it seems important to investigate the Raman spectrum of mix-crystals of the alkali-halide type, preferably under different conditions. We should obtain from such an investigation valuable information on the more or less perfect statistical structure.

FINAL REMARKS

We have considered the mix-crystal with 50 percent of both components. However, the gradual decrease of the frequency of the reflection maximum, with increasing percentage of the heavier ion, is readily understandable from general theorems about the frequency change with the substitution of heavier atoms.

Our results do not apply to molecular crystals in which molecules are practically independent units, as in a gas, but in oriented and fixed positions. In this case, a mix-crystal would be approximately equivalent to a mixture of molecules and one would expect a superposition of the component spectra. This seems to be confirmed by observations of the Raman effect of mix-crystals of substituted benzenes.[4]

[4] M. Vuks, Acta Physicochim. U.R.S.S. **6**, 327 (1937) and S. C. Sirkar a. I. C. Bishui, Indian J. Phys. **11**, 417 (1937). I thank Dr. B. D. Saksena for drawing my attention to these results at the 1950 Symposium on Molecular Spectroscopy, Columbus, Ohio.

THE JOURNAL OF CHEMICAL PHYSICS VOLUME 19, NUMBER 2 FEBRUARY, 1951

The Reactions of Methyl Radicals. II. The Abstraction of Hydrogen Atoms from Paraffins

A. F. Trotman-Dickenson,* J. R. Birchard, and E. W. R. Steacie
Division of Chemistry, National Research Council, Ottawa, Canada

(Received September 19, 1950)

The reactions of methyl radicals formed by the photolysis of acetone and deutero-acetone with nine paraffins have been studied from 25°C to 340°C. If the combination of methyl radicals requires no activation energy, then the activation energies found for the abstraction of hydrogen atoms are as follows: ethane, 10.4; *n*-butane, 8.3; 2-methyl propane, 7.6; *n*-pentane, 8.1; 2,2-dimethyl propane, 10.0; *n*-hexane, 8.1; 2,3-dimethyl butane, 6.9 and 7.8; 2,3,4-trimethyl pentane, 7.9; 2,2,3,3-tetra-methyl butane, 9.5 (all values in kcal). The collision theory steric factors of these reactions are all less than 10^{-3}.

INTRODUCTION

THIS paper is the second of a series describing experiments carried out as part of a quantitative survey of the reactions of methyl radicals. In the first paper,[1] in future referred to as Part I, we described experiments on the high temperature photolysis of acetone which were necessary before it could be used as a source of methyl radicals for the study of their reactions with other compounds. Here are described, in

* National Research Council of Canada Postdoctorate Fellow. Present address: Dept. of Chemistry, University of Manchester, Manchester, England.

[1] A. F. Trotman-Dickenson and E. W. R. Steacie, J. Chem. Phys. **18**, 1097 (1950).

the first section, further experiments on the photolysis of light and heavy acetone using radiation of different wavelengths and, in the second section, experiments with paraffin hydrocarbons.

We have recently reviewed[2] the literature on the reactions of methyl radicals in detail and will not discuss it further here.

METHOD

When acetone is photolyzed alone at high temperatures, methane and ethane are produced by the reactions

$$2CH_3 = C_2H_6 \qquad (2)$$

$$CH_3 + CH_3COCH_3 = CH_4 + CH_2COCH_3. \qquad (3)$$

In the presence of a hydrogen-containing substance, RH, methane is also produced by

$$CH_3 + RH = CH_4 + R. \qquad (1)$$

It appears most unlikely that either methane or ethane is produced in any other way.

From the first scheme, it can be seen that when acetone is photolyzed

$$R_{CH_4} = k_3[CH_3][CH_3COCH_3]$$
$$R_{C_2H_6} = k_2[CH_3]^2,$$

where R_{CH_4} and $R_{C_2H_6}$ are the rates of formation of methane and ethane, $[CH_3]$ and $[CH_3COCH_3]$ the concentrations of these species, and k_3 and k_2 the rate constants for reactions (3) and (2). Hence,

$$k_3/k_2^{\frac{1}{2}} = R_{CH_4}/R_{C_2H_6}^{\frac{1}{2}}[CH_3COCH_3].$$

Provided that light of uniform intensity is used, the quantities on the right-hand side of this equation may be found experimentally, and so the value of $k_3/k_2^{\frac{1}{2}}$ at any temperature may be determined.

When a mixture of acetone and neopentane is photolyzed, we have, using the same notation as above,

$$R_{CH_4} = k_3[CH_3][CH_3COCH_3] + k_1[CH_3][C_5H_{12}]$$
$$R_{C_2H_6} = k_2[CH_3]^2.$$

Hence,

$$R_{CH_4}/R_{C_2H_6}^{\frac{1}{2}} = k_3/k_2^{\frac{1}{2}}[CH_3COCH_3] + k_1/k_2^{\frac{1}{2}}[C_5H_{12}].$$

Since we can find $k_3/k_2^{\frac{1}{2}}$ by the photolysis of acetone alone at any temperature, it is possible by using this relation to find $k_1/k_2^{\frac{1}{2}}$. A series of experiments in which $k_1/k_2^{\frac{1}{2}}$ has been determined in this way over a range of temperature is described below. Similar experiments have been carried out to find $k_1/k_2^{\frac{1}{2}}$, where k_1 is the rate constant of reaction (1) and RH is some other paraffin. This procedure for the determination of $k_1/k_2^{\frac{1}{2}}$ will be referred to as Method I.

An alternative approach, which we shall refer to as Method II, is the photolysis of mixtures of heavy acetone with hydrocarbons. In this case the reactions producing methane and ethane are

$$CD_3 + RH = CD_3H + R \qquad (1^*)$$

$$CD_3 + CD_3COCD_3 = CD_4 + CD_2COCD_3 \qquad (3^*)$$

$$2CD_3 = C_2D_6. \qquad (2^*)$$

Then, as before for heavy acetone alone,

$$k_3^*/k_2^{*\frac{1}{2}} = R_{CD_4}/R_{C_2D_6}^{\frac{1}{2}}[CD_3COCD_3],$$

while in the presence of a hydrocarbon

$$k_1^*/k_3^* = R_{CD_3H}[CD_3COCD_3]/R_{CD_4}[RH],$$

the notation being the same as before. R_{CD_3H}/R_{CD_4} can be determined experimentally. Only 2 or 3 percent of the total acetone present was photolyzed, so that the initial ratio $[CD_3COCD_3]/[RH]$ may be taken as remaining constant throughout the run. In Part I, $k_3'/k_2'^{\frac{1}{2}}$ was determined over a range of temperatures where k_3' and k_2' are the rate constants for reactions (3) and (2) in a system where the heavy acetone photolyzed is 68 percent acetone-d_6 and 32 percent acetone-d_5. A correction term must be applied to the ratio $k_3'/k_2'^{\frac{1}{2}}$ to find $k_3^*/k_2^{*\frac{1}{2}}$. This correction is necessary because the hydrogen atoms in the acetone react with methyl radicals nearly three times as fast as the deuterium atoms. A correction must also be applied to the ratio R_{CD_3H}/R_{CD_4} because CD_3H is formed in the photolysis of the heavy acetone alone. Thus we can find k_1^*/k_3^*. $k_3^*/k_2^{*\frac{1}{2}} = k_1^*/k_2^{*\frac{1}{2}}$ at any convenient temperature.

By Method I we have found the relation between $k_1/k_2^{\frac{1}{2}}$ and $k_1'/k_2'^{\frac{1}{2}}$ for 2,2-dimethyl propane (runs 178, 179, and 180), where k_1' is the rate constant for the reaction corresponding to reaction (1) for radicals from heavy acetone containing 32 percent acetone-d_5. We find that the temperature dependence of the two ratios is the same and that $(k_1/k_2^{\frac{1}{2}})/(k_1'/k_2'^{\frac{1}{2}}) = 1.17$. We have assumed that this deviation from unity is due to the different rates of combination of light and heavy methyl radicals; if this is true, the ratio will be independent of $[RH]$ and the value of k_2'/k_2^* will be very close to unity. This seems to be the most reasonable explanation; however, since the deviation is small, no likely alternative assumption would affect our results. This correction has been applied to all the results obtained by Method II in order to find $k_1/k_2^{\frac{1}{2}}$.

Method II has a number of advantages. First, the possibility of the formation of ethane by means other than reaction (2) is not important, as no measurement of ethane formation is made. Second, the possibility of formation of methane by decomposition of the radical R is unimportant, as such methane would not be deuterated. Third, the determination of the ratio $CD_3H:CD_4$ can be made very accurately and rapidly with the mass spectrometer; the determination is facilitated by the fact that "residuals" do not often occur at the mass peaks 19 and 20 used for the determination. Fourth,

[2] A. F. Trotman-Dickenson and E. W. R. Steacie, paper presented at the Minneapolis Symposium of the American Chemical Society. To appear in J. Phys. and Colloid Chem.

a very simple system of temperature-controlled traps will separate the "noncondensables" from the other reaction products; the mass spectrometer analysis is improved by the removal of most of the carbon monoxide by combustion in a copper oxide tube. This, however, is not essential and need not be quantitative. Fifth, fast reactions may be studied more readily by this method than by Method I, as in these cases the amount of ethane formed is too small for accurate measurement.

The collision theory of chemical kinetics states that $k=PZ\exp(-E/RT)$, where k is the rate constant, P the steric factor, Z the collision number, and E the activation energy for the reaction. Hence,

$$k_1/k_2^{\frac{1}{2}}=P_1Z_1\exp[-(E_1-\tfrac{1}{2}E_2)/RT]/P_2^{\frac{1}{2}}Z_2^{\frac{1}{2}}.$$

Since we can determine $k_1/k_2^{\frac{1}{2}}$ and $E_1-\frac{1}{2}E_2$ experimentally and calculate Z_1 and Z_2 from the kinetic theory of gases, making reasonable assumptions about the collision diameters of the several species, we can find $P_1/P_2^{\frac{1}{2}}$. It is very unlikely that the steric factor for the combination of methyl radicals is greater than unity, so this is a maximum value for the steric factor of reaction (1). When P_2 has been determined, it will be possible to calculate the value of P_1 and the absolute values of the rate constant k_1.

EXPERIMENTAL

The apparatus was basically the same as that used in Part I. A second reaction system was added which was more suitable for the study of compounds having a vapor pressure below 6 cm at room temperature. This system was used for the "A" series of runs. The light source was a Hanovia S-500 medium pressure mercury arc. The light was roughly collimated by a polished aluminum cylinder 10 cm long and 4 cm internal diameter. This arrangement has the advantage that it does not project an image of the source on to the cell and furnishes reasonably uniform illumination on the front face of the cell but is unsuitable for actinometry. A similar optical arrangement in conjunction with the old reaction system was used for runs 239–243. Three filters were used as follows:

Filter A—A chlorine filter at atmospheric pressure.

Filter B—A Corex A filter (also known as 9–54 or 7910) with 50 percent transmission at 2450A.

Filter C—A Corex D filter (also known as 9–53 or 9700) with 50 percent transmission at 2875A.

The transmissions were measured on a Beckman spectrophotometer. The peaks of the absorption curves are at about 2775A for both light and heavy acetone. The extinction coefficients for the two compounds were found to be the same within the limits of experimental error.

All runs for which no duration is given were of approximately one hour. The concentration of each component in the reaction mixtures was about 1.8 $\times10^{-6}$ mole/cc.

The quartz reaction cell of the new system was 10 cm long and had a volume of 175 cc. Throughout, the volume of the cell has been used for the calculation of rate constants. The cell was placed in an aluminum block furnace similar to that used for the other system. The reactants were measured in a calibrated volume and then condensed in a small trap attached to the cell. The total volume of the cell, this trap, and the connecting tubing as far as the float in the heated float-valve mercury cutoff was 191 cc. The analysis of the reaction products was carried out as before.

MATERIALS

The light acetone used was Mallinckrodt Analytical Reagent grade which had been refluxed over potassium permanganate, distilled and stored over drierite.

The heavy acetone was made for us by Dr. L. C. Leitch in this laboratory; three different samples were used containing 31 percent-d_5, 32 percent-d_5, and 32 percent-d_5.

The hydrocarbons used were Phillips Research Grade products except for the 2,3,4-trimethyl pentane, which was a standard sample of the National Bureau of Standards, and the 2,2,3,3-tetramethyl butane, which was a gift from Dr. F. D. Rossini of the National Bureau of Standards. All these reagents except for the last were reported to contain less than 0.3 M percent impurity. Our experiments show that the small quantities of other paraffins which are the most probable impurities would have little effect upon the results obtained.

TABLE I. The photolysis of acetone.

Run	Temp. (°K)	Acetone concentration (micromoles/cc)	Time (sec)	Products (micromoles) CO	Methane	Ethane	$k_3/k_2^{\frac{1}{2}}$ $\times10^{13}$
			Acetone—no filter				
A.11	397	2.79	3925	13.2	3.30	11.8	5.34
A.21	411	3.04	3900	11.7	4.54	8.07	8.18
A.20	429	2.88	3960	11.6	5.84	6.76	12.1
A.22	457	2.99	4050	12.5	10.6	4.49	25.5
A.18	487	2.99	3900	13.9	15.2	3.09	44.8
A.16	528	2.78	3903	16.3	21.0	1.34	101
A.8	543	2.88	4560	23.2	31.9	1.70	122
			Acetone—filter B				
A.12	398	3.01	5760	18.6	5.13	14.5	5.72
A.19	430	2.90	3902	10.0	5.67	5.50	13.0
A.10	453	3.02	3720	15.3	11.3	6.27	23.9
A.24	492	2.79	4425	11.3	13.5	1.83	52.3
A.23	523	2.86	4505	14.1	18.9	1.09	91.2
			Heavy acetone—no filter				
243	416	3.69	3020	21.3	2.48	18.6	2.63
241	463	3.64	2402	18.0	5.78	12.6	8.51
242	499	3.53	2528	18.7	11.3	9.2	19.5
240	543	3.55	3500	29.2	28.3	6.49	49.0
			Heavy acetone—filter C				
A.26	423	3.08	3000	15.9	1.69	14.4	2.56
A.27	455	2.85	3180	16.7	3.70	13.6	6.06
A.25	495	2.88	4200	24.0	11.3	14.3	15.5
A.28	558	2.85	3000	19.0	19.5	4.87	54.8

TABLE II. The reaction of methyl radicals with paraffins (Method I).

Run	Temp. (°K)	Acetone Concentration (micromoles/cc)	Hydrocarbon Concentration (micromoles/cc)	Time (sec)	Products (micromoles) CO	Methane	Ethane	$k_1/k_2^{\frac{1}{2}}$ ×10¹³
			Ethane+heavy acetone					
185	389	1.84	1.81	24350	24.45	1.95	24.6	0.50
183	403	1.87	1.84	22700	24.60	3.10	22.4	0.91
186	422	1.84	1.84	24800	26.15	5.35	20.5	1.58
181	454	1.82	1.88	11520	13.15	5.75	8.55	3.96
184	480	1.84	1.88	24200	17.7	19.2	13.5	6.96
188	500	1.83	1.83	23560	27.5	24.5	10.6	9.45
189	522	1.87	1.84	24200	27.40	30.70	4.3	24.2
187	523	1.81	1.80	24750	27.80	31.60	4.75	24.0
192	544	1.79	1.74	25600	26.10	34.40	4.33	18.6
182	567	1.73	1.84	14600	17.90	25.20	1.95	25.4
			n-Butane					
127	395	1.84	1.73	7870	19.39	5.75	15.14	5.13
124	395	1.79	1.83	9690	19.40	6.20	13.16	5.31
125	412.5	1.74	1.89	10000	18.60	9.60	11.67	8.17
129	413	1.82	1.76	7410	18.00	7.91	12.00	7.77
130	443	1.80	1.81	8120	21.95	16.45	9.73	16.45
128	471	1.53	1.87	7900	17.60	19.00	4.54	28.61
			2-Methyl propane					
153	349	1.80	1.78	8960	10.29	2.06	10.52	2.79
156	369	1.86	1.71	8380	12.66	3.94	9.95	5.78
154	398	1.96	1.74	7760	13.38	7.62	7.95	12.0
157	422	1.79	1.75	7190	11.50	9.80	5.15	19.0
152	446	1.87	1.76	8520	14.80	16.50	3.50	34.6
155	467	1.91	1.81	8000	14.30	18.80	1.93	52.0
			n-Pentane					
202	362	1.95	1.89	10340	12.22	2.56	10.14	2.71
200	377	1.81	1.79	9800	13.45	3.65	10.12	4.03
198	392	1.84	1.77	11100	11.25	5.15	7.29	6.21
203	413	1.82	1.82	10100	13.43	8.65	6.74	10.75
201	430	1.83	1.81	8450	11.19	9.41	4.34	15.6
197	451	1.83	1.79	10100	10.9	12.6	2.26	26.2
			2,2-Dimethyl propane					
171	411	1.85	1.75	9100	12.39	4.16	8.55	1.81
166	413	1.85	1.71	9620	15.16	5.04	10.55	2.04
172	440	1.27	2.10	15400	16.57	9.06	8.32	3.64
164	460	1.76	1.72	9700	15.78	12.25	5.92	6.58
170	480	1.39	2.66	14050	17.30	17.80	3.85	10.57
167	502	1.88	1.89	9400	15.5	18.82	2.14	16.4
165	534	1.85	1.75	9070	15.00	23.20	1.07	31.0
169	565	1.26	2.46	14820	19.1	40.1	1.00	48.0
			2,2-Dimethyl propane+heavy acetone					
178	432.5	1.80	1.84	13760	16.16	4.64	11.5	2.77
180	451	1.77	1.80	10900	12.28	5.42	7.55	4.57
179	481	1.81	1.80	14100	23.7	12.81	7.15	9.70
			n-Hexane					
205	365	1.80	1.80	10100	10.82	2.82	8.90	3.57
207	385	1.85	1.83	9600	11.44	5.02	7.60	6.74
204	413	1.82	1.78	10410	14.00	10.00	6.63	13.0
208	433	1.85	1.74	11050	15.03	14.07	4.71	21.7
206	457	1.89	1.83	10880	15.20	18.70	2.85	34.0
			2,3-Dimethyl butane					
148	300	1.81	1.77	21400	5.36	1.17	11.05	1.245
151	318	1.86	1.77	16500	8.12	1.93	10.94	2.35
149	336	1.81	1.69	13300	12.19	3.46	11.15	4.37
145	357.5	1.84	1.74	11520	17.35	6.17	12.35	7.58
143	379	1.97	1.87	8340	15.30	8.70	8.55	13.85
146	412	2.61	1.07	7470	18.57	13.83	10.50	28.3
142	443	1.83	1.76	9340	18.34	23.16	3.54	52.4
144	463	1.81	1.73	8510	15.60	22.70	1.93	68.5

RESULTS

It is convenient to present and discuss first the results of further experiments on the photolysis of acetone alone. The results are given in Table I and are plotted in Fig. 1. The lines drawn on Fig. 1 correspond to those drawn on Fig. 1 of Part I. The points which correspond to the experiments described here show that there is no sensible change in the activation energy when different light sources are used and that the change in the absolute rates found is small. The agreement is the more impressive because the "A" series of runs was carried out by a different operator using different

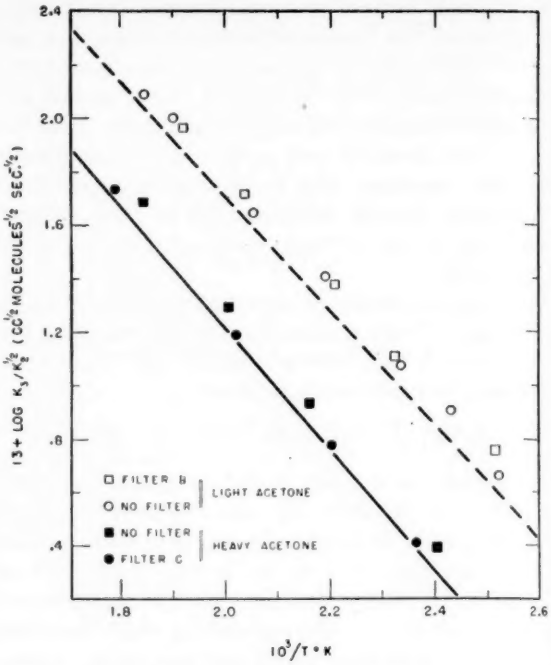

FIG. 1. Arrhenius plot for the reaction of methyl radicals with acetone.

reaction and analysis systems and different samples of acetone.

We have not sufficient knowledge of the factors which affect the absolute reaction rate to explain the changes found quantitatively, some of which are probably due to alteration of the effective reaction volume as the distribution of the light absorption varies. We have therefore presented the experimental results fairly fully in order that when more is known about this, the necessary corrections can be made. The corrections

TABLE III. The reaction of methyl radicals with paraffins (Method II).

Run	Temp. (°K)	[Hydrocarbon]/[Acetone]	CD_3H/CD_4	$k_1/k_2^{\frac{1}{2}}$ ×10¹³
		2,3-Dimethyl butane		
A.63	439	1.00	20.2	57.5
A.60	476	1.05	16.8	115
A.59	520	0.93	12.3	235
A.61	566	1.06	11.2	427
		2,3,4-Trimethyl pentane		
A.46	414	0.93	17.98	26.9
A.48	442	0.90	15.06	50.0
A.51	474	1.01	13.35	91.5
A.45	514	0.97	11.21	182
A.50	557	0.89	8.36	324
A.52	602	1.00	7.97	561
A.47	605	1.02	8.24	575
		2,2,3,3-Tetramethyl butane		
A.56	435	0.93	2.63	6.63
A.58	478	1.01	2.55	17.0
A.53	517	0.99	2.43	36.3
A.57	557	1.02	2.21	66.0
A.55	605	1.00	2.22	141

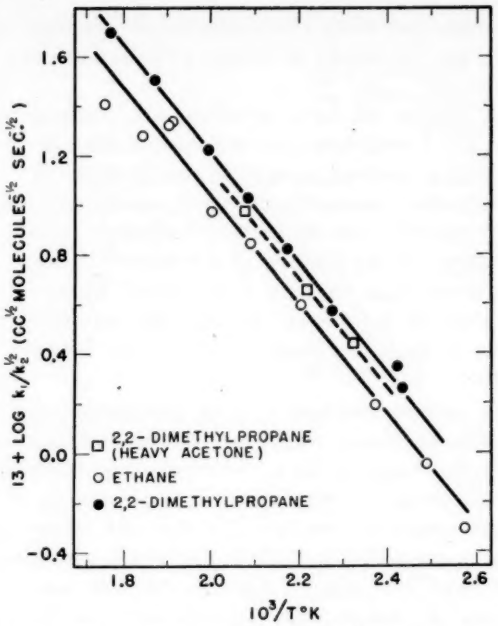

FIG. 2. Reaction of methyl radicals with ethane and neopentane.

will amount, at the most, to some 20 percent for the relative rate constants obtained by Methods I and II and so can have no effect upon our conclusions.

The results obtained in our experiments on the photolysis of acetone in the presence of paraffin hydrocarbons are given in Tables II and III and are plotted in Figs. 2–5.

We studied the photolysis of light and heavy acetone in the presence of 2,2-dimethyl propane and found, as can be seen from Fig. 2, a slight difference between $k_1/k_2^{\frac{1}{2}}$ and $k_1'/k_2'^{\frac{1}{2}}$, which we ascribed to a difference between k_2 and k_2'. There is no difference in the slopes of the lines.

The scatter of the points obtained for ethane at high

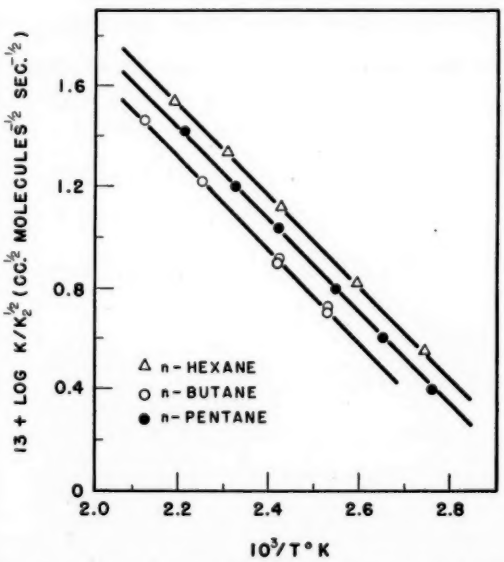

FIG. 3. Reaction of methyl radicals with normal paraffins.

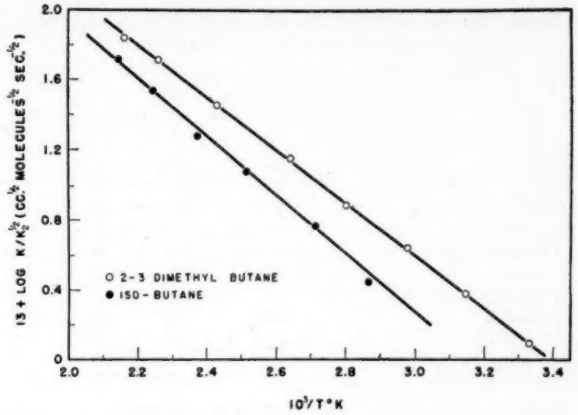

FIG. 4. Reaction of methyl radicals with branched-chain paraffins.

temperatures could be completely explained by errors of 5/10,000 in the ratio of C_2D_6 to C_2H_6 found on the mass spectrometer, and we believe that it is due to this cause.

The activation energies $E_1-\frac{1}{2}E_2$ and the relative steric factors $P_1/P_2^{\frac{1}{2}}$ found are given in Table IV together with the collision diameters used for the steric factor calculation and the values of $k_1/k_2^{\frac{1}{2}}$ found at 182°C. The rate constants are expressed in molecules, cc, and seconds.

The difference in the two values found for $E_1-\frac{1}{2}E_2$ for 2,3-dimethyl butane is greater than the probable experimental error. No reasonable allowance for the contribution of the primary hydrogen atoms removes the discrepancy. The same sample of reagent was used for both sets of runs, though an interval of some nine months separated them. There appear to be two possible explanations: either an impurity was present in one

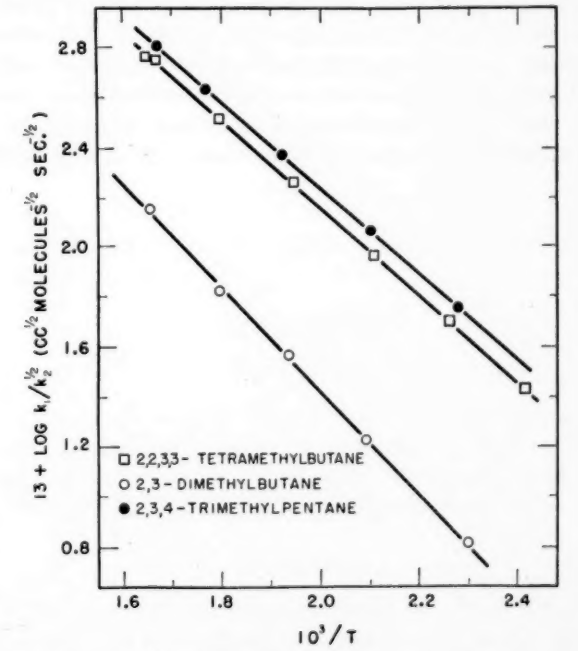

FIG. 5. Reaction of methyl radicals with branched-chain paraffins.

TABLE IV. The reaction of methyl radicals with paraffins. Activation energies and steric factors.

Compound	Collision diameter A	$E_1-\frac{1}{2}E_2$ kcal	$k_1/k_2^{\frac{1}{2}}$ $\times 10^{12}$ at 182°C	$P_1/P_2^{\frac{1}{2}}$ $\times 10^4$
Ethane	5.0	10.4	3.8	6
n-Butane	5.8	8.3	21	3
2-Methyl propane	5.9	7.6	42	3
n-Pentane	6.1	8.1	27	3
2,2-Dimethyl propane	6.0	10.0	6.3	6
n-Hexane	6.4	8.1	33	3
2,3-Dimethyl butane				
Method I	6.4	6.9	68	2
Method II		7.8	78	6
2,3,4-Trimethyl pentane	6.7	7.9	65	8
2,2,3,3-Tetramethyl butane	6.7	9.5	10	7

set of runs, or the plots are slightly curved owing perhaps to the presence of methyl radicals possessing excess energy. At the moment not enough is known to settle this point. It should, however, be noted that in experiments (to be described in Part IV) carried out with cyclopentane concordant results were given by Method I and Method II.

We obtained evidence in a number of cases for the decomposition of the alkyl radicals produced in reaction (1). This was particularly striking in the case of *n*-butane at 250°C, as shown by the value of $\frac{1}{2}CH_4+C_2H_6/CO$ being about 1.2. It is also noticeable for 2,2-dimethyl propane, where the radical presumably breaks down to methyl and 2 methyl propene.

DISCUSSION

In this work we have assumed that all the methane is produced by reaction (1), where RH is acetone or a paraffin, and that no methane is produced by the disproportionation reaction of methyl with an alkyl radical. It is very difficult to obtain information on this point; however, there are radicals such as the 2,2-dimethyl propyl, 2,2,3,3-tetramethyl butyl, and acetonyl with which disproportionation would not immediately give an olefin and consequently will be much less probable. The results obtained in these cases fall in line with those obtained with the majority of paraffins which would not be likely if disproportionation were important.

The results we have obtained are summarized in Table IV. From them two conclusions may be drawn. First, the activation energies of the reactions of methyl with paraffins containing primary, secondary, and tertiary hydrogens are distinctively different, the activation energy for the removal of a tertiary hydrogen atom being lower than that for a secondary which is lower than that for a primary. Second, the maximum value for the P factor in these reactions lies between 10^{-3} and 10^{-4}.

This second conclusion is of particular interest in view of the recent paper by Evans and Szwarc[3] in which they stated that there was no experimental evidence for low steric factors in the reactions of type (1) and predicted theoretically that the steric factors lay between unity and 10^{-2}. The work which we describe here is evidence that the steric factors for the reaction of methyl with paraffins are less than 10^{-3}. This conclusion receives further support from the findings of other workers which we have recently reviewed.[2] The same point has been made by Dorfman and Gomer,[4] who based their deductions largely upon work done at the University of Rochester. It appears, therefore, that the conclusions reached by the transition state method in these cases are incorrect, and that, in fact, more reactions are known with low steric factors than with high. There thus appears to be no such thing as a "normal" steric factor, and it remains for experiment to decide the matter in each case.

ACKNOWLEDGMENT

We wish to thank Miss Frances Gauthier and Dr. F. P. Lossing of this laboratory for the mass spectrometric analyses.

[3] M. G. Evans and M. Szwarc, Trans. Faraday Soc. **45**, 940 (1949).

[4] L. M. Dorfman and R. Gomer, Science **110**, 439 (1949).

The Reactions of Methyl Radicals. III. The Abstraction of Hydrogen Atoms from Olefins

A. F. TROTMAN-DICKENSON* AND E. W. R. STEACIE
Division of Chemistry, National Research Council, Ottawa, Canada
(Received September 19, 1950)

The abstraction of hydrogen atoms from eight olefins by deutero-methyl radicals formed in the photolysis of deutero-acetone has been investigated over a temperature range from 180°C to 340°C. The activation energies of those reactions have been determined relative to the activation energy of the combination of methyl radicals. The activation energies are 10.0 kcal for ethylene and 7.5±0.3 kcal for the other seven olefins. The collision theory "P" factors are all of the order of 10^{-3} or less.

INTRODUCTION

THIS paper is the third in a series on the quantitative study of the reactions of methyl radicals. In the first paper,[1] Part I, we described some experiments on the photolysis of acetone which had to be made before it could be used as a source of methyl. In the second paper,[2] Part II, we described further experiments on acetone alone using light of different wavelengths and on the photolysis of mixtures of acetone and paraffins. Here we describe experiments on the photolysis of heavy acetone in the presence of olefins made to determine the effect of structure upon the rate of removal of hydrogen atoms from the olefins by methyl.

The only previous quantitative work on these reactions is that of Taylor and Smith,[3] who studied the photolysis of mercury dimethyl in the presence of propene. The results show that the abstraction of hydrogen is fast compared with the abstraction of hydrogen from paraffins, but they are not suitable for the calculation of rates or activation energies because no estimate can be made of the methyl radical concentrations. As we have shown elsewhere,[4] the assumption upon which their estimate of the activation energy was based is not valid.

METHOD

The method used was that described in Part II as Method II. When heavy acetone is photolyzed in the presence of hydrogen-containing compounds, methane is formed only by reaction (1*) and (3*):

$$CD_3+RH=CD_3H+R \qquad (1^*)$$

$$CD_3+CD_3COCD_3=CD_4+CD_2COCD_3; \qquad (3^*)$$

and ethane is formed only by reaction (2*):

$$2CD_3=C_2D_6. \qquad (2^*)$$

So it can be seen that

$$R_{CD_3H}=k_1^*[CD_3][RH]$$
$$R_{CD_4}=k_3^*[CD_3][CD_3COCD_3],$$

where R_{CD_3H} and R_{CD_4} are the rates of formation of CD_3H and CD_4, the terms in square brackets are the concentrations of the species, and k_1^* and k_3^* are the rate constants for the reactions. Hence,

$$k_1^*/k_3^*=R_{CD_3H}[CD_3COCD_3]/R_{CD_4}[RH].$$

Since the reaction is only carried to two or three percent of completion, the initial concentrations of the acetone and the hydrogen-containing compound may be used in the equation. The ratio of CD_3H to CD_4 is readily determined by the mass-spectrometric analysis of the methane formed. Previously, we have determined $k_3^*/k_2^{*\frac{1}{2}}$ over a wide range of temperatures, so that $k_1^*/k_2^{*\frac{1}{2}}$ may now be found. $k_1/k_2^{\frac{1}{2}}$, the ratio of the rate constants for the corresponding reactions with light methyl radicals has been found by adding a correction of 18 percent to $k_1^*/k_2^{*\frac{1}{2}}$, as determined in Part II. A further correction as described in Part II is necessary to allow for the fact that the acetone used was not completely deuterated. We have determined $k_1/k_2^{\frac{1}{2}}$ for the olefins over a range of temperature, so we can calculate $E_1-\frac{1}{2}E_2$, where E_1 and E_2 are the activation energies of the reactions, and $P_1/P_2^{\frac{1}{2}}$, where P_1 and P_2 are the collision theory steric factors given by the equation

$$P_1/P_2^{\frac{1}{2}}=k_1Z_2^{\frac{1}{2}}\exp[(E_1-\tfrac{1}{2}E_2)/RT]/k_2^{\frac{1}{2}}Z_2,$$

where Z_1 and Z_2 are the collision numbers for the reacting species.

EXPERIMENTAL

Apparatus

The apparatus was the same as that used for runs 239–243 described in Part II, with the addition to the optical system of a Corex A filter (now designated as 7910 or 9–54) with 50 percent transmission at 2450A.

Materials

The heavy acetone was prepared for us by Dr. L. C. Leitch of this laboratory from heavy acetic acid. Analysis of this acetone by the parent mass peaks at 64

* National Research Council of Canada Postdoctorate Fellow. Present address: Chemistry Department, University of Manchester, Manchester, England.

[1] A. F. Trotman-Dickenson and E. W. R. Steacie, J. Chem. Phys. 18, 1097 (1950).

[2] Trotman-Dickinson, Birchard, and Steacie, J. Chem. Phys. 19, 163 (1951).

[3] H. S. Taylor and J. O. Smith, J. Chem. Phys. 8, 543 (1940).

[4] Steacie, Darwent, and Trost, Faraday Soc. Discussions 2, 80 (1947); A. F. Trotman-Dickenson and E. W. R. Steacie, J. Phys. Chem. (to be published).

and 63 showed that it contained 32 percent acetone-d_6. This impurity was allowed for in calculating the results.

The ethylene, propene, 1-butene, *cis*-2-butene, and 2-methyl propene were Phillips Research Grade hydrocarbons. The 1-pentene, 3-methyl-1-butene, and 2-3-dimethyl-2-butene were standard samples from the National Bureau of Standards. Except for the *cis*-2-butene, which was reported to contain 3.8 M percent impurity which was probably *trans*-2-butene, none of the hydrocarbons was reported to contain more than 0.7 M percent impurity. The most probable impurities are paraffins which would have a negligible effect upon our results.

Results

The experimental results are given in Table I and Fig. 1. The activation energies found are given in Table II. Both $E_3^*-E_1^*$ and $E_1-\frac{1}{2}E_2$ are given because the first quantity is more accurate being directly determined, while the second quantity includes any error made in determining $E_3^*-\frac{1}{2}E_2$. For comparison of the various members of the series, the first quantity is more suitable; but the second is needed for calculation of steric factors and for comparison with many of our other results.

Except in the case of ethylene there was no evidence for the addition of methyl to the double bond of the olefin or of polymerization. There was a slight decrease in the total pressure in the reaction system during the runs with ethylene such as would correspond to about 10 percent dimerization. It appeared that a very small amount of high boiling substance was formed. For this reason the results with ethylene are probably less accurate than those for the other compounds. A consideration of the method of obtaining results which we have used shows that the results for the relative rates and for the activation energies will not be greatly affected by small amounts of polymerization.

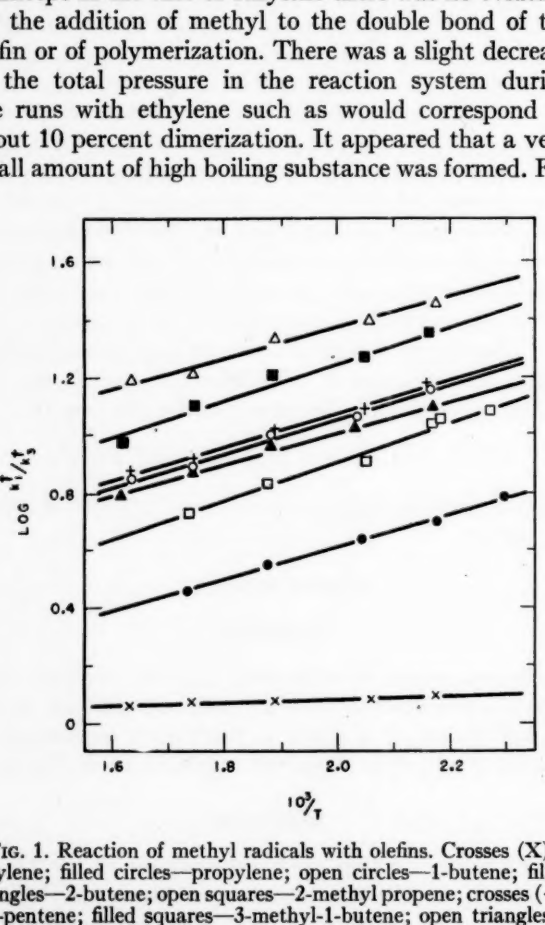

FIG. 1. Reaction of methyl radicals with olefins. Crosses (X)—ethylene; filled circles—propylene; open circles—1-butene; filled triangles—2-butene; open squares—2-methyl propene; crosses (+)—1-pentene; filled squares—3-methyl-1-butene; open triangles—2,3-dimethyl-2-butene.

TABLE I. The reaction of methyl radicals with olefins,

Run	Temp. (°K)	Acetone pressure (mm)	Olefin pressure (mm)	$\frac{R_{CD_3H}}{R_{CD_4}}$	$\frac{k_1^*}{k_3^*}$
			Ethene		
298	461	54.0	52.7	1.53	1.25
304	486	56.3	57.5	1.54	1.21
292	531	61.2	62.0	1.52	1.20
301	575	67.2	66.8	1.46	1.18
295	613	71.0	70.0	1.42	1.14
			Propene		
270	436	50.7	50.8	6.33	6.02
266	460	52.2	52.8	5.39	5.03
260	490	56.5	59.7	4.89	4.34
264	533	63.5	65.0	3.93	3.54
262	577	66.8	64.8	3.07	2.86
			1-Butene		
277	462	54.8	55.7	15.03	14.5
271	492	57.0	59.2	12.33	11.6
279	532	61.8	61.8	10.23	9.93
273	574	66.8	66.1	7.97	7.75
275	613	70.5	70.3	7.31	7.01
			2-Butene		
278	461	55.0	51.5	11.84	12.3
272	493	58.3	55.5	10.16	10.4
280	532	61.6	63.0	9.48	8.98
274	574	67.1	64.7	7.46	7.43
276	615	71.0	71.0	6.42	6.12
			2-Methyl propene		
267	441	5.07	5.00	12.3	12.1
265	459	5.38	5.27	11.40	11.3
269	461	52.4	52.8	11.49	11.0
259	489	56.1	56.6	8.42	8.04
263	533	62.0	61.3	7.05	6.83
261	577	66.4	67.1	5.72	5.36
			1-Pentene		
283	461	56.1	55.3	14.84	14.8
289	489	57.8	58.3	12.86	12.4
281	531	63.3	67.0	10.80	10.0
287	572	67.5	65.6	8.43	8.37
285	619	71.9	69.6	7.44	7.37
			3-Methyl-1-butene		
284	462	64.2	64.2	22.7	22.4
290	489	56.9	55.4	19.23	18.2
282	531	62.0	63.0	16.29	15.7
288	574	67.5	70.5	12.36	12.6
286	619	72.2	71.1	9.75	9.30
			2-3 Dimethyl-2-butene		
297	461	54.1	53.1	27.51	28.0
303	487	58.9	57.0	24.26	24.7
291	530	64.0	54.3	18.44	21.4
300	575	65.3	63.1	16.80	16.2
294	614	72.0	56.1	12.50	15.6

In this table and in Fig. 1. $k_1'/k_3' = 1.35k_1^*/k_3^*$, where k_1 and k_3' refer to experiments in which the deutero-acetone contains 68 percent acetone-d_8 and 32 percent acetone-d_6.

DISCUSSION

A comparison of the rates and activation energies found for the reaction of methyl radicals with ethylene

and propene permits two conclusions. First, that the rate of abstraction of a vinylic hydrogen atom is considerably less than the rate for an allylic hydrogen in the temperature range studied. Second, that the abstraction of a vinylic hydrogen requires a greater activation energy than the abstraction of an allylic hydrogen.

The relative values of $k_1/k_2^{\frac{1}{2}}$ for 1-butene and 1-pentene show that hydrogen atoms in the β- or γ-position make a negligible contribution to the rate constant. This could have been inferred from the results obtained for paraffins.

The values of $E_3^*-E_1^*$ for all the olefins studied, except ethylene, lie in the range 7.8 ± 0.3 kcal. The variation is about the same size as the probable experimental error and shows no systematic trend. There is no dependence of activation energy upon structure as occurred so markedly with the paraffins. If two reactions have the same steric factor, a difference of 0.2 kcal in the activation energy corresponds to a difference in rates of only 20 percent in the middle of our temperature range, so that all variation in rates greater than this must be attributed to changes in steric factor. In Table II the values of $k_1/k_2^{\frac{1}{2}}$ at 253°C divided by the number of active hydrogen atoms are given; here, ethylene is considered to have four equivalently active hydrogen atoms; propene has three; 1-butene, two; and 3-methyl-1-butene, one, since we have shown that hydrogen atoms in the α-position to the double bond are much more reactive than the others in the molecule. The variation in reactivity of the primary, secondary, and tertiary hydrogen atoms in the α-position to the double bond is well marked. We intend to discuss these facts later in conjunction with others which we have discovered from the investigation of other compounds.

Recently there have been a number of investigations on the reactions of olefins which have some bearing on the results described here. Melville and Robb[5] have studied the reactions of hydrogen atoms with olefins. They attribute the disappearance of the hydrogen atoms to addition to the double bond of the olefin; however, from our results it seems possible that in some cases the combination with a hydrogen atom from an olefin may be the way in which the hydrogen atoms are removed. Hinshelwood, Danby, and Raal[6] have studied the photolysis of acetaldehyde in the presence of a number of olefins. They develop a very complicated mechanism to explain their results and from it deduce the activation energy for the addition of a methyl radical to ethylene. The deduction depends upon the assumption that the mean number of ethylene units contained in the polymeric molecules produced is independent of temperature. One of the most important factors determining the size of the polymer molecules is the breakdown of the growing polymer radical to an olefin and a small alkyl radical. The activation energy of such steps can be estimated from thermochemical evidence to be more than 15 kcal, and this value has been confirmed by Bywater and Steacie.[7] So it is unlikely that the assumption, and hence the activation energy, of Hinshelwood and his co-workers is correct.

Table II. Activation energies and steric factors.

Compound	Collision diameter A	$E_3^*-E_1^*$ kcal	$E_1-\frac{1}{2}E_2$ kcal	$k_1/k_2^{\frac{1}{2}}$ $\times10^{12}$ at 253°C	$P_1/P_2^{\frac{1}{2}}$ $\times10^4$	$k_1/k_2^{\frac{1}{2}}$ $\times10^{12}$ at 253°C per "active" H atom
Ethylene	4.8	0.3	10.0	25	9	6.3
Propene	5.4	2.6	7.7	75	3	25
1-Butene	5.6	2.7	7.6	210	8	110
cis-2-butene	5.6	2.6	7.7	185	7	30
2-Methyl propene	5.8	3.0	7.3	145	4	25
1-Pentene	6.0	2.7	7.6	220	8	110
3-Methyl-1-butene	6.0	2.9	7.4	315	9	315
2-3 Dimethyl-2-butene	6.1	2.5	7.8	435	17	40

The rate constants are expressed in molecules, cc, and seconds.

Bolland[8] has studied the reaction of R—O—O-radicals with olefins in autoxidation reactions. These reactions are very similar to the reactions of methyl radicals with olefins, but there is little correspondence between his results and ours. Bolland relied upon an empirical relation between the logarithms of the velocity constants and the activation energies of the reactions to determine the exact activation energies which he quotes. As such relations are not universal or generally very accurate, it is not surprising that his activation energy differences are not found by us.

The steric factors which we find for the abstraction of hydrogen atoms from olefins are all low, since the values given for $P_1/P_2^{\frac{1}{2}}$ in Table II are maximum values for P_1. We intend to discuss the magnitude of steric factors in these and similar reactions more fully later in this series of papers.

ACKNOWLEDGMENT

We wish to thank Miss F. Gauthier and Dr. F. P. Lossing of this laboratory for the mass-spectrometer analyses.

[5] H. W. Melville and J. C. Robb, Proc. Roy. Soc. (London) **202**, 181 (1950).

[6] C. J. Danby and C. N. Hinshelwood, Proc. Roy. Soc. (London) **A179**, 169 (1941); Raal, Danby, and Hinshelwood, J. Chem. Soc. 1949, 2225 (1949).

[7] S. Bywater and E. W. R. Steacie, J. Chem. Phys. (to be published).

[8] J. L. Bolland, Quart. Rev. **3**, 1 (1949); Trans. Faraday Soc. **46**, 358 (1950).

The Mercury ($^3P_1$) Sensitized Decomposition of Normal and Iso-Butane at High Temperatures

S. BYWATER* AND E. W. R. STEACIE
Division of Chemistry, National Research Council, Ottawa, Canada
(Received November 3, 1950)

The mercury ($^3P_1$) sensitized decomposition of normal and iso-butane at high temperatures is described. The reactions of both hydrocarbons result in the formation of decomposition products of butyl radicals at temperatures above 250°C. In the case of normal butane this reaction gives methane, ethane, ethylene, and propylene; and with iso-butane, only methane and butane. Activation energies are assigned to the various radical decomposition steps.

INTRODUCTION

THE investigation of the mercury photosensitized decomposition of propane[1] and ethane[2] at high temperatures has yielded information on the thermal stability of the ethyl and propyl radicals.

Previous work on the photosensitized decomposition of normal butane[3] and iso-butane[4] was carried out at temperatures below 250°C. Under these conditions the various butyl radicals showed no signs of decomposition. The reaction has here been carried out up to 400°C in order to obtain products of the butyl radical decomposition.

EXPERIMENTAL

The reaction has been carried out using a static system of conventional design. Unreversed λ2537 was obtained from a low pressure mercury arc with neon (3 mm) as carrier gas. The light was roughly collimated by a quartz lens and passed through a quartz reaction cell contained in a concentric aluminum block furnace. The intensity of the incident light was found to be 1.38×10^{-5} einstein/hr as previously described.

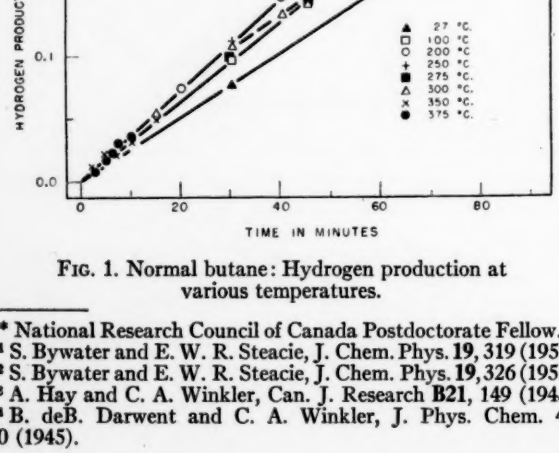

FIG. 1. Normal butane: Hydrogen production at various temperatures.

Normal and iso-butane were obtained in cylinders from the Phillips Petroleum Company (research grade). These were certified as being 99.78 percent and 99.88 percent pure, respectively, traces of impurity being saturated hydrocarbons. The gas used was therefore subjected to only bulb-to-bulb distillation and rigorous degassing before use. The apparatus was exactly as described by Bywater and Steacie[1] except that the gas analysis system was altered to include a low temperature still similar to that described by LeRoy.[5] This consisted of a primary trap immersed in liquid nitrogen, maintained at −125°C by means of a heating coil, followed by a long columnar trap with a temperature gradient along its length. After removal of noncondensible gases with the latter at liquid nitrogen temperature, ethane and ethylene were pumped off by maintaining the base of the column at −160° and the top some 20° higher. Blank experiments showed a 96 percent recovery of a small amount (0.150 cc N.T.P.) of ethane mixed with a large amount (50 cc N.T.P.) of normal butane. The recovered ethane was found by mass spectrometer analysis to be completely uncontaminated by butane. It was impossible to recover more than 60 percent of a similar amount of propane in a large excess

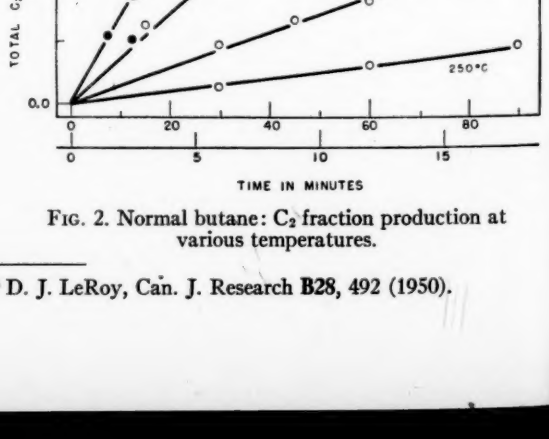

FIG. 2. Normal butane: C_2 fraction production at various temperatures.

* National Research Council of Canada Postdoctorate Fellow.
[1] S. Bywater and E. W. R. Steacie, J. Chem. Phys. **19**, 319 (1951).
[2] S. Bywater and E. W. R. Steacie, J. Chem. Phys. **19**, 326 (1951).
[3] A. Hay and C. A. Winkler, Can. J. Research **B21**, 149 (1943).
[4] B. deB. Darwent and C. A. Winkler, J. Phys. Chem. **49**, 150 (1945).
[5] D. J. LeRoy, Can. J. Research **B28**, 492 (1950).

of butane with this apparatus. Propane and propylene were therefore not normally analyzed, but typical experiments were fractionated in a more efficient still closer in design to that of Savelli, Seyfried, and Filbert.[6] The C_2 fraction was analyzed for ethylene by means of the Blacet-Leighton microanalysis apparatus. The non-condensible fraction was analyzed for methane by combustion over copper oxide at 280°C.

RESULTS

Experiments were carried out at a constant pressure of butane or iso-butane of 20 cm. This high pressure was chosen by consideration of the results obtained using propane. Under these conditions the reaction was shown to be much simpler than at lower pressures, where the results are complicated by some of the products quenching the ($^3P_1$) mercury atoms. Using higher pressures also makes the occurrence of radical recombination reactions less important. At this pressure

TABLE I.

Production of methane and hydrogen from iso-butane at 20 cm total pressure.

Iso-butane Temp. °C	cc CH_4/hr	cc H_2/hr	cc/hr non-chain (by extrapolation)	Δ(chain H_2)	[all quantities cc N.T.P.]
26°	...	0.154	...	...	
100°	...	0.181	...	...	
200°	...	0.197	...	...	
300°	0.040	0.212	...	...	
325°	0.088	0.219	0.214	0.005	
350°	0.145	0.270	0.217	0.053	
375°	0.248	0.402	0.219	0.183	
400°	0.436	0.801	0.233	0.568	

Production of methane and total C_2 hydrocarbons from normal butane.

Normal butane Temp. °C	CH_4 production (cc/hr)	C_2 production (cc/hr)	[all quantities cc N.T.P.]
250°	0.039	0.030	
275°	0.136	0.085	
300°	0.360	0.214	
350°	1.74	1.07	
375°	3.22	2.05	

the quantum yield of hydrogen formation at room temperature for both iso-butane and normal butane is 0.50. This value is identical with the quantum yield from propane at high pressures.

NORMAL BUTANE

Up to 250°C no reaction product is detectable other than hydrogen and a heavy fraction. The hydrogen production reaches a maximum at 200°C. Thereafter the initial rate is equal to that at 200°C but begins to fall off with time (Fig. 1). Presumably an equal amount of octane is produced,[2,3] corresponding to the heavy fraction present.

Above 250°C with normal butane, appreciable amounts of methane, ethane, ethylene, and propylene are formed (Table II). Double bond analyses made on twelve typical C_2 fractions from various runs showed

[6] Savelli, Seyfried, and Filbert, Ind. Eng. Chem. (Anal.) 13, 868 (1941).

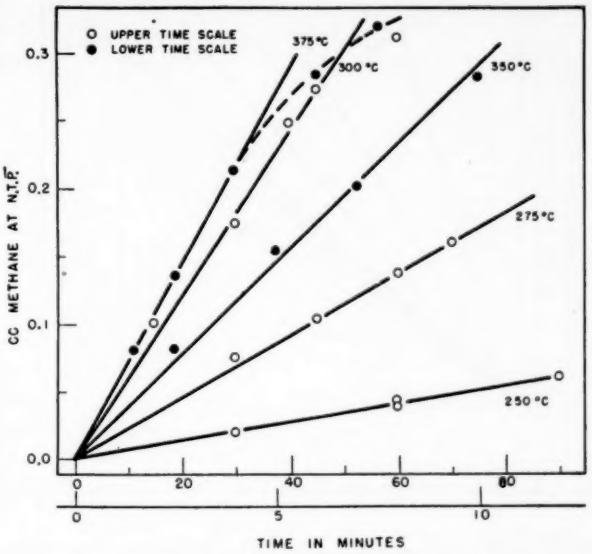

FIG. 3. Normal butane: Methane production at various temperatures.

that an average of 55 percent of the C_2 fraction was ethylene, variation between 53 and 57 percent being normal. The C_3 fraction is roughly equivalent to the amount of methane formed. Exact estimation of the quantity of this fraction was difficult since it was always contaminated with butane. Usually it was found to be around 85 percent propylene. A further cut was found to produce further small quantities of propylene contaminated heavily with butane. The agreement between methane and propylene production has therefore partially resulted by cancellation of these two factors.

The rate of total C_2 fraction and methane formation with time at various temperatures is shown in Figs. 2 and 3 and Table I. The activation energy calculated from these results (Fig. 4) corresponds to 23 kcal for both C_2 and methane formation. Although the experi-

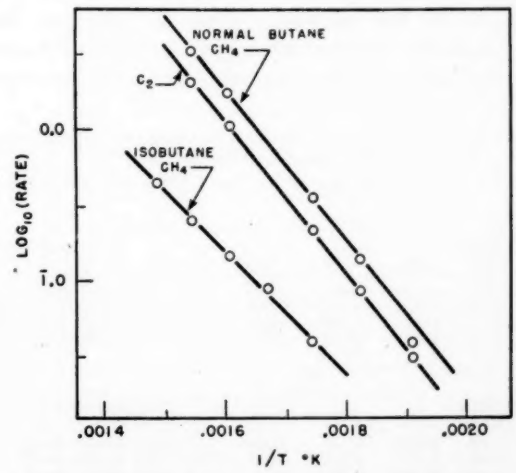

FIG. 4. Activation energy plots for the formation of CH_4 and total C_2 fraction for the two butanes.

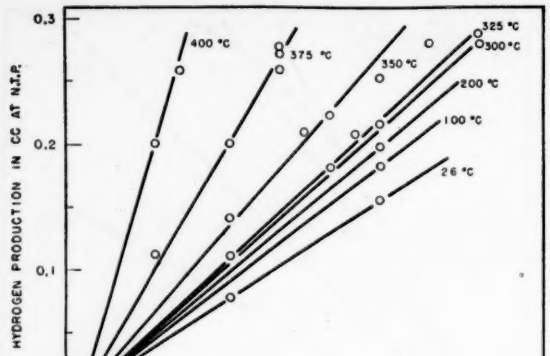

FIG. 5. Iso-butane: Hydrogen production at various temperatures.

ments were carried out at constant pressure rather than constant concentration, no appreciable error will result from using concentration units in this calculation. Thermal blank experiments at 375°C show that only 0.5 percent of the products are due to thermal reaction at this temperature.

ISO-BUTANE

With iso-butane, the hydrogen production increases continuously with temperature (Fig. 5). At a temperature of 300°C, appreciable quantities of methane are formed. No appreciable amounts of ethane or ethylene could be detected at any temperature. Complete product analysis (Table II) gave erratic results for the formation of C_3 hydrocarbons. From the results, it is clear that in some cases the C_3 was incompletely removed and in others appreciable amounts of butane were carried over. No thermal reaction could be detected even at 400°C.

The rate of methane formation at various temperatures is shown in Fig. 6, an activation energy of 18.5 kcal (Fig. 4) is obtained from the Arrhenius plot. Above 350°C the quantum yield of hydrogen rises sharply and has values above unity. A chain mechanism producing hydrogen atoms must occur. The activation

TABLE II. Complete analyses on several typical experiments with *n*-butane and iso-butane.

Normal butane Temp. °C	Time (min)	H_2	CH_4	C_3	C_4	[all quantities cc N.T.P.]
275°	60	0.182	0.136	0.082	0.104	C_3 83% double bond
300°	30	0.108	0.174	0.091	0.195	C_3 83% double bond
350°	7	0.034	0.200	0.109	0.204	C_3 77% double bond
375°	6	0.024	0.282	0.178	0.307	C_3 82% double bond
Iso-butane Temp. °C	**Time (min)**	H_2	CH_4	C_3	[all quantities cc N.T.P.]	
325°	80	0.278	0.119	0.079	C_3 46% double bond	
350°	70	0.279	0.167	0.088	C_3 50% double bond	
375°	40	0.259	0.161	0.63	C_3 21% double bond	
400°	20	0.259	0.147	0.167	C_3 61% double bond	

energy for this step has been calculated by subtracting the amount of hydrogen produced by the non-chain mechanism from the total hydrogen production (Fig. 7), by extrapolation of the low temperature results (Table I). This extra hydrogen production plotted logarithmically (Fig. 8) *vs* reciprocal temperature gives an apparent activation energy for the chain step of 40 kcal.

DISCUSSION

The low temperature results are consistent with the basic mechanisms postulated by Hay and Winkler[1] and Darwent and Winkler.[4]

$$\mathrm{Hg}(^1S_0)+h\nu=\mathrm{Hg}(^3P_1) \qquad 0$$
$$\mathrm{Hg}(^3P_1)+\mathrm{C_4H_{10}}=\mathrm{C_4H_9}+\mathrm{H}+\mathrm{Hg}(^1S_0) \qquad \Phi I_{abs}$$
$$\mathrm{H}+\mathrm{C_4H_{10}}=\mathrm{C_4H_9}+\mathrm{H_2} \qquad k_2$$
$$2\mathrm{C_4H_9}=\mathrm{C_8H_{18}} \qquad k_3$$

together with a quenching step which results in $(^3P_0)$ mercury atoms and no C—H bond split. This has been expressed as a factor Φ in the quenching step

FIG. 6. Iso-butane: Methane production at various temperatures.

which is temperature dependent. The reactions

$$\mathrm{H}+\mathrm{C_4H_9}=\mathrm{C_4H_{10}} \qquad k_4$$
$$2\mathrm{C_4H_9}=\mathrm{C_4H_8}+\mathrm{C_4H_{10}} \qquad k_5$$
$$\mathrm{H}+\mathrm{C_4H_8}=\mathrm{C_4H_9} \qquad k_6$$

which can conceivably occur but are unlikely by analogy with the experimental evidence on propane decomposition are not here considered. If they caused the low quantum yield rather than quenching inefficiency, the rate of hydrogen production would be again ΦI_{abs}, where Φ has a different significance being a ratio of rate constants.

At higher temperatures, radical decomposition products appear. By analogy with the previous work on propane and ethane we may expect the following reactions

$$\mathrm{C_4H_9}=\mathrm{C_2H_4}+\mathrm{C_2H_5} \qquad k_7$$
$$\mathrm{C_4H_9}=\mathrm{C_3H_6}+\mathrm{CH_3} \qquad k_8$$
$$\mathrm{C_4H_9}=\mathrm{C_4H_8}+\mathrm{H} \qquad k_9$$

followed by

$$\mathrm{C_2H_5}+\mathrm{C_4H_{10}}=\mathrm{C_2H_6}+\mathrm{C_4H_9} \qquad k_{10}$$
$$\mathrm{CH_3}+\mathrm{C_4H_{10}}=\mathrm{CH_4}+\mathrm{C_4H_9} \qquad k_{11}$$

The methyl radical produced will not decompose further since it is known to be thermally stable up to very high temperatures. The ethyl radical will not appreciably decompose until 425°C and so will also be thermally stable in these experiments.

The experiments described earlier confirm that these reactions occur, ethane and ethylene being formed in roughly equal quantities. Similarly, the rates of formation of methane and propylene are roughly equivalent. On the basis of the aforementioned mechanism, neglecting terms such as $\frac{1}{2}E_\Phi$ or $\frac{1}{2}E_3$ which will be small compared to the experimental error, $E_7=E_8=23$ kcal, for normal butane; and $E_8=18.5$ kcal, $E_9=40$ kcal for iso-butane.

The two possible branched chain radicals produced by the decomposition of iso-butane could not split to form C_2 fragments without an extensive rearrangement of the carbon skeleton. Thus reaction (7) would be impossible in this case. This is confirmed by the absence

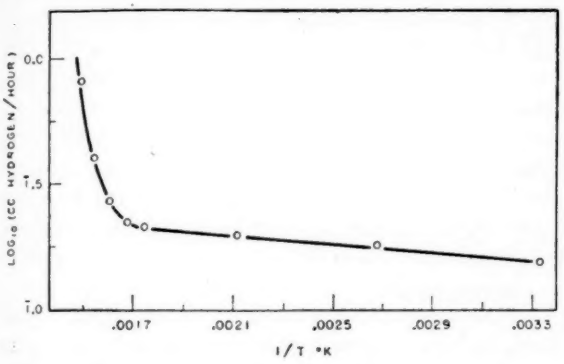

FIG. 7. Iso-butane: Activation energy plot for the total hydrogen production.

of ethane and ethylene in these experiments. There appears no obvious reason why the two straight chain radicals produced from normal butane should not decompose via reaction (9) but the products are not found experimentally. With normal butane reaction (8) is found to be approximately 3.3 times as fast as reaction (7). On the simplest possible basis one would expect a factor of two in the rates since there are two possible bonds to break for reaction (8) and only one for reaction (7). There must, therefore, be some other effect in the steric factor which increases this ratio still further.

No previous estimate appears in the literature for the activation energies of reactions (7), (8), (9). It is possible to estimate the heats of these reactions if the various carbon-hydrogen bond strengths in the butanes are known. Butler and Polanyi[7] estimate the primary

[7] E. T. Butler and M. Polanyi, Trans. Faraday Soc. **38**, 19 (1942).

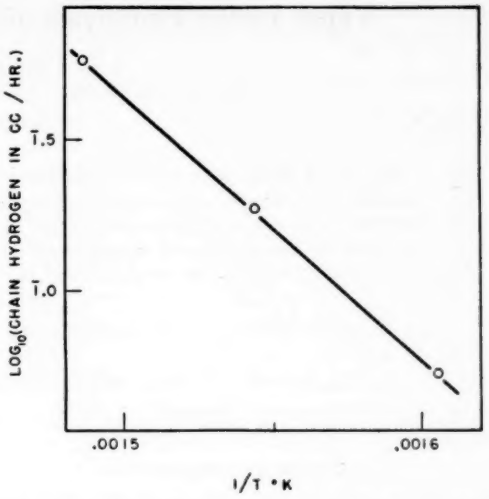

FIG. 8. Iso-butane: Activation energy plot for the chain step.

C—H bond strength in normal butane and the tertiary C—H bond strength in iso-butane. No estimate is available for the other two C—H bond types however, and in any case Butler and Polanyi's values must be considered inaccurate. It is certain that the various C—H bond strengths in the butanes cannot be greater than the value in ethane which is known with more certainty. Thus we can estimate minimum heats of reaction using heats of formation from tables.[8]

In this way $\Delta H_7=\Delta H_8\geqslant 21$ kcal (normal butane) and $\Delta H_9\geqslant 33$ kcal (iso-butane). The experimental activation energies are thus reasonable assuming approximately 2 kcal for the activation energy of the back reaction. The values suggest a mean C—H bond strength in normal butane very little lower than in ethane and in iso-butane a value some 5 kcal lower. This confirms the impression gained from the propane results[1] that the mean C—H bond strength in propane is only around 2 kcal lower than in ethane and suggests that all Butler and Polanyi's bond strengths with the exception of the ethane values are too low, particularly for the secondary and tertiary C—H bonds.

The experimental value of E_8 for iso-butane is much too low since the true value cannot be less than the corresponding value for normal butane. It may be that in this case side reactions have complicated the mechanism to some extent.

ACKNOWLEDGMENTS

The complete Ward-still analyses described in Table H and double bond analysis were carried out by Mr. R. Pilon to whom our thanks are due.

[8] Selected values of the properties of hydrocarbons. U. S. National Bureau of Standards, Washington, D. C.

THE JOURNAL OF CHEMICAL PHYSICS VOLUME 19, NUMBER 2 FEBRUARY, 1951

Vapor Phase Photolysis of Formaldehyde at Wavelength 3130A

J. G. CALVERT* AND E. W. R. STEACIE
Division of Chemistry, National Research Laboratories, Ottawa, Canada

(Received September 1, 1950)

The vapor phase photolysis of formaldehyde at wavelength 3130A has been investigated at high temperatures. The experimental results indicate that the rate of hydrogen formation is directly proportional to the first power of the intensity of absorbed light, and at constant intensity of absorbed light the rate is accelerated by the addition of formaldehyde or inert gas with about equal efficiency. Propylene and nitric oxide inhibit the rate. The mechanism of the photo-decomposition is suggested to be:

$$H_2CO+h\nu=HCO+H$$
$$H+H_2CO=H_2+HCO \quad E\leqq 5 \text{ kcal}$$
$$HCO=H+CO \quad E\geqq 13 \text{ kcal}$$
$$HCO+(\text{Wall})=\text{Products}+(\text{Wall}).$$

INTRODUCTION

TWO primary processes have been suggested in explanation of formaldehyde photolysis:

$$H_2CO+h\nu\rightarrow HCO+H \quad (I)$$
$$\searrow$$
$$CO+H_2. \quad (II)$$

Early investigators concluded that (II) was the only important primary process at wavelengths of absorbed light greater than 2750A.[1] However more recent investigations indicate that process (I) occurs to some extent even at the longer wavelengths. Akeroyd and Norrish[2] using radiation from a full mercury arc found that the rate of formaldehyde photo-decomposition was strongly temperature dependent. Gorin[3] found that large quantities of hydrogen iodide were formed in photolyses of formaldehyde-iodine mixtures at wavelength 3130A. In view of these results there can be little doubt that primary process (I) occurs in the formaldehyde photolysis. However, the experimental results of the previous investigations are incomplete, and definite conclusions as to the mechanism of the chain photo-decomposition are impossible. The present study of the formaldehyde photolysis was made to correlate the previous results, to aid in establishing the nature of the secondary reactions which follow primary process (I), and to test the possibility of the use of formaldehyde photolysis as a source of hydrogen atoms for the study of abstraction reactions of the type

$$H+RH\rightarrow H_2+R.$$

EXPERIMENTAL PROCEDURE

(a) *Photolysis System*

The vapor pressure of formaldehyde monomer in equilibrium with polymer is about 370 mm at 100°C;[4] thus to retain formaldehyde monomer up to 370 mm pressure without rapid polymerization all surfaces in contact with the vapor must be kept at a temperature of 100°C or above. This was accomplished in the present work by preventing contact between the formaldehyde vapor and surfaces which could not be heated (stopcocks, mercury valves, etc.). The parts of the photolysis system which were in contact with formaldehyde vapor were the photolysis cell, glass circulating pump, trap, quartz spiral manometer, two metal valves, and connecting tubing. These parts were suspended in a large air thermostat which was maintained at the temperature 100±1°C by a system of heaters, Fenwal regulator, and circulating fan.

The photolysis cell was made from fused quartz tubing, 15.0 cm in length and 3 cm diameter with plane parallel quartz windows fused on the ends. The volume of the cell was 104 cm. The cell was placed in a cylindrical electrically heated furnace about 6 cm inside diameter.

In series with the photolysis cell were a glass circulating pump (magnetically operated) and a trap. Connected to this system was a quartz spiral manometer.

The formaldehyde storage bulb and the main vacuum system were connected to the photolysis system through metal valves (Hoke bellows valves, type 434). The valves were contained in the thermostat, and the valve handles extended through the wall of the thermostat housing.

(b) *Optical System*

A Hanovia type A burner operated with 3.0 amp current from a 200-v dc supply was used as the radiation source in all of the experiments. The radiation from the lamp passed through a series of filters for isolation of the 3130A line of the mercury arc spectrum.[5] A spectrogram of the radiation passing through the filter system indicated that there was no appreciable intensity of any wavelength other than 3130A. The intensity of the 3130A line of the arc decreased slowly with use; the intensity after about 400 hours operation had decreased

* National Research Council of Canada Postdoctorate Fellow; Present address: Chemistry Department, Ohio State University, Columbus 10, Ohio.

[1] (a) R. G. W. Norrish and F. W. Kirkbride, J. Chem. Soc. 1518 (1932). (b) F. Patat, Z. physik. Chem. **B25**, 208 (1934); T. Locker and F. Patat, **B27**, 431 (1934).

[2] E. I. Akeroyd and R. G. W. Norrish, J. Chem. Soc. 890 (1936).

[3] E. Gorin, J. Chem. Phys. **7**, 256 (1939).

[4] H. H. Nielson and E. S. Ebers, J. Chem. Phys. **5**, 824 (1937).

[5] R. Hunt and W. Davis, J. Am. Chem. Soc. **69**, 1415 (1947).

TABLE I. Production of methyl alcohol and carbon monoxide in the thermal decomposition of formaldehyde.

Temp. °C	Moles of product $\times 10^6$ CO	CH_3OH
295	1.9	3.8
295	8.2	10
295	8.4	8.1
255	13	13.7
255	2.0	2.1

to about 0.7 of the original value. For a given series of runs the intensity of the arc was substantially constant.

The light beam was well collimated by a series of lenses and stops which were so arranged that a homogeneous beam of radiation filled the cell volume almost completely.

Absolute intensity measurements were made by uranyl oxalate actinometry. Relative intensities of the light transmitted through the full and empty cell were determined throughout the work by means of a multiplier photo-tube (IP-21) and circuit.[6] These were attached behind the cell and outside the thermostat.

(c) *Preparation of Materials*

Liquid monomeric formaldehyde was prepared as described by Spence and Wild.[7] The liquid was stored at dry ice temperatures for periods of 30 days or more without serious polymerization; it was warmed slightly when a sample of formaldehyde gas was desired.

The hydrocarbons used in this work were commercial c.p. products. Nitric oxide was prepared by reduction of nitrite ion with iodine.[8]

(d) *Analysis of Products*

Mass spectrometric and chemical analyses indicated that the only noncondensable products from photolyses of formaldehyde are carbon monoxide and hydrogen. These products from most experiments were analyzed by combustion using the Blacet-Leighton gas analysis procedure. Noncondensable products from photolyses of formaldehyde mixtures with hydrocarbons or nitric oxide were analyzed by the mass spectrometer, since traces of hydrocarbons or nitric oxide in the noncondensable products prevent accurate analysis by the combustion method.

EXPERIMENTAL RESULTS

I. Thermal Decomposition of Formaldehyde

It was found that the products of long photochemical runs at temperatures above 150°C and low intensities of absorbed light consisted of carbon monoxide in great excess of the quantity of hydrogen produced. These results indicated the possibility of the occurrence of a thermal reaction producing carbon monoxide, and several dark runs were made to test this possibility. Carbon monoxide and methyl alcohol were found as the major products of the thermal decomposition in the temperature range 150 to 350°C. The methyl alcohol was identified by mass spectrometric analyses of the condensable fraction remaining after removal of excess formaldehyde by polymerization. Results of several analyses of products of the thermal reaction are presented in Table I. The thermal reaction was investigated in this work only as was necessary to correct rates of photo-chemical decomposition, and such corrections were always small except in a few runs at low intensities. Analysis of products from thermal decompositions at temperatures above 300°C indicated that small but increasing quantities of hydrogen were formed in addition to carbon monoxide as temperatures increased. However, there was no thermal correction to photo-chemical rates of hydrogen formation in the photolyses at temperatures below 300°C, and the largest thermal correction to this rate in photolyses at 397°C was only 10 percent.

TABLE II. Rate of hydrogen formation at various temperatures: (CH_2O), 0.0058_2M; intensity of absorbed light, about 7.6×10^{11} quanta/cc-sec.

Temp. °C	$d(H_2)/dt$, ml $\times10^6$/sec.	Approximate quantum yield of hydrogen
100.7	2.86	1.0
156.5	5.54	1.9
195.7	15.6	5.4
233.3	45.1	16
255.4	75.3	26
270.3	108.0	38
295.2	197.5	69

II. Photo-Decomposition of Formaldehyde Vapor

(a) *Effect of Temperature on Rate of Hydrogen Formation*

Table II summarizes the results from several photolyses at constant formaldehyde concentration and absorbed light intensity. Rates of hydrogen formation are reported in column (2) of Table II as volume of hydrogen in ml (STP) which was produced per second. These units are used for all rates reported in this paper. Concentrations are reported in moles/liter, *M*. (The concentration of 0.0058_2M is equivalent to a gas pressure at 136 mm at 100°C.)

(b) *Effect of Intensity of Absorbed Light on Rate of Hydrogen Formation*

Figure 1 illustrates the results of experiments at different light intensities and various fixed formaldehyde concentrations and temperatures. The light intensity was varied in these experiments by inserting in the light path neutral density filters or Pyrex plates.

[6] R. W. Engstrom, J. Opt. Soc. Am. **37**, 420 (1947).
[7] R. Spence and W. Wild, J. Chem. Soc. **1935**, 338 (1935).
[8] W. A. Noyes, J. Am. Chem. Soc. **53**, 515 (1931).

(c) *Effect of Formaldehyde and Carbon Dioxide Concentrations on Rate of Hydrogen Formation*

Table III summarizes the results obtained from photolyses at varied formaldehyde concentration and also the results of experiments with mixtures of formaldehyde and carbon dioxide at various concentrations and at several temperatures. The fraction of the incident light which was absorbed by the formaldehyde, Q_m, is given in column (d). Since the rate of hydrogen formation is directly proportional to the absorbed light intensity (see the preceding section), the measured rates of hydrogen formation, column (c), were multiplied by $7.6\times10^{11}/I_a$ in column (f) to eliminate the variations in rate due to changes in incident or absorbed light intensities. This procedure corrects the measured rates to a constant absorbed light intensity of 7.6×10^{11} quanta/cc-sec.

(d) *Effect of Various Foreign Gases on Rate of Hydrogen Formation*

Definite amounts of several hydrocarbon gases and carbon dioxide were mixed with a given pressure of formaldehyde. Gases were chosen which were condensable at liquid nitrogen temperature, so that hydrogen and carbon monoxide products could be separated easily. The data of Table IV summarize the effect of the presence of the various gases on the rate of hydrogen formation. The rates in part (b) of Table IV were corrected for thermal reaction; the correction was about six percent of the total rate of hydrogen formation.

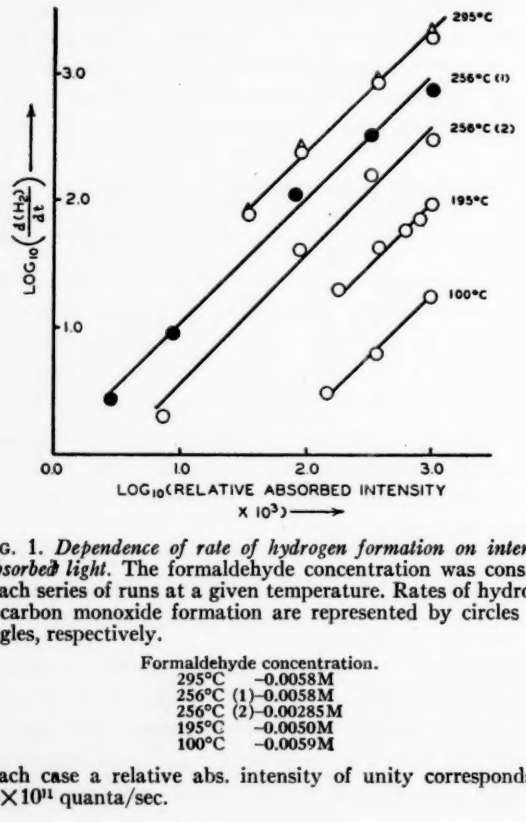

FIG. 1. *Dependence of rate of hydrogen formation on intensity of absorbed light.* The formaldehyde concentration was constant for each series of runs at a given temperature. Rates of hydrogen and carbon monoxide formation are represented by circles triangles, respectively.

Formaldehyde concentration.
295°C −0.0058M
256°C (1)−0.0058M
256°C (2)−0.00285M
195°C −0.0050M
100°C −0.0059M

In each case a relative abs. intensity of unity corresponds to *ca.* 6×10^{11} quanta/sec.

TABLE III. Effect of formaldehyde and carbon dioxide concentrations on rate of hydrogen formation. (Reaction volume 104 cc).

(a) $(CH_2O)\times10^3$, M.	(b) $(CO_2)\times10^3$, M.	(c) $d(H_2)/dt\times10^5$ ml/sec	(d) Q_m	(e) $I_a\times10^{-11}$ q/cc-sec	(f) (c)(7.6)/(e)
(a) Temp. 195°C					
13.35	—	2.35	0.77	8.28	2.16
10.36	—	1.89	0.67	7.26	1.98
5.86	—	1.08	0.48	5.15	1.59
5.06	—	0.93	0.43	4.66	1.51
2.61	—	0.413	0.25	2.74	1.15
5.85	0.80	1.10	0.48	5.15	1.62
5.85	1.97	1.21	0.48	5.15	1.79
5.85	2.96	1.23	0.48	5.15	1.82
5.85	3.52	1.27	0.48	5.15	1.88
5.85	4.28	1.33	0.48	5.15	1.96
5.85	5.86	1.44	0.48	5.15	2.13
(b) Temp. 255°C					
9.00	—	11.93	0.67	10.1	8.99
5.81	—	7.54	0.53	8.00	7.15
2.88	—	3.02	0.31	4.70	4.88
1.36	—	1.08	0.16	2.41	3.41
6.05	0.83	4.93	0.54	5.01	7.46
6.05	2.25	5.66	0.54	5.01	8.58
6.05	3.38	5.86	0.54	5.01	8.89
6.05	4.74	6.74	0.54	5.01	10.2
(c) Temp. 295°C					
11.42	—	28.0	0.79	8.15	26.1
5.65	—	13.26	0.54	5.56	18.1
2.85	—	4.81	0.32	3.32	11.0
1.46	—	1.41	0.18	1.85	5.79
2.87	0.85	6.01	0.32	3.69	12.4
2.87	1.81	6.91	0.32	3.69	14.2
2.87	2.92	8.44	0.32	3.69	17.4
2.87	4.55	10.5	0.32	3.69	21.6
2.87	6.16	11.1	0.32	3.69	22.8
(d) Temp. 347°C (Rate corrected for thermal reaction)					
7.65	—	60.9	0.67	7.69	60.1
5.76	—	41.5	0.57	6.54	48.2
4.36	—	25.9	0.47	5.45	36.1
3.86	—	22.6	0.43	4.93	34.9
2.06	—	6.9	0.26	2.98	17.6
1.20	—	2.1	0.16	1.81	8.8
3.86	2.63	33.7	0.43	4.93	51.9
(e) Temp. 397°C (Rate corrected for thermal reaction)					
9.56	—	203	0.78	8.66	178
7.74	—	161	0.71	7.90	155
5.95	—	106	0.61	6.85	118
4.19	—	66.1	0.49	5.42	93
3.17	—	39.7	0.40	4.45	68.0
2.39	—	25.7	0.32	3.58	54.5
1.82	—	13.2	0.25	2.82	35.5

(e) *Inhibition of Formaldehyde Photolysis by Propylene and Nitric Oxide*

The effects of added propylene and nitric oxide on the rate of hydrogen formation are summarized in Tables V and VI, respectively.

DISCUSSION

I. Thermal Decomposition

The data suggest the occurrence of a mode of thermal decomposition represented by the over-all reaction (1).

$$2CH_2O\rightarrow CO+CH_3OH. \quad (1)$$

The authors believe that this reaction has not been reported previously.†

The rates were erratic and the temperature coefficient was low (about 14 kcal). This suggests that the thermal reaction is heterogeneous.

II. Photo-Decomposition of Formaldehyde

The following mechanism for the high temperature formaldehyde photolysis is consistent with the results obtained in this work:

$$CH_2O+h\nu=H+HCO \quad (2)$$

$$H+H_2CO=H_2+HCO \quad (3)$$

$$HCO=H+CO \quad (4)$$

$$HCO+(Wall)=Products+(Wall). \quad (5)$$

The importance at low temperatures of intramolecular hydrogen and carbon monoxide formation, primary process (II) of the Introduction, cannot be determined from the present work. At high temperatures it is unimportant.

Reaction (5) probably involves the reaction of the formyl radical with an adsorbed hydrogen atom, reforming formaldehyde, or reaction with an adsorbed formyl radical to give either formaldehyde and carbon monoxide or glyoxal. The occurrence of reaction (5) necessitates the diffusion of formyl radicals to the walls of the cell, and an inverse dependence of the rate of reaction (5) on the concentration of formaldehyde or other gas present, (M), is expected. However, the lifetime of a large fraction of the formyl radicals may be long and the mean path travelled by them great compared to their distance from the cell wall; in such a case there would be little dependence of the rate of (5) on (M). If the lifetime of the formyl radicals is short so that the mean path traveled by them is small compared to their distance from the cell wall, then the rate of (5) is expected to be inversely proportional to (M). Thus the rate of reaction (5) may be represented as inversely proportional to $(M)^n$, where $0 \leqq n \leqq 1$, to include the possibility of very long and very short-lived formyl radicals. The assumption of this mechanism for formaldehyde photolysis leads to the rate expression (6).

$$\frac{d(H_2)}{dt}=\frac{d(CO)}{dt}=I_a\cdot\phi_I\left[1+\frac{2k_4(M)^n}{k_5(Wall)}\right], \quad (6)$$

where $0 \leqq n \leqq 1$. Discussion of the evidence which sup-

TABLE IV. Effect of various foreign gases on rate of hydrogen formation.

Run no.	Foreign gas	$d(H_2)/dt$ ml×10⁶/sec
(a) Temp. 257°C; (CH_2O), 0.00589M; foreign gas conc., 0.00461M; I_a, 7.6×10¹¹ quanta/cc-sec		
1	(none)	73.4
2	CO_2	104
3	C_3H_8	118
4	iso-C_4H_{10}	119
5	n-C_4H_{10}	113
6	n-C_5H_{12}	116
7	C_6H_6	61.1
8	C_3H_6	0.4
9	(none)	75.3
(b) Temp. 351°C; (CH_2O) and foreign gas conc., 0.00386M; I_a, 6.3×10¹¹ quanta/cc-sec		
1	(none)	344
2	CO_2	608
3	iso-C_4H_{10}	592
4	n-C_4H_{10}	660
5	$(CH_3)_4C$	670
6	(none)	350

TABLE V. Inhibition of formaldehyde photolysis by propylene: (CH_2O), 0.00580M; I_a about 3.9×10¹¹ quanta/cc-sec.

Run no.	$(C_3H_6)\times10^4$, M	$d(H_2)/dt\times10^6$ ml/sec
(a) Temp. 101°C		
1	—	1.8
2	4.6	0.88
3	60	0.54
4	199	0.46
(b) Temp. 172°C		
5	—	4.30
6	4.4	1.81
7	8.7	1.34
(c) Temp. 250°C		
8	—	35.0
9	2.2	21.4
10	18.8	6.3
11	57.2	2.1
12	76.9	0.5
(d) Temp. 300°C		
13	—	108
14	2.8	62.9
15	11.9	22.9
16	40.1	7.4
17	—	96.0

TABLE VI. Inhibition of formaldehyde photolysis by nitric oxide: (CH_2O), 0.00580M; I_a, about 4.2×10¹¹ quanta/cc-sec.

Run no.	$(NO)\times10^5$, M	$d(H_2)/dt\times10^6$, ml/sec
(a) Temp. 198°C		
1	—	8.96
2	9.5	4.82
3	19.0	3.20
4	28.5	1.23
5	37.7	1.26
6	48.9	1.16
7	—	8.45
(b) Temp. 250°C		
8	—	37.1
9	4.9	0.84
10	9.1	1.7
11	19.0	0.94
12	29.7	2.6
13	—	35.0

† A private communication to the authors from Mr. J. E. Longfield states that Mr. Longfield and Dr. W. D. Walters of Rochester University have obtained other evidence of this mode of thermal decomposition during recent investigations of radical sensitized thermal decompositions of formaldehyde.

ports the proposed mechanism is given in the following sections.

(a) *Effect of Intensity of Absorbed Light on Rate of Hydrogen Formation*

The data are represented graphically in Fig. 1. The photo-chemical rates of carbon monoxide production are represented in Fig. 1 by triangles. These data show that carbon monoxide and hydrogen are formed in equal amounts photochemically within experimental error.

The slopes of the best straight lines through the experimental points in Fig. 1, as determined by the method of least squares, are 0.98 (carbon monoxide rates) and 0.95 (hydrogen rates) at 295°C, 0.98 and 1.04 at 256°C and (CH_2O), 0.00580M-(1) and 0.00285M-(2) respectively, 0.88 at 195°C, and 0.93 at 100°C. Within the experimental error the rate of hydrogen formation (and photo-chemical carbon monoxide) at each temperature studied is directly proportional to the first power of the intensity of absorbed light. This evidence indicates that wall termination of chains is important in the formaldehyde photolysis [a reaction such as (5)] and argues strongly against formaldehyde photolysis mechanisms which involve gas phase chain termination steps.[2,3]

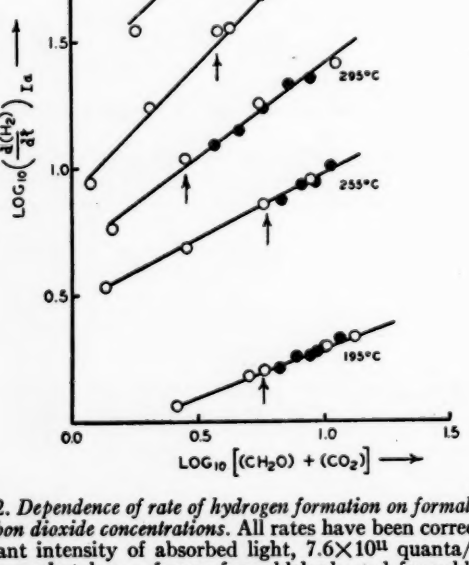

FIG. 2. *Dependence of rate of hydrogen formation on formaldehyde and carbon dioxide concentrations.* All rates have been corrected to a constant intensity of absorbed light, 7.6×10^{11} quanta/cc-sec. Data from photolyses of pure formaldehyde and formaldehyde-carbon dioxide mixtures are represented by open and closed circles, respectively. In experiments with added carbon dioxide the formaldehyde concentration was fixed at the values indicated by arrows.

(b) *Effect of Formaldehyde and Carbon Dioxide Concentration on Rate of Hydrogen Formation*

The data in Table III are represented graphically in Fig. 2. The open circles represent data from photolyses of pure formaldehyde; the closed circles represent data from photolyses of formaldehyde and carbon dioxide mixtures. In experiments with added carbon dioxide the formaldehyde concentration was fixed at the values indicated by the small arrows, and increasing amounts of carbon dioxide were added. The logarithm of the sum of the concentrations of formaldehyde and carbon dioxide are plotted in these experiments. The data of Fig. 2 indicate a remarkable similarity between the effect of formaldehyde concentration and carbon dioxide concentration on rate of hydrogen formation when the intensity of absorbed light is held constant. It appears that the role of formaldehyde concentration in the rate expression, aside from the absorption of light, may be played by an inert gas, and reaction (3) cannot be the rate determining step in the formaldehyde photolysis. It may be suggested that the increase in concentration of formaldehyde or inert gas slows reaction (5), the diffusion of radicals to the wall (where chain termination must occur as indicated in the above section), and increases the chain length.

The slope of the best lines through the data for pure formaldehyde photolysis given in Fig. 2 are 0.38 at 195°C, 0.52 at 255°C, 0.73 at 295°C, 1.03 at 347°C, and 0.94 at 397°C. The slope of the best lines through the data for carbon dioxide-formaldehyde mixtures in Fig. 2 are 0.41 at 195°C, 0.59 at 255°C, and 0.76 at 295°C. These slopes represent the power, n, to which formaldehyde (or carbon dioxide) concentration, (M), appears in the rate expression at each temperature. The results are in agreement with the rate expression (6). At low temperatures the effect of formaldehyde or other gas concentration on the rate is small, $n\rightarrow0$, indicating very long-lived formyl radicals and possibly a significant contribution to the rate of hydrogen formation from the temperature independent term of relation (6). At intermediate temperatures, where only the temperature dependent term of (6) is important, the effect of gas concentration on the rate is more pronounced, $0.5\leqq n\leqq1$, reflecting the decrease in the average lifetime of the formyl radicals with increasing temperature. At elevated temperatures, 350°C and above, the rate of hydrogen formation is directly proportional to the gas concentration, $n=1$, indicating that the distance to the cell wall must be large for most formyl radicals compared to the average distance the radicals can diffuse during their lifetime at these temperatures.

Carbon dioxide is not unique in its effect of increasing the rate of photolysis of formaldehyde. The increase in the rate of the formaldehyde photolysis on addition of an inert gas was first observed by Style and Sum-

mers.[9] They stated that added hydrogen and nitrogen increased the rate of formaldehyde photolysis at temperatures above 100°C, but no account of the evidence has been published. The data of Table IV summarize the effect of added hydrocarbon gases on the rate of hydrogen formation in the formaldehyde photolysis. The acceleration in rate produced by the saturated hydrocarbons is very similar and in general is slightly greater than that produced by carbon dioxide. It is difficult to explain the acceleration in rate without resort to a mechanism involving the retardation of reaction (5) and the resultant increase in reactions (4) and (3).

The present results appear to contradict the findings of Akeroyd and Norrish[2] who reported that the rate of formaldehyde photolysis at high temperatures was proportional to $I_a^{\frac{1}{2}}$ (CH_2O). These authors photolyzed formaldehyde with the full ultraviolet spectrum of a mercury arc at several pressures and temperatures in a reaction cell 25 cm in length. It was assumed that the radiation was completely absorbed at all pressures used, and therefore the experiments were at constant intensity of absorbed light. However, the fraction of light absorbed at wavelength 3130A, near the maximum of absorption of formaldehyde, in a path length of 25 cm is 0.96 at 400 mm, 0.79 at 200 mm, and 0.54 at 100 mm (pressures used by Akeroyd and Norrish referred to temperature 100°C). Since the light source was not monochromatic and the fractions of light absorbed are large in most cases, the reported rates cannot be corrected with justification to a constant absorbed intensity. However, if one assumes that the light of wavelength 3130A represents the main part of the absorbed radiation and utilizes to correct these data the direct proportionality between absorbed intensity and rate, then it is found that the results of Akeroyd and Norrish are not inconsistent with the present findings; the data corrected in this manner indicate the power to which formaldehyde appears in the rate expression increases from 0.15 at 100°C to 0.78 at 350°C.

(c) *Effect of Temperature on Rate*

A logarithmic plot of the rate data of Table II *vs.* $1/T$ is given in Fig. 3. The curvature of the plot at low temperatures seems to indicate the importance of the temperature independent term of relation (6) in photolyses at low temperatures. The slope of the straight line portion of the curve corresponds to an activation energy of 13.4 kcal/mole. This value is in reasonable agreement with the values 16.4 and 12 kcal/mole reported by Akeroyd and Norrish[2] and Style and Summers[8] respectively from studies of the formaldehyde photolysis using the full mercury arc.

In terms of the proposed mechanism for the formaldehyde photolysis this apparent activation energy is equal to E_4-E_5. E_5 is presumably a chain terminating reaction involving recombination or disproportionation of radicals on the wall, and it is probable that E_5 is small; on the basis of this assumption the 13.4 kcal may be taken as an estimate of E_4. Gorin has estimated from results of the photolysis of acetaldehyde-iodine mixtures that $E_4 \geqq 26$ kcal/mole.[10] A critical assumption necessary to the method of calculation used by Gorin is that there is no reaction between formyl radicals and iodine at temperatures up to 130°C. The results of more recent and detailed studies of the acetaldehyde-iodine photolysis by Blacet, Heldman,[11] and Loeffler[12] indicate that all formyl radicals produced in the acetaldehyde photolysis at temperatures of 60°C and above react with iodine. Thus one cannot rule out the present interpretation of the mechanism of formaldehyde photolysis on the basis of the divergence of the present estimate of E_4 and that made by Gorin. The present results are in agreement with a recent estimate of $E_4 \geqq 14$ kcal/mole from results of the butyraldehyde photolysis.[13]

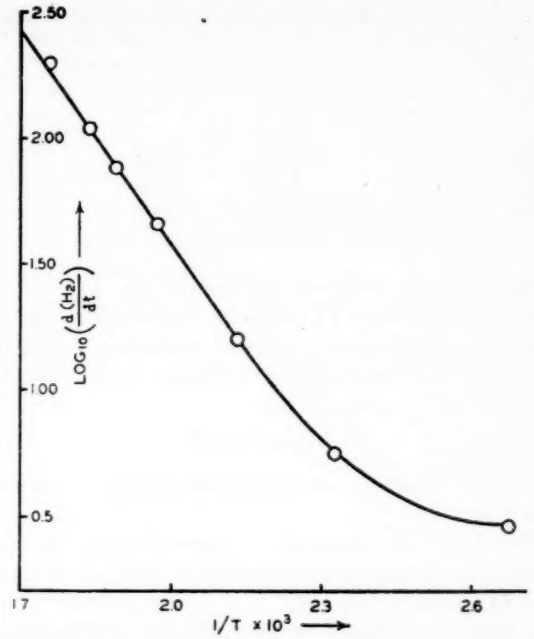

FIG. 3. *Dependence of rate of hydrogen formation on temperature.* Formaldehyde concentration was 0.00582M; the intensity of absorbed light was constant at about 7.6×10^{11} quanta/cc-sec. The slope of the straight line portion of the plot corresponds to an apparent activation energy of 13.4 kcal/mole.

(d) *Inhibition of Formaldehyde Photolysis by Propylene*

In the suggested reaction mechanism for the formaldehyde photolysis, reaction (3) represents the only fate of hydrogen atoms and all of the evidence points to its rapid occurrence. It was desirable to obtain some

[8] D. W. G. Style and Summers, Trans. Faraday Soc. **35**, 899 (1939).

[10] E. Gorin, Acta Physicochim. U.R.S.S. **9**, 681 (1938).

[11] F. E. Blacet and J. D. Heldman, J. Am. Chem. Soc. **64**, 889 (1942).

[12] F. E. Blacet and D. E. Loeffler, J. Am. Chem. Soc. **64**, 893 (1942).

[13] F. E. Blacet and J. G. Calvert, J. Am. Chem. Soc. (to be published).

TABLE VII. Experimental results from a preliminary investigation of the photolysis of formaldehyde-propane-d_8 mixtures.

Temp. °C	(CH_2O) $\times 10^3$M	(C_3D_8) $\times 10^3$M	$\frac{d(HD)}{dt}/\frac{d(H_2)}{dt}$	k_8/k_3
203	3.48	6.65	0.038	0.020
219	4.86	4.84	0.021	0.021
263	3.15	5.89	0.056	0.030
300	2.83	5.55	0.088	0.045

estimate of the order of magnitude E_1. The data of runs 7 and 8 of Table IV indicate an inhibition of photolysis with benzene and a marked inhibition with added propylene. The experimental evidence in the literature indicates that reaction (7) is

$$H+C_3H_6=C_3H_7 \qquad (7)$$

very rapid[14] and has an activation energy of not more than 5 kcal.

Photolyses of mixtures of formaldehyde and propylene were made in an attempt to study the relative rates of reactions (3) and (7) at several temperatures. The results of these experiments are summarized in Table V. If we assume that the reaction of hydrogen atoms alone accounts for the observed inhibition of formaldehyde with added propylene, then it is possible to estimate from the data of Table V the relative rates of reactions (3) and (7) at various temperatures. The assumption is made that reactions (3) and (7) are of equal velocity and $(C_3H_6)/(CH_2O)=k_3/k_7$ at the conditions of concentration which result in one-half total inhibition at a given temperature. This treatment of the data indicates that within the experimental error k_3/k_7 is independent of the temperature; hence $E_3=E_7$, and therefore $E_3\leqq 5$ kcal/mole. This estimate is in agreement with the results of Geib,[15] who from studies of reaction (3) by the discharge-tube method concluded that $E_3\leqq 5$ kcal/mole.

(e) *Formaldehyde Photolysis as a Source of Hydrogen Atoms for the Study of Hydrogen Abstraction Reactions*

The results which have been presented indicate clearly that hydrogen atoms are produced in formaldehyde photolysis. However, all of the evidence points to the rapid occurrence of reaction (3), and it cannot be determined from the results whether abstraction reactions of the type

$$H+RH\rightarrow H_2+R$$

(where RH represents a hydrocarbon molecule) are sufficiently fast to compete measurably with reaction (3) at reasonable pressures and temperatures. Several mixtures of formaldehyde and propane-d_8‡ were photolyzed, and the hydrogen and deuterium hydride in the products were determined by mass spectrometric analysis to estimate the relative importance of hydrogen abstraction from formaldehyde and propane. The results of these experiments are summarized in Table VII. The only important reaction leading to hydrogen formation in these experiments is reaction (3), and it is reasonable to assume that deuterium hydride is formed only by reaction (8).

$$H+C_3D_8\rightarrow HD+C_3D_7. \qquad (8)$$

On the basis of this mechanism for hydrogen and deuterium hydride formation the results lead to the estimates of k_8/k_3 which are given in Table VII. The temperature dependence of k_8/k_3 indicates that E_8-E_3 is about 4.5 kcal/mole. These preliminary experiments demonstrate that formaldehyde photolysis may be used as a convenient source of hydrogen atoms for the study of hydrogen abstraction reactions. Further work is in progress on the photolysis of mixtures of formaldehyde with deuterated hydrocarbons (and formaldehyde-d_2 with ordinary hydrocarbons) from which information concerning hydrogen abstraction reactions may be obtained.

ACKNOWLEDGMENT

The authors wish to thank Drs. F. P. Lossing and A. W. Tickner for the mass spectrometric analyses, Dr. D. M. Miller for the preparation and purification of the nitric oxide, and Dr. L. C. Leitch for the preparation of the propane-d_8 used in this work.

[14] (a) W. J. Moore and H. S. Taylor, J. Chem. Phys. **8**, 504 (1940). (b) H. W. Melville and J. C. Robb, Proc. Roy. Soc. (London) **A196**, 445 (1949).

[15] K. H. Geib, Ergeb. exakt. Naturwiss. **15**, 44 (1936).

‡ Propane-d_8 was prepared by the reduction of propine-d_4 with deuterium on a nickel catalyst. The propine-d_4 had been prepared by the reaction of deuterium oxide on magnesium carbide. Mass spectrometric analysis indicated that the deuterated propane was about 70 percent C_3D_8 and 28 percent C_3D_7H.

The Mercury Photo-Sensitized Decomposition of Methyl Chloride

C. R. MASSON* AND E. W. R. STEACIE
Chemistry Division, National Research Council, Ottawa, Canada
(Received October 19, 1950)

A study has been made of the mercury photo-sensitized decomposition of methyl chloride over a pressure range of 10 mm to 640 mm, a temperature range of 72°C to 328°C, and a threefold variation in light intensity. The stoichiochemical equation for the reaction at 250°C and 160-mm pressure is $3CH_3Cl=HCl+0.97CH_4+0.49C_2H_4Cl_2+0.41Hg_2Cl_2+0.24C_2H_4+0.18CH_2=CHCl+0.15C+0.07C_2H_6+0.02H_2+0.01C_2H_2$. At high pressures, the following mechanism is shown to be consistent with the experimental results:

$$\begin{aligned} Hg(6^3P_1)+CH_3Cl &= Hg(6^1S_0)+CH_3+Cl \\ CH_3+CH_3Cl &= CH_4+CH_2Cl \\ Cl+CH_3Cl &= HCl+CH_2Cl \\ CH_2Cl+CH_2Cl &= C_2H_4Cl_2 \\ Hg+CH_2Cl &= HgCl+CH_2 \\ HgCl+HgCl &= Hg_2Cl_2 \\ CH_2+CH_2 &= C_2H_4 \end{aligned}$$

The first of these reactions is shown to have a quantum efficiency of unity. From the effect of added CO_2 on the reaction, an approximate value of $\sigma^2=5.7\times10^{-16}$ cm² has been calculated for the quenching cross section of methyl chloride.

INTRODUCTION

FEW studies have been made of the photolysis of the alkyl chlorides, probably because of the transparency of these substances down to about λ2400A. Investigation by mercury photo-sensitization therefore seems worthwhile, and the present paper describes an investigation of the mercury photo-sensitized decomposition of the first member of the series, methyl chloride.

The photolyses of methyl bromide and methyl iodide have been studied, the latter fairly extensively.[1] The first attempt to elucidate completely the nature of the products was made by West and Schlessinger,[2] who studied the decomposition of methyl iodide vapor at 300 mm and 25°C, using λ2537A radiation. The products were chiefly methane, with small amounts of ethane and ethylene; about a third of the iodide decomposed appeared as CH_2I_2. The quantum yield becomes appreciable in the presence of silver foil; but in its absence it is very low,[3–5] and it is uncertain whether this is due to the reaction of methyl radicals with iodine atoms or with iodine molecules or both. The reaction $CH_3+I_2=CH_3I+I$ has been shown by Andersen and Kistiakowsky[5] to have a very low activation energy. Schultz and Taylor,[6] in some recent work, have concluded that "hot" methyl radicals are formed in the primary reaction.

Similarly, in the case of methyl bromide[7] the main products are methane and bromine, and very low quantum yields are observed. It is of interest to compare these results with the results of the present investigation.

EXPERIMENTAL

The apparatus used was of the conventional type. The reaction cell was cylindrical in form and was constructed of fused quartz with plane quartz windows 2 mm thick at each end. The cell was 120 mm long and had an internal diameter of 35 mm. A mercury reservoir was attached to the cell by a tube entering near the rear window. The cell was connected to the rest of the apparatus by a similar tube attached near the front window. This arrangement was chosen to insure that the entire cell would be filled with mercury vapor during a run.

The cell was enclosed in a cylindrical, electrically heated furnace constructed in two sections for ease of removal, and fitted with plane quartz windows 3 mm thick at each end. Current for the furnace was taken through a Variac transformer from a 1 kva Sorensen constant voltage regulator. The temperature, as indicated by a copper-constantan thermocouple placed near the rear window of the cell, was controlled manually to ±1°C during a run. The temperature of the mercury reservoir was controlled independently of that of the furnace by means of a separate winding.

A U-shaped mercury-rare gas resonance lamp with oxide coated electrodes served as source of λ2537A radiation. The lamp was fed from a 6000-v neon sign transformer with a Variac in the primary circuit.

---

* National Research Council of Canada Postdoctorate Fellow, 1948–50. Present address: Department of Chemistry, University of Rochester, College of Arts and Science, Rochester 3, New York.

[1] For a review of the literature up to 1945, see E. W. R. Steacie, *Atomic and Free Radical Reactions* (Reinhold Publishing Corporation, New York, 1946), pp. 237, 454.

[2] W. West and L. Schlessinger, J. Am. Chem. Soc. **60**, 961 (1938).

[3] J. R. Bates and R. Spence, J. Am. Chem. Soc. **53**, 1689 (1931); Trans. Faraday Soc. **27**, 468 (1931).

[4] G. Emschwiller, Ann. chim. **17**, 413 (1932).

[5] H. G. Andersen and G. B. Kistiakowsky, J. Chem. Phys. **11**, 6 (1943).

[6] R. D. Schultz and H. A. Taylor, J. Chem. Phys. **18**, 194 (1950).

[7] A. Gordon and H. A. Taylor, J. Am. Chem. Soc. **63**, 3435 (1941).

The current through the lamp was controlled manually at 70±1 mA during a run. A polished aluminum reflector was placed behind the lamp to increase the available intensity. An approximately parallel light beam was produced by means of a single lens and stop. A convenient check on the light intensity was provided by allowing a small fraction of the light emergent from the cell to fall on a photo-multiplier tube placed a short distance from the rear end of the furnace.

The reaction system, consisting of cell, mercury reservoir, and a small U-trap, was isolated from the rest of the apparatus by two mercury cutoffs. One of these, which was used also for measuring the pressure of gas in the system, led to a further series of cutoffs, traps, and bulbs for purification and storage of gases. The other cutoff, which was fitted with ground-glass float valves, led to the analysis system.

The first part of the analysis system, consisted of a liquid-air trap, a modified Ward still,[8] and a small McLeod gauge, all in series. This part could be isolated from the rest by means of a further cutoff with float valves. The volume between the two cutoffs (including the volume of the McLeod gauge) was 177 cc. The remainder of the analysis system consisted of a mercury diffusion pump in series with a combined Toepler pump and gas burette. By means of stopcocks, the mercury diffusion pump could be by-passed so that the Toepler pump alone could be used for withdrawing products if desired.

The methyl chloride used in this work was obtained in cylinders from the Ohio Chemical and Manufacturing Company. After degassing and several bulb-to-bulb distillations, mass spectrometer analysis revealed the presence of several percent vinyl chloride as impurity. By continuous pumping from a bulb surrounded by a pentane mush at −130°C the amount of this impurity could be reduced to about 0.4 percent. Methyl chloride thus purified was stored in a 2-liter bulb behind a mercury cutoff, and final purification of relatively small quantities was effected before each run by means of the Ward still. Mass spectrometer analysis showed that, on fractional distillation, with the foot of the Ward column held at −127°C, all the vinyl chloride distilled over along with the first ten percent of the methyl chloride fraction. Experiments showed that the presence of 0.4 percent vinyl chloride had no effect on the rate of production of the main products at 150-mm pressure and 250°C. Since vinyl chloride itself is an important product of the reaction, however, its exact determination becomes rather uncertain unless it is completely removed at the start.

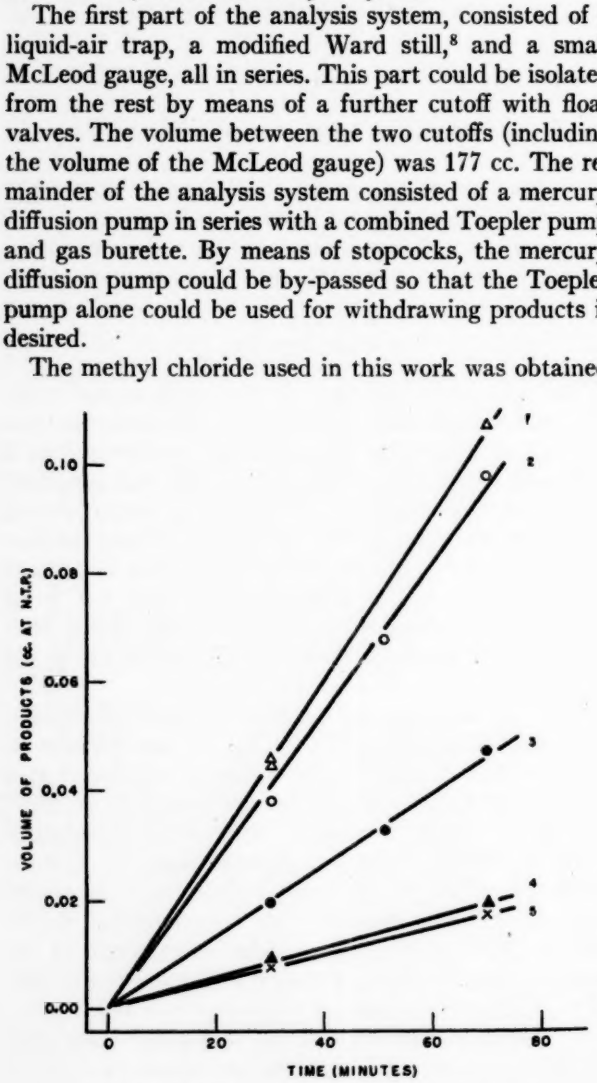

FIG. 1. Effect of duration of run on major products: (1) HCl, (2) CH_4, (3) $C_2H_4Cl_2$, (4) C_2H_4, (5) $CH_2=CHCl$.

Preliminary experiments showed the main products of the reaction to be methane, hydrogen chloride, 1,2-dichloroethane, ethylene, and vinyl chloride, along with small quantities of hydrogen, ethane, acetylene, and methylene chloride. Methane and hydrogen were pumped off using liquid nitrogen as refrigerant. Hydrogen was removed by oxidation over copper oxide at 280°C, and the remaining gas was shown by combustion to be 100 percent methane. The presence of small amounts of hydrogen in the noncondensables was further checked by mass spectrometer analysis.

After removal of the noncondensables, all other products, along with unchanged methyl chloride, were frozen into the first trap of the analysis system; and the mixture of gases was then separated into convenient fractions by Ward still analysis. Hydrogen chloride was removed along with the C_2 hydrocarbons. This fraction was analyzed for C_2 hydrocarbons on the mass spectrometer. It was not possible to measure the hydrogen chloride directly, since the peak heights for this compound vary according to the total time the sample remains in the mass spectrometer system. The hydrogen chloride in these samples was therefore obtained by difference.

Vinyl chloride was pumped off along with the first part of the unchanged methyl chloride, the percentage of vinyl chloride being subsequently determined on the mass spectrometer. The unchanged methyl chloride was removed by continuous pumping, the temperature at the foot of the Ward still being kept constant at −108°C. The heavier fraction was then taken off. The mass spectrum of this fraction showed it to consist mainly of 1,2-dichloroethane with occasional small quantities of methylene chloride. Accurate analysis was not possible, probably owing to the extreme readiness with which these products dissolve in the stopcock grease of the mass spectrometer system. Infrared an-

[8] E. C. Ward, Ind. Eng. Chem. Anal. Ed. **10**, 169 (1938). D. J. Le Roy, Can. J. Research **B28**, 492 (1950).

TABLE I. Effect of time and mercury vapor concentration on products of reaction (temperature of reaction cell = 250°C).

Run	Press. (mm)	Time (min)	(Hg) (°C)	Products (cu mm at N.T.P.) CH_4	H_2	C_2 hydrocarbons +HCl	C_2H_2	C_2H_4	C_2H_6	HCl	vinyl chloride	$C_2H_4Cl_2$
105	161	30	190	38.0	0.3	58.38	1.5_3	8.5_1	3.3_4	45.0	7.5_6	19.6
98	158	51	190	67.7	1.2	88.0	...	...	...	...	...	32.6
106	159	70	190	98.0	2.1	126.7	0.96	18.46	5.3_8	107.2	17.1	47.3
107	157	51	129	70.2	1.6	73.4	trace	6.5_5	1.6_2	65.2	...	38.6
110	160	60	25	14.0	0.0_5	...	...	...	...	...	...	...
79	295		190	0.00	0.00	0.00					...	1.3

alysis also showed this fraction to consist exclusively of these two compounds, with dichloroethane as the predominant constituent. This analysis was performed on the collected heavy products from twelve runs done at 10-mm pressure and 110°C.

In addition to the above gaseous products, two solid products were found. One of these was a white deposit which accumulated on the window of the reaction cell at low temperatures, cutting down the light intensity during a run. In runs at low pressures, this deposit could be conveniently sublimed out of the reaction cell at 110°C; in runs at higher pressure (>100 mm) it was necessary to maintain the temperature of the cell at about 250°C in order to keep the window clear. For this reason, most of the runs were done at the latter temperature. The white deposit was found to be insoluble in hot water and in hot mineral acids, and has been assumed to be mercurous chloride.

The second solid product was a dark deposit which also formed on the window of the cell. This deposit, although very slight and not readily observed, cut down the light intensity considerably if allowed to accumulate and had therefore to be removed after each run. This was done by admitting oxygen at a few mm pressure into the cell and flaming the window to almost a dull red heat. The product of oxidation was separated from excess oxygen by means of the Ward still, and had a vapor pressure corresponding to that of carbon dioxide. No other oxidation products could be detected, and it is concluded that this deposit consists of carbon.

On account of the observation that small amounts of oxygen have a marked effect on the nature of the products, it was necessary to ensure that the last traces of oxygen were completely removed from the system before each run. After oxygen had been present in the system, therefore, the cell, mercury reservoir, and connecting tubing were thoroughly flamed. The cell was then kept at 250°C overnight and pumped out continuously. Finally, the reaction system was flushed out with methyl chloride and pumped down to 10^{-5} mm, before the next run was commenced. Unless such precautions were taken, reproducible results could not be obtained.

RESULTS

The effect of mercury vapor concentration and of the duration of a run on the volume of the products are shown in Table I. The figures in the fourth column denote the temperature of the mercury reservoir. In run 110, where the mercury reservoir was at room temperature, the system was allowed to equilibrate overnight before the run was commenced. In all other experiments, a period of about one hour was allowed for equilibration of mercury vapor before starting the run. Run 79 was a blank experiment in which the system was allowed to stand for 90 minutes without irradiation in order to check the possibility of a thermal reaction. In Fig. 1, the volume of the main products is plotted against time of irradiation for runs 105, 98, and 106.

TABLE II. Effect of pressure of methyl chloride on rate of formation of products (temperature of cell = 250°C; temperature of Hg reservoir = 190°C).

Run	Press. (mm)	Time (min)	Rate (cu mm/hour) CH_4	H_2	C_2 hydrocarbons +HCl	C_2H_2	C_2H_4	C_2H_6	HCl	$CH_2=CHCl$	heavy products	CO_2 from deposit	Remarks
92	8.5	46	87.2	4.2	115.1	1.3	16.1	2.1_5	95.6	39.3	10.4	...	
83	9.7	60	90.2	3.1	134.0	1.6	17.5	0.7	114.2	35.0	11.5	12	
91	26.0	60	92.9	1.9	129.0	0.6_5	19.2	2.6	106.6	...	20.0	...	CH_2Cl_2 found
93	55.7	60	89.4	0.4	119.5	0.2_3	19.9	4.3	95.1	...	30.0	...	CH_2Cl_2 absent
94	88.9	40.6	85.5	0.4	115.9	0.0	29.5	6.6	79.8	...	33.4	...	CH_2Cl_2 absent
87	137	45	78.8	1.3	104.7	0.0	27.1	2.6	75.0	19.4	35.6	...	CH_2Cl_2 absent
A*	159		79.9	1.3	109.5	1.9	16.4	5.6	90.7	14.9	39.4	16	
86	272	50	79.3	0.0	98.8	0.0	22.2	6.2	70.4	...	45.6	11	
88	354	60	79.7	1.3	99.7	0.0	16.7	5.1	77.9	...	49.5	...	CH_2Cl_2 absent
84	442	60	77.5	0.5	98.5	0.0	12.4	7.9	78.2	...	44.0	11	CH_2Cl_2 absent
90	600	45	80.1	2.1	89.7	0.0	8.0	3.1	78.6	...	53.2	...	CH_2Cl_2 absent
85	640	43	71.9	2.1	82.0	0.0	18.8	9.1	54.1	...	53.0	...	CH_2Cl_2 absent

* A mean of runs 98, 105, and 106.

TABLE III. Effect of added oxygen on reaction (temperature of cell = 250°C; temperature of mercury reservoir = 190°C).

Run	Press. CH_3Cl (mm)	Press. O_2 (mm)	Time (min)	Rate (cu mm/hr) CH_4	H_2	HCl	C_2H_2	C_2H_4	C_2H_6	Heavy products	Remarks CH_2Cl_2	H_2O	CO_2
81	10.5	*10^{-4}	60	80.6	4.4	55.3	2.9	18.3	1.4	39.6	found	found	found
75	150	*10^{-4}	90	80.7	1.4	44.3	0.0	21.1	2.7	62.8	nil	found	nil
78	328	*10^{-4}	60	89.6	1.8	41.9	0.0	19.9	5.2	106.0	nil	found	found
76	512	*10^{-4}	51	77.8	2.9	47.4	0.0	21.9	4.6	150.5	nil	found	found
82	624	*10^{-4}	45.7	72.5	2.0	21.1	0.1	15.4	9.6	91.8	nil	found	found
89	48.5	1.5	87	19.3	2.9	0.0	0.0	6.1	3.2	92.5	nil	found	9.7

* Cell pumped to 10^{-4} mm at room temperature after admitting oxygen. Not flamed.

It is evident that the rates of production of the main products are independent of the duration of the run.

Table II illustrates the effect of the pressure of methyl chloride on the rates of production of the products. The heavy products from most of these runs were analyzed qualitatively for methylene chloride with the mass spectrometer. The results of these analyses, given in the last column of the table, show that methylene chloride is a product of the reaction only at low pressures (<55.7 mm). Further evidence that this fraction consists only of dichloroethane at higher pressures was obtained by using a small McLeod gauge on the analysis system as a rough dew point apparatus. The heavy products from a run at 159 mm were compressed into the closed capillary of the gauge, and the dew point obtained graphically. These measurements gave a value of 85.5 mm for the vapor pressure of this fraction at 26°C, as compared with the value of 82.5 mm for $C_2H_4Cl_2$, obtained from the data of Pearce and Peters.[9] In the analysis of C_2 hydrocarbons from runs 105 and 106 (included in run A), the sensitivity of the mass spectrometer was roughly three times higher than in the other analyses. This may account for the detection of a trace of acetylene in these runs; this product was not otherwise observed except in runs at low pressures.

The results in Table III illustrate the effect of small quantities of oxygen on the reaction. With the exception of run 89, the oxygen present in these experiments arose from a failure to remove all traces of this gas after oxidizing the carbon deposit. Small amounts of carbon dioxide were generally detected in the C_2 fraction of these runs, while significant quantities of water were obtained in the heavy products. The carbon dioxide formed in run 89 was quantitatively pumped off along with the C_2 hydrocarbons and measured accurately; the HCl spectrum was completely absent in this analysis. Relatively little dichloroethane was observed in the heavy products from run 89. Most of this fraction consisted of water, and an unidentified, non-chlorine-containing compound, probably methylal, with large peaks at mass 76 and 44. No carbon deposit was formed in this run, while the deposit of mercurous chloride appeared to be relatively large. In Fig. 2, the rate of methane production, in the presence and absence of oxygen, is plotted against the pressure of methyl chloride, while Fig. 3 shows the corresponding plot for hydrogen chloride. The inhibiting effect of traces of oxygen on the rate of formation of HCl is marked; it is also evident that similar traces of oxygen have no effect on the rate of production of methane. The presence of 3 percent oxygen in the system completely suppresses the formation of hydrogen chloride and considerably lowers the yield of methane.

The effect of pressure on the rate of formation of the heavy products is illustrated in Fig. 4.

Figure 5 shows the effect of variations in light intensity on the major products. The production of all products is proportional to the intensity.

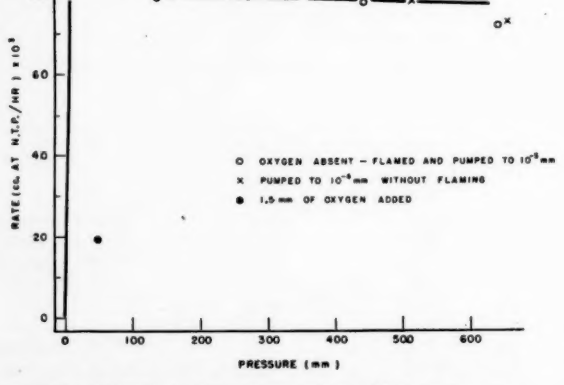
RATE (cc AT N.T.P./HR) x 10³
PRESSURE (mm)
O OXYGEN ABSENT – FLAMED AND PUMPED TO 10⁻⁴ mm
× PUMPED TO 10⁻⁴ mm WITHOUT FLAMING
● 1.5 mm OF OXYGEN ADDED

FIG. 2. Effect of pressure and of added oxygen on rate of CH_4 production.

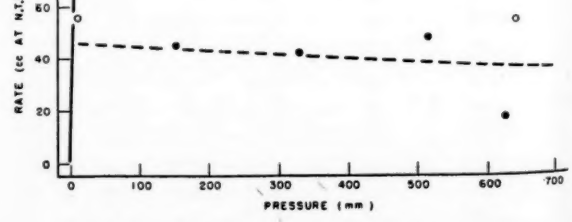

FIG. 3. Effect of pressure and of added oxygen on rate of HCl production.

[9] J. N. Pearce and P. E. Peters, J. Phys. Chem. 33, 873 (1929).

TABLE IV. Effect of temperature.

Run	Temp. °C	Press. (mm)	Hg °C	Time (min)	Rate (cu mm/hr) CH_4	H_2	C_2H_4	C_2H_6	HCl	$CH_2=CHCl$	$C_2H_4Cl_2$
103	328	160	190	36	87.8	1.2	17.8	3.2	115.8	26.8	37.8
A	250	159	190	...	79.9	1.3	16.4	5.6	90.7	14.9	39.4
104	190	159	190	50	73.6	0.0	...	...	...	18.0	36.4
108	131	158	130	40	64.3	0.4	0.5	9.7	71.9	9.5	36.9
101	72	159	72	19.75	45.3	0.9	21.4	11.5	55.1	4.72	32.5

In Table IV are presented the results of a series of runs at different temperatures. The temperature coefficients are all small. Arrhenius plots give reasonably good straight lines in all cases, from which the following activation energies are obtained:

$$E_{CH_4}=0.8 \text{ kcal.}$$
$$E_{HCl}=1.1 \text{ kcal.}$$
$$E_{CH_2=CHCl}=2.4 \text{ kcal.}$$
$$E_{C_2H_4Cl_2}=0.2 \text{ kcal.}$$

The effect of added carbon dioxide on the reaction is shown in Table V. These runs were done with a slightly different optical set-up, so that the yields are not comparable with other runs. The yields of HCl and heavy products are not given here, since the experiments were performed before the necessity for excluding traces of oxygen was realized. The fact that oxygen was present in the system was shown by the detection of water in the heavy products. The amount of oxygen present, however, was very small, so that the yields of methane are not appreciably affected. These results will be discussed later.

Quantum Yields

The quantum yield of the reaction was determined using monochloracetic acid as actinometer. With the reaction cell at 250°C, the mercury reservoir at 190°C, and a methyl chloride pressure of 158.5 mm, the following quantum yields were obtained:

$$\phi CH_4=1.00;\ \phi HCl=1.03;\ \phi C_2H_4Cl_2=0.51;$$
$$\phi C_2H_4=0.25;\ \phi CH_2=CHCl=0.19;$$
$$\phi C_2H_6=0.07_2;\ \phi H_2=0.025;\ \phi C_2H_2=0.00_7.$$

From this the over-all quantum yield of methyl chloride disappearance under these conditions is 3.09. These values will be uncertain to about 15 percent, since no allowance has been made for the small amount of radiation not consisting of λ2537A emitted by the lamp.

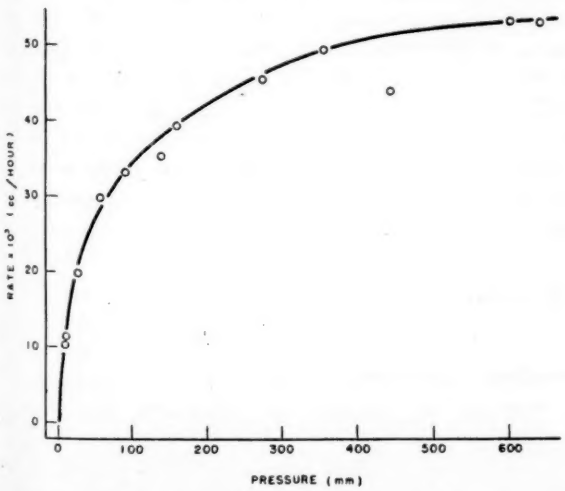

FIG. 4. Effect of pressure on rate of production of heavy products.

DISCUSSION

From the aforementioned results, the stoichiochemical equation for the reaction at 160-mm pressure and 250°C may be written

$$3CH_3Cl=0.97CH_4+HCl+0.49C_2H_4Cl_2$$
$$+0.41Hg_2Cl_2+0.24C_2H_4+0.18CH_2=CHCl$$
$$+0.15C+0.07C_2H_6+0.02H_2+0.01C_2H_2.$$

The amount of mercurous chloride formed has been estimated from the chlorine deficiency in the gaseous products. That mercury vapor is used up in the reaction is shown by the observation (Table I) that the yield of methane is greatly decreased when the temperature of the mercury reservoir is lowered from 190°C to 25°C, other conditions remaining the same.

No ethyl chloride could be detected in the products,

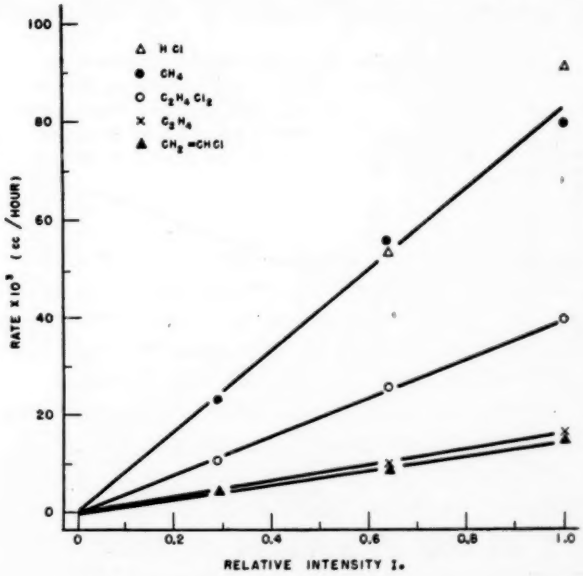

FIG. 5. Effect of light intensity on products.

TABLE V. Effect of added CO_2 (temperature of cell = 110°C; temperature of Hg reservoir = 100°C).

Run	Press. CH_3Cl (mm)	Press. CO_2 (mm)	Time (min)	Rate (cu mm/hr) CH_4	H_2	C_2H_2	C_2H_4	C_3H_6
60	10.0	0	180	83.8	2.5	0.0	11.7	trace
64	9.5	1.15	180	75.2	2.5	1.9	8.6	trace
62	11.0	10.5	240	60.7	1.7	5.7	6.2	trace
61	10.5	51.0	120	33.0	1.0	present	present	trace

although its presence was sought for repeatedly in the methyl chloride fraction. This is of interest, since Lee and LeRoy[10] have reported its formation in the reaction of excited mercury atoms with hydrogen-methyl chloride mixtures.

One of the main features of the reaction is the equivalence of the methane and hydrogen chloride yields at pressures above 100 mm, as shown in Figs. 2 and 3. This suggests that these products are formed by related mechanisms. The most significant feature of the reaction is the strong inhibition of hydrogen chloride formation by oxygen under conditions which leave the yield of methane unaffected. These two observations give important information concerning the primary process. If, as has been generally found in mercury photo-sensitized reactions, the primary process involves the rupture of a C−H bond, methane and hydrogen chloride could be formed in equivalent amounts by the following sequence of reactions:

$$Hg(6^3P_1)+CH_3Cl=Hg(6^1S_0)+H+CH_2Cl \quad (A)$$

$$H+CH_3Cl=HCl+CH_3 \quad (B)$$

$$CH_3+CH_3Cl=CH_4+CH_2Cl. \quad (2)$$

This scheme, however, predicts that the yield of methane would be lowered correspondingly with the yield of hydrogen chloride on addition of oxygen. The fact that this does not occur suggests strongly that the primary step is the breaking of the C−Cl bond.

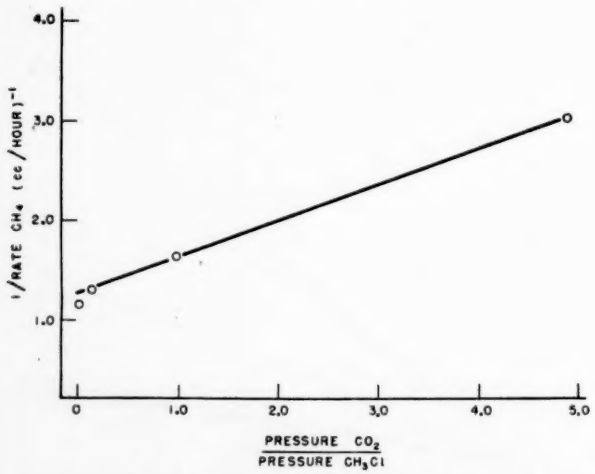

FIG. 6. Plot of $1/R_{CH_4}$ against $[CO_2]/[CH_3Cl]$.

[10] G. L. Lee and D. J. LeRoy, Can. J. Research **B28**, 500 (1950).

CH_4 and HCl would then arise by the following reactions:

$$Hg(6^3P_1)+CH_3Cl=Hg(6^1S_0)+CH_3+Cl \quad (1)$$

$$CH_3+CH_3Cl=CH_4+CH_2Cl \quad (2)$$

$$Cl+CH_3Cl=HCl+CH_2Cl, \quad (3)$$

which explains the effect of oxygen, since chlorine-atom reactions are notoriously sensitive to it, and the equivalence in yield of the two main products.

Since $\phi_{CH_4}\approx\phi_{HCl}\approx 1$, reaction (1) must have a quantum efficiency of unity. It is of interest to compare these results with the low quantum yields found in the photolyses of methyl bromide and iodide, where the primary split is also rupture of the carbon halogen bond. In these cases, the reactions corresponding to reaction (3), *viz.*,

$$Br+CH_3Br=CH_2Br+HBr \quad (3a)$$

and

$$I+CH_3I=CH_2I+HI \quad (3b)$$

are endothermic, while reaction (3) is exothermic.[11] The activation energies of reactions (3a) and (3b) will therefore be considerably higher than the activation energy of reaction (3), so that the combination of bromine or iodine atoms either with themselves or with methyl radicals will become much more important, thus lowering the quantum yields.

Dichloroethane undoubtedly arises by reaction (4):

$$CH_2Cl+CH_2Cl=C_2H_4Cl_2. \quad (4)$$

In the absence of other competing reactions for the chloromethyl radical, the quantum yield of dichloroethane formation would be expected to be unity. Actually $\phi_{C_2H_4Cl_2}$ is very low at low pressures and approaches asympototically a value of about 0.67 as the pressure is increased. This observation, along with the formation of mercurous chloride, may be partly explained by the reaction

$$Hg+CH_2Cl=HgCl+CH_2 \quad (5)$$

followed by

$$HgCl+HgCl=Hg_2Cl_2. \quad (6)$$

Ethylene would then be formed by

$$CH_2+CH_2=C_2H_4. \quad (7)$$

The fact, however, that vinyl chloride is formed at low pressures at the expense of dichloroethane as shown in

[11] See reference 1, p. 244.

Table II indicates that further reactions of the chloromethyl radical take place. The abstraction of a hydrogen atom from the chloromethyl radical by either a methyl radical or a chlorine atom, and subsequent combination of the CHCl radical with methylene is a possible source of vinyl chloride at low pressures. Such reactions would not alter the quantum yields of methane and hydrogen chloride. Vinyl chloride may also be formed at low pressures by reactions subsequent on quenching by ethylene. Further experiments would be required to test the verity of these suggestions, but it seems fairly certain that reactions (1) to (7) describe the main course of the decomposition at high pressures.

According to the above mechanism, $\phi_{C_2H_4Cl_2}+\phi_{C_2H_4}$ should be unity at high pressures. Owing to a fairly wide scatter in the experimental results for ethylene, it is not possible to estimate the quantum yield of this product exactly at high pressures. Taking, however, a mean value of approximately 0.25 for this quantity, we find a value of 0.92 for the sum of the above quantum yields at 600-mm pressure. Further support for the above mechanism comes from the low experimental activation energies found for methane and hydrogen chloride. The temperature coefficients for the rates of production of these two products should be zero by the above mechanism, and actually are very low.

The results in Table V, showing the effect of added carbon dioxide on the reaction, also lend support to the above mechanism. The decrease in yield of methane on adding carbon dioxide may be expected to be due to the quenching reaction

$$Hg(6^3P_1)+CO_2=Hg(6^1S_0)+CO_2 \qquad (8)$$

in competition with reaction (1). From reactions (1), (2), and (8) by the usual stationary state treatment we obtain

$$\frac{1}{R_{CH_4}}=\frac{1}{I_a}+\frac{k_8}{k_1 I_a}\frac{(CO_2)}{(CH_3Cl)}, \qquad (1)$$

where R_{CH_4} represents the rate of methane production, k_1 and k_8 are the velocity constants for reactions (1) and (8), and the terms in parentheses denote concentrations. A linear relationship should therefore obtain between $1/R_{CH_4}$ and $(CO_2)/(CH_3Cl)$. This plot is shown in Fig. 6. From the slope of the line and the value of the intercept at $(CO_2)/(CH_3Cl)=0$, we obtain a value of 1/2.19 for the ratio k_8/k_1.

Using this result, we may obtain an approximate value for the quenching cross section of methyl chloride. This works out to be 5.7×10^{-16} cm^2, which seems a reasonable value.

Acknowledgment.—We are indebted to Dr. F. P. Lossing and Miss Frances Gauthier for the mass spectrometer analyses and to Dr. R. N. Jones for the infrared spectra.

THE JOURNAL OF CHEMICAL PHYSICS VOLUME 19, NUMBER 2 FEBRUARY, 1951

The Infrared and Raman Spectra of Condensed Nitric Oxide*

A. Lee Smith, William E. Keller, and Herrick L. Johnston
Cryogenic Laboratory and Department of Chemistry, The Ohio State University, Columbus, Ohio

(Received October 2, 1950)

The infrared and Raman spectra of liquid and solid nitric oxide have been studied in an attempt to prove the existence of the $(NO)_2$ molecule. The liquid has four strong Raman lines at 1861, 262, 196, and 167 cm^{-1}; two weaker Raman lines at 1760 and 487 cm^{-1}; and two strong infrared bands at 1863 and 1770 cm^{-1}. Several weaker infrared bands can be satisfactorily assigned as combinations by using the observed strong infrared and Raman frequencies. The spectra were found to be due exclusively to a dimer which probably exists as a bent ONNO molecule.

INTRODUCTION

NITRIC oxide is unique among stable diatomic molecules in that it possesses an odd electron. This electron indicates that a moderately stable dimer might form. According to Pauling,[1] however, a three-electron bond stabilizes the NO molecule to such an extent that the heat of dimerization becomes negative. Data on the magnetic susceptibility of the gas[2] to 112.8°K show excellent agreement with theory, indicating that dimerization of the gas is negligible at temperatures below the boiling point (121.36°K). This conclusion is substantiated by the findings of Johnston and Weimer,[3] who showed from data of state that association at the boiling point is less than 0.5 percent.

It is fairly well established, however, that nitric oxide molecules in the liquid state are polymerized. This is inferred from the unusually high and strongly temperature-dependent heat capacity of the liquid as well as

* This work was supported in part by the ONR under contract with the Ohio State University Research Foundation.

[1] Pauling, *Nature of the Chemical Bond* (Cornell University Press, Ithaca, N. Y., 1945), p. 266.

[2] Wiersma, De Haas, and Capel, Leid. Comm. 212*b*.

[3] Johnston and Weimer, J. Am. Chem. Soc. **56**, 625 (1934).

from its high entropy of vaporization,[4] from its magnetic rotatory power,[5] and from its magnetic susceptibility.[6] The degree of association, calculated from this magnetic data, is found to be of the order of 95 percent. Polymerization is further evidenced by data of state on compressed gases[7,8] and by the appearance of an anomalous frequency (260 cm^{-1}) in the Raman spectrum of the liquid.[9]

The absorption spectrum of liquid nitric oxide has been studied in the visible and ultraviolet regions of the spectrum by Vodar[10] and by Bernstein and Herzberg,[11] who found strong continuous absorption from 4000A to shorter wavelengths and from 5600A to longer wavelengths, with maximum transmission near 4600A. The spectrum was not temperature dependent. It was suggested that the continuous absorption is due to the molecule $(NO)_2$.

Rice,[12] on the basis of a thermodynamic treatment, concludes that the liquid is almost completely associated, and calculates the heat of dissociation to be 3910 and 2870 cal per M of $(NO)_2$ in the liquid and gas, respectively. This result agrees quite well with a heat of dissociation of 4000 cal calculated from other sources.[8] It is interesting to note that Johnston and Giauque,[4] in their paper on the heat capacity of solid and liquid nitric oxide, report a discrepancy of $\frac{1}{2}R\ln 2$ between the observed and calculated entropy. They suggest that this difference could be accounted for if the solid were a mixture of two polymerized isomers in equal amount.

In the present investigation, we have observed the infrared and Raman spectra of the liquid and solid in an attempt to find direct evidence for the dimer and to deduce its structure.

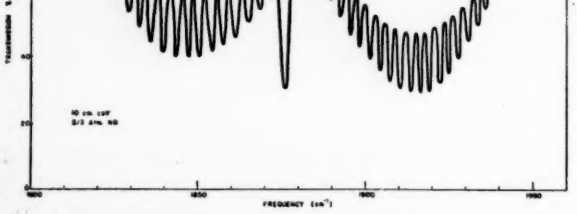

FIG. 1. Infrared spectrum of NO gas.

[4] Johnston and Giauque, J. Am. Chem. Soc. **51**, 3194 (1929).
[5] Bizette and Tsai, Compt. rend. **204**, 1638 (1937).
[6] Bizette and Tsai, Compt. rend. **206**, 1288 (1936).
[7] Duclaux, J. Phys. Radium [vii] **8**, 277 (1937).
[8] Eucken and d'Or, Nachr. Gesell. Wiss. Göttingen, Mathphysik. Kl. (1932), p. 107.
[9] Vodar, Jardillier, and Mayence, Compt. rend. **222**, 1343 (1946).
[10] Vodar, Compt. rend. **204**, 1467 (1937).
[11] Bernstein and Herzberg, J. Chem. Phys. **15**, 77 (1947).
[12] Rice, J. Chem. Phys. **4**, 367 (1936).

EXPERIMENTAL

Nitric oxide was prepared according to the method of Johnston and Giauque, and our product should contain less than 0.001 M percent impurity. Infrared spectra were obtained with a model 12-B Perkin-Elmer spectrometer, using a variable thickness low temperature transmission cell.[13] Sample thicknesses ranged from 0.05 to 1.5 mm. The entire region from 400 to 6000 cm^{-1} was investigated, using LiF, NaCl, and KBr prisms. Careful corrections were made for water vapor absorption.

Raman spectra were obtained with a Lane-Wells spectrograph and power supply, using a special low temperature cryostat[14] in which the sample could be maintained at any temperature between 20° and 300°K. The Hg 4358 line was used for excitation, since liquid nitric oxide is transparent in the region 4000 to 5600A. The method of polarized incident light was employed for depolarization measurements.

RESULTS

Gaseous nitric oxide was found to give the now well-known infrared vibration-rotation spectrum consisting of P, Q, and R branches, with the rotational lines nicely resolved and the band center at 1876 cm^{-1} (Fig. 1) in agreement with the data of Nielsen and Gordy.[15] Spectra of the liquid and solid in this region are shown in Fig. 2. It is seen that a considerable change takes place in the spectrum upon passing to the liquid, with the 1876-cm^{-1} band being replaced by two intense bands at 1770 and 1863 cm^{-1}. Several weaker bands can also be seen. The solid shows even more complication, and while the 1862-cm^{-1} absorption has sharpened, the 1770-cm^{-1} band has apparently split and some new bands have appeared. The first vibrational overtones, shown in Fig. 3, consist of a very broad general absorption with three sharp bands at the center, in both the liquid and the solid.

A microphotometer tracing of the Raman spectrum

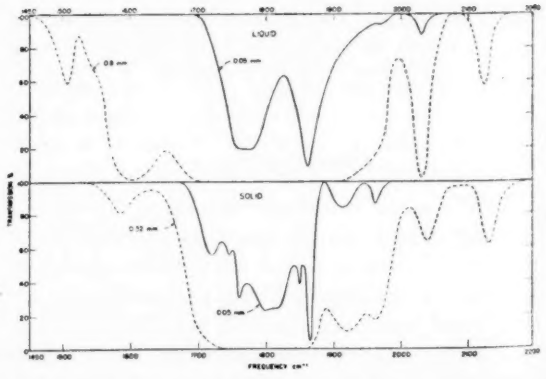

FIG. 2. Infrared absorption spectra of liquid and solid nitric oxide.

[13] Holden, Taylor, and Johnston, J. Opt. Soc. Am. **40**, 757 (1950).
[14] Taylor, Smith, and Johnston, J. Opt. Soc. Am. (to be published).
[15] Nielsen and Gordy, Phys. Rev. **56**, 781 (1939).

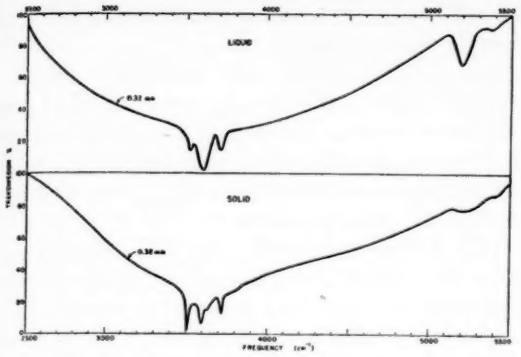

FIG. 3. Vibrational overtones in liquid and solid nitric oxide.

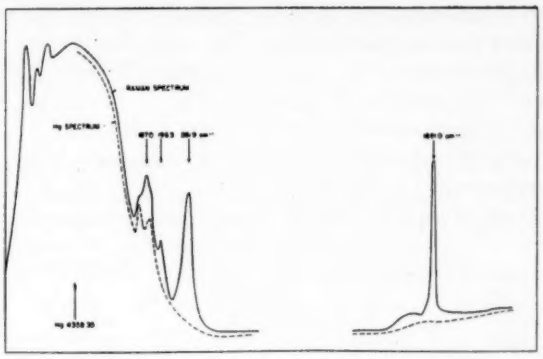

FIG. 4. Microphotometer tracing of the Raman spectrum of of liquid nitric oxide.

of the liquid is shown in Fig. 4. Four lines can be seen definitely, the most intense at 1861 cm^{-1}, and three somewhat weaker lines at low frequencies. With a 64-hr exposure, very weak lines seem to be present at about 486 and 1760 cm^{-1}. The solid showed no trace of a Raman spectrum even with exposures sufficiently long to record the four most intense lines of the liquid.

Table I shows a summary of the observed frequencies. The strong bands at 1770 and 1863 cm^{-1} can be assigned immediately as fundamentals, and the bands around 3600 cm^{-1} are evidently overtones or combinations of the two strong fundamentals. It is important to note that the entire infrared spectrum of the liquid can be accounted for in terms of the two strong infrared frequencies and the frequencies observed in the Raman spectrum.

DISCUSSION AND INTERPRETATION

Although various explanations could be considered for the observed spectra of the condensed nitric oxide, only two are logically possible. First, more than one species of the molecule is present; the extraneous material could be a monomer, a polymer with two or more configurations, another oxide of nitrogen, or some other impurity. Second, the polymer could contain two, three, four, or more NO molecules. The spectra, however, are believed to be exclusively those of the dimer since the frequencies do not coincide with those of any logical foreign molecules nor with that of the gas. Furthermore, the preparation and purification procedures are known to be effective. The low value of the magnetic susceptibility of the liquid precludes the existence of a monomer or trimer, and it would be unusual if a tetramer were to have only five observable fundamental frequencies. We cannot eliminate the possibility of the dimer existing with two configurations, but if this is the case, it seems unlikely that the structures would be radically different. There is no marked temperature dependence of the band intensities in the liquid (or in the solid above 40°K), indicating that the liquid does not dissociate appreciably even near its boiling point.

In order to show the effect of temperature and of concentration on the degree of dimerization, infrared spectra of solutions of nitric oxide in liquid nitrogen and in liquid krypton were studied. Krypton was chosen because its liquid range (116-121°K) coincides in part with that of nitric oxide. The pure rare gas was obtained

TABLE 1. Frequencies in cm^{-1} of infrared bands and Raman lines in condensed nitric oxide.

Band No.	Liquid I.R.	Liquid Raman	Solid I.R.	Assignment
1	~5390* V.W.		~5390* V.W.	$2F_1+F_2$
2	~5200* V.W.		~5200* V.W.	$2F_2+F_1$ and/or $3F_2$
3	3708 M.		3712 M.	$2F_1$
4	3600 S.		3596 M.	F_1+F_2
5	3515 M.		3507 M.	$2F_2$
6	2124 W.		2130 W.	F_1+F_3
7	2032 M.		2038 W.	F_1+F_5 and/or F_2+F_3
8	1965 M.		1962 M.	F_2+F_4
9			1918 M.	F_2+F_5
10	1863 V.S.	1861 S. (P)	1865 V.S.	F_1
11			1850 W.	
12			1822 S.	
13	(1783)		1795 S.	
14	1770 V.S.	1760 V.W.(?)	1760 S.	F_2
15			1745 V.W.(?)	
16			1715 M.	
17	1600 M.		1586 V.W.	F_1-F_3 and/or F_2-F_5
18	1545 V.W.(?)			
19	1506 W.			F_2-F_3
20			519 V.W.	$2F_3$
21		487 V.W.(?)	486 V.W.	
22		262 S. (P)		F_3
23		196 W.		F_4
24		167 M.		F_5

* Calibration uncertain to about ±30 cm^{-1}.

from the Matheson Company (Joliet, Illinois) and used without further purification. The mole fraction of NO in krypton was 0.017, and in nitrogen it was slightly larger. The results are shown in Fig. 5. It can be seen that at a temperature of 117°K, the diluted nitric oxide is partially dissociated into the monomer which is vibrating with a frequency of 1872 cm^{-1}. At the temperature of liquid nitrogen, almost complete association

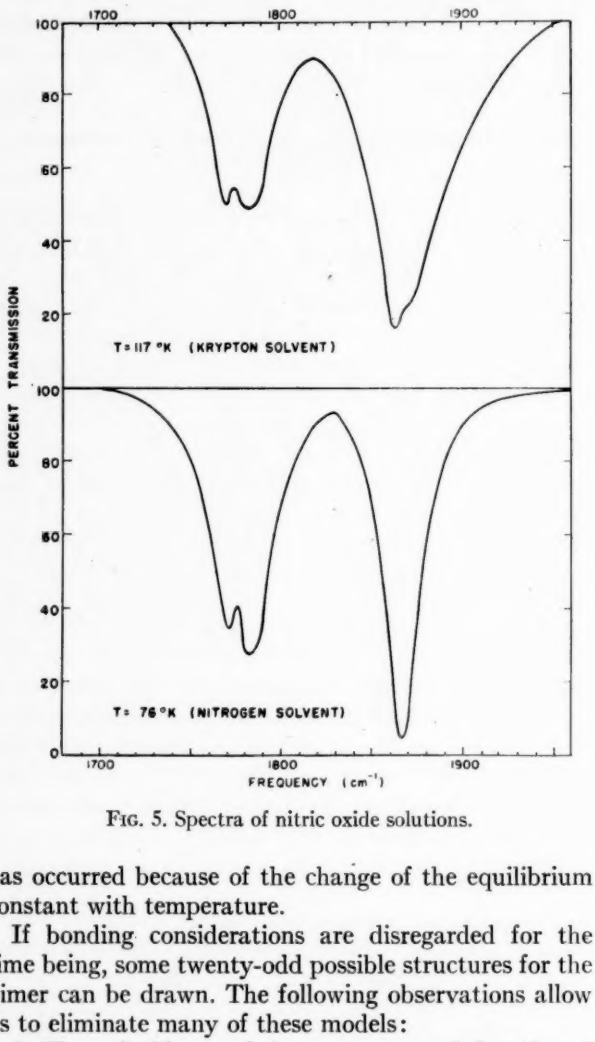

FIG. 5. Spectra of nitric oxide solutions.

has occurred because of the change of the equilibrium constant with temperature.

If bonding considerations are disregarded for the time being, some twenty-odd possible structures for the dimer can be drawn. The following observations allow us to eliminate many of these models:

1. The coincidence of the same strong infrared and Raman band at 1860 cm^{-1} makes a structure with a center of symmetry unlikely. The appearance of the 1770 and 1860 overtones and of the combination of two Raman polarized bands (1865+262) in the infrared, all of which occur with appreciable intensity, lend support to this conclusion.

2. The frequencies of the stretching modes are sufficiently high to indicate the presence of at least a double bond between the O and the N. This requirement, plus the difficulty of writing electronic configurations, eliminates all NOON structures as well as the triangular and square models.

3. The NONO type structures are somewhat questionable for reasons given in the preceding paragraph. Furthermore, nitrogen and oxygen are enough alike so that one would expect the in-phase and out-of-phase stretchings to have very different intensities in the infrared, but this is not observed. It is true, however, that while these considerations weaken the case for the NONO linkage, they do not exclude it. This configuration, while a possibility, is somewhat less probable than those considered subsequently.

Three possibilities remain, all of the bent ONNO type. The models in which the ONN bond angles are different (point groups C_s and C_1) appear to be highly unlikely, so we are left with the two bent structures belonging to point groups C_2 and C_{2v}, which is what we expect from valence considerations anyway. It is difficut to choose between these two structures.

Frequency assignments for the liquid can be partially made on the basis of available evidence, but the fact that one fundamental has not been found makes a complete assignment impossible. Since the 1863-cm^{-1} line is polarized, it must be of species A and thus arises from the symmetrical NO stretching. This leaves $\nu = 1770$ cm^{-1} as caused by the asymmetric stretch.[16]

Not much can be said concerning the low vibrational frequencies (in view of their proximity) other than the fact that the polarized 262-cm^{-1} line arises from a symmetrical motion. The 487-cm^{-1} frequency is difficult to explain; it may be the sixth fundamental but it apparently does not combine with the other fundamentals, and yet it cannot be satisfactorily assigned as a combination or overtone.

A possibility which has not been dealt with is that low-lying electronic levels may be present; the data are insufficient to settle this point.

[16] This band behaves in an interesting fashion in the diluted liquid. It apparently is split into two components, one at 1770 cm^{-1} and the other at about 1785 cm^{-1}. It is unlikely that these are two different fundamentals, and the splitting may be due to the existence of two kinds of dimer molecules. It appears that a further splitting occurs in the solid, giving rise to the bands at 1760 and 1795 cm^{-1}.

An Averaged Field Calculation of the Polarity of the Carbon-Hydrogen Bond

CHARLES R. MUELLER AND HENRY EYRING
Department of Chemistry, University of Utah, Salt Lake City, Utah
(Received October 19, 1950)

Considering the carbon-hydrogen bond as an isolated unit, and including the effect of the interelectronic repulsions, a quantum-mechanical calculation of the polarity of this bond is made. The bond dipole is found to be C^+H^-. On the basis of these calculations, the effect of change in hybridization on the C—H dipole, and the similar effect of replacement of hydrogen in a hydrocarbon by a highly electronegative substituent, is qualitatively discussed. It is predicted that, in both cases, there will be a tendency for the dipole moment to reverse itself.

IN view of the theoretical importance of the carbon-hydrogen bond, both for organic chemistry and as a test of the L.C.A.O. (Linear combination of atomic orbitals), approximation, it seems desirable to carry out a quantum-mechanical treatment which includes the interelectronic forces. To do this it is necessary to consider the bond as an isolated system. The method used below, therefore, represents a compromise between carrying out a wave mechanical treatment, for example, of a methane molecule in the manner that Coulson[1,2] has done, omitting these repulsive terms, and a self-consistent field treatment in the same manner. The complexities of the mathematics force us either to follow Coulson, or to adopt the method used here.

Because of the large magnitude of these repulsive electronic terms, which have heretofore been neglected, it seems necessary to treat the system as we have done. In view of the general agreement of localized and non-localized molecular orbital treatments, the eigenfunctions used here seem to possess no special disadvantage over those previously used.

We will also review the validity of certain other customary approximations, particularly that for E_c, the energy of an electron, which later becomes bonding, in the isolated carbon atom. Using the usual central field approximation,

$$E_c=\int \varphi_c(-1/2\nabla^2-Z_c/R_c+f)\varphi_c d\tau, \qquad (1)$$

where Z_c is the effective nuclear charge of the isolated atom, and f is the interelectronic repulsive potential.

In Section I the eigenfunctions, Hamiltonian, methods of integration and variation are described. The notation used is that developed by Coulson.[3]

In Sec. II we obtain an approximate value for the quantity, E_c, and discuss its relation with the ionization potential. It is particularly important to consider the reorganization energy accompanying ionization.

In Sec. III the selection of nuclear charges is discussed. After a brief consideration of the theoretical factors a value, 2.868 a.u., is selected for the effective nuclear charge of the carbon atom in the molecule and 1.00 a.u. for the hydrogen atom on the basis of energetic considerations.

In Sec. IV the variation of the coefficients of the atomic orbitals and dipole moments with effective nuclear charge is considered. It is found that for those charges selected above a dipole moment of 0.23 D. C^+H^- is found. On the basis of this curve, it is predicted that with the substitution of a highly electronegative group on an alkane, the moment will tend to reverse itself. It is also predicted that a similar shift will occur with a change in type of hybridization. These predictions are then compared to experiment and are found to be in general agreement in regard to all these particulars.

I. THE EIGENFUNCTIONS AND HAMILTONIANS

In the calculations which follow, we have adopted the notation used by Coulson[3] in the self-consistent field treatment of the hydrogen molecule.

The complete wave function for the two electrons is

$$\Psi=\psi(1)\psi(2)\{\alpha(1)\beta(2)-\alpha(2)\beta(1)\}. \qquad (2)$$

Here α and β are the spin wave functions, and since these play no part in the energy calculations they shall be henceforth omitted.

The Hamiltonian is

$$H=h+G(1), \qquad (3)$$

where

$$h=2\{-1/2\nabla^2-Z_c/R_c-Z_h/R_h\}, \qquad (4)$$

and where $G(1)$ is the interaction potential, in turn defined by

$$G(1)=\int \frac{\psi^2(2)}{R_{12}} d\tau_2. \qquad (5)$$

The eigenfunctions $\psi(1)$ and $\psi(2)$ are linear combinations of the tetrahedral carbon and hydrogen atomic orbitals and are of the same analytical form as those proposed by Slater,[4] except that the nuclear charges in the exponents of the eigenfunction are varied. In all cases these effective nuclear charges are held equal to the corresponding quantities in the Hamiltonian, and

[1] C. A. Coulson, Trans. Faraday Soc. **33**, 388 (1937).
[2] C. A. Coulson, Trans. Faraday Soc. **38**, 433 (1942).
[3] C. A. Coulson, Proc. Cambridge Phil. Soc. **34**, 204 (1938).
[4] J. C. Slater, Phys. Rev. **36**, 57 (1930).

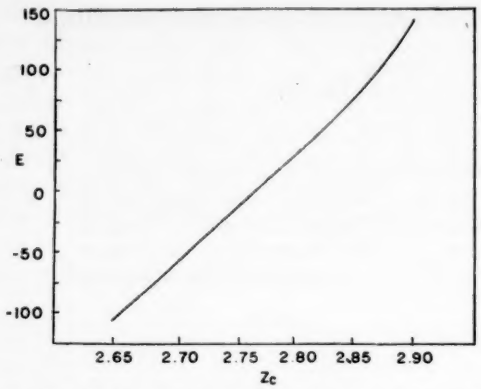

FIG. 1. Variation of binding energy (E) in kcal with effective nuclear charge of carbon (Z_C).

are normalized to unity.

$$\psi(2)=a\varphi_{cte}+b\varphi_h, \tag{6}$$

$$a^2+2abS+b^2=1. \tag{7}$$

The values of the integrals were obtained from the tables prepared by Kotani and Amemiya[5] or were integrated by the authors.

The variation was performed, graphically first, until the quantities H_{hh}, H_{cc}, and E were constant in the third decimal place (0.3–0.5 percent) where these quantities have the usual significance, and then, the results substituted into the equation (cf. Coulson[6]).

$$a^2/b^2=(H_{hh}-E)/(H_{cc}-E). \tag{8}$$

II. THE VALUE OF E_c

Since there are no empirical rules for effective nuclear charges in molecules, one must select the value which gives the best binding energy. This, in turn, depends on the calculation of the energy of the electrons, which later become binding, in the isolated atoms, and the nuclear repulsions which present no difficulties. This quantity, E_c, has been defined in Eq. (1).

We must now investigate the relationship of this quantity, the ionization potential, and the quantity, E_c', defined by an exactly analogous equation except that the effective nuclear charges of the isolated atom have been replaced by those in the molecule.

We shall, for the time being, neglect those inter-electronic forces designated by f. We will first establish a relationship between E_c and the ionization potential, and then one between E_c' and E_c.

The energy required for ionization can, for the sake of convenience, be divided into three parts: the energy necessary to remove an electron from a central field, which is unchanged by its removal; the gain of electronic energy of those residual electrons due to lessened shielding; and the gain energetically of these same electrons due to lessened repulsive forces. We shall designate these quantities by E_1, E_2, and E_3, respectively.

Assuming the virial theorem to hold for our eigenfunctions,

$$E_1=Z_c^2/2n_c^2a_0. \tag{9}$$

If we then use Slater's rules[4] the value of E_2 is obtained from the equation:

$$E_2=\frac{3Z_c^2}{2n_c^2a_0}-\frac{3}{2n_c^2a_0}(Z_c+0.35)^2. \tag{10}$$

The value of E_3 is extremely difficult to estimate, and we shall only discuss qualitatively the magnitude of the error caused by its omission. This error is limited by the relative smallness of the repulsive terms in comparison with those previously considered and, by the fact that we are interested only in the differences between E_c and E_c'. It will be seen from the results in Sec. IV that such an omission has the effect of forcing the choice of a slightly higher Z_c and a slightly lower value of a^2/b^2 for this charge than is given on the graph.

Thus, it is hoped that, in large measure, these opposing effects will cancel one another. Since this cannot be exactly so, the exact magnitudes of the calculated dipoles should not be taken too seriously.

Using the Slater[4] effective nuclear charges, Z_c equal to 3.25, we obtain a value of 11.92 ev for the ionization potential. Since the ionization potential of the carbon $2p$ electron is 11.21 ev, and that of the s electron slightly more, it is at least consistent if we write E_c as

$$E_c=Z_c^2/2n_c^2a_0, \tag{11}$$

where Z_c is 3.25.

For the corresponding term in the molecule we shall use the same expression but with changed nuclear charge. This, of course, implies that the energy represented by E_c shall vary with the square of Z_c. The repulsive terms which we have omitted, in general, vary with the first power. Since the total variation

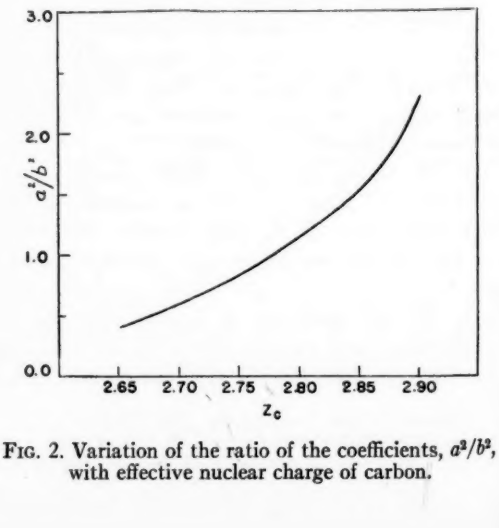

FIG. 2. Variation of the ratio of the coefficients, a^2/b^2, with effective nuclear charge of carbon.

[5] M. Kotani and A. Amemiya, Proc. Phys.-Math. Soc. Japan **22**, Extra Number (1940).
[6] C. A. Coulson, Proc. Cambridge Phil. Soc. **33**, 112 (1937).

between the effective nuclear charge in molecule and free atom is only 12 percent, we shall not correct for the resultant error.

III. THE EFFECTIVE NUCLEAR CHARGE

The variation of binding energy with effective nuclear charge is given in Fig. 1. From this, it is seen, that the best choice for the Z_c is 2.868, corresponding to the observed binding energy of 98.2 kcal given by Pitzer.[7] As for the nuclear charge of hydrogen, values ranging from 0.9[1] to 1.19[8] have been used. For simplicity and ease of calculation, the value of 1.00 has been chosen.

As for Z_c, the values, which have been used, range from 1.19,[9] 1.76,[1] to 3.25 for crude calculations.

Certainly, there is no limitation so far as precedent is concerned. From the theoretical viewpoint, at least three factors are involved. In the process of chemical combination the atoms should exhibit some "united atom characteristics." This tends to cause a slight rise in nuclear charge.

Secondly, there is a small screening increment due to the presence of an additional bonding electron in the region of the nuclei.

Thirdly, there is some tendency for the bonding electrons to form a separate "group" as Slater[4] uses the term, and this tends to reduce the charge. All that can be said is that the effective nuclear charge seems to be somewhat lower than in the free atom.

It is interesting to note, that by including the repulsive electronic field our effective nuclear charge varies from that of the atom by only 12 percent, while Coulson,[1] neglecting the former, used a Z_c (1.76), 54 percent of the free atom.

IV. THE VARIATION OF THE COEFFICIENTS AND DIPOLE

In Figs. 2 and 3, respectively, the variation of these quantities is shown with changing effective nuclear charge. It should be noticed that the variation in both cases is very rapid.

The dipole moments were obtained from the usual quantum-mechanical formula.

$$M=-2e(\bar{R}_c-R_{ch}/2), \tag{12}$$

where

$$R_c=a^2\int \varphi_{cte}^2 R_c d\tau+2ab\int \varphi_{cte}\varphi_h R_c d\tau+b^2\int \varphi_h^2 R_c d\tau. \tag{13}$$

The value of M obtained for Z_c equal to 2.868 was 0.23 D., C^+H^-, which appears to be in satisfactory agreement with the observed values of 0.30–0.40 D., C^+H^-. It should be noted, however, that a small change in nuclear charge tends to cause a considerable change in magnitude.

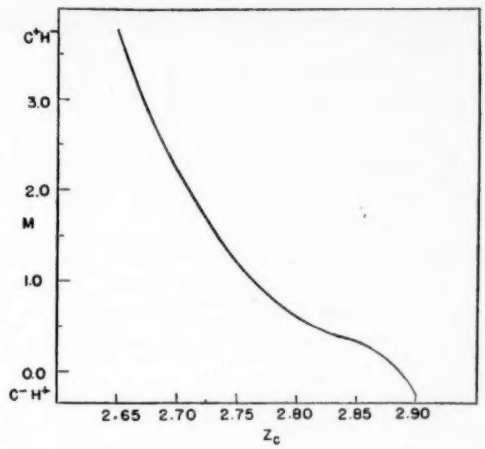

FIG. 3. Variation of dipole moment in Debye units with effective nuclear charge of carbon.

In the alkyl halides, for example, roughly 1/5 of an electronic unit is pulled from the region of the carbon atom to that of the halogen. In the bond, itself, this results in an increase of the nuclear charge due to lessened shielding, causing a change of around 1/15 to about 1/25, depending on what shielding constant one uses. The change in Z_c in the adjacent bonds will then be some fraction of this amount. We should, therefore, expect a tendency to reverse the dipole moment with increasing electronegativity of substituent.

Qualitatively, one can also predict the same sort of change as one passes from sp^3 to sp^2 and sp hybridization. From the tables compiled by Kotani and Amemiya,[5] one finds that in this range of effective nuclear charge, there is about a 2 percent increase in the overlap integral as one changes from sp^3 to sp^2 hybridization. One then expects a very small change in overlap energy. The change in H_{hh} should also be quite small.

Surprisingly enough, it also appears that the change in H_{cc} is also not very large. The value of the integral,

$$K_{\alpha\beta}=\int (\varphi_{c\alpha}\varphi_{c\beta}/R_h)d\tau \tag{14}$$

has been selected as a typical case in this range of effective nuclear charge.

For $Z_c\times R_{ch}/2=3.00$ in atomic units, $2K_{ss}/Z_c=0.3139$, $2K_{sp}/Z_c=0.1247$, $2K_{pp}/Z_c=0.3785$. However,

$$\int (\psi^2_{cte}/R_h)d\tau=0.4709\times 2/Z_c, \tag{15}$$

$$\int (\varphi^2_{c\ \text{trigonal}}/R_h)d\tau=0.4704\times 2/Z_c. \tag{16}$$

The other attractive integrals are almost unchanged, and the repulsive integrals are only slightly reduced. For these reasons, it seems that the primary effect of

[7] K. Pitzer, J. Am. Chem. Soc. **70**, 2140 (1948).
[8] S. Weinbaum, J. Chem. Phys. **1**, 317 (1949).
[9] N. Bayliss, J. Chem. Phys. **17**, 1353 (1949).

hybridization is caused by the change in the effective nuclear charge.

Because the *s* electrons are, on the average, closer to the nucleus and, hence, are shielded less, the effective nuclear charge should be greater for *s* than for *p* electrons. The changes of hybridization should result in increased nuclear charge, since they increase the *s* character of the orbitals.

As a result there should be a shift of the electronic charge cloud toward the carbon atom, making the hydrogen atom more positive. This seems to be borne out by the increase in acidity as one passes from ethane to ethylene and acetylene.

The quantum-mechanical calculations by Coulson,[2] by Hirschfelder as reported by Smyth[10] and corrected by Coulson,[2] and by the authors, agree as to the direction of the moment. They also agree as to the general magnitude (0.50, 0.40, 0.23 D.), and to the fact that the moment arises from the orientation of the overlap electron cloud. For example, it should be noted that the ratio of a^2/b^2 is 1.75 for our calculated dipole moment.

It is, of course, impossible to review all of the experimental evidence concerning these predictions and, for a fuller review, the reader is referred to the article by Gent.[11]

As for the general magnitude, spectroscopic measurements by Foley[12] give a value of 0.307 D. for the moment in CH_4. Timm and Mecke[13] give 0.30 D. for $CHCl_3$, 0.26 D. for CH_2Cl_2, and 0.25 D. for CH_3Cl. The direction of the moments is indeterminate. The same sort of sequence was also reported for the corresponding brominated methanes. If the direction of the moments in chloroform and methylene chloride is C^-H^+, then the change of moment is as predicted. The direction in methyl chloride would then probably be the same.

Walsh[14–16] argues that if the polarity is C^+H^- in the hydrocarbons, then the properties of this bond should be similar to those of the carbon-halogen bonds. He demonstrates the existence of this parallelism by means of force constant, thermochemical, and bond length data. While this seems reasonable, it should be noted that the similarity between these kinds of bonds is confined to the overlap portion of the electronic cloud. The cloud is denser around the carbon atom in the C—H bond and denser around the halogen atom in the carbon-halogen bond.

On the whole, one should state that the evidence seems to indicate a polarity as calculated, and a dipole moment of 0.30 D. However, the evidence does not seem to be conclusive.

[10] C. P. Smyth, J. Phys. Chem. **41**, 209 (1937).
[11] W. Gent, Quart. Rev. Chem. Soc. **4**, 383 (1948).
[12] R. Foley, Phys. Rev. **69**, 628 (1946).
[13] B. Timm and R. Mecke, Z. physik. Chem. **98**, 363 (1935).
[14] A. D. Walsh, J. Chem. Soc. 400 (1948).
[15] A. D. Walsh, Faraday Soc. Disc. **2**, 18 (1947).
[16] A. D. Walsh, Trans. Faraday Soc. **43**, 68 (1947).

THE JOURNAL OF CHEMICAL PHYSICS VOLUME 19, NUMBER 2 FEBRUARY, 1951

The Thermal Hydrogen-Oxygen Reaction at Relatively Low Temperatures

H. P. BROIDA* AND O. OLDENBERG
Lyman Laboratory of Physics, Harvard University, Cambridge, Massachusetts
(Received July 13, 1950)

In the behavior of the thermal hydrogen-oxygen reaction there is an apparent discrepancy. The *second explosion* of the thermal reaction occurs over a wide range of low temperatures down to 350°C, even though the rate of *steady thermal reaction* is very nearly zero. The authors used a criterion stated by Lewis and von Elbe to show that the same volume chain which explains the reaction at higher temperatures applies to the low temperature range. The inhibition period within the low pressure explosion region and the branching of the chains are briefly discussed.

I. PROBLEM

THE theory of the thermal hydrogen-oxygen reaction, introduced in general terms by Kassel[1] and worked out in great detail by Lewis and von Elbe,[2,3,4] has been confirmed by numerous measurements of Lewis and von Elbe. Furthermore, Willbourn and Hinshelwood[5] have apparently confirmed the essential steps of the chain in a higher temperature range, in which they retarded the reaction by covering the surface of the vessel with KCl. The general theory accounts for the second explosion limit. This limit is characterized by a sudden, large increase in the rate of the reaction with decreasing total pressure. While at a certain pressure of a few centimeters, the rate of the reaction is exceedingly

* Now at the National Bureau of Standards, Washington, D. C.
[1] L. S. Kassel, Chem. Revs. **21**, 331 (1937).
[2] B. Lewis and G. von Elbe, *Combustion, Flames, and Explosions of Gases* (Cambridge University Press, London, England, 1938).
[3] B. Lewis and G. von Elbe, J. Chem. Phys. **10**, 366 (1942).
[4] "Third symposium on combustion" (The Williams and Wilkins Co., Baltimore, Maryland, 1949), p. 484.
[5] G. N. Hinshelwood and A. H. Willbourn, Proc. Roy. Soc. (London) **A185**, 353–380 (1946).

slow, at an only slightly lower pressure it is infinitely rapid. The pressure at which this large change in rate occurs is the second explosion limit.

In this paper, we are concerned with the contrasting behavior of the *second explosion limit* and the *rate of the steady reaction* at the low temperature range. This range is, say, from 500° down to 350°C; this latter temperature is the lowest at which the second explosion has been observed. The rate of the steady reaction becomes too low for easy measurement below 500°C; but by extrapolation from rates above 500°, the rate at 350°C and at 2 cm Hg is computed to be a negligible 10^{-13} mm Hg per minute. Accordingly, we face the problem that the second explosion still occurs at temperatures at which the steady reaction is practically absent. The contrasting behavior just described gives the impression that at lower pressures the second explosion is unrelated to the rate of the steady reaction. However, above 500°C such a relation has been satisfactorily established by the theory of Lewis and von Elbe. We want to correlate with the theory the apparent discrepancy of the occurrence of the explosion in spite of the absence of a measureable steady reaction.

For this purpose we used the following method. In 1942 Lewis and von Elbe[3] published measurements which are applicable as a critical test of their theory. They had explored the second explosion limit between 480° and 570°C as a function of the relative composition of the exploding gases and admixed inert gases. Since their observations agreed so well with the predictions of their theory, this test confirmed the theory in the high temperature range. Because the theory seemed questionable for very low temperatures (down to 350°C), we have applied their test to this lower temperature range (Secs. III and IV).

The results of Sec. IV lead to essential agreement with the theory except that they suggest a doubt with respect to the initiating reaction at low temperature. The initiating reaction is further discussed in Sec. V. By a very sensitive instrument we have been able to trace reaction rates in large Pyrex vessels to a temperature as low as 350°C at total pressures between 8 cm and 60 cm Hg (Sec. VI).

Sec. VII is concerned with the question of the temperature at which the branching of the chains becomes prominent in the steady reaction. This is to be judged by the temperature coefficient of the rate.

II. EXPERIMENTAL ARRANGEMENT

In order to measure very small pressure changes we used a manometer built by Prof. G. B. Kistiakowsky.[6] It has a helix of eleven turns of thin elliptic quartz tubing, closed at one end and sealed at the other to the system. The spiral is immersed in an envelope in which the pressure can be set at will. Essentially, this instrument measures a pressure difference in a manner similar to that of a Bourdon gauge. A small mirror attached to the bottom of the helix serves as an indicator. A system of twin photo-tubes in a bridge circuit permits a sensitive and stable reading with an accuracy of 0.01 mm mercury. In most of the experiments to be described the envelope was evacuated. This limited the pressure range from 0 to 6 cm, but had the advantage of making the instrument rather independent of ambient temperature.

The reaction vessel was heated in a cylindrical oven (inside diameter, 22 in.; inside height, 31 in.) and was kept at constant temperature (±0.1°C) by a bridge controlled thyratron thermostat built by Kennedy and Hooper, Cambridge.[7] The top and bottom of the oven were supplied with manually controlled heaters. Temperatures were read with a Chromel-Alumel thermocouple calibrated against the melting point of zinc. Because of the aging of the thermocouple, the readings taken within intervals of days and weeks are not closer than one degree. In most of the experiments reported subsequently, a change of temperature of 1°C causes a change of 2 percent in the pressure of the second explosion limit.

Spherical Pyrex vessels were used. Since in the mixing process the last admitted gas remained relatively unmixed in the inlet tube, a suitable correction was applied. The vessels were washed with Ivory Flakes and rinsed with boiling distilled water. Coating with KCl was done by either of two methods. Clean vessels were rinsed with a hot, saturated solution of cp grade KCl and gradually dried. Alternatively, saturated cp grade KOH solution, which adheres more uniformly to the walls, was used; the KOH was changed to KCl by a stream of dry HCl. The B_2O_3 coating was made as described by McLane.[8]

Hydrogen and oxygen were prepared electrolytically and purified by passing over hot platinum asbestos and P_2O_5. Tank nitrogen was used, specified as 99.5 percent pure; the impurities were oxygen and rare gases. All stopcocks were lubricated with Apiezon L grease.

In many experiments the procedure was as follows. The reaction vessel was evacuated, rinsed with hydrogen, and filled with hydrogen to a pressure above the second explosion limit. For the rapid admission of oxygen, an "outer chamber" of known volume and temperature was filled with oxygen of such a pressure that after opening the stopcock the reaction vessel contained the desired mixture proportion and total pressure. For the determination of the second explosion limit, the pressure in the reaction vessel was reduced to about 2 mm above the explosion limit within 20 to 30 sec; the final pumping to the explosion was done gradually in about 40 sec, while the pressure was followed by the quartz spiral.

The best reproducible values were determined as follows. Since it appeared that various agents may lower the tendency toward the explosion, the highest value of

[6] This type of construction is described by Mr. W. E. Vaughan, Rev. Sci. Instr. **18**, 192 (1947).

[7] Now called Spencer-Kennedy Laboratories.

[8] C. K. McLane, J. Chem. Phys. **17**, 379–385 (1949).

the limit was determined. First, a preliminary value was found by the withdrawal method. Then the mixture at a predetermined pressure was reduced to the pressure of the explosion limit by allowing the gas to flow into a fixed volume within a few seconds. This was done for various final pressures within a few tenths of a millimeter of mercury. The second explosion limit was defined as the highest pressure at which the explosion occurred. The second limit determined by this procedure was reproducible for a set of runs within less than 1 percent. Below 500°C the difference of less than $\frac{1}{10}$ of a millimeter was the difference between a negligible rate and an explosion.

Sometimes, particularly in large vessels, self-heating of the mixture at the second explosion limit was evident from the following observation. Just prior to the large pressure *decrease*, which gave evidence of the explosion, a small, sudden *increase* of pressure was observed.

III. THEORY

Since the complex facts regarding the three explosion limits have been described in detail,[2,3] we shall give only a brief outline of the various individual steps and specify only those necessary to explain the second explosion limit.

The second explosion limit gives evidence regarding the various steps of the reaction and has the distinction of being the most reproducible feature of the thermal reaction. However, this limit gives no direct information about the initiating reaction. This is understood as follows. Any explosion limit is defined by the requirement,

$$\text{rate of branching} = \text{rate of breaking.}$$

This defines the explosion as the property of individual chains, irrespective of the number of chains started per second. Here we presuppose no interaction between chains and no internal heating. Hence, the explosion limit does not depend on the initiating reaction; it is necessary only that some chains start within the observable time interval.

Since it is known that hydrogen peroxide is formed in the thermal reaction, a complete theory must account for its production. Hence, Lewis and von Elbe have introduced steps involving hydrogen peroxide. These steps, however, do not seem to affect the explosive characteristics of the chain but are concerned with the products of the chain. Therefore, for our purpose, it is permissible to simplify the scheme by assuming H_2O as the product and so keep the computations much simpler than they would be introducing the intermediate formation of H_2O_2. Nevertheless, the success of such schemes for special purposes must not be interpreted as excluding the intermediate formation of H_2O_2.

The reaction scheme adopted for the explanation of the second explosion limit at low temperatures assumes the usual chain continuation in the volume and chain destruction at the surface. The first six steps are identical with those of Willbourn and Hinshelwood. Another chain breaking step is needed to explain the new low temperature observations of the second explosion limit. The loss of hydrogen atoms (step 7) is the most plausible step which fits the experimental data; also this step has been assumed by other authors as breaking the chains at very low pressure, i.e., below the first explosion limit.

1. $OH+H_2 \rightarrow H_2O+H,$
2. $H+O_2 \rightarrow OH+O,$
3. $O+H_2 \rightarrow OH+H,$
4. $H+O_2+M \rightarrow HO_2+M,$
5. $HO_2 \xrightarrow{\text{surface}} \frac{1}{2}H_2O+\frac{3}{4}O_2,$
6. $HO_2+H_2 \rightarrow H_2O+OH,$
7. $H \xrightarrow{\text{surface}} \frac{1}{2}H_2.$

Steps 2 and 3 are the branching steps. Step 4 if followed by the surface reaction 5 is chain breaking. If, instead, 4 is followed by the volume reaction 6, the chain is continued.

The breaking effect of the surface depends on the chance for one or the other carrier to reach the surface. The chain carrier HO_2 may be consumed by 5 or 6. In our experiments at low temperature and pressure, since 6 is rare and practically absent, the formation of HO_2 by 4 is necessarily followed by 5 and so breaks the chain. H is consumed by 2 or 4 or 7. At very low pressure 4 is absent, which limits the competition to 2 and 7. Since 2 is rare because of its high activation energy, at lower pressures 7 breaks the chains. (O and OH have short lives because of the high probabilities of 1 and 3; under most conditions this eliminates surface recombinations of O or OH.)

Suppose we start from conditions which favor a steady reaction. When the pressure is decreased, the triple collision 4 loses out as compared with 2. Hence, the breaking fails and the explosion of the second limit occurs. At still lower pressures there follows a certain range of explosion. Finally, at further decreasing pressure the surface reaction 7 begins to compete with 2 and breaks the chain. This stabilizes the reaction and is responsible for the first explosion limit and the steady reaction at still lower pressures. We are concerned here mainly with the upper limit of this explosion region, the second explosion limit.

The discussed reaction supplemented by other reaction steps, which are needed for the explanation of the rates, leads to a complicated expression for the rate.[9] The condition for the total pressure P_2 at the second explosion limit is, as derived by Lewis and von Elbe,

$$P_2 = 2k_2T/k_4, \tag{1}$$

[9] Derived in the thesis of H. P. Broida.

where k with a subscript means the rate constant of one or the other step. This simple equation for P_2 holds under many conditions. However, later we shall need to consider corrections due to the effects of steps 6 and 7.

Lewis and von Elbe further analyzed k_4 by introducing the idea that, in step 4, each of the constituent gases has its own chain breaking efficiency. This leads to the expansion of Eq. (1) into

$$\frac{1}{P_2}=\frac{k_4'}{2k_2T}(f_{H_2}+k_{O_2}f_{O_2}+k_Mf_M)=\frac{k_4'\alpha}{2k_2T}. \qquad (2)$$

The letter f with a subscript indicates the fractional concentration of a constituent gas and k_4' the absolute efficiency of H_2 in step 4, whereas k_{O_2} and k_M indicate the efficiencies of O_2 and M *relative* to that of H_2. This means that the efficiency of H_2 is arbitrarily taken as a standard. The factors k_2 and k_4' are temperature dependent. α is an abbreviation for the bracket.

We have varied the relative concentrations of the gases over the widest possible range. In the first case in which no inert gas is added, $f_M=0$; and the equation simplifies to

$$\frac{1}{P_2}=\frac{k_4'}{2k_2T}[(k_{O_2}-1)f_{O_2}+1]. \qquad (3)$$

This shows that k_4'/k_2 and k_{O_2} are derived from a linear plot of $1/P_2$ against f_{O_2}.

In the presence of an inert gas the complete equation describes a linear relation between $1/P_2$ and f_M. For the stoichiometric mixture, it is

$$\frac{1}{P_2}=\frac{k_4'}{2k_2T}\frac{2+k_{O_2}}{3}\left\{\left(\frac{3k_M}{2+k_{O_2}}-1\right)f_M+1\right\}. \qquad (4)$$

We need a supplement to this theory owing to the fact that deviations are found for large hydrogen concentrations. Since we are dealing with pressures of only a few cm, the plausible explanation is that here the same breaking mechanism enters which is the major mechanism effective at very low pressure, below the first limit. This step is the adsorption at the wall of H atoms (step 7); among the chain carriers H atoms have the longest life. In the absence of a foreign gas this leads to the equation

$$\frac{1}{P_2}=\frac{k_4'[(k_{O_2}-1)f_{O_2}+1]}{k_2T[1+\{1+b(1-k_{O_2})-b/f_{O_2}\}^{\frac{1}{2}}]}, \qquad (5)$$

where $b=k_4'k_7/k_2^2$. Equation 5 depends upon the assumption that the rate constant of step 7 is independent of pressure. The constant b, which involves the new step 7, is evaluated by the following procedure. Since b is of the order of 0.01 to 0.1, except for small values of f_{O_2}, the last equation is approximated by Eq. 3, in which step 7 was neglected. Hence, the first approximation to k_4'/k_2 and k_{O_2} is obtained from the straight line portion of the curve. More specifically,

$$k_4'/k_2=2I_O \quad \text{and} \quad k_{O_2}=I_1/I_O,$$

where I_O and I_1 indicate the two intercepts for $f_{O_2}=0$ and $f_{O_2}=1$, respectively. The constant b, which supplies the value of k_7 is found by adjusting the theoretical curve to the experimental points.

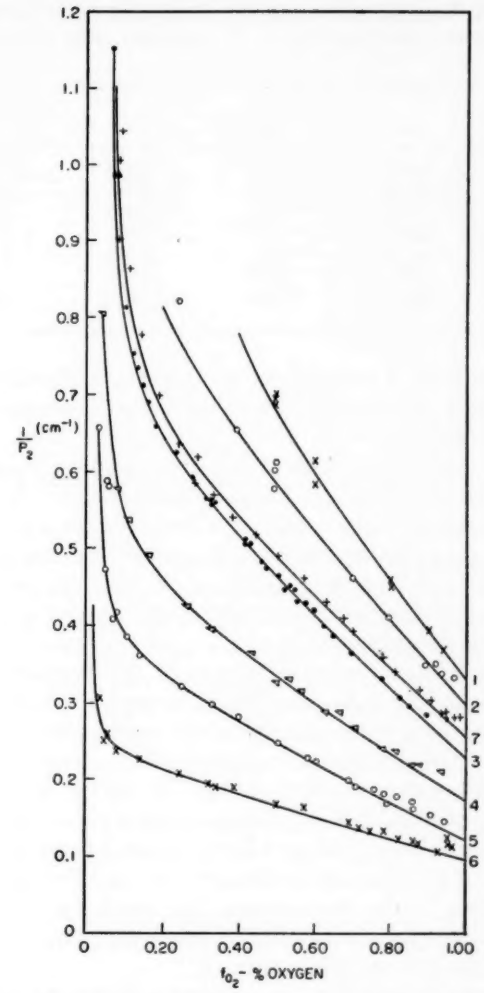

FIG. 1. Second explosion limit as a function of the relative oxygen concentration. (The numbers of the curves refer to Table I.)

IV. RESULTS REGARDING THE SECOND EXPLOSION LIMIT

The most consistent and reliable values of the second explosion limit at low temperatures were obtained in a 3-liter spherical vessel covered with KCl. Figure 1 shows the experimental points; the solid lines are the theoretical curves from Eq. 5 and the constants listed in Table I. The curves are well approximated by straight lines for large values of f_{O_2}. The relative efficiency in step 4 of O_2 (that is, k_{O_2}) was constant except at the highest temperature used, 496°C. The average value of 0.34 for k_{O_2} confirms the value of 0.35 obtained by Lewis and von Elbe[3] at higher temperatures. The seeming de-

TABLE I. Large KCl vessel III. (Constants found by fitting experimental points of Fig. 1. No. indicates order of series of runs.)

No.	t°C	k_{O_2}	b	k_3T/k_4' (cm of Hg)
1	434.5	0.34	0.095	0.525
2	435.5	0.35	0.08	0.594
7	444.3	0.36	0.075	0.705
3	449.5	0.33	0.07	0.730
4	463.4	0.34	0.055	0.980
5	478.6	0.335	0.045	1.35
6	496.0	0.40	0.015	2.09

viation from a constant at the highest temperature is explained by the continuation of the chain through step 6 (Eq. 6).

The vertical portions of Fig. 1 at small f_{O_2} show the junction of the first and second explosion limits. In clean Pyrex this junction occurs at a lower temperature for a given f_{O_2}; this agrees with the larger recombination efficiency of hydrogen atoms on Pyrex than on KCl surfaces.[10] The percentage of oxygen at this junction depends directly upon b.

The temperature dependence of the constant b is shown in Fig. 2. In our limited range $b=k_4'k_7/k_2^2$ was more nearly a linear function of the temperature than an exponential function, which would be anticipated. The resulting value of about 40 kcal/M for the activation energy of step 7 is high. This apparent activation energy possibly is explained as follows: since adsorbed water makes a glass surface ineffective for the recombination of atoms, it may be assumed that increasing temperature makes the dry fraction of the surface larger and so promotes the recombination.

Figure 3 shows the logarithmic dependence of the second explosion limit on the absolute temperature. Theoretically, the second explosion limit depends on the temperature by the relation

$$P_2/T=\text{const}\exp[-(E_2-E_4)/RT].$$

(This implies that the relative efficiency in step 4, that is, k_{O_2}, does not depend on the temperature.) E_2 and E_4 are the activation energies of reactions 2 and 4, respectively. As expected, the lines for the different relative concentrations of f_{O_2} are parallel. The slope of the lines gives the activation energy of 22.0 kcal per M for E_2-E_4. Since step 4 presumably has no activation energy, this number gives the activation energy of step 2. In another vessel of the same size, also covered with KCl, the activation energy found was 21.6 kcal/M. In a smaller KCl-covered vessel the value was 21.0 kcal/M. These values do not agree well with the 17 kcal/M obtained by Lewis and von Elbe. (The higher value of 26 kcal/M obtained by Hinshelwood and Willbourn is criticized by Lewis and von Elbe,[11] who object to an approximation which at the high temperature of these experiments would cause an error. However, the same approximation seems justified at our much lower temperature range.)

Results obtained in other vessels will be summarized briefly. In a small KCl vessel, the measured activation energy E_2-E_4 was 21 kcal/M; this is in agreement with the value previously reported. In a large Pyrex vessel, that is, under widely different conditions, E_2-E_4 was 21.7 kcal/M. Here k_{O_2} had an average value of 0.40; this reasonably well confirms the value in KCl.

This value of k_{O_2} showed a small variation with temperature, increasing from 0.37 at 378°C to 0.44 at 464°C. The differences of these values from those in KCl and this slow increase with the temperature may be explained by taking into account step 6 which becomes more probable with increasing temperature and pressure. (For the detail see the thesis of H. P. Broida.) This argument leads to an energy of activation for E_6-E_6 of about 10 kcal/M. This unexpectedly high value compares with the figure obtained by Willbourn and Hinshelwood at high temperature in KCl covered vessels (5 kcal/M).

We have also measured the efficiency of nitrogen and of water as a third body in step 4 at temperatures between 443° and 492°C. Our average result of 0.42 for k_{N_2} is in good agreement with that of other investigators working above 500°C. At 453°C, k_{H_2O} was 6.7. The values determined by Lewis and von Elbe are 10.4 at 480°C and 14.6 at 570°C. This comparison confirms the suggestion of Lewis and von Elbe[3] that k_{H_2O} is temperature dependent. The value calculated from kinetic theory is only 0.6. The large value observed, about 20 times the kinetic value, connected with its temperature dependence suggests that the water enters into the reaction in a more complicated manner.[12]

McLane[8] found that rinsing a Pyrex vessel with B_2O_3 increases the lifetime of H_2O_2 and makes its decomposition more reproducible. However, the hydrogen-oxygen reaction was not rendered more reproducible than it is in a Pyrex vessel. Although the behavior was erratic, the characteristics of a B_2O_3-coated vessel were more like those of a KCl-coated than a clean Pyrex vessel.

Our main conclusion is that the second explosion limit measured at comparatively low temperatures over the widest possible range of mixture composition confirms the Lewis and von Elbe theory. In the various ranges, the steps applied are as follows. Through a considerable intermediate range the steps 1, 2, 3, 4, and 5 represent the observed limits. At lower temperature and pressure, adsorption of H atoms (step 7) becomes effective, while at higher temperature and pressure step 6 is no longer negligible.

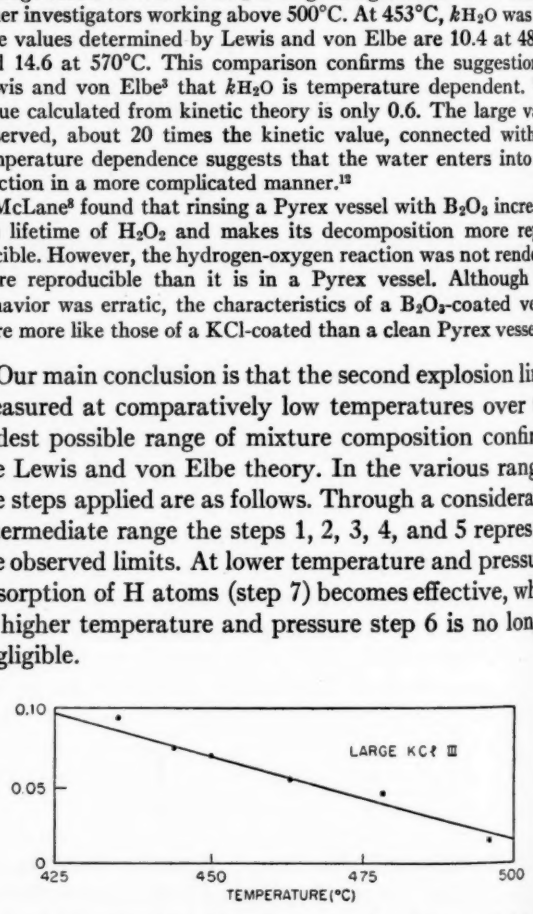

FIG. 2. b as a function of temperature. (Values from Table I.)

[10] W. V. Smith, J. Chem. Phys. **11**, 110 (1943).
[11] Reference 4, p. 491.
[12] V. Vojevodsky, J. Phys. Chem. (U.S.S.R.) **20**, 1285 (1946), introduces the step $HO_2+H_2O=H_2O_2+OH$ into the reaction scheme. This step, however, does not remove the present difficulty since it attributes to the H_2O molecule a chain *continuing*, not a chain *breaking*, effect.

V. INITIATING REACTION

The initiating reaction appeared to be well established for high temperatures by the work of Willbourn and Hinshelwood.[5] They offered two separate arguments indicating that the thermal dissociation of H_2 initiates the chains. First, the energy of activation of the initiating reaction (not the total reaction which is affected by the branching chain) is about 100 kcal/M, that is, just the energy of dissociation of H_2. Second, when the relative concentrations of H_2 and O_2 were varied, the rate obtained indicated that the reaction starts from the dissociation of H_2 molecules and not from the possible competing reaction $H_2+O_2 \rightarrow OH+OH$.

Lewis and von Elbe,[4] however, present a conclusive argument against this initiation by thermal dissociation of H_2. They compare the number per second of sufficiently energetic collisions with the rate of the initiating reaction and find a deficiency of the collisions by the factor 10^{13}. In addition, they use the rate constants and activation energies of their 1942 paper to present curves agreeing reasonably well with the experimental data of Willbourn and Hinshelwood. Therefore, they prefer the thermal dissociation of H_2O_2 as the initiating reaction. This requires only 50 kcal/M and has a much more reasonable steric factor. The obvious difficulty is that there is no H_2O_2 initially present in the mixture of H_2 and O_2. Hence, they are forced to assume a subsidiary reaction taking place at the wall and supplying traces of H_2O_2. These traces multiply in the volume. So far, one would conclude that the over-all rate would be proportional to the rate of the subsidiary production of H_2O_2 at the wall. In order to circumvent this situation, Lewis and von Elbe assume that H_2O_2 reaches a steady concentration which is independent of the rate of its first formation. This is accomplished by assuming that the growth of H_2O_2 is limited by collisions with chain carriers:

$$H+O_2+H_2O_2 \rightarrow H_2O+O_2+OH$$

and

$$HO_2+H_2O_2 \rightarrow H_2O+O_2+OH.$$

Hence, in this scheme the chains are not independent, since two chain carriers, H_2O_2 and HO_2, react with one another. For the purpose of the mathematical treatment Lewis and von Elbe describe the same scheme as follows. They assume that in the first place traces of H_2O_2 are generated by an unspecified, rare process. It does not need to be specified, since the ultimate concentration of H_2O_2 depends not on this process but on the balance of more frequent processes, generating and consuming H_2O_2. On this basis they consider the thermal dissociation of H_2O_2 as the initiating reaction.

This unusual argument compares to that which explains the concentration of neutrons in the nuclear reactor. In the first place one assumes an unspecified, rare process generating a few neutrons. The ultimate concentration of neutrons, however, does not depend on this rare initiating process but on the balance of more frequent processes, generating and consuming neutrons. The concentration of electrons and ions in an electric discharge through a gas is of the same character.

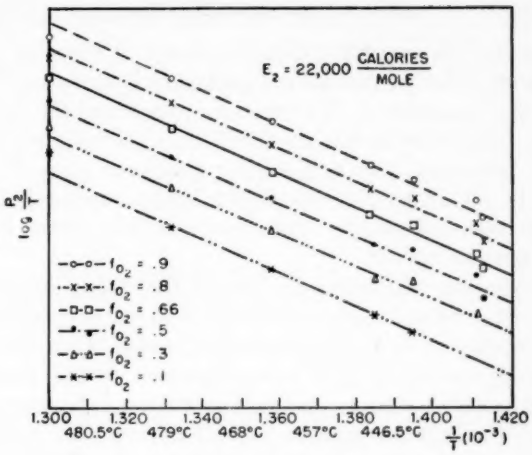

FIG. 3. Logarithmic dependence of the second explosion limit on the absolute temperatures.

In order to explore the initiating reaction at the lower temperature range, an attempt was made to measure its activation energy at comparatively low temperatures. However, these low rates were found to be so erratic that no conclusions could be drawn. Somewhat better results were obtained by the method used by Willbourn and Hinshelwood. These authors varied the relative concentrations of H_2 and O_2 in the high temperature range (570–600°C) and found variations of the rate which did not agree with the assumption of $H_2+O_2 \rightarrow 2OH$. Our experiments in a three-liter Pyrex vessel at temperatures down to 350°C agree with these results and indicate that at a constant temperature the rate of the reaction is proportional to the product of the total pressure and the square of the percentage of hydrogen.

In the low temperature range, down to 350°C, the discrepancy from which we started is as follows. The absence of a noticeable steady reaction and the explosion, which is attributed to a volume chain, need to be reconciled. Our conclusion is that a measurable rate is unnecessary as long as a chain is started during the period of observation. Since within the scheme of the steady reaction, the initiating step has by far the highest activation energy, initiation is expected to be very rare. However, it is known that at temperatures below 500°C a surface reaction persists which occasionally may liberate carriers into the volume and thus start the same volume chain known at high temperature.[13] Although chains start so rarely that the steady reaction fails to reach a noticeable rate, the starting process may be sufficient to initiate the chains. The explosion does not require that many chains start per second but only that the chains are long, that is, branching exceeds breaking.

[13] C. N. Hinshelwood and A. T. Williamson, *The Reaction between Hydrogen and Oxygen* (Clarendon Press, Oxford, 1934), p. 5.

VI. INHIBITION PERIOD

Lewis and von Elbe found a source of error in the determination of the second explosion limit caused by too slow pumping as the pressure approached the limit. Slow manipulation has the effect that the steady reaction occurring above the limit produces some H_2O, which, in turn, by its large effect in step 4, breaks chains. Thus the explosion is suppressed and the pressure of the limit is lowered.

Under our conditions the rate of the steady reaction above the second explosion limit was so low that such an accumulation of H_2O was easily avoided. In order to investigate the effect of pumping speed on the second limit, a series of runs was made in a large KCl vessel at 527°C; at this temperature in KCl the reaction is slow. The surprising result was that the second limit was *lowered* by *faster* pumping. The same effect was found in all vessels, large or small, clean Pyrex or KCl-covered. If the pressure was rapidly reduced to the value at which explosion occured for slow pumping, the explosion took place after a noticeable time lag. It was ascertained that this lag was not due to a slight change of the temperature. The lag was much more pronounced in large vessels and at lower temperature. It was short if the final pressure reached was considerably below the second explosion limit. No consistent results were found for variations of fo_2 except that time lags were found at small fo_2 under conditions in which none were found at large fo_2.

This inhibition period is probably caused by the time necessary to build up a sufficient quantity of chain carriers. Nalbandjan[14] has shown the existence of a true induction period in the explosion peninsula. He was able to explain the experimental results by considering the rate of change of H atom concentration. Our observed time lags at the second limit are consistent with the predicted dependence of the induction period on temperature and vessel size.

VII. BRANCHING *VERSUS* NONBRANCHING

Lewis and von Elbe[3] have discussed the opposed interpretations of the chains as branched or nonbranched. It seems to us that the statements made by the various authors do not seriously disagree. Oldenberg and Sommers[15] plotted the log of the rates in the conventional fashion against $1/T$ in order to apply the criterion of Semenoff for branched chains. According to Semenoff's theory, these curves are straight lines for nonbranched chains but curve up at increasing temperature for branching chains. Over a considerable temperature interval the curves are straight. Such straight lines had been found much earlier by Prettre.[16] The authors interpreted these observations as an argument for nonbranched chains; they did not exclude the possibility of branching processes at higher temperatures.

Lewis and von Elbe correctly called attention to a source of error (effect of water vapor produced during the mixing) and repeated the observations; but their result was the same: "but for the highest temperatures, the curves approximate straight lines." This result is compatible with their theory and indicates that above about 550°C the branching dominates. However, at lower temperatures the branching gradually recedes. Although the reaction still consists of the same chain with a changed probability of the steps, the rate does not depend as much upon the branching. This is compatible with the numerical values given by Lewis and von Elbe. The competition between branching and nonbranching is identical with the competition between reactions 2 and 4. The k values given by Lewis and von Elbe permit the computation of the fate of an H atom. For example, at 510°C it is 30 times as probable that an H atom goes into the breaking step 4 than that it goes into the branching step 2. (If, by way of an approximation, we neglect the branching step 2 as compared with the breaking step 4 for this temperature range, we arrive at a chain which is identical with the Bonhoeffer-Haber chain.) According to Semenoff, the straight line characteristic of the plot of the logarithm of rate as a function of the reciprocal of the absolute temperature indicates a nonbranching mechanism. Thus, over a considerable temperature range of the volume reaction, the chain branching is small compared to the chain breaking.

Thanks are due Professor G. B. Kistiakowsky for the loan of his sensitive manometer.

[14] A. Nalbandjan, Acta Physicochimica U.R.S.S. **19**, 483–507 (1944).

[15] O. Oldenberg and H. S. Sommers, Jr., J. Chem. Phys. **9**, 573 (1941).

[16] M. Prettre, J. chim. phys. **33**, 189 (1936).

The Effect of Pressure on the Melting of Several Methyl Siloxanes

P. W. BRIDGMAN
Jefferson Physical Laboratory, Harvard University, Cambridge, Massachusetts
(Received October 10, 1950)

Previous experiments had left open the possibility that the melting phenomena of the methyl siloxanes might be an exception to the universal behavior of all other known substances, namely, that there is no experimental evidence for a critical point between solid and liquid or for a maximum or temperature asymptote on the melting curve. The special apparatus necessary for an examination of the siloxanes in this respect has been constructed, and it has been found that they do not constitute any exception. The abnormality of their melting behavior is sufficiently explained by abnormal subcooling effects connected with the abnormally large increase of viscosity of these substances under pressure.

INTRODUCTION

PREVIOUS measurements on the viscosity and compressibility of a number of methyl siloxanes, i.e., the series of compounds with the formula:

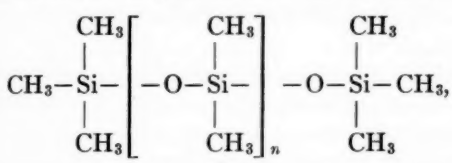

where n runs from 0 (dimer) to 6 (octamer), brought to light an unusual state of affairs with respect to the melting phenomena of these substances.[1] The normal melting point of these substances at atmospheric pressure is confined within the range from $-59°$ to $-86°$. Within this range, there is no regular progression with molecular weight; but the melting temperature oscillates back and forth as one progresses in the series toward increasing molecular weight. This behavior is anomalous, the usual behavior in a series of similar compounds being for the melting point to increase with increasing molecular weight, as in the series of alcohols, for example. Not only this, but the effect of pressure on the melting point is anomalous in that only a single one of the compounds, namely, the dimer, in the experiments referred to above which were made at 25°C, was brought to freeze by the action of pressure, all the other from the trimer to the octamer remaining liquid over a pressure range reaching up to 40,000 kg/cm². It would be normal for the members of the series of higher molecular weights to be brought to freeze first by the action of pressure.

These facts raised the question whether there may be something drastically different from normal in the melting mechanisms of these compounds. In particular, might the abnormality be of such a kind as to vitiate the generalization which I had made from every other known experiment on the effect of pressure on melting temperature? This generalization is that there is no critical point between liquid and solid, but the melting curve continues to rise indefinitely with increasing pressure, and the difference of volume between liquid and solid decreases with rising pressure in such a way that there is no indication that the volume difference will extrapolate to zero. The reason for this generalization about the melting curve is, I think, not even yet adequately explained theoretically, so that there is still an inclination in some quarters to regard a continuous passage from liquid to solid, such as would be implied by a critical point, as a possibility to be seriously considered. The failure of pressures up to 40,000 kg/cm² to force the trimer or any higher members of the series to freeze at room temperature might mean that room temperature is above a critical point for these substances, or might mean that the melting curve has a maximum at a lower temperature, a maximum as well as a critical point being ruled out by the experimental generalization. As long as there was no adequate theoretical background, it seemed to me that the suspicion that the generalization might not be valid could be laid only by direct experimental attack, although I had already stated[2] that it seemed probable that the failure of the solid phase to appear was a subcooling effect due to the abnormally great increase of the viscosity of these substances under pressure.

APPARATUS AND EXPERIMENTAL METHOD

Specially constructed apparatus is necessary because the former techniques are not applicable to these siloxanes, because there seems to be no suitable liquid with which to transmit pressure to them. Mercury cannot be used, because it freezes in the range of pressure and temperature anticipated; and there seems to be no other liquid which is not miscible with the siloxanes to some extent. A modification of the method used in the experiments to 40,000 kg/cm² was therefore indicated, in which the siloxane was completely enclosed in a lead capsule, and pressure transmitted to it by the collapse of the capsule. The pressure range of the experiments anticipated here was much lower than 40,000, so that an uncertainty in the pressure due to the strength of the capsule which before might be tolerable was now out of the question. The new apparatus must, therefore, be of such proportions that the error due to the restraining effect of the capsule is small enough to be eliminatable.

[1] P. W. Bridgman, Proc. Am. Acad. 77, 117–128, 129–145 (1949).

[2] Reference 1, page 145.

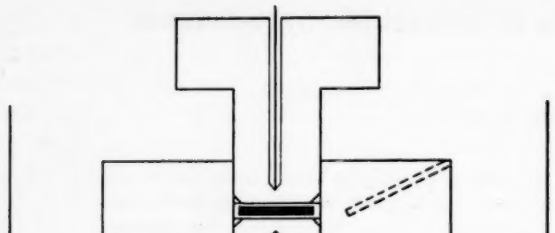

FIG. 1. General scheme of the apparatus. The liquid is shown in black, sealed into a lead disk-shaped capsule.

The apparatus is shown in Fig. 1. The pressure vessel takes the form of a heavy steel collar 4-inch o.d., $\frac{3}{4}$-inch i.d. and $1\frac{1}{8}$ inch thick. The interior is given a smooth finish. Pressure is applied by means of two pistons inserted from the two ends. The maximum pressure reached in these experiments was something over 6000 kg/cm², although the apparatus is capable of considerably more. The lead capsule containing the fluid is $\frac{3}{16}$ inch thick, and its cylindrical walls are 0.042 inch thick. The conical brass sealing rings shown in the diagram prevented lead from leaking past the pistons. By making the capsule thin compared with the diameter, it is obvious that the effect of friction on the cylindrical surface is much reduced; and by making the walls thin, the effect of the resistance of the lead to plastic yield is minimized. In general, the difference of pressure at a fixed piston position with increasing and decreasing pressure was of the order of 200 kg/cm², or 100 kg/cm² on the mean. The actual error should be materially less than this, because the differences were consistent. The volume changes were obtained from the relative displacements of the pistons, measured with an Ames 1/10,000-inch jeweled gauge, mounted on a yoke and connected to the pistons with two feeler rods, as indicated. These feeler rods took off the displacement from points near the flat ends of the pistons, thus avoiding error from the elastic distortion of the pistons. Readings were smooth and consistent to a small fraction of the smallest gauge divisions, or to two or three 1/100,000ths inch.

Temperature was controlled by a bath contained in the can built around the lower piston as indicated. The bath liquid for temperatures below 0°C was alcohol, cooled by the addition of CO_2 snow, and stirred with three turbine stirrers. Temperature was read with a copper-constantan thermocouple inserted into a well drilled in the side of the pressure vessel as indicated and connected with a short period galvanometer of sufficient sensitivity. Temperature control was manual. My assistant, Mr. Charles Chase, continually watched at the galvanometer during the experiment and added CO_2 snow as the galvanometer indicated. The control was considerably better than 1 degree. Automatic control was not attempted because the small number of measurements anticipated did not justify the time that would have been demanded for the construction of the apparatus. Temperatures above 0° were by a water bath, also controlled manually.

The pistons were pushed together in a standard 3.5-inch press. This was actuated by a hand pump, and was coupled to a 0.25-inch free piston gauge. The pressures were controlled by manipulating the weights of the free piston gauge. The general method of measurement was the same as in all my other determinations of meltings under pressure, namely, by measuring piston displacement at constant temperature.

The material I owe to the courtesy of Mr. Shailer L. Bass of the Dow Corning Company; it was the identical material which had been formerly used in measurements to 40,000 kg/cm².

In addition to the measurements under pressure, the melting temperatures at atmospheric pressure were also determined. At first it was attempted to find these points by the method of temperature arrest. The material was placed in a test tube with a thermocouple in the center of the mass. The tube was cooled by immersing in liquid air, and the temperature indicated by the thermocouple recorded as a function of time. This was done both for cooling and for the spontaneous warming on removal from liquid air. Temperature arrest points were found, but it proved that these were not reliable indications of the equilibrium temperature between solid and liquid because of the great degree of sub-cooling which these substances will tolerate and the sluggishness of crystallization or melting when it occurs. The method could doubtless be made to work more satisfactorily by the construction of suitable apparatus; but with the crude apparatus which I used temperature gradients were so great that a temperature arrest at the point of the thermocouple did not necessarily indicate a freezing or melting at that point, but only a freezing or melting at some other neighboring point and at a different temperature, the heat set free there during the process being sufficient to upset the regular march of temperature at the couple. Better freezing points at atmospheric pressure were given by the temperatures indicated by the couple when it was used as a stirrer in a mush of liquid and solid. There was a further difficulty in determining the atmospheric freezing points because sometimes it was very difficult to make the crystalline solid appear, but a glass formed instead which was not always easy to distinguish from the true solid. As it was, I succeeded in getting atmospheric freezing points of only the dimer, trimer, and tetramer. No certain results could be found for the pentamer and hexamer; although these could be made to "solidify," the solid was a mixture of glass and perhaps some true crystal, the latter present in too small amount to yield any

definite equilibrium temperature. In the following, I have preferred to use as more reliable the melting temperatures at atmospheric pressure determined at the Dow Corning Research Laboratory.[3] They give for the melting temperatures of the dimer, trimer, and tetramer −68°, −86°, −76°, respectively, against my values −70°.8, −87°.0, and −71°.2.

In making the pressure measurements, the general scheme of attack, in order to minimize as far as possible difficulties due to subcooling and sluggishness, was to start at the lower temperatures, where freezing is presumably easier, and work up, taking pains to go from each temperature to the next higher with pressure high enough to maintain the solid phase, so that in this way, one could be sure of at least getting a melting at the next higher temperature even if direct formation of the solid out of the liquid at that temperature might prove to be impossible. In principle, it would be possible by this method to find the melting at any temperature and pressure, no matter how high, even after the solid had been lost, by again lowering the temperature and approaching the melting through the solid phase induced at lower temperatures and pressures. Such manipulations were attempted here in only one or two cases, since the lowering of the temperature of the whole apparatus after obtaining a melting at a higher temperature was a matter of some inconvenience. Furthermore, such did not prove necessary, because it soon appeared how the land lay. To anticipate, it was as I had surmised; there is no abnormality in the course of the melting curve or in the volume relations, but all the appearance of possible abnormality is connected with the sluggishness of the reaction, which is much accentuated by the enormous effect of pressure on viscosity.

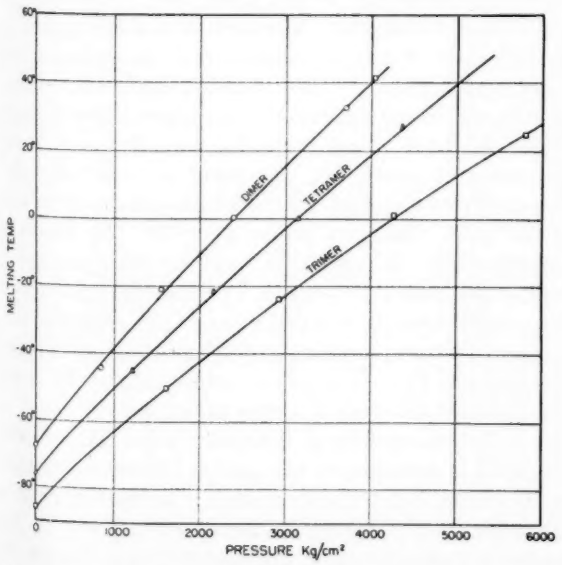

FIG. 2. The melting temperatures of the three lowest methyl siloxanes as a function of pressure.

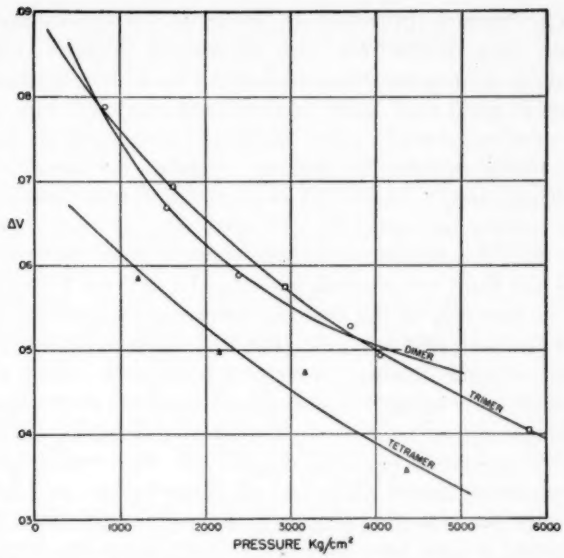

FIG. 3. The change of volume on freezing in cm³/gm of the three lowest methyl siloxanes as a function of pressure.

THE EXPERIMENTAL RESULTS

Results were obtained under pressure only for the first three members of the series, the dimer, trimer, and tetramer. In spite of two attempts, I did not succeed in making the hexamer freeze in the pressure apparatus. In the second of these attempts I employed all the wiles at my command. The liquid in the capsule was inoculated with scraps of glass wool, asbestos, and mica, it being well known that freezing often is initiated at the right kind of surface. I had long ago found that glass wool is often effective in initiating a stubborn freezing. The capsule thus inoculated was kept in liquid nitrogen overnight before mounting in the pressure apparatus. In the pressure apparatus pressure was raised to over 6000 kg/cm² at −40° and released; temperature was then lowered to −70° and pressure applied to 4000 and pressure then released to nearly atmospheric. From here the apparatus was allowed to warm slowly to nearly 0°, the pressure spontaneously rising during the warming to 4000 again. All this was without effect.

The freezing results for the dimer, trimer, and tetramer are given in Figs. 2 and 3; in Fig. 2 the melting temperatures as a function of pressure, and in Fig. 3 the changes of volume on melting, in cm³/gm, as a function of pressure. Table I contains various melting parameters at even pressure intervals as obtained from the smooth curves drawn through the experimental points of Figs. 2 and 3. As already mentioned, the melting temperatures at atmospheric pressure given in the table are the values determined at the Dow Corning Laboratory. For the sake of smoothness, an additional significant figure has been arbitrarily added to the Dow Corning results.

[3] Hunter, Warrick, Hyde, and Currie, J. Am. Chem. Soc. **68**, 2284-2290 (1946).

The freezing pressures as given in the figures and table were determined with decreasing pressure. On increase of pressure subcooling of the liquid was in most cases so great that when freezing once started it ran to completion, so that a point could not be obtained on the two-phase system. On release of pressure, however, melting always started at once without superheating and a reading could be obtained on the two-phase system. This reading was usually made when the solid was less than half melted, and may be in error because of the lowering of the freezing point due to impurities. The pressure taken at this point was the indicated pressure, without attempt at correction for the effect of friction and strength of capsule. Error from this effect is in the opposite direction from error due to impurity, and I optimistically hoped that the two would approximately cancel. However, all three liquids were not equally pure, so that the error from this procedure is greater for some than for others. Impurity in the dimer was noticeably greater than for the others, judging by the premature rounding of the corner of the melting curve on release of pressure. The rounding of the corners for the dimer got progressively worse on successive runs at successively higher temperatures; it is to be considered whether there might have been some decomposition.

Of the three substances measured, the trimer was notably the most difficult to get to freeze. Even after the recent occurrence of the solid phase in the capsule, excess pressures of the order of 2000 kg/cm² were required at all temperatures to induce freezing, against something of the order of 1000 for the tetramer and 700 for the dimer. The tetramer on two occasions showed an effect found only a few times previously, namely, that on the first increase of pressure beyond the freezing point, the freezing does not run, but does run on release of pressure from its maximum. On the first set-up with the tetramer pressure was raised at 0° to 6200 kg/cm², without freezing; temperature was then lowered at constant pressure to −50° without freezing, and at this temperature pressure released, whereupon freezing took place on reaching 4.000. On the second set-up, the initial application of pressure was made at −44.8°. Again pressure was raised to 6200 kg/cm² without freezing. On release of pressure at the same temperature freezing occurred at 4300 kg/cm². It suggests itself that the process of nucleus formation is multiple. The high pressure results in the formation of some sort of complex which predisposes to the formation of a nucleus of the crystal when the pressure has been sufficiently reduced so that the viscosity can be overcome.

TABLE I. Melting curve parameters.

Pressure kg/cm²	Temp. °C	$\frac{dT}{dp}$	ΔV cm³/gm	Latent heat kg cm/gm	$\frac{\Delta S}{\tau}$ kg cm/gm	$p\Delta V$ kg cm/gm	ΔE kg cm/gm
			Dimer				
0	−68.0	0.0318					
500	−52.5	0.0302	0.0840	613	2.78	42.0	571
1000	−37.7	0.0288	0.0746	610	2.59	74.6	535
2000	−10.2	0.0265	0.0623	618	2.35	124.6	493
3000	+15.5	0.0251	0.0551	634	2.20	165.3	469
4000	+40.2	0.0242	0.0505	654	2.09	202.0	452
			Trimer				
0	−86.0	0.0240					
500	−74.3	0.0230	0.0825	713	3.59	41.2	672
1000	−63.0	0.0220	0.0760	728	3.45	76.0	652
2000	−41.9	0.0201	0.0654	752	3.25	130.8	621
3000	−22.6	0.0186	0.0568	765	3.05	170.4	595
4000	−4.2	0.0173	0.0500	778	2.89	200.0	578
5000	+12.5	0.0161	0.0445	791	2.77	222.5	569
6000	+28.0	0.0150	0.0394	793	2.63	236.4	557
			Tetramer				
0	−76.0	0.0269					
500	−62.7	0.0259	0.0661	537	2.55	33.0	504
1000	−50.0	0.0250	0.0612	547	2.45	61.2	486
2000	−25.7	0.0235	0.0525	553	2.23	105.1	448
3000	−2.9	0.0222	0.0452	552	2.04	135.6	416
4000	+18.7	0.0211	0.0389	538	1.84	155.6	382
5000	+39.6	0.0203	0.0335	518	1.65	167.5	350

In addition to the melting parameters certain other partial thermodynamic information can be obtained from the various curves of piston displacement against pressure at various temperatures. In the first place, the measurements would be capable of yielding compressibilities if made over a sufficient range and with that purpose in view. It was checked roughly, within 3 or 4 percent, that the compressibility of the dimer agrees with the previously published value up to 3500. No attempt was made to wring the last possible drop of information on this point out of the data, since if this were the purpose, it would be preferable to obtain new data with this object specially in view.

The difference of slopes of the isothermals above and below the melting gives the difference of compressibility between liquid and solid phases. In all cases the solid is less compressible; as far as I know, this is a generalization without exception. The best numerical values for the difference of compressibility were obtainable at the lower temperatures. The following numerical values were found for the difference of compressibility between liquid and solid at the reversible melting point at the temperatures given. For the dimer at −44° the compressibility of the liquid is 0.0000162 greater than that of the solid. For the trimer at −50° the excess of compressibility is 0.0000128; and for the tetramer at −45°, the excess is 0.0000130. The pressure unit in these compressibilities is the kg/cm², and the compressibility is referred to unit volume of the liquid at atmospheric pressure and 25°, using in the computations the densities given by the Dow Corning Laboratory.

A sufficient number of isotherms were taken to give the effect of pressure on the average thermal expansion of the trimer and tetramer over a temperature range of the order of 75°. The results are given in Table II. The figures in parentheses at atmospheric pressure are the Dow Corning results for the temperature range 25° to 100°. As usual, thermal expansion decreases with rising pressure. The table indicates a large increase of expansion on passing from 500 kg/cm² to atmospheric

pressure. This recalls the unusually large drop of compressibility of this class of substance in the low pressure range. The present figures would indicate that the thermal expansion is fully as variable with pressure as the compressibility; usually the compressibility is more variable than expansion.

CONCLUSION

Figures 2 and 3 and Table I contain the answer to the question which prompted this investigation. The thermodynamic parameters which might indicate anything abnormal in the character of the melting curve, and which, in particular, might indicate by the way in which they extrapolate whether a critical point or a maximum temperature or a temperature asymptote is to be anticipated, are quite like those of all other substances investigated, with no suggestion of any abnormality. In particular, the difference of volume between liquid and solid when plotted against either pressure or temperature is convex toward the pressure or temperature axis with no indication that it will ever vanish by cutting the axis, as it must if there is a critical point or maximum temperature. The slope of the melting curve, dt/dp, when plotted against either pressure or temperature is also convex toward pressure or temperature axis, with no suggestion that it will ever vanish, as it must if there is a maximum temperature or a temperature asymptote. The latent heat changes comparatively little along the melting curve; it rises after a flat minimum for the dimer, rises continuously for the trimer, and falls for the tetramer after a flat maximum. If there were a critical point, the latent heat would extrapolate to zero; and furthermore, the extrapolated pressure or temperature at which it vanishes would have to be the extrapolated pressure or temperature at which the volume difference vanishes, which does not occur.

TABLE II. Thermal expansion as function of pressure.

Pressure kg/cm²	Trimer, mean expansion −50° to +25°	Tetramer, mean expansion −45° to +27°
0	(0.00145)	(0.00131)
500	0.00035	0.00055
1000	0.00030	0.00049
1500	0.00027	0.00044
2000	0.00025	0.00041
3000	0.00023	0.00035
4000	0.00022	0.00031

There is, therefore, nothing in the behavior of these unusual substances to vitiate the generalization from all other experiments on the effect of pressure on melting. This generalization is that there is no present experimental reason to anticipate anything except an indefinite rise of the melting curve with increasing pressure, with continually decreasing curvature, with a difference of volume between the two phases convex toward pressure or temperature axis and with no indication of any eventual vanishing, and with no indication of a critical point, maximum temperature, or temperature asymptote. The failure to find the melting curve at room temperature of any of these substances except the dimer, which gave rise to this investigation, must be ascribed to the abnormally rapid increase of viscosity of these substances under pressure, which would prevent the formation of a nucleus of the solid. The other abnormalities in the melting phenomena as indicated by the unusual sequence of the melting temperatures with increasing molecular weight will probably have to wait for their elucidation until the x-ray structure of the solid phases has been determined. If the different polymers crystallize in different systems, there would be a basis for irregularity in the sequence of melting temperatures.

Binding Regions in Diatomic Molecules*

THEODORE BERLIN†
Department of Chemistry, University of Michigan, Ann Arbor, Michigan
(Received June 16, 1950)

The concept of intramolecular binding is given a precise definition in a way that relates binding to the forces acting on the nuclei in a diatomic molecule. A consequence of the definition is that the space around the nuclei may be separated into binding and antibinding regions. These regions are described and they depend on the Coulomb law of force and on the ratio of the nuclear charges: the internuclear distance is simply a scale parameter. The influence of a single electron on the binding due to other electrons is briefly discussed.

I. INTRODUCTION

A KNOWLEDGE of the electron distribution in a molecule is a fundamental requirement for the understanding of the chemical behavior of the molecule. The difficulties involved in obtaining an accurate wave function for other than the simplest molecules $(H_2)^+$ and H_2 are very great. The approximate methods which have been devised yield results which, in general, are only roughly in agreement with experiment. In this paper, the approach to the problem of binding shall be essentially qualitative.

It is the purpose of this paper to consider binding in diatomic molecules and to develop the idea of binding regions in the space around the nuclei. The word "binding" shall be defined in such a way that it relates to the *forces* acting on the nuclei in the molecule. Thus, *binding* shall be distinguished from *bonding* which is usually[1] related to the *energy* of the molecule. The bonding by a single electron is related to the energy of this electron in the molecule; in the same sense, the binding by a single electron will be related to the forces exerted by this electron on the nuclei.

In this study it is supposed that the diatomic molecule is free and, therefore, exists in stationary energy states determined by the appropriate Schrödinger Eq. (1). The charge distribution in such states is independent of the time, and it can be expected that the consideration merely of the electrostatic interaction between the nuclei and the electronic charge distribution within the molecule may be helpful for the understanding of its properties (Comm. II). Thus, it will be examined whether such a relatively simple picture can be considered as a desirable approximation.

It will be first shown on the basis of wave mechanics that the electric forces exerted on the nuclei by the molecular electron distribution can be interpreted from the electrostatic viewpoint when the molecule is in a stationary state, even though this charge distribution is dependent on the electronic motion. A definition of binding in terms of the electric forces will then be given. Electron spin and the Pauli principle will then be taken into account, and the electrostatic viewpoint will be shown to be maintained. Some consequences of the definition, such as the separation of space into binding and antibinding regions, and the influence of a single electron on the binding due to other electrons will be discussed.

II. THE WAVE MECHANICAL FOUNDATION

In describing the electronic wave function of a diatomic molecule, the usual Born-Oppenheimer[2] approximation is assumed, that is, the nuclei are assumed to be fixed at a given internuclear distance R. The electronic wave function ψ_e and the molecular energy E_e (not including the energy arising from nuclear motion) satisfy the Schrödinger equation

$$H\psi_e=(T+V)\psi_e=E_e\psi_e, \tag{1}$$

where T, the electronic kinetic energy operator

$$=-\frac{h^2}{8\pi^2 m}\sum_{i=1}^{N}\left(\frac{\partial^2}{\partial x_i^2}+\frac{\partial^2}{\partial y_i^2}+\frac{\partial^2}{\partial z_i^2}\right);$$

V, the potential energy

$$=\frac{Z_1Z_2e^2}{R}-\sum_{i=1}^{N}\left(\frac{Z_1e^2}{r_{1i}}+\frac{Z_2e^2}{r_{2i}}\right)+\sum_{i<j}\frac{e^2}{d_{ij}};$$

N is the number of electrons in the molecule; x_i, y_i, z_i are the Cartesian coordinates of the ith electron; r_{1i} is the distance of the ith electron from the nucleus of charge $+Z_1e$; r_{2i} is the distance of the ith electron from the nucleus of charge $+Z_2e$; and d_{ij} is the distance between the ith and jth electrons.

The internuclear distance, R, occurring in V is regarded as an external parameter. In general, E_e will be a function of R, and ψ_e will depend on R in addition to the coordinates of all the electrons. The equilibrium value of R, R_{eq} is that value which minimizes $E_e(R)$.

It is important for this study to show the validity of

* Communication VII on "The Electronic Structure of Molecules." See the previous communications: II, T. Berlin and K. Fajans, J. Chem. Phys. **10**, 691 (1942); VI, K. Fajans and T. Berlin, Phys. Rev. **63**, 309 (1943). See also K. Fajans, Chem. Eng. News **27**, 900 (1949). These papers will be referred to as Comm. II or VI and CEN.

† Present address: Department of Physics, Johns Hopkins University, Baltimore 18, Maryland.

[1] G. Herzberg, *Molecular Spectra and Molecular Structure I* (Prentice-Hall, Inc., New York, 1939).

[2] M. Born and R. Oppenheimer, Ann. Physik **84**, 457 (1927).

the relation

$$\partial E_e/\partial R=\langle\partial V/\partial R\rangle_{Av}$$
$$\equiv\int\cdots\int\psi_e^*(\partial V/\partial R)\psi_e d\tau_1 d\tau_2\cdots d\tau_N, \quad (2)$$

where $d\tau_i=dx_i dy_i dz_i$ and the integration is over all space.

Equation (2) was derived by Hellmann[3] and by Feynman,[4] but their derivations have been criticized by Coulson and Bell.[5] It will be shown, however, that Eq. (2) is valid under the conditions stated by the former authors.

Following Feynman, let us suppose that the Hamiltonian H of a system contains a parameter λ, and that the system is in a stationary state ψ. Therefore, $H\psi=E\psi$, where E is the energy of the state, and we shall assume that $\int\psi^*\psi d\tau=1$. We then have

$$E=\int\psi^*H\psi d\tau,$$

and

$$\partial E/\partial\lambda=\int\psi^*(\partial H/\partial\lambda)\psi d\tau$$
$$+\int(\partial\psi^*/\partial\lambda)H\psi d\tau+\int\psi^*H(\partial\psi/\partial\lambda)d\tau.$$

As H is a self-adjoint operator,

$$\int\psi^*H(\partial\psi/\partial\lambda)d\tau=\int(\partial\psi/\partial\lambda)H\psi^*d\tau.$$

Since $H\psi=E\psi$ and $H\psi^*=E\psi^*$, we have

$$\partial E/\partial\lambda=\int\psi^*(\partial H/\partial\lambda)\psi d\tau$$
$$+E\int(\partial\psi^*/\partial\lambda)\psi d\tau+E\int\psi^*(\partial\psi/\partial\lambda)d\tau,$$

$$\partial E/\partial\lambda=\int\psi^*(\partial H/\partial\lambda)\psi d\tau$$
$$+E(\partial/\partial\lambda)\int\psi^*\psi d\tau=\int\psi^*(\partial H/\partial\lambda)\psi d\tau,$$

because

$$(\partial/\partial\lambda)\int\psi^*\psi d\tau=(\partial/\partial\lambda)1=0.$$

The kinetic energy operator T is independent of λ. Hence,

$$\partial H/\partial\lambda=(\partial T/\partial\lambda)+(\partial V/\partial\lambda)=\partial V/\partial\lambda.$$

Consequently,

$$\partial E/\partial\lambda=\int\psi^*(\partial V/\partial\lambda)\psi d\tau.$$

This concludes Feynman's derivation, when $\lambda=R$.

We may also consider the following derivation of Eq. (2). Let $\lambda'=\lambda+\delta\lambda$ and $H'\psi'=E'\psi'$, the primes denoting the use of λ'. If T is independent of λ, then

$$H'=T+V'=T+V+(\partial V/\partial\lambda)\delta\lambda+\cdots=H+H_1.$$

Now H_1 can be regarded as a perturbation, the unperturbed wave equation being $H\psi=E\psi$. Applying the usual perturbation theory, we find that

$$\lim_{\delta\lambda\to0}\frac{E'-E}{\delta\lambda}=\frac{\partial E}{\partial\lambda}=\int\psi^*\frac{\partial V}{\partial\lambda}\psi d\tau,$$

assuming that ψ is normalized to unity.

The objection raised by Coulson and Bell to Eq. (2) is as follows. Since $E=\bar{H}$, then

$$\partial E/\partial\lambda=\partial\bar{H}/\partial\lambda=(\partial\bar{T}/\partial\lambda)+(\partial\bar{V}/\partial\lambda).$$

If $\partial E/\partial\lambda=\langle\partial V/\partial\lambda\rangle_{Av}$, then Feynman, according to Coulson and Bell, must have implied that

$$\text{(a)}\quad\partial\bar{T}/\partial\lambda=0\qquad\text{(b)}\quad\partial\bar{V}/\partial\lambda=\langle\partial V/\partial\lambda\rangle_{Av}. \quad (3)$$

However, as the latter point out, it can be shown that

$$\partial\bar{T}/\partial\lambda\neq0\quad\text{and}\quad\partial\bar{V}/\partial\lambda\neq\langle\partial V/\partial\lambda\rangle_{Av}, \quad (4)$$

and, as a consequence, Eq. (2) must be incorrect.

If we identify λ with the internuclear distance R of a diatomic molecule, then it is physically plain that the relations (4) are correct. However, the relations (3) are not implied in the derivation of Eq. (2), as Coulson and Bell assume. The following analysis, which follows Hellmann in principle, demonstrates why the relations (4) and Eq. (2) do not contradict each other. The fundamental reason for their coexistence is the assumption of a stationary state for all values of the parameter λ and the associated fact that the eigenvalue E is an extremum for a certain class of variations of the wave function ψ.

The relation $\partial E/\partial\lambda=\partial\bar{H}/\partial\lambda=\langle\partial H/\partial\lambda\rangle_{Av}$ does not imply $\partial\bar{T}/\partial\lambda=\langle\partial T/\partial\lambda\rangle_{Av}$ and $\partial\bar{V}/\partial\lambda=\langle\partial V/\partial\lambda\rangle_{Av}$. The reason for this is simply that ψ is neither an eigenfunction of the operator T nor of the operator V, whereas ψ is an eigenfunction of $H=T+V$.

The fact that E is an eigenvalue implies that if the eigenfunction ψ is varied by $\delta\psi$, then for H unvaried,

$$\delta E=\delta\int\psi^*H\psi d\tau=\int\delta\psi^*H\psi d\tau+\int\psi^*H\delta\psi d\tau=0.$$

The relation holds when the variation function $\delta\psi$ is well behaved. Now let $\delta\psi=(\partial\psi/\partial\lambda)\delta\lambda$. We expect, in general, that $(\partial\psi/\partial\lambda)$ will be a well-behaved function and so will define a suitable $\delta\psi$. Then,

$$\int(\partial\psi^*/\partial\lambda)H\psi d\tau+\int\psi^*H(\partial\psi/\partial\lambda)d\tau=0.$$

[3] H. Hellmann, *Einführing in die Quantenchemie* (Leipzig, 1937), p. 285.
[4] R. P. Feynman, Phys. Rev. **56**, 340 (1939).
[5] C. A. Coulson and R. P. Bell, Trans. Faraday Soc. **41**, 141 (1945).

Since T does not depend on λ, this equation can be written as

$$(\partial\bar{T}/\partial\lambda)+\int(\partial\psi^*/\partial\lambda)V\psi d\tau + \int\psi^*V(\partial\psi/\partial\lambda)d\tau=0. \quad (5)$$

Since

$$\partial\bar{V}/\partial\lambda=\langle\partial V/\partial\lambda\rangle_{Av}+\int(\partial\psi^*/\partial\lambda)V\psi d\tau + \int\psi^*V(\partial\psi/\partial\lambda)d\tau,$$

we are immediately led to Eq. (2).

The reason for the coexistence of Eqs. (4) and (2) is clear. The assumption of the stationary state for all λ implies that when a change $\delta\lambda$ is made, then both ψ and V are changed, and that the change in the average kinetic energy due to the change in ψ is just canceled by that part of the change of the average potential energy which is due to the change in ψ. Thus, the resulting change in E is given by the average of the change in V.

III. A DEFINITION OF BINDING

The external force, which may be purely mechanical, required to hold the nuclei fixed at the distance R is

$$F=-\partial E_e/\partial R=-\langle\partial V/\partial R\rangle_{Av}.$$

As the interelectronic distances d_{ij} are independent of R,

$$\frac{\partial V}{\partial R}=-\frac{Z_1Z_2e^2}{R^2}+\sum_{i=1}^{N}\left(\frac{Z_1e^2}{r_{1i}^2}\frac{\partial r_{1i}}{\partial R}+\frac{Z_2e^2}{r_{2i}^2}\frac{\partial r_{2i}}{\partial R}\right),$$

and

$$F=\frac{Z_1Z_2e^2}{R^2}-\sum_{i=1}^{N}\int\cdots\int\psi_e^* \times\left(\frac{Z_1e^2}{r_{1i}^2}\frac{\partial r_{1i}}{\partial R}+\frac{Z_2e^2}{r_{2i}^2}\frac{\partial r_{2i}}{\partial R}\right)\psi_e d\tau_1\cdots d\tau_N. \quad (6)$$

We can integrate over all the electron coordinates except those of the ith electron. Therefore, let

$$\rho_i(x_i, y_i, z_i)=\int\cdots\int'\psi_e^*\psi_e d\tau_1\cdots d\tau_N, \quad (7)$$

the prime signifying the omission of the integration over the coordinates of the ith electron. ρ_i is the probability density of the ith electron at x_i, y_i, z_i regardless of where all the other electrons might be, and $e\rho_i d\tau_i$ is the magnitude of the charge of the ith electron in the volume element $d\tau_i$. Then,

$$F=\frac{Z_1Z_2e^2}{R^2}-\sum_{i=1}^{N}\int\left(\frac{Z_1e^2}{r_{1i}^2}\frac{\partial r_{1i}}{\partial R}+\frac{Z_2e^2}{r_{2i}^2}\frac{\partial r_{2i}}{\partial R}\right)\rho_i d\tau_i.$$

The quantity in parentheses depends only on the point in space. If we fix our attention on the point x, y, z in the volume element $d\tau$, we may write

$$F=(Z_1Z_2e^2/R^2)-\int[(Z_1e^2\partial r_1/r_1^2\partial R) + (Z_2e^2\partial r_2/r_2^2\partial R)]\rho d\tau, \quad (8)$$

where

$$\rho(x, y, z)=\sum_{i=1}^{N}\rho_i(x, y, z)$$

and $e\rho d\tau$ is the magnitude of the total electronic charge at the point x, y, z in the volume element $d\tau$; r_1, r_2 are the distances of the point x, y, z from Z_1, Z_2, respectively.

The electrostatic model of the molecule is shown in Fig. 1.

The derivative $\partial r_1/\partial R$ must be found when r_2 is fixed and R is changed. Thus, $\partial r_1/\partial R=\cos\theta_1$ and $\partial r_2/\partial R=0$. In a similar way, $\partial r_1/\partial R=0$ and $\partial r_2/\partial R=\cos\theta_2$. Adding the two resulting expressions for F and dividing by 2, we may write

$$F=(Z_1Z_2e^2/R^2)-\tfrac{1}{2}e^2\int f\rho d\tau, \quad (9)$$

where

$$f=(Z_1/r_1^2)\cos\theta_1+(Z_2/r_2^2)\cos\theta_2.$$

The quantity ef is simply the component along the internuclear axis of the total force exerted on the nuclei by a unit negative charge at x, y, z,

When F is positive, the external force prevents the nuclei from flying apart, i.e., prevents R from increasing. When F is negative, the external force prevents the nuclei from moving together, i.e., prevents R decreasing. The equilibrium value of R is to be determined by $F=0$.

The quantity ρ is positive and never changes sign. Therefore, we can separate the integral in Eq. (9) into regions where $f>0$ and $f<0$.

$$F=(Z_1Z_2e^2/R^2)-\tfrac{1}{2}e^2\int_{f>0}f\rho d\tau-\tfrac{1}{2}e^2\int_{f<0}f\rho d\tau. \quad (10)$$

The negative charge in regions where $f>0$ reduces the value of F, i.e., *binds* the nuclei, while negative charge in regions where $f<0$ increases the value of F. Consequently, we may define binding in the following manner. Negative charge in a region of space where f is positive is *binding*; negative charge in a region of space where f is negative is *antibinding*. The binding region, $f>0$, is separated from the antibinding region, $f<0$, by the

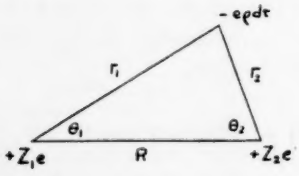

FIG. 1. The electrostatic model of a diatomic molecule.

surface of revolution $f=0$ (the internuclear axis is the axis of symmetry).

IV. ELECTRON SPIN AND THE PAULI PRINCIPLE

The preceding analysis has neglected electron spin and the Pauli Exclusion Principle and, therefore, does not yet apply to a real molecule. Consequently, we shall reconsider the problem taking into account both spin and the Pauli principle. We shall find that the preceding results are essentially unchanged and, therefore, can be applied to real molecules.

We again assume that the appropriate Schrödinger equation is Eq. (1). This means that we are neglecting all magnetic interactions involving the electron spin, but this neglect is justified to a high degree of approximation. However, each electron is now described by four coordinates, the three positional coordinates (x_i, y_i, z_i for the ith electron) and a spin coordinate (s_i for the ith electron) which takes on the two discrete values, $\pm\frac{1}{2}$. The total electronic wave function is now Ψ_e, which must involve the spin coordinates for all the electrons as well as the positional coordinates. The requirement of the Pauli Exclusion Principle is that Ψ_e is totally antisymmetric, that is, interchanging the positional and spin coordinates of any pair of electrons changes the sign of Ψ_e. Furthermore,

$$H\Psi_e=E_e\Psi_e, \tag{1'}$$

although H does not involve the spin coordinates.

The analysis of Sec. II is entirely valid if we replace $\int d\tau_i$ by $\int_{s_i} d\tau_i$, where the latter symbol means integrating the positional coordinates of the ith electron over all space and summing over the two spin values of the ith electron, and if we assume that a change in R does not introduce any important spin interactions. The normalization of the wave function now means

$$\int_e \Psi_e^*\Psi_e d\tau \equiv \int_{s_1}\int_{s_2}\cdots\int_{s_N}\Psi_e^*\Psi_e d\tau_1 d\tau_2\cdots d\tau_N=1,$$

and

$$\partial E_e/\partial R=\langle\partial V/\partial R\rangle_{Av} \equiv \int_{s_1}\cdots\int_{s_N}\Psi_e^*(\partial V/\partial R)\Psi_e d\tau_1\cdots d\tau_N. \tag{2'}$$

Continuing with Sec. III, we have

$$F=\frac{Z_1Z_2e^2}{R^2}-\sum_{i=1}^{N}\int_{s_1}\cdots\int_{s_N}\Psi_e^* \times\left(\frac{Z_1e^2}{r_{1i}^2}\frac{\partial r_{1i}}{\partial R}+\frac{Z_2e^2}{r_{2i}^2}\frac{\partial r_{2i}}{\partial R}\right)\Psi_e d\tau_1\cdots d\tau_N. \tag{6'}$$

We can integrate over the coordinates and sum over the spins of all electrons except those of the ith electron. Therefore, let

$$P_i(x_i, y_i, z_i, s_i)=\int_{s_1}\cdots\int_{s_N}{}'\Psi_e^*\Psi_e d\tau_1\cdots d\tau_N, \tag{11}$$

the prime signifying the omission of the integration over the coordinates and of the summing over the spin of the ith electron.

Since $\Psi_e^*\Psi_e$ is the probability density for a given spatial configuration of the electrons with a given arrangement of spins, $P_i(x_i, y_i, z_i, s_i)$ is the probability density of the ith electron at x_i, y_i, z_i with the spin s_i regardless of the spatial and spin configuration of all the other electrons.

We now write

$$F=\frac{Z_1Z_2e^2}{R^2}-\sum_{i=1}^{N}\int_{s_i}\left(\frac{Z_1e^2}{r_{1i}^2}\frac{\partial r_{1i}}{\partial R}+\frac{Z_2e^2}{r_{2i}^2}\frac{\partial r_{2i}}{\partial R}\right)P_i d\tau_i. \tag{12}$$

However, we can still sum over the spin s_i. Then

$$\sum_{s_i} P_i(x_i, y_i, z_i, s_i)=\rho_i(x_i, y_i, z_i), \tag{13}$$

where $\rho_i(x_i, y_i, z_i)$ has essentially the same meaning as the ρ_i in Sec. III; i.e., ρ_i is now the probability density of the ith electron at x_i, y_i, z_i regardless of its own spin and the spatial and spin configuration of all the other electrons. The quantity $e\rho_i d\tau_i$ is the magnitude of the charge of the ith electron in the volume element $d\tau_i$. The remaining discussion in Sec. III is unchanged.

Consequently, Eq. (9) is still valid with $e\rho d\tau$ still interpretable as the magnitude of the total electronic charge at the point x, y, z in the volume element $d\tau$, and the results can be applied to real molecules.

It possibly might appear strange that a simple electrostatic interpretation of the force exerted on the nuclei by the electrons in a molecule is valid, even though electron spin and the Pauli principle are taken into account. The usual "exchange" terms do not appear in the analysis. Exchange does not appear because our analysis deals with the complete electronic wave function and its rigorous interpretation. Exchange terms appear when explicit form is given to Ψ_e. Nevertheless, it must be remembered that the component parts of an explicit form for Ψ_e are not rigorously interpretable in general as physically meaningful wave functions. Furthermore, the analysis illustrates the role of the Pauli principle as a restrictive principle, that is, only those solutions of Eq. (1') which are totally antisymmetric in addition to being regular, square integrable, and mutually orthogonal are to be taken as physically meaningful. It is only these wave functions which should yield a charge distribution agreeing with experiment.

It should be noted that for a stationary state of a

molecule at equilibrium the relation

$$Z_1Z_2e^2/R_e^2=\tfrac{1}{2}e^2\int f\rho d\tau \tag{14}$$

is formally correct, to the approximation considered here, for *any* regular, square integrable solution of Eq. (1) or (1′). However, Eq. (14) has physical content only if ρ is either the experimentally determined charge distribution of the molecule or the charge distribution computed by means of the correct wave function Ψ_e.

Once the rules for defining a physically sensible wave function have been set down, then within that framework the primary factors available for a description of molecular behavior are the forces between particles (which are mainly coulomb forces) and whatever quantum numbers are inherent in the problem.

V. BINDING AND ANTIBINDING REGIONS

At this point we shall investigate the nature of the surface separating the binding and the antibinding regions. Since the surface is one of revolution, we need only discuss the plane curve

$$f=(Z_1/r_1^2)\cos\theta_1+(Z_2/r_2^2)\cos\theta_2=0.$$

A suitable coordinate system is shown in Fig. 2. Let

$$x=\tfrac{1}{2}R\xi,\quad y=\tfrac{1}{2}R\eta,\quad \alpha=Z_1/Z_2\leqslant 1.$$

Then

$$r_1^2=(\tfrac{1}{2}R+x)^2+y^2=\tfrac{1}{4}R^2[(1+\xi)^2+\eta^2],$$
$$r_2^2=(\tfrac{1}{2}R-x)^2+y^2=\tfrac{1}{4}R^2[(1-\xi)^2+\eta^2],$$
$$r_1\cos\theta_1=\tfrac{1}{2}R+x=\tfrac{1}{2}R(1+\xi),$$
$$r_2\cos\theta_2=\tfrac{1}{2}R-x=\tfrac{1}{2}R(1-\xi),$$

and the equation of the curve becomes

$$\{\alpha(1+\xi)/[(1+\xi)^2+\eta^2]^{\frac{3}{2}}\}+\{(1-\xi)/[(1-\xi)^2+\eta^2]^{\frac{3}{2}}\}=0.$$

The points $\xi=\pm 1$, corresponding to the position of the nuclei, shall be excluded for the moment. There is no solution for η when $-1<\xi<+1$, as both terms of the equation are positive. Therefore, we shall first consider the range $1<\xi<\infty$.

Let

$$0<u=(\xi-1)/\alpha(\xi+1)<1/\alpha.$$

Then, the equation of the curve may be written

$$(1-u^{\frac{2}{3}})\eta^2=u^{\frac{2}{3}}(\xi+1)^2-(\xi-1)^2=(u^{\frac{2}{3}}-\alpha^2u^2)(\xi+1)^2. \tag{15}$$

Since the right side of the equation is always positive, a solution for η is possible only for $u<1$. As $u\to 1$, $\eta^2\to\infty$; but $\alpha<1$, and, therefore, $1/\alpha>1$. Consequently, $u=1$ is a permissible value. This equation, $u=1$, defines the limiting value of ξ for $\xi>1$, i.e.,

$$\xi=(1+\alpha)/(1-\alpha)>1.$$

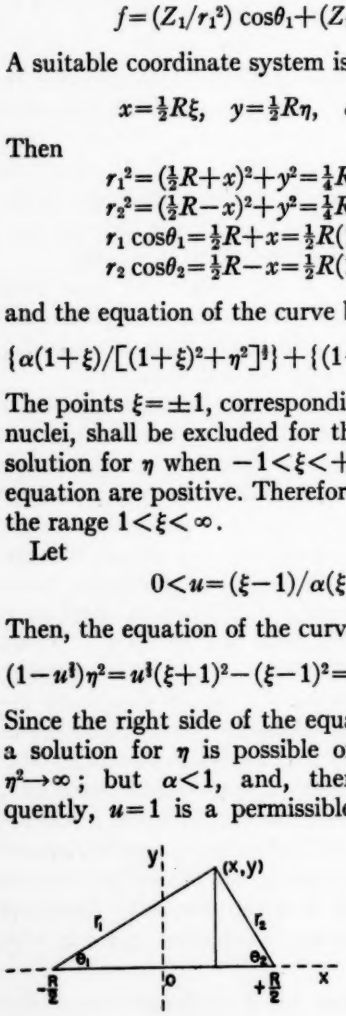

FIG. 2. The coordinate system.

The point $\xi=+1$ offers no difficulty. Let $\xi=1+\epsilon$, where $\epsilon\to+0$. Then $u\simeq\epsilon/2\alpha$, and $\xi\simeq 1+2\alpha u$ as $u\to+0$. Therefore, $(1-u^{\frac{2}{3}})\eta^2\simeq\eta^2\simeq 4u^{\frac{2}{3}}$, or $\eta\simeq\pm 2u^{\frac{1}{3}}$. Hence, $\eta\to 0$. Furthermore,

$$d\eta/d\xi\simeq\pm\tfrac{2}{3}u^{-\frac{1}{3}}du/d\xi\simeq\pm u^{-\frac{1}{3}}/3\alpha.$$

Thus, $d\eta/d\xi\to\pm\infty$, and the curve enters the point $\xi=+1$ at right angles.

For the region $-\infty<\xi<-1$, let us simply change the sign of ξ in the equation for the curve by defining $\xi=-\xi'$, and also set $\beta=1/\alpha>1$. Then we have

$$\{\beta(1+\xi')/[(1+\xi')^2+\eta^2]^{\frac{3}{2}}\}+\{(1-\xi')/[(1-\xi')^2+\eta^2]^{\frac{3}{2}}\}=0.$$

Utilizing the previous analysis, let $0<u=(\xi'-1)/\beta(\xi'+1)<1/\beta$. Thus,

$$(1-u^{\frac{2}{3}})\eta^2=(u^{\frac{2}{3}}-\beta^2u^2)(\xi'+1)^2. \tag{16}$$

Since $\beta>1$ one has $1/\beta<1$ and the point $u=1$ is excluded. A solution for η is possible only if $u^{\frac{2}{3}}-\beta^2u^2\geqslant 0$. This leads to the result that

$$1<\xi'\leqslant[(\beta)^{\frac{1}{3}}+1]/[(\beta)^{\frac{1}{3}}-1]=[1+(\alpha)^{\frac{1}{3}}]/[1-(\alpha)^{\frac{1}{3}}].$$

Consequently, η remains finite and the curve is closed. The curve enters the points

$$\xi=-1\text{ and }\xi=-[1+(\alpha)^{\frac{1}{3}}]/[1-(\alpha)^{\frac{1}{3}}]$$

at right angles. A sketch of the curve $f=0$ for $\alpha=\frac{1}{2}$ is shown in Fig. 3.

In the case of a homonuclear molecule, $\alpha=1$, the regions are, of course, symmetrical and the curve $f=0$ is open. The curve is shown in Fig. 4. An interesting feature is the following. The curve approaches a straight line asymptotically as $x\to\infty$. For ξ large, $u\simeq 1-2/\xi$. Now,

$$(1-u^{\frac{2}{3}})\eta^2=u^{\frac{2}{3}}(1-u^{\frac{2}{3}})(1+u^{\frac{2}{3}})(\xi+1)^2.$$

Therefore,

$$\eta=\pm u^{\frac{1}{3}}(1+u^{\frac{2}{3}})^{\frac{1}{2}}(\xi+1),$$

and

$$\eta\to\pm\sqrt{2}\xi+0(1/\xi). \tag{17}$$

The asymptotic line passes through the origin and $\tan\theta=\sqrt{2}$. Thus, 2θ equals 109°28′, the tetrahedral angle. This result is due to the Coulomb force law, for if the force between charges varied inversely as the nth power of the distance, then $\tan\theta=(n)^{\frac{1}{2}}$.

VI. DISCUSSION

Although the electrons cannot be strictly individualized in the many-electron molecule, it is usually a good approximation and physically fruitful to do just that. In the method of molecular orbitals the distinction of bonding and antibonding electrons is based on the criterion whether the energy level of a given electron is

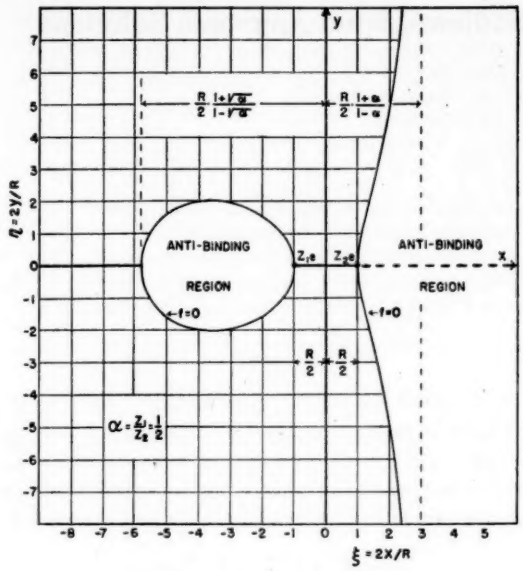

FIG. 3. Binding and antibinding regions in a heteronuclear molecule.

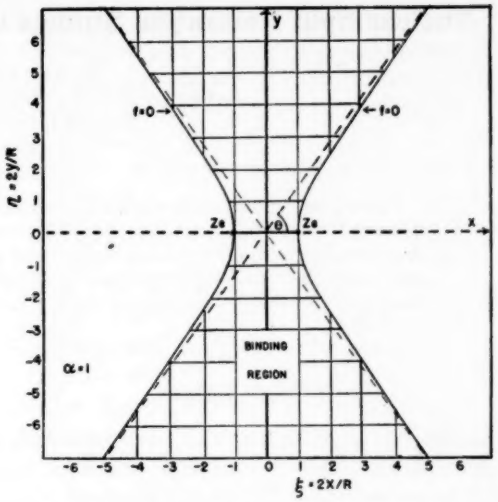

FIG. 4. Binding and antibinding regions in a homonuclear molecule.

lowered or raised respectively in the transition from separated atoms to the molecule. Applying the consideration of the forces exerted by an electron on the nuclei in an analogous manner, we shall say that an electron moves predominantly in the binding or antibinding region when $\int f\rho d\tau$ is positive or negative, respectively. The quantity $e\rho$, the charge density of the single electron, is a function of the internuclear distance. The sign of $\int f\rho d\tau$ gives a more exact interpretation of the expressions "binding region between the cores" and "antibinding region beyond the cores" (CEN).

It is not easy to classify generally the types of charge distribution which are binding or antibinding. Two simple distributions which give rise to a net binding effect are the following.

(a) An electron distribution which has one of the two nuclei as a center of symmetry is binding. This is so because the electron exerts no net force on the nucleus which is the center of symmetry, and the electron attracts the other nucleus. This point of view led (see CEN) to the conclusion that, e.g., in N_2 the four K electrons do contribute to the binding of the two N^{7+} nuclei because they screen the positive charge of the latter and reduce it to the charge of the cores N^{5+}.

(b) For an electron distribution which has elliptical symmetry with respect to the two nuclei as foci, it can be shown that $\int f\rho d\tau$ is also positive.

The binding behavior of a single electron has been investigated (Comm. VI) on the basis of the effect which the addition of the Nth electron to a system containing $N-1$ electrons has on the internuclear distance and the more sensitive force constant. The experimentally determined effect is the result of two factors which are not independent of each other.

(a) The Nth electron can move predominantly either in the binding or in the antibinding region.

(b) The Nth electron always repels the remaining N-1 electrons and, in general, reduces their binding effect.

Thus, if one finds that the addition of the Nth electron strengthens the binding, this indicates that this electron moves predominantly in the binding regions and that its binding action outweighs the effect of reducing the binding of the remaining electrons. This seems to be the case, e.g., in N_2 and HCl.

However, if one finds that the addition of the Nth electron weakens the binding, there are two alternatives. Either the electron moves predominantly in the antibinding region, as seems to be the case (Comm. VI) in hydrides of the type $BeH=e^-(Be^{2+})(H^-)$, or in spite of moving predominantly in the binding region, the binding effect of the electron is outweighed by its effect of reducing the binding action exerted by the other electrons; this was concluded to be the case in CO (CEN).

In forthcoming papers the above points of view will be applied in more detail for the elucidation of the binding in various molecules.

ACKNOWLEDGMENT

The author wishes to thank Professor K. Fajans for the many illuminating discussions of this problem. He also has to thank Dr. Beth Cook Hillig for calculating part of the data for the figures.

The grant from the Horace H. Rackham School of Graduate Studies during the academic year 1943–1944 is sincerely appreciated.

Nuclear Spin Relaxation Studies in Dilute Sodium-Liquid Ammonia Solutions

R. NEWMAN* AND R. A. OGG, JR.†
Lyman Laboratory of Physics and Mallinckrodt Chemical Laboratory, Harvard University, Cambridge, Massachusetts
(Received June 23, 1950)

The nuclear spin relaxation times of the protons in dilute solutions of sodium in liquid ammonia have been measured at 30 Mc/sec over the room temperature-dry ice range. The data can be interpreted on the basis of an associative equilibrium existing between paramagnetic and diamagnetic solute species. This is in agreement with the results of the conventional magnetic susceptibility measurements. The paramagnetic component of the solutions seems to be about one-tenth as effective as a cupric ion in inducing nuclear relaxation.

INTRODUCTION

CHEMICAL equilibria in which reactant and product species differ in magnetic moment may be studied experimentally by direct magnetic susceptibility measurements over a suitable range of concentrations and temperatures. This method has been applied, for example, to study the dissociation of substituted ethanes (dissolved in organic solvents) into the corresponding substituted free methyl radicals.[1] The procedure demands very high precision susceptibility measurements, since in dilute solutions the diamagnetism of the solvent may well exceed in magnitude the paramagnetism of the solute species.

The nuclear spin relaxation phenomenon[2,3] offers another approach to experimental study of chemical equilibria of the type mentioned above. It provides a method of measuring the concentration of a species characterized by a permanent magnetic moment of its molecules. If, for example, the relaxation time T_s of solvent molecule protons is studied in a solution containing a paramagnetic solute, then

$$1/T_s = 1/T_p + \gamma^2 C \mu_{eff}^2 F(a, D_s, D_p, \tau). \quad (1)$$

Here T_p denotes the proton relaxation time in the pure solvent; γ is the nuclear gyromagnetic ratio of the proton; C is the concentration of solute particles having magnetic moment μ_{eff}. The function F depends upon a, the distance of closest approach of a paramagnetic solute particle and a solvent proton, and upon the diffusion coefficients D_s and D_p of the solute particles and solvent molecules respectively. The dependence of F upon a is an inverse one. In a limiting case, where the relaxation process is determined solely by diffusion of solvent molecules around the paramagnetic solute particle

$$F \propto 1/aD_p. \quad (2)$$

F will in general also depend upon τ, the electronic paramagnetic relaxation time of the solute particles. In most cases, previously studied, this dependence can be neglected but each case must be considered individually.

For a given temperature Eq. (1) may be rewritten as

$$\Delta(1/T) = 1/T_s - 1/T_p = \alpha C. \quad (3)$$

The proportionality constant α, is in general temperature dependent. At a given temperature it may be evaluated, in principle, by measurements of the relaxation time of the pure solvent and of a single solution of known concentration. The measurement of relaxation times may then be used to find the concentrations of unknown solutions of the same solute.

If an equilibrium

$$A_2 \rightleftarrows 2A$$

is established, with equilibrium constant K and only the species A is paramagnetic, then

$$\Delta(1/T) = \alpha C_A,$$
$$C_A^2/C_{A_2} = K, \quad C_A + 2C_{A_2} = C_{tot}. \quad (4)$$

In principle two measurements of $\Delta(1/T)$ for solutions of differing known total solute concentration C_{tot} enable the determination of the quantities α and K. Of course in practice it is necessary to obtain a large number of relaxation time measurements, over the widest accessible concentration range, for results of satisfactory accuracy. Such sets of measurements, taken at different temperatures, allow for the determination of the temperature dependence of K.

It had previously been proposed[4] that in a solution of an alkali or alkaline earth metal in liquid ammonia the negative ion constituent consists in part of trapped single electrons (in $^2S_{\frac{1}{2}}$ states) and in part of trapped electron pairs (in $^1S_0$ states). The equilibrium between the two species may be represented by the equation

$$e_2 \rightleftarrows 2e$$

and was presumed to be rapidly attained. It is seen that this equilibrium is of the type discussed above, e_2 being diamagnetic, while e should have a magnetic moment of 1.73 Bohr magnetons.

It was in the hope of throwing further light on this

* DuPont Postdoctoral Fellow in Chemistry (1949–50).
† Work performed while on leave from Stanford University, California.
[1] E. Müller, I. Müller-Rodloff, and W. Bunge, Ann. der Chem. **520**, 235 (1935). E. Müller and I. Müller-Rodloff, **521**, 89 (1935). M. F. Roy and C. S. Marvel, J. Am. Chem. Soc. **59**, 2622 (1937).
[2] N. Bloembergen, E. M. Purcell, and R. V. Pound, Phys. Rev. **73**, 679 (1948).
[3] F. Bloch, W. W. Hansen, and M. Packard, Phys. Rev. **70**, 474 (1946).
[4] R. A. Ogg, Jr., J. Chem. Phys. **14**, 114 (1946), p. 295.

proposal and the alternatives to it that the present study was undertaken. It should be emphasized that although these measurements can, to a certain extent, define the properties of the paramagnetic particles, they can give no information about diamagnetic particles. In other words, while they may enable us to distinguish between alternative proposals for the nature of the paramagnetic particle (singly trapped electrons, solvated electrons etc.), they cannot say anything about alternatives for the diamagnetic species (trapped electron pairs, diatomic metal molecules etc.). For this latter purpose other data need to be invoked.

EXPERIMENTAL PROCEDURE

With the exception of a few preliminary tests with lithium solutions, all measurements were made with solutions of metallic sodium in anhydrous liquid ammonia. The solutions were contained in small sealed capsules of Pyrex glass. The capsules were prepared by constricting one leg of a Faraday tube. The latter was provided with a small side arm on the other leg and was attached at the bend, through another small constriction, to a standard taper ground joint.

A small bit of metallic sodium, freshly cut from the interior of a large piece, was introduced into the small side arm, which was then sealed. The tube was attached to a high vacuum line and exhausted, with repeated flashings with dried ammonia gas. The latter was admitted to the line from a reservoir filled with the liquid containing dissolved sodium. The capsule was flamed repeatedly during the evacuation to bake out water retained by the glass. The sodium was carefully distilled in high vacuum and appeared as a bright mirror in the Faraday tube. By cooling with an acetone-dry ice bath, the desired quantity (of the order of two cc) of anhydrous liquid ammonia was condensed in the tube, which was then sealed off at the upper constriction. A portion of the sodium, which had been distilled into the tube, was dissolved and the relatively concentrated solution was allowed to stand for some time in the capsule in order to further remove retained moisture. After decantation of the solution to the other arm of the tube, the ammonia was distilled back into the capsule. Part of the condensation was performed on the still unused portion of the sodium, which was thereby carried down into the capsule. By controlling the amount of metal which was carried down, the concentration could be adjusted to about the desired value, judged approximately by the depth of the blue color. After the solution had been prepared the capsule and contents were cooled with dry ice and the capsule was finally sealed off at the constriction. After the measurements of relaxation time were completed (see below) the concentration of the solution was determined by standard chemical analysis.

Despite the above precautions, considerable trouble was encountered with fading of the solutions, due to the formation of metal amide. The chemical analysis yielded only the initial concentration of the metal solutions. The uncertainty due to fading was minimized by preparing the solutions immediately before measurements and by keeping them at dry ice temperature if any delays occurred. However, this chemical instability proved to be the single greatest source of error and unfortunately reduces the nature of the studies to a semi-quantitative one.

The apparatus used for the relaxation time measurements has already been described.[2,5,6] It consisted of a conventional nuclear resonance bridge circuit, a water-cooled electromagnet operated from storage batteries and a thermostating system for the sample. All of the measurements reported here were made at 30 Mc/sec. The set of saturation curves was calibrated by means of the directly measured relaxation time of pure liquid ammonia at 20°C. The values of the relaxation times relative to the adopted value of $T_p(20°)$ have a probable error of about ±seven percent.

To minimize the uncertainties due to chemical instability of the solutions, measurements were usually initiated within thirty minutes after preparation. A saturation curve was first determined at room temperature. The sample was then cooled to about −65° and the measurement was repeated. Usually measurements were then made at two additional temperatures intermediate between these limits. The entire series of measurements on a given sample of solution required approximately five hours. In several cases the room temperature measurement was repeated after completion of the series with no significant change in results. This is an indication that the extent of chemical decomposition during the series of measurements was relatively small.

In several cases the samples were allowed to stand a few days after measurements, with resultant complete disappearance of the blue color. The relaxation time at a given temperature for such a solution was found to be indistinguishable from that for pure liquid ammonia. This indicates that the sodium amide has no magnetic moment, which is certainly to be expected.

Measurements were also made on a 0.01 molar solution of cupric nitrate in liquid ammonia. This was done in order to have experimental comparison with a paramagnetic solute which does not undergo the type of association reaction discussed above.

EXPERIMENTAL RESULTS AND DISCUSSION

Figure 1 shows the typical behavior of the measured relaxation times for several solutions as a function of temperature. In Fig. 2 the experimentally determined quantity

$$\Delta(1/T)/C_{Na}$$

is plotted as a function of the metal concentration C_{Na}. Because of the considerable scattering only the data for the two extremes of the temperature range are given in the figure.

[5] A. M. Sachs, Ph.D. thesis, Harvard University, (1949).
[6] E. Turner, Ph.D. thesis, Harvard University, (1949).

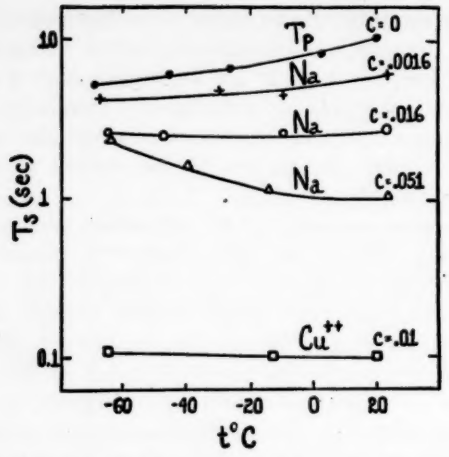

FIG. 1. Relaxation time *vs.* temperature curves for representative sodium-liquid ammonia solutions.

In the case of a simple paramagnetic solute uncomplicated by the type of associative equilibrium discussed above, the plot of $\Delta(1/T)/C$ against C should be a horizontal line. The monotonic trend of the curves in Fig. 2 is indicative of an equilibrium in which the associated species has a magnetic moment considerably less than that of the dissociation products (we can assume the moment of the associated species to be zero). The proper test of the equilibrium law would involve the exact determination of the intercept at $C=0$ at a given temperature. As is seen from Eq. (4) this would yield the value of the proportionality constant α, since at infinite dilution the solute is presumably entirely in the dissociated paramagnetic form. The constancy of the parameter K could then be tested from the experimental values of $\Delta(1/T)$ at various finite values of the total solute concentration. Unfortunately, all experimental errors, both from the chemical instability of the solutions and from the limited precision of the relaxation time values, become most serious in the vitally important region of extreme dilution. This produces a consequent large uncertainty in the extrapolated value of α.

However, the form of the equilibrium law may be tested from the behavior of solutions sufficiently concentrated so that the degree of dissociation is relatively small. If the equilibrium law is that postulated in Eq.

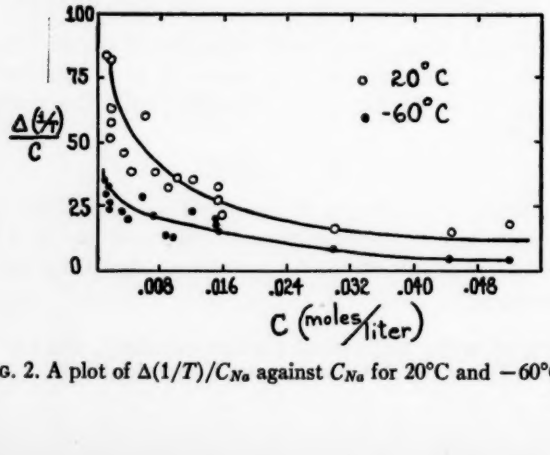

FIG. 2. A plot of $\Delta(1/T)/C_{Na}$ against C_{Na} for 20°C and −60°C.

(4), it is readily seen that

$$\log[\Delta(1/T)/C_{Na}]=-\tfrac{1}{2}\log C_{Na}+\tfrac{1}{2}\log(K\alpha^2/2). \quad (5)$$

A plot of the experimental values (dealing with solutions of concentration greater than $0.008M$) of $\log[\Delta(1/T)/C_{Na}]$ at a given temperature against $\log C_{Na}$ can be fitted by a straight line whose slope is approximately $-\frac{1}{2}$. While the experimental precision leaves much to be desired, it is believed that this constitutes some confirmation of the validity of this type of association equilibrium law.

It is to be emphasized that this simple mass law description is approximately valid only in very dilute solutions. Deviations at higher concentrations are clearly indicated by the imminent crossing of two of the representative curves shown in Fig. 1. In view of the relatively small dielectric constant of liquid ammonia as compared to water, for example, ideal behavior for electrolyte solutions could scarcely be expected.

It is to be noted that $\Delta(1/T)$ for the simple paramagnetic solute Cu^{++} is practically temperature independent. This might suggest that the curves in Fig. 2 should have nearly the same intercept α_{Na}. If this is taken to be about 10^2 on the scale shown,‡ the respective best values of K corresponding to the previously mentioned association equilibrium (Eq. (4)) are some 3×10^{-3} mole/liter at 20°C and 7×10^{-4} at −60°C. Despite the low precision of the data (and granted the above assumptions) the trend of K with temperature seems to be indicated, i.e., the dissociation of the diamagnetic species A_2 is an endothermic process.

The value of α for the Cu^{++} ion, which has approximately the same μ_{eff} as an electron with spin only, is found from the observed relaxation time to be 10^3 in the units used in Fig. 2. It is of some interest to inquire why the paramagnetic component of the metal solution should make a less effective contribution than the Cu^{++} ion to the relaxation process by about a factor of ten. We again assume, with the justification given, that α_{Na} equaled approximately 10^2. Bloembergen's results[2] for various paramagnetic cations in aqueous solutions essentially showed that F could be regarded as a constant for the different ions studied. There is no reason to suppose that this is not a general rule for all solvents provided that no complex ion structures, which would exclude solvent molecules, are formed. In this sense then, the paramagnetic particles in the solutions of sodium in ammonia show anomalous behavior. It is not possible here to determine the origin of the discrepancy between F (or α) values for the metal solution and for the normal paramagnetic ion. However, it is perhaps worth noting

‡ This value of α can be justified by a comparison of our data with the magnetic susceptibility measurements (see concluding paragraph). If it is assumed that the paramagnetic particles are localized spin-only electrons, then the limiting molar susceptibility at infinite dilution is known approximately. Since, at a given temperature, the limiting molar susceptibility and α should be proportional to one another, the value of the latter quantity can be found by comparing our data with the susceptibility data at definite concentrations.

that such a discrepancy is compatible with the assumption of a large cavity radius for a paramagnetic singly trapped electron[4] (see Eqs. (1)–(3)).

The results of the present study are at least qualitatively similar to those of the measurements of Huster and of Freed and Sugarman of the magnetic susceptibility of dilute metal-ammonia solutions.[7,8] That is, both the conventional susceptibility measurements and the current data suggest an endothermic dissociation of the type discussed above.

[7] E. Huster, Ann. d. Physik **33**, 477 (1938).
[8] S. Freed and N. Sugarman, J. Chem. Phys. **11**, 354 (1943).

ACKNOWLEDGMENT

One of us (R.N.) would like to express his appreciation to the E. I. DuPont de Nemours Company for the fellowship under which this work was done.

THE JOURNAL OF CHEMICAL PHYSICS VOLUME 19, NUMBER 2 FEBRUARY, 1951

Electron Diffraction by Transmission through Thin Liquid Films

CARROLL W. LUFCY, FELIX S. PALUBINSKAS,* AND LOUIS R. MAXWELL
U. S. Naval Ordnance Laboratory, Silver Spring, Maryland
(Received July 24, 1950)

Electron interference has been obtained by the transmission of 50-kv electrons through thin liquid films of the silicones: DC703, DC500, and DC200; and the hydrocarbons: octoil, castor oil, and glycerine. A commercial electron microscope (RCA, type EMU) was used after modification of the specimen holder. The electron diffraction patterns obtained from the hydrocarbons were all practically the same. They were characterized by three complete diffraction halos. The Bragg spacings (d) for octoil were found to be 4.93A, 2.26A, and 1.23A. These distances compare closely with values obtained previously for electron diffraction in liquid phytol ($C_{20}H_{39}OH$), Nujol, and Cenco pump oil. The patterns obtained for the silicones were significantly different from those of the hydrocarbons. Four complete rings were observed for DC703, giving d values of 8.17A, 4.18A, 1.97A, and 1.27A. The DC500 and DC200 fluids showed only three rings with Bragg spacings of 7.40A, 3.96A, and 1.27A; the ring which occurred at $d=1.97$A for DC703 was absent. The accepted Si—O distance of 1.60A is in agreement with the above data; however, the Si—O—Si—O angle is found to be approximately 104°. Such conclusions were confirmed by density calculations.

INTRODUCTION

An earlier investigation by Maxwell[1] obtained electron diffraction patterns by the transmission of electrons through thin liquid films. Several liquids containing straight chain carbon molecules were studied. With the recent availability of new liquids having suitable vapor pressure and surface tension, it became apparent that additional information regarding the structure of liquids could be obtained by the electron diffraction method. It is of interest to examine, in addition to hydrocarbons, the silicones where the carbon chain is replaced by a silicon-oxygen chain.

EXPERIMENTAL ARRANGEMENT

An RCA type EMU electron microscope was modified to accommodate electron diffraction by liquids. Following the method developed previously,[1] a thin film of the liquid under investigation was placed in the electron beam, and transmission photographs were obtained.

An improved type of holder was developed with which it was possible to reform the thin films in the microscope without disturbing the vacuum. The holder was a piece of flat 4-mil brass shim stock, containing a 1-mm diameter aperture, soldered to a brass sleeve in such a manner that it could be mounted on the reflection specimen holder pin of the microscope. A piece of No. 14 (B&S) enameled Cu wire was soldered to the end of the diffraction stage and bent so as to lie flat against the holder when it was set normal to the axis of the electron beam. It was then possible by making use of the transverse motion control of the pin to move the holder with respect to the copper wire or "wiper." A small drop of the liquid under investigation was placed between the wire wiper and the holder; and by a transverse motion of the pin the holder could be moved under the wire, thus wiping a thin film of the liquid over the aperture. The holder could then be moved back so as to bring the aperture and film into the electron beam.

The electron microscope is equipped with an ion neutralizer gun by which low voltage electrons are sprayed onto the diffraction specimen stage to neutralize any positive charge that might develop on the specimen during electron bombardment. In the present work the ion neutralizer was used to reduce the thickness of the liquid films. The film was irradiated by electrons from the ion neutralizer, causing local heating and increased evaporation of the film. When the films were too thick, the central beam spot would shift erratically;

* Now at Iowa State College, Ames, Iowa.
[1] L. R. Maxwell, Phys. Rev. **44**, 73 (1933).

but it could be easily brought to a stable position through the use of the ion neutralizer.

The diffraction patterns obtained from gold films were used for calibration ($a_0=4.068$A). The positions of the interference rings from the liquid films were read visually. Bragg spacings, corresponding to the first-order diffraction, were obtained from these measurements. Three to five photographs were measured for each specimen studied. The probable error in the above Bragg spacings was about one percent. At least two observers were used for each photograph measured. The energy of the electron beam was held constant to within ± 0.02 of one percent at a value close to 50,000 volts.

RESULTS

The liquids investigated are classified into three groups: (a) long chain hydrocarbons, (b) short chain hydrocarbons, and (c) long chain siloxane polymers. The hydrocarbons showed a similar type of interference pattern characterized by three diffraction rings, while the siloxanes gave a pattern different in appearance from the hydrocarbons, with a new interference ring occurring at small angles. Typical photographs characteristic of the hydrocarbons and the siloxanes are shown in Fig. 1.

A summary of the values obtained for the Bragg spacings (d) is given in Table I. Cenco pump oil gave d values in good agreement with the results reported by Maxwell.[1] For octoil the spacings increased slightly with respect to Cenco pump oil, while for castor oil they decreased slightly, with the exception of the outermost ring. In the case of glycerine three spacings were found comparable to Cenco pump oil but with corresponding smaller d values; the smallest for any of the hydrocarbons studied. The innermost or first interference ring appeared for DC703 at a d value of 8.17A; and for DC500 and DC200 at slightly lower values. The third maximum was absent for DC500 and DC200, while the fourth diffraction ring was present for all three siloxanes at about the same Bragg spacing. The interference patterns exhibited by the hydrocarbons give rise to the same type of pattern with comparatively small differences existing between them.

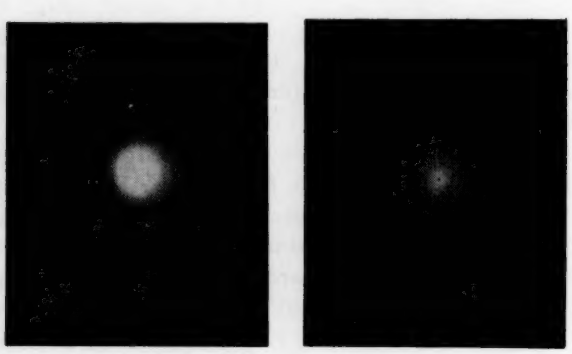

(a) (b)

FIG. 1. Typical electron diffraction photographs of (a) octoil and (b) silicone DC703.

TABLE I. Summary of Bragg spacings found for various liquids.

Type	Name	Bragg spacings (A) 1st maximum	2nd maximum	3rd maximum	4th maximum
Straight chain carbon	Cenco pump oil (93050-C)	Absent	4.74	2.15	1.21
Straight chain carbon	Castor oil	Absent	4.53	2.08	1.21
Straight chain carbon	Glycerine $C_3H_5(OH)_3$	Absent	4.42	2.07	1.19
Straight chain carbon with phenol group on one end	Octoil	Absent	4.93	2.26	1.23
Straight chain silicon-oxygen with phenyl side groups	Silicone DC 703	8.17	4.18	1.97	1.27
Straight chain silicon-oxygen with methyl side groups	Silicone DC 500	7.27	3.98	Absent	1.25
	Silicone DC 200	7.40	3.69	Absent	1.27

DISCUSSION

As discussed previously[1] the Bragg spacing occurring at about 4.6A for the long chain carbon compounds has been attributed by Stewart,[2] from x-ray investigations of liquid paraffins, to the distance between adjacent molecules measured in a plane perpendicular to the axis of the molecules. The spacing at approximately 1.21A agrees with the distance between the projection of neighboring carbon atoms on the axis of the molecule; the C—C—C angle is assumed to be 106 degrees. It is assumed, on this basis, that there is enough coupling between adjoining molecules to define a Bragg plane perpendicular to the axis of the molecule. Having made this postulate there should exist other planes of a diagonal sort which could give rise to a spacing in the neighborhood of 2.0A as observed.

The silicones DC500 and DC200† are members of the polymer homologous series having the formula[3]

$$(CH_3)_3SiO-[(CH_3)_2SiO]_n-Si(CH_3)_3,$$

where n is approximately 36 and 132, respectively. DC703 is a copolymer containing both methyl and phenyl groups attached to the silicon atom as side groups. The length of the DC703 molecule is not known; but, judging from its viscosity, it may be assumed to be at least as long as the DC200 molecule. As in the case of the hydrocarbons, we interpret the spacing corresponding to the first maximum to be the distance between adjoining molecules. The separations are considerably greater than those for the hydrocarbons, which is evidently caused by the existence of the side groups, particularly for DC703 having phenyl side groups. The larger spacing of 8.17A for DC703 as compared to 7.27A and 7.40A for DC500 and DC200, respectively, can be associated with the difference in length between the phenyl and methyl groups.

[2] G. W. Stewart, Phys. Rev. 31, 174 (1928).

† Poly Methyl Siloxane polymers supplied by Dow Corning Corporation, Midland, Michigan.

[3] Dow Corning Silicone Notebook, Fluid Series 3, September, 1948.

In the silicones we have a Si−O−Si chain. If we take the Si−O−Si−O bond angle from Sauer and Mead[4] as 160°±15° and the Si−O distance[5] as 1.60A, we would expect an interference ring at about 1.58A on the same basis that we accounted for the 1.21A spacing in the hydrocarbons. The electron diffraction results, however, give a spacing of about 1.26A in disagreement with the above structure. To obtain agreement, the electron diffraction results require a Si−O−Si−O bond angle of 104°—close to the C−C−C bond angle—for a Si−O distance of 1.60A.

It is noticed that the third maximum is absent for DC500 and DC200, while it is present for DC703. DC500 and DC200 have methyl side groups, while DC703 contains phenyl side groups. It is therefore concluded that the scattering from the phenyl groups gives rise to the third maximum, as in the case of the hydrocarbons.

Another theoretical approach is one used by Warren[6] for x-ray diffraction from liquids, where the intensity of coherent scattering $I(sl_{ij})$ is considered for all possible orientations in space in a manner similar to that used for free gas molecules. $I(sl_{ij})$ is given by

$$I(sl_{ij})\sim\sum_{i=1}^{n}\sum_{j=1}^{n}\psi_i\psi_j\frac{\sin sl_{ij}}{sl_{ij}};\quad s=4\pi\sin(\tfrac{1}{2})\theta/\lambda, \qquad (1)$$

where θ is the angle of scattering and l_{ij} is the distance between the ith and jth atoms, ψ_i and ψ_j are the scattering amplitudes. $\sin sl_{ij}/sl_{ij}$ has a strong positive first maximum at $sl_{ij}=7.72$, from which l_{ij} can be calculated as

$$l_{ij}=0.614\lambda/\sin(\tfrac{1}{2})\theta, \qquad (2)$$

which is the Ehrenfest-Keeson relation for closely packed spheres.

[4] R. O. Sauer and D. J. Mead, J. Am. Chem. Soc. **68**, 1794 (1946).
[5] B. E. Warren, Phys. Rev. **45**, 657 (1934).
[6] B. E. Warren, Phys. Rev. **44**, 969 (1933).

TABLE II. Results of density calculations of liquids from electron diffraction data.

Liquid	Density (gm/cc) Square	Hexagonal	Known	Remarks
DC 200	0.995	1.15	0.973[a]	Si−Si distance between ends of adjacent molecules assumed to be 2A
DC 500	0.927	1.07	0.953[a]	
Glycerine	1.69	1.95	1.26[b]	End group of C−H
	1.17	1.35		End group of C−O−H
Phytol $C_{20}H_{40}O$	1.03	1.19	0.852[b]	From electron diffraction data by Maxwell (reference 1)

[a] Density values obtained from Dow Corning Notebook, Third Series, No. 3, September, 1948.
[b] Lange, *Handbook of Chemistry* (Handbook Publishers, Inc., Sandusky, Ohio, 1941), fourth edition.

The intensity of electron scattering from a liquid would necessarily have a strong contribution in Eq. (1) arising from the coherent scattering between nearest and next-nearest neighbors in each molecule. For the fourth maximum, which must correspond to the distance between nearest neighbors, values of 1.5A and 1.6A are obtained by the use of Eq. (2) for the C−C and Si−O distances, respectively, agreeing with the values obtained above. For the distance between next-nearest neighbors we find, for the long chain hydrocarbons, poorer agreement, a value of 2.5A to be compared with the expected distance of 2.4A.

DENSITY CONSIDERATIONS

Densities of the liquids studied were computed on the basis of the above structural data. For the siloxanes DC200 and DC500 the length of the Si−O distance projected on the axis of the molecule was taken as 1.26A, which requires the Si−O−Si angle of 104°. The intermolecular distance was taken to be equal to the Bragg spacings for the first observed maximum for the molecules given in Table I. The density was calculated both for a square array and for a close-packed hexagonal array, with the results shown in Table II. The densities calculated for the square array give better agreement with the known values.

Note on Orthogonal Atomic Orbitals*

J. C. SLATER
Massachusetts Institute of Technology, Cambridge Massachusetts
(Received October 16, 1950)

It is shown that orthogonal atomic orbitals, as introduced by Wannier for solid-state problems and by Löwdin for molecular problems, do not lead to a simple way of eliminating the non-orthogonality problem in the Heitler-London method. Thus, if a calculation of the H_2 molecule is made using orthogonal atomic orbitals in place of ordinary atomic orbitals, proceeding by the simple Heitler-London method, the resulting diagonal energy of the lowest state shows no energy minimum. The orthogonal atomic orbitals are suitable for use, however, if we make a complete perturbation calculation, and for this purpose they are as convenient as LCAO's, but not appreciably superior.

WANNIER[1] a number of years ago showed how by making linear combinations of molecular orbitals in a periodic potential problem one can set up functions similar to ordinary atomic orbitals, but having the very desirable property of being orthogonal to each other. Löwdin[2] has recently pointed out the possibility of doing an essentially similar thing in the study of molecules. These orbitals have a number of uses in formulating perturbation problems in molecular and solid-state structure, arising mainly because of their orthogonality: in setting up diagonal and nondiagonal components of the energy matrix, we have none of those terms arising from non-orthogonality integrals which so much complicate the ordinary study of molecular structure using the Heitler-London method. On account of the probable considerable use of these functions, it is worth while suggesting a name for them, and it seems natural to suggest Orthogonal Atomic Orbitals, which might well be abbreviated OAO, falling in line with the various abbreviations for Molecular Orbitals (MO), Atomic Orbitals (AO), Linear Combinations of Atomic Orbitals (LCAO), introduced by Mulliken.

It might be thought, and Löwdin suggests, that the use of OAO's would bring a very easy answer to the old problem of the neglect of non-orthogonality integrals in the Heitler-London treatment of chemical valence. It is well known that the chemists have found it very useful to set up a theory of molecular binding following the general lines of the Heitler-London method, but neglecting all non-orthogonality integrals, and that they have been able to correlate this type of theory surprisingly well with experiment. Yet the non-orthogonality integrals usually are by no means negligible; they are in many cases very large. We might hope that we could formulate a theory of valence, formally like the Heitler-London theory, but starting from the beginning with OAO's instead of with AO's. Then the non-orthogonality integrals would automatically be absent, and everything would work out just according to the findings of the chemists. Most unfortunately, this attractive hope is not justified, and the purpose of the present note is to point out the reason why, using the old and familiar example of the H_2 molecule.

I. FORMULATION OF THE H_2 PROBLEM IN TERMS OF OAO'S

Let the ordinary $1s$ atomic orbital around one of the two nuclei of the H_2 molecule be denoted a, that around the other nucleus as b. If the coordinates of an electron be denoted 1 (or 2), we may write these orbitals as $a(1)$, $b(1)$, etc. Let the two functions be normalized, and let the non-orthogonality integral $\int a(1)b(1)dv_1$ be denoted by α. We may then set up the two OAO's for this case by writing functions

$$A(1)=c_1a(1)+c_2b(1),$$
$$B(1)=c_2a(1)+c_1b(1), \tag{1}$$

where c_1, c_2 are to be chosen so as to make A and B normalized and orthogonal. These requirements lead to the conditions

$$c_1^2+c_2^2+2c_1c_2\alpha=1,$$
$$2c_1c_2+(c_1^2+c_2^2)\alpha=0. \tag{2}$$

These equations can be easily solved for c_1 and c_2; since we shall not require the formulas, we do not bother to write down the solutions. Clearly, in the limit of infinite separation, when α goes to zero, the only solutions are $c_1=1$, $c_2=0$, or $c_1=0$, $c_2=1$, leading to the ordinary AO's; but as α increases, the c's deviate from these values, in such a way that if c_1 is positive, c_2 is negative, leading to the possibility of satisfying the orthogonality condition. We can also arrive at the same final answer for the OAO's in other ways. First, we can set up LCAO's, $(a+b)/[2(1+\alpha)]^{\frac{1}{2}}$ and $(a-b)/[2(1-\alpha)]^{\frac{1}{2}}$, which we may call I and II. These functions are normalized and orthogonal. Then, adapting the scheme of Wannier to the problem, we can set up combinations $(\mathrm{I}\pm\mathrm{II})/\sqrt{2}$. It is only a matter of algebra to prove that the resulting functions are the same ones which we have set up in (1). Or we can use the method of Löwdin, which is considerably more complicated in appearance because it is designed for more general cases than the present; it also can be shown to lead to the same result.

Now let us use these OAO's to set up the perturbation

* The work described in this paper was supported in part by the Signal Corps, the Air Materiel Command, and ONR, through the Research Laboratory of Electronics.

[1] G. H. Wannier, Phys. Rev. 52, 191 (1937).
[2] P. O. Löwdin, J. Chem. Phys. 18, 365 (1950).

problem of the H_2 molecule. It is well known[3] that if we have two electrons and require that they be found in the orbitals a or b, there will be four resulting states, a triplet and three singlets. As far as the orbital part of the wave function is concerned, the wave functions are written in the Heitler-London theory in the following form:

$$\text{Triplet: } \frac{1}{[2(1-\alpha^2)]^{\frac{1}{2}}}[a(1)b(2)-b(1)a(2)]. \quad (3)$$

$$\text{Singlet No. 1: } \frac{1}{[2(1+\alpha^2)]^{\frac{1}{2}}}[a(1)b(2)+b(1)a(2)]. \quad (4)$$

$$\text{Singlet No. 2: } \frac{1}{[2(1+\alpha^2)]^{\frac{1}{2}}}[a(1)a(2)+b(1)b(2)]. \quad (5)$$

$$\text{Singlet No. 3: } \frac{1}{[2(1-\alpha^2)]^{\frac{1}{2}}}[a(1)a(2)-b(1)b(2)]. \quad (6)$$

Of these the triplet is the ordinary repulsive Heitler-London state, singlet No. 1 is the ordinary attractive Heitler-London state, singlets Nos. 2 and 3 are polar states. When we consider the matrix components of energy or unity between these various wave functions, we find that on account of symmetry the only non-vanishing components are between singlets Nos. 1 and 2. Thus, we have a perturbation problem, resulting in a quadratic secular equation, between these two states; the triplet and singlet No. 3, are already in final form, as far as we can approximate them with functions constructed from the $1s$ atomic orbitals.

Our suggested scheme is now to replace the AO's a and b by the OAO's A and B in (3), (4), (5), (6), the only changes being the obvious ones of normalization (the terms α^2 being absent in the denominators on account of the orthogonality of A and B). When we do this, and write the resulting functions in terms of a and b, by means of Eqs. (1) and (2), we find that (3)[4] and (6) are unchanged; but (4) and (5) are replaced by

Singlet No. 1:

$$\frac{1}{\sqrt{2}}\frac{1}{1-\alpha^2}\{[a(1)b(2)+b(1)a(2)] - \alpha[a(1)a(2)+b(1)b(2)]\}, \quad (7)$$

Singlet No. 2:

$$\frac{1}{\sqrt{2}}\frac{1}{1-\alpha^2}\{[a(1)a(2)+b(1)b(2)] - \alpha[a(1)b(2)+b(1)a(2)]\}. \quad (8)$$

In other words, by using the OAO's, and proceeding as in the Heitler-London method, the singlet No. 1, which would represent the wave function of the ground state in the ordinary Heitler-London approximation, has taken on some of the character of the polar state. We can now find the diagonal matrix component of energy with respect to the function (7). We shall not go into the details of this calculation. The integrals involved are mostly the same as those met in the ordinary Heitler-London theory of H_2. The remaining integrals are easy to evaluate, and have already been met in earlier calculations (as those mentioned in reference 3). The author has carried out the calculations, however, with the disconcerting result that the diagonal energy of the state (7) shows no minimum similar to that shown by the function (4), which Heitler and London identified with the ground state of H_2. In other words, the modification of (4) produced by adding the contribution $-\alpha[a(1)a(2)+b(1)b(2)]$ of polar state has altered the function so profoundly that it no longer forms any sort of approximation to the ground state of the molecule. It is for this reason that it, unfortunately, seems impossible to use the OAO's as a starting point for a modified Heitler-London theory of valence avoiding the difficulty of non-orthogonality integrals. We shall see in the next section why this is the case.

Of course, a more accurate treatment than the Heitler-London result is obtained by solving the perturbation problem between states (4) and (5). When this is done (the results of such a calculation are presented graphically in reference 3 of J. C. Slater), it is found that the final function representing the ground state, the optimum combination of (4) and (5), has an energy only very slightly lower than that of (4), so that the function (4) itself forms a very good approximation to the best function, over the whole range of internuclear distance. It is for this reason that the Heitler-London method has had such great success. On the other hand, the modified wave function for the polar state is considerably different from (5), and results in a much more repulsive state than the diagonal energy of (5) would indicate. If in a similar way we make linear combinations of (7) and (8) to solve the perturbation problem, it is obvious that the final energy levels and wave functions will be just as if we started with (4) and (5), since (7) and (8) are themselves combinations of (4) and (5). On the other hand, the final wave functions for the ground state, being very nearly the same as (4), will be decidedly different from (7), the latter forming a poor approximation to the ground state.

II. INTERPRETATION OF THE PROPERTIES OF OAO'S, AO'S, AND LCAO'S

In the preceding section we have stated the facts regarding the formulation of the H_2 problem in terms of OAO's; let us now try to understand physically why these results come about. To do this, we shall adopt a method of treating wave functions as vectors, which one

[3] See J. C. Slater, Phys. Rev. **35**, 509 (1930); S. Weinbaum, J. Chem. Phys. **1**, 593 (1933).

[4] Löwdin (reference 2) uses the case where all spins are parallel to discuss the connection between the method of OAO's and the ordinary Heitler-London method. We see that this was an unfortunate choice, since in the simple case of H_2 this case with parallel spins leads to identical results in the two cases, whereas the ground state, which is the one of real interest, does not.

often talks about in general discussions of wave mechanics, but seldom uses for graphical discussion. We recall that a normalized wave function u_1 can be considered to be a unit vector in a function space. The scalar product of two such vectors u_1 and u_2 is the nonorthogonality integral $\int u_1 u_2 dv$. Thus, if they are orthogonal, this scalar product is zero. If they are not, however, we may write α as $\cos\theta$, interpreting θ as the angle between the vectors. If we make a linear combination of two such vectors, we can combine them by the ordinary parallelogram law. If we have only two such vectors, or functions, we can plot them in a plane, and get a very physical picture of what is going on.

The two vectors (4) and (5) can be represented by unit vectors, the first being the nonpolar, the second the polar, Heitler-London function. If we multiply these and integrate over $dv_1 dv_2$, the result is $2\alpha/(1+\alpha^2)$, which then may be regarded as the cosine of the angle between the vectors. When R, the internuclear distance, is infinite, $\alpha=0$, and the angle is 90°. As R decreases, however, the angle very rapidly decreases until at the actual distance of separation in the molecule it is only about 20°. In other words, the nonpolar and polar functions are far from linearly independent for small R. This, of course, is to be expected, since as R goes to zero the two functions become identical. When we carry out our perturbation calculation, the resulting perturbed functions, unlike these unperturbed ones, are of course orthogonal to each other. One of them, corresponding to the ground state, proves for all values of R to be quite close to the function (4); but the other one, being at right angles to it, must depart widely from the function (5). Since we do not ordinarily care about this state, we do not ordinarily worry about the fact that (5) is not a good wave function when using the Heitler-London method. In Fig. 1, we now give plots of the sort we have described, for several internuclear distances. In each case we have plotted the correct linear combination of (4) and (5) to represent the ground state along the x axis, the other correct combination along the y axis. We see how the function (4) lies close to the x axis for the whole range of R's, verifying the remarkable accuracy of the Heitler-London function.

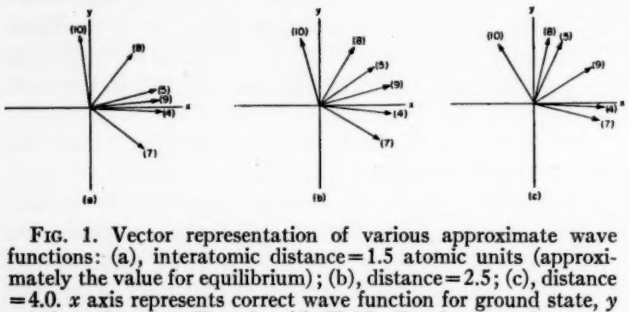

FIG. 1. Vector representation of various approximate wave functions: (a), interatomic distance=1.5 atomic units (approximately the value for equilibrium); (b), distance=2.5; (c), distance =4.0. x axis represents correct wave function for ground state, y axis for polar state. Function (4), Heitler-London nonpolar state; (5), Heitler-London polar state; (7) and (8), functions formed from OAO's; (9) and (10), functions formed from LCAO's. Numbering of vectors agrees with numbering of equations in the text.

In Fig. 1, we have plotted not only (4) and (5), but two other sets of functions as well. One is the set (7) and (8) of functions formed from OAO's. The other is the set of functions corresponding to the use of LCAO's. If we assume that both electrons are in the orbital I of Section 1, or both in orbital II, respectively, the corresponding wave functions prove to be

$$\frac{1}{2(1+\alpha)}\{[a(1)b(2)+b(1)a(2)] + [a(1)a(2)+b(1)b(2)]\}, \quad (9)$$

$$\frac{1}{2(1-\alpha)}\{[a(1)b(2)+b(1)a(2)] - [a(1)a(2)+b(1)b(2)]\}. \quad (10)$$

These functions, and (7) and (8), can be easily proved to have interesting geometrical relationships, shown in Fig. 1. The function (9) is the bisector of the angle between (4) and (5), and (10) is orthogonal to (9). The functions (7) and (8) form the 45° bisectors of the functions (9) and (10). Once we know these facts, the relations of (7), (8), (9), (10) to the best wave function of the ground state, represented by the x axis in Fig. 1, become obvious.

At large distances R, the functions (4) and (5) are orthogonal to each other; the first lies along x, the second along y. In this case, the LCAO (9), being the bisector of these, lies along the 45° line, and the function (7), formed from OAO's, lies along the x axis. Thus, for large R, the function (9) forms a very bad approximation to the ground state, illustrating the well-known failure of the MO or LCAO method for large internuclear distances. In this limit, on the other hand, the function (7), formed from OAO's, forms a good approximation, as it must, since the OAO's reduce to AO's at large R. As R decreases, however, the situation changes entirely. The functions (4) and (5) approach each other, having only a small angle between, so that (9), the function formed from LCAO's, being the bisector, must lie close to (4), and, hence, close to the correct ground state. This is the origin of the fact that the LCAO method gives good approximations to the molecular states at small internuclear distances, without the necessity of applying perturbation methods. At small R, on the other hand, since (9) is a fairly good approximation, and since (7) is 45° to it, it is clear that (7) forms a very poor approximation to the ground state, so that the OAO's do not furnish a good starting point for building a wave function for the ground state, though the AO's, leading to (4), do.

For the further interpretation of Fig. 1, we may ask how the energy of any one of the wave functions is to be determined. If u_1, u_2 represent the x and y axes, that is, the correct linear combinations of (4) and (5), and if the diagonal energies of these states are H_1 and H_2, then we can show at once that the energy of a state represented

by a vector at an angle θ to the x axis will be $H_1 \cos^2\theta + H_2 \sin^2\theta$. If we set up an ellipse with semi-axes $1/H_1^{\frac{1}{2}}$, $1/H_2^{\frac{1}{2}}$ along the two axes, and set up a vector at angle θ, this vector will intersect the ellipse at a point whose distance from the origin is $1/H^{\frac{1}{2}}$, where H is the energy appropriate to this vector or wave function. It is at once obvious, then, that a vector close to the x axis will correspond to a very nearly correct energy. On the other hand, two vectors at 45° to the axes, as (7) and (8) approximately are at small R, will correspond to the same energy. Thus, the energies of these states will approach each other at small R, this common energy forming a compromise between the attractive and repulsive states represented by the x and y axes in Fig. 1, explaining the lack of attractive nature in the function (7) formed from OAO's, which we have mentioned in Sec. I.

III. CONCLUSION

Of all the various functions which we have considered, only the Heitler-London function (4) lies close to the correct wave function over the whole range of R. Therefore, if we wish to set up an unperturbed wave function which, without application of perturbation theory, represents accurately the correct wave function over wide ranges of R, we find nothing approaching the Heitler-London function in accuracy. If this is the case in hydrogen, we may assume the same thing to hold in more complicated molecules as well. But the non-orthogonality integrals are very large and important, and we must not expect to be able to neglect them and still retain any pretense of making an accurate calculation.

If we wish to use a perturbation calculation, making linear combinations of a number of unperturbed wave functions, then we can get better results; and then we are freed from the necessity of using Heitler-London type functions, with the awkward results of non-orthogonality. In that case, we can start either with molecular orbitals (or LCAO's), or with OAO's; the final result will be the same in either case if we carry out the perturbation calculation conscientiously. Either of these starting points will have the convenience of orthogonal orbitals, so that the calculation of matrix components of energy and unity will be simple. There are ordinarily advantages, however, in the use of LCAO's, as opposed to OAO's, since we have seen that the function built up properly of LCAO's represents a fairly good approximation to the actual wave function of the molecule at small R; this is the basis of the usual application of LCAO's for discussing molecular structure, without carrying out a perturbation calculation. There are, on the other hand, certain problems, such as that of distorted lattices, for which the OAO's are particularly convenient; but their usefulness is probably somewhat restricted in ordinary problems of molecular structure.

The Jones Reductor: A Model for the Kinetics of Chromatography*

KERRO KNOX† AND HENRY C. THOMAS‡
Brookhaven National Laboratory, Upton, New York, and the Sterling Chemistry Laboratory, New Haven, Connecticut

(Received September 11, 1950)

The Jones reductor can be made to assume a steady state of operation in the reduction of ferric sulfate. Its behavior under such conditions strongly indicates that the rate limiting process is the diffusion of ferric ion through a static film of solution around the solid particles. This is particularly evidenced by the exponential dependence of the extent of reduction on the square root of the flow rate. The behavior of the reductor as a function of zinc ion concentration, zinc amalgam particle size, and temperature, also agrees with this result.

IN searching for a simplified model in which to study the processes of importance in the behavior of chromatographic columns, we have noticed that the well-known Jones reductor can, under certain circumstances, be made to assume a steady state of operation. The study of the kinetics of fast reactions by measurements of steady-state conditions in flowing systems has long been a procedure of recognized utility. If one attempts to apply the method to a heterogeneous system in which perhaps a solid reactant is fixed in the stream of a reacting solution, and if a steady state is actually found, such that the concentration of the dissolved reactant does not vary with time at a point in the system, then the concentration of the reacting solid is either not varying, or else this concentration does not appear in the rate law. Thus, the method for heterogeneous systems is not general; its utility depends on an accident of chemical kinetics, or on a limiting case in the particular application.

The reducing action of zinc amalgams has been studied by many workers. The investigations of Liebhafsky[1] and of Stone and Hume[2] are of special interest in this connection. It appears that in the case of ferric ion, which is reducible by mercury as well as by zinc, the amalgam surface remains constant in its reducing efficiency. This is not true for the reduction of ions unaffected chemically by mercury; in the cases of the vanadate and chromic ions the efficiency of a Jones reductor falls off rapidly as the reactions proceed. We were thus led to set up a model of a chromatographic column using a Jones reductor supplied with a rapid stream of ferric sulfate solution. In order to avoid complicating effects due to the change in the composition of the solution as it passed through the reductor, zinc sulfate solutions rather than pure water were used as solvent. Studies have been made of the effects of the following parameters on the extent of reduction of the iron: flow rate, iron concentration, column length, particle size, zinc concentration, temperature, the extent of amalgamation of the zinc particles, and the *p*H of the solutions.

EXPERIMENTAL

Solutions were forced up through the columns by pressure supplied from a tank of nitrogen. The flow rates were controlled by adjusting a stopcock at the outlet of the column. In most of the experiments, the solution reservoir was maintained at 25° in a regulated bath. Runs were also made at 0° and at 40°. The rate of flow was measured on one of three suspended-ball flow-meters, which covered the range 0–1000 ml/min. Three interchangeable columns, of 1.15 cm inside diameter, allowed weights of zinc amalgam of 7.5, 15, and 30 g, corresponding to column lengths of approximately 2, 4, and 8 cm. The zinc was supported on a thin layer of glass wool, and a barrier of glass wool was laid over the top of the zinc. The exit end of the column was filled with glass beads to minimize the dead volume.

Two sizes of zinc pellets were used, 16–24 standard screen mesh and 50–60 mesh, corresponding to average particle diameters of 0.840 mm and 0.274 mm. These were amalgamated to mercury percentages of 0.5, 1, and 5. The amalgamated pellets were aged for about 48 hours before use. By this time, the amalgam surface had become hard; the pellets would pack as discrete particles into a column. Charging the columns was accomplished by slowly pouring the zinc into the tube filled with water while rapidly tapping its side. Considerable care was taken to standardize this procedure in order to obtain reproducible columns. This object was probably not entirely accomplished. Furthermore, the columns usually showed a shrinkage of about ten percent during the course of an experiment.

Stock solutions in ca. 1.0, 0.5, or 0.25 molar zinc sulfate were prepared with ferric sulfate at iron concentrations of 0.0125, 0.025, and 0.05 molar. Reagent grade chemicals were used with no further purification. The *p*H of the solutions, as determined by a glass electrode, was adjusted to 2.00 with concentrated sulfuric acid. A run was also made with the *p*H at 1.34.

In order to realize a nearly steady state in a column,

* Research conducted under the auspices of the AEC. The material for this paper has been taken from a dissertation prepared by Kerro Knox at the Brookhaven National Laboratory and submitted to the Faculty of the Graduate School of Yale University in partial fulfillment of the requirements for the degree of Doctor of Philosophy, June 1950.

† Present address: Department of Physical Chemistry, Cambridge, England.

‡ Present address: Sterling Chemistry Laboratory, New Haven, Connecticut.

[1] H. A. Liebhafsky, J. Am. Chem. Soc. **59**, 452 (1937).

[2] H. W. Stone and D. N. Hume, Ind. Eng. Chem., Anal. Ed. **11**, 598 (1939).

TABLE I. Column run No. 1.

(For conditions see Table II)
20.00 ml of completely reduced stock solution
=21.33 ml of the Ce IV used

Flow rate (ml/min)	Ce IV (ml)	$-\ln c_{exit}/c_{input}$
5.05	20.91	3.93
5.05	21.00	4.17
5.25	20.56	3.32
5.25	20.70	3.52
5.25	20.80	3.70
12.70	19.09	2.26
12.70	19.17	2.29
33.30	16.41	1.47
33.30	16.87	1.57
104	12.56	0.89
104	12.57	0.89
104	12.64	0.90

a procedure of preliminary washing was adopted in which a solution containing iron at 0.05M at a *p*H of 2.00 was passed through the column for two hours at a rate of about 35 ml per minute. Under this treatment, the reducing power of the column became essentially constant.

Total iron determinations were done with the aid of a Jones reductor and carefully standardized ceric sulfate solutions using ferroin as indicator. For the zinc analysis of the stock solutions, iron was first separated by a double precipitation with ammonia, and the zinc determined by precipitation as the ammonium phosphate.

The flow-meters were first calibrated with an iron-zinc solution in which the zinc concentration was 0.941 M and the iron concentration about 0.048 M. New calibrations were found to be necessary only for changes in zinc concentration; the relatively small changes in iron content were without appreciable effect.

In a typical run, after the column had been pretreated and shown to have reached a steady state for a constant flow rate, the iron-zinc solution was switched into the column at a rate sufficiently low to ensure nearly complete reduction. A series of determinations of extent of reduction was made at arbitrary intervals of flow rate up to the maximum rate that the apparatus would allow. Each point was determined in duplicate, and at the end of the run an earlier point was again checked to ascertain that reproducible data were being obtained. To illustrate the character of the results, the complete data of a single experiment are given in Table I. The sensitivity to lack of experimental precision of the Fe III concentration ratio, c (exit)/c_0 (input), is apparent from these data. Values corresponding to nearly complete reduction must be disregarded in any discussion of the results.

Table II contains a summary of the conditions and results of all of the experiments. In the two runs made at 0°, to avoid recalibration of the flow-meters, two reservoir bottles were introduced into the system between the meters and the column. These bottles were cooled in crocks of crushed ice. The warm solution from the flow-meter entered the first bottle at the top, displacing the cold, more dense, solution from the bottom of the first bottle to the top of the second. The column, also cooled in ice, received its solution from the bottom of the second bottle. For the run at 40°, a single reservoir bottle and the column were mounted in a thermostat at this temperature. The cool solution from the flow-meter passed into the bottom of this bottle, and the column received its solution from the top.

DISCUSSION

Flow Rate. The data of each of the twenty-two runs are adequately described by the expression

$$c = c_0 \exp(-S/\dot{v}^{\frac{1}{2}}).$$

S has been determined graphically as the slope of the logarithmic plot with $\dot{v}$, the flow rate, measured in milliliters per minute. The values of S, for the various runs, are given in Table II. The character of the agreement between the runs intended to be identical will be seen in Fig. 1. Runs 1 and 2, and Runs 3, 4, and 5 were done with conditions nearly alike. Except at the low flow rates, the agreement is satisfactory. Within a single run the exponential dependence on $1/\dot{v}^{\frac{1}{2}}$ is in excellent agreement with the data.

We are immediately led to the presumption that the rate limiting process in the reductor column is the diffusion of the ferric ion up to the amalgam surface through a nearly static liquid film. The steady-state behavior of a column with such a rate law may readily be shown to result in the following expression for the concentration

$$c = c_0 \exp(-3Dx/r\Delta r\dot{v}d).$$

The important assumptions underlying this expres-

TABLE II. Summary of results.

Run No.	Zn M	Fe M	Column length, g	Temp.	Percent amalgam	Zn mesh	Slope S
1	0.934	0.04789	30	25	5	16–24	8.88
2	0.934	0.04789	30	25	5	16–24	
3	0.934	0.04789	15	25	5	16–24	
4	0.934	0.04789	15	25	5	16–24	5.00
5	0.940	0.04825	15	25	5	16–24	
6	0.934	0.04789	7.5	25	5	16–24	2.84
7	0.940	0.04825	15	0	5	16–24	3.90
8	0.934	0.02408	15	25	5	16–24	(5.00)
9	0.934	0.02408	15	25	1	16–24	6.48
10	0.454	0.04512	15	25	5	50–60	18.0
11	0.452	0.02289	15	25	5	16–24	6.02
12	0.452	0.02289	15	25	5	50–60	(18.0)
13	0.452	0.02289	7.5	25	5	50–60	9.36
14	0.452	0.02279	15	25	1	50–60	24.4
15	0.452	0.02289	15	25	0.5	50–60	23.4
16	0.452	0.02279	15	0	5	50–60	15.0
17	0.452	0.02282	15	40	5	50–60	17.0
18[a]	0.452	0.02282	15	25	5	50–60	19.2
19	0.448	0.01136	15	25	5	50–60	(18.0)
20	0.230	0.04362	15	25	5	50–60	
21	0.227	0.02281	15	25	5	50–60	23.8
22	0.224	0.01132	15	25	5	50–60	

[a] *p*H 1.34.

sion are given by Boyd, Adamson, and Myers.[3] The film thickness, Δr, will vary inversely approximately as the square root of the flow rate,[4] which leaves us with the dependence of $\ln(c/c_0)$ on flow rate as actually found. In the above expression, D is the diffusion coefficient of the ferric ion; r, the particle radius; x, the column length measured in terms of the mass of zinc contained therein; and d, the density of zinc amalgam particle.

Iron Concentration. That the effect of changes in ferric ion concentration has been adequately swamped by the high zinc concentrations will be seen from the circles in Fig. 1 for run 8 as compared to the line for runs 3, 4, 5. This is again shown by the comparison of runs 10, 12, and 19; and runs 20, 21, and 22. In the following discussion, we may thus disregard the actual iron concentrations and consider only the ratios.

Column Length. Both in the diffusion limited case as well as in the kinetics for a chemical reaction at the solid-liquid interface, one expects a simple exponential dependence of c/c_0 on column length. How nearly this is realized is apparent from the slopes for runs 1, 2; runs 3, 4, 5; and run 6. Theoretically, these slopes should be in the ratio 4:2:1. Experimentally, we find 3.13:1.76:1.00. For the smaller particles, runs 12 and 13 give the ratio 1.92:1.00, while 2:1 is expected. Increase in column length consistently gives too small an increase in efficiency. This deviation from simple behavior is well outside any experimental uncertainty, at least for the coarser particles. A possible explanation for this effect lies in the fact that hydrogen gas is evolved in the column. As the gas is swept downstream it very probably collects, in part, in the interstices of the particles, thus shielding the iron from the action of the zinc. One would expect the effect to increase with column length. In fact, the observed decrease in efficiency is roughly proportional to column length.

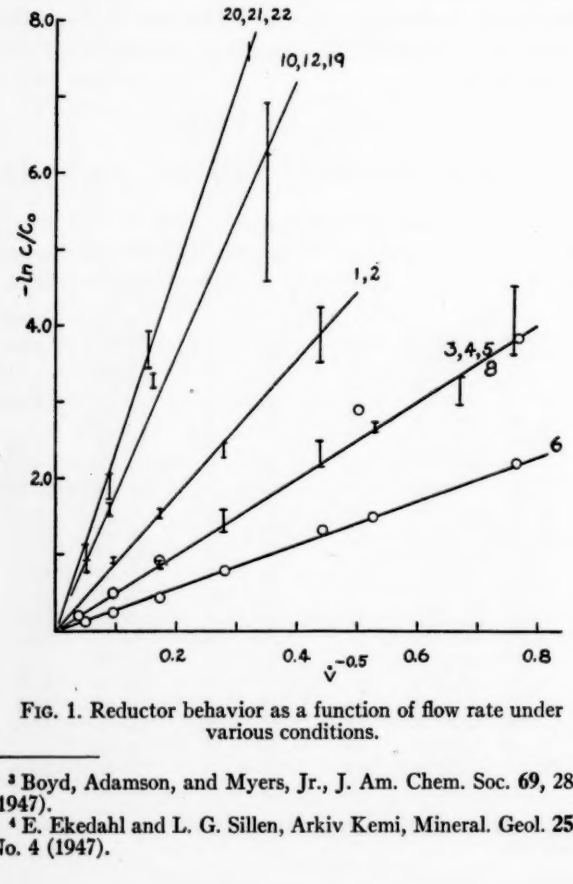

FIG. 1. Reductor behavior as a function of flow rate under various conditions.

Particle Size. A comparison of run 11 with runs 10, 12, and 19 gives the dependence on particle size; the slopes are in the ratio 1.00:2.95. The ratio of the average particle diameter is 3.07:1.00. The efficiency of the column is nearly inversely proportional to the particle radius, as is called for by the theory. It should be noted, however, that this dependence results as well from the discussion of the case for an interfacial reaction as the controlling mechanism. We have here no further evidence for a decision between the two cases.

Zinc Concentration. Comparisons of run 8 with run 11, and of runs 10, 12, and 19 with runs 20, 21, and 23, show that a decrease of the zinc concentration in the region 0.25−1.0M results in an increase in the efficiency of the column. This effect is to be expected for the diffusion mechanism only. A decrease in the viscosity of the solution, resulting from a decrease in zinc concentration, will cause a decrease in the film thickness, Δr, and a consequent increase in S. An effect on the diffusion constant of the iron is also to be expected. Indeed, if the minimum in D lies near 1M, as might be expected, then we have a complete qualitative explanation of the observed variations in S.

Temperature. Some idea of the effect of temperature on performance is to be had from a comparison of runs 3, 4, and 5 at 25°, with run 7 at 0°, and of run 16 (0°), run 12 (25°), and run 17 (40°). The experiments at 0° and 25° give an activation energy of 1.2−1.6 kcal. Since the film diffusion mechanism can be considered as fairly well established, we are here essentially computing the temperature coefficient of $D/\Delta r$, a no doubt complicated function of the viscosity of the solution. No simple physical significance, therefore, can be attached to this estimate of activation energy. Unfortunately, the run at 40° fails to add anything to our knowledge. At the higher temperature a marked darkening of the iron solution occurred. Increased hydrolysis evidently caused a change in the character of the ionic species present; the efficiency of the column actually decreased with the increase in temperature from 25° to 40°.

Percentage Amalgamation and pH. Runs 8 and 9, 12, and 14 indicate a thirty percent increase in efficiency caused by lowering the mercury content from five percent to one percent. An effect apparently inconsistent with this result is observed in the comparison of runs 14 and 15. We must suppose, however, that there does exist a real dependence on the mercury content. This fact indicates that the complete kinetic picture of the

[3] Boyd, Adamson, and Myers, Jr., J. Am. Chem. Soc. **69**, 2836 (1947).
[4] E. Ekedahl and L. G. Sillen, Arkiv Kemi, Mineral. Geol. **25A**, No. 4 (1947).

zinc reductor is much more complex than thus far implied. No further studies have been made on this point.

A comparison of runs 12 and 18 indicates a small dependence on pH. However, the results of run 18 are suspect in that at this low pH a considerably greater hydrogen evolution was observed. Run 18 does show that small accidental deviations in pH from the value 2.00 selected for the experiments would have but little effect on the results.

THE JOURNAL OF CHEMICAL PHYSICS VOLUME 19, NUMBER 2 FEBRUARY, 1951

The Fluorescence of Acetone Vapor*

G. W. Luckey† and W. Albert Noyes, Jr.
Department of Chemistry, University of Rochester, Rochester, New York
(Received October 4, 1950)

An apparatus has been designed and built for the study of low fluorescence intensities. The "blue" fluorescence of acetone vapor has been investigated from pressures of about 1 mm to pressures of about 200 mm, at temperatures from 25°C to 300°C both with and without the addition of foreign gases, such as O_2, NO, N_2, and $(CH_3CO)_2$.

It is found at temperatures over about 100°C, and in the presence of O_2 and NO, that there is no structure in the fluorescence of acetone which can be detected, and the wavelength of the intensity maximum is different from that found at 25°C. The shapes of the quenching curves are such as to demand at least two upper electronic states which participate directly or indirectly in the fluorescence phenomenon. This is in agreement with previous work. The photo-chemical data necessitate a high probability of predissociation of the initially formed state together with a small lifetime probably determined by the rate of predissociation. At least one other upper state, formed from the first through collisions, must be relatively insensitive to collisional deactivation. A complete theory cannot be given, but some important aspects are clear.

SINCE the first observations of the fluorescence of acetone vapor were made by Damon and Daniels,[1] many articles have appeared which have served to elucidate one aspect or another of the relatively complex phenomena associated with this problem.[2]

The present work was undertaken to complete some of the data, and to attempt to arrive at a consistent picture of the phenomena. It is impossible, as so often happens in problems of this type, to present a mechanism which explains all of the data satisfactorily, and to prove that the mechanism is a unique solution to the problem. Nevertheless, it is believed that the present work limits possibilities to a smaller number than heretofore.

EXPERIMENTAL

The acetone was Baker's analyzed, distilled in a column of approximately 30 plates with a 10:1 reflux ratio, and with retention of the middle third, which was dried by anhydrous copper sulfate. Final purification was accomplished by bulb-to-bulb distillation in the vacuum line.

Oxygen was prepared by heating potassium permanganate and by passing it through a trap cooled to the temperature of liquid nitrogen. Linde Nitrogen was passed through heated copper turnings and a trap immersed in liquid nitrogen. Nitric oxide was prepared by a method previously described,[3] which was based on a reaction used by Johnston and Giauque.[4]

An Alpine burner (Hanovia Manufacturing Company) was used as a radiation source for most of the work, but a General Electric AH-6 arc was used for several of the experiments. The radiation penetrating a 1-mm radius hole was collimated by a quartz lens of 140-mm focal length, and passed through the color filter combination of Hunt and Davis.[5] The radiation consisted principally of the group of lines at 3130A and a small amount of radiation at 3341A. Because of pressure broadening, the radiation from the AH-6 arc was not as monochromatic as that from the Alpine burner.

The radiation transmitted through the cell was measured with a G.E. 929 photo-cell and an electrometer circuit using a *V X* 41 *A* tube. The photo-current was balanced by current from a Leeds and Northrup student type potentiometer. The balance point drifted with time, but could be centered on the galvanometer scale by adjustment of the resistor in the electrometer plate circuit.[6]

* This research was supported in part by Contract N6onr-241, Task I with the ONR, United States Navy.

† Eastman Kodak Company Fellow in physical chemistry at the University of Rochester during 1949–50.

[1] G. H. Damon and F. Daniels, J. Am. Chem. Soc. **55**, 2363 (1933).

[2] R. E. Hunt, and W. A. Noyes, Jr., J. Am. Chem. Soc. **70**, 467 (1948) give a bibliography of most of the work until 1948. Later references will be given at their appropriate places in this article.

[3] W. A. Noyes, Jr., J. Am. Chem. Soc. **53**, 514 (1931).

[4] H. L. Johnston and W. F. Giauque, J. Am. Chem. Soc. **51**, 3194 (1929).

[5] R. E. Hunt and W. Davis, Jr., J. Am. Chem. Soc. **69**, 1415 (1947).

[6] The authors wish to thank Professor S. N. Van Voorhis, of the Department of Physics, for suggesting the circuit used with the

The fluorescent radiation passed through two diaphragms and was focused by a quartz lens on the cathode of the photo-multiplier tube. Scattered ultraviolet radiation was removed by a Corning, No. 738, glass filter. The fluorescent radiation was "chopped" thirty times per second by a four-bladed aluminum sector mounted on a steel shaft turned by a belt drive from a speed reducer motor combination. The intensity was measured by an *IP*21 photo-amplifier tube using a synchronous amplifier designed by Dr. Van Voorhis.[7] The circuit employed the principle of synchronous detection which has been used by several workers, notably Michels[8,9] and Cosens.[10]

Some difficulty was experienced with amplifier noise. The sources of noise with an *IP*21 have been discussed by Engstrom.[11] Cooling units of some type might have led to some improvement,[12,13] but the apparatus was sufficiently sensitive to make most of the measurements described with an accuracy of 2 to 3 percent, and it was felt that construction of a cooling unit was not necessary.

It was found to be extremely difficult to construct a cell of material which would not in itself fluoresce. A special *T*-shaped quartz cell was ordered with a main limb 12.5 cm in length, and an internal diameter of 3.2 cm. The observation window was 2.2 cm in diameter, and the stem of the *T* was 2.9 cm in diameter at the cross bar, tapering down to 9-mm tubing which was sealed to the vacuum system with a quartz-Pyrex graded seal. The background produced by the cell amounted to about 2 percent of the fluorescence at 140°C and 150-mm pressure. No background emission could be detected, under the above conditions, after the outside of the cell was painted with "optical black" lacquer.

Both fluorescence and transmission amplifiers were calibrated before and after each measurement. For the fluorescence amplifier, this was done with a standard blue radium-activated phosphor, with an intensity of 0.5 microlambert, which was purchased from the United States Radium Corporation.[14] The phosphor remained constant within about 1 percent. The transmission amplifier was calibrated by a 6-volt headlight lamp operated at reduced voltage, and filtered through 2 mm of cobalt blue glass. The transmission amplifier was found to be linear within experimental error.

It is unnecessary to describe the vacuum line and gas techniques in detail, since they resemble customary procedures used in studies of this type.

Measurements of pressures greater than 25 mm were made on a mercury cutoff used as a manometer. Below 25 mm a Gaertner cathetometer was used to measure the difference in level. The maximum error in pressure measurements in the range 25 to 50 mm, was 1 to 2 percent. Pressures below 1 mm were measured on a McLeod gauge.

Most of the spectrograms were taken with a large Bausch and Lomb spectrograph with a reciprocal dispersion of about 16A/mm in the range used. Some of the pictures were taken with a small Bausch and Lomb spectrograph with a reciprocal dispersion of about 32A/mm. For low intensities, a three prism, high speed spectrograph was used.[15] The reciprocal dispersion of this instrument was about 40A/mm.

The absolute fluorescence quantum yield measurements were made by a method suggested by Dr. J. E. LuValle of the Eastman Kodak Company. This method may be summarized as follows: (1) An Eppley bismuth-silver thermopile was standardized with the aid of a Bureau of Standards radiation standard. (2) The thermopile was then used to measure the incident intensity at various wavelengths. (3) By means of a mirror, the incident light was reflected to the surface of the *IP*21 photo-multiplier tube. (4) Wratten neutral density filters, calibrated by a Beckmann spectrophotometer, were used to reduce the incident intensity to a value approximating the fluorescent intensity. (5) The 3660A mercury line was isolated by a 2-mm Corning glass No. 5860, and a 2-mm Corning glass No.

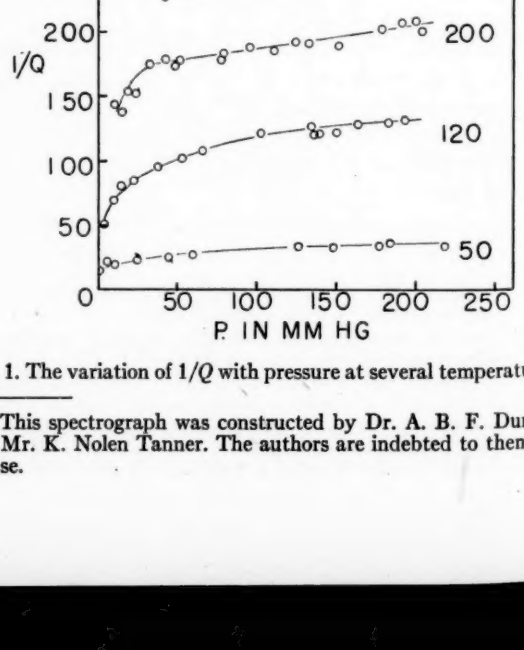

FIG. 1. The variation of $1/Q$ with pressure at several temperatures.

V X 41 *A* tube. The details of the circuit may be found in the Ph.D. thesis of G. W. Luckey, University of Rochester, 1950. Penick, D. B., Rev. Sci. Instr. **6**, 115 (1935) has discussed several electrometer circuits, and the conditions for their stability.

[7] A similar circuit has been described recently by D. Marlow, and J. C. Pemberton, Rev. Sci. Instr. **20**, 724 (1949) and earlier by G. M. B. Dobson, Proc. Phys. Soc. (London) **43**, 324 (1931). The details of the amplifier design and operation are given in the Ph.D. thesis of George W. Luckey, Department of Chemistry, University of Rochester, 1950. This thesis has also been distributed as a report to the ONR, under Contract N6onr-241, Task Order I.

[8] W. C. Michels, and N. L. Curtis, Rev. Sci. Instr. **12**, 444 (1941).

[9] W. C. Michels and E. D. Redding, Rev. Sci. Instr. **20**, 566 (1949).

[10] C. R. Cosens, Proc. Phys. Soc. (London), **46**, 818 (1934).

[11] R. W. Engstrom, J. Opt. Soc. Am. **37**, 420 (1947).

[12] E. F. Coleman, Electronics **19**, 220 (1946).

[13] R. W. Engstrom, Rev. Sci. Instr. **18**, 587 (1947).

[14] The authors wish to thank Professor Brian O'Brien and the Institute of Optics, University of Rochester, for calibration of the phosphor.

[15] This spectrograph was constructed by Dr. A. B. F. Duncan and Mr. K. Nolen Tanner. The authors are indebted to them for its use.

TABLE I. Sensitivity of the photo-multiplier-amplifier circuit.

Wavelength	Quanta/second	Scale divisions on 1 megohm scale
3660A	6.3×10^4	2.4
5460A and 5790A	6.3×10^4	1.01
Blue phosphor	6.3×10^4	0.83

738. The 5460 and 5790A mercury lines were isolated by the Hunt-Davis solution filters, and 2 mm of Corning No. 3387 glass. Concentrations of the solutions were adjusted so that observation of the source, with a hand spectrograph, showed the desired lines only. (A very small amount of 4900A radiation was present). The radiation always passed through 10 cm of water to reduce infrared radiation. (6) The *IP*21 tube was thus calibrated at 5460 to 5790A and at 3660A, and the calibrations agreed with those given by Engstrom[13] within about 25 percent. (7) From calibration of the photo-amplifier and the values of the relative fluorescence efficiency at 50°, the absolute efficiency could be calculated on the assumption that the fluorescent beam behaved as a line source.

The absolute fluorescence efficiency determined in this way is certainly not very accurate, but it is estimated to be correct within a factor of 2 or 3. (See Table I.)

RESULTS

The existence of structure in the blue fluorescence of acetone, at room temperature, has already been reported.[16] It became evident that the effect of foreign gases and of increase in temperature on this structure might be important to the understanding of the theory. The principal results follow:

(1) At temperatures from 120°C to 150°C, the fluorescence showed no structure. The wavelength at maximum intensity shifted from about 4500 to 4550A at room temperature, to about 4300A at the higher temperatures.

(2) Oxygen at pressures of 20 to 100 mm at room temperature caused the structure to disappear and caused the same wavelength shift as an increase in temperature.

(3) Nitrogen at pressures up to 50 mm had no effect on the appearance of the fluorescence spectrum.

(4) Nitric oxide was not studied in this connection.

(5) A mixture of 80 mm of biacetyl and 200 mm of acetone showed no structure in the blue part of the spectrum at room temperature.

The fluorescence quenching data on pure acetone may be summarized as follows:

(1) A Stern-Volmer plot of $1/Q$ *vs* P does not give a straight line at any temperature up to 200°C, but at 200° and at 300°C, a straight line is obtained over a considerable range. (See Fig. 1). ($1/Q$ is the inverse of the fluorescence efficiency. The values in column 4 of Table II are in arbitrary units. To obtain the inverse of the absolute fluorescence efficiency, these values should be multiplied by about 15.)

(2) The fluorescence efficiency is independent of the incident intensity over the range studied.

(3) At 50°C, and a pressure of 150 mm, the absolute fluorescence efficiency is about 2×10^{-3}.

(4) The error in the pressure dependence of $1/Q$ is probably not more than three percent at any given

[16] Luckey, Duncan, and Noyes, J. Chem. Phys. **16**, 407 (1948).

TABLE II. Quenching of acetone fluorescence under various experimental conditions

Acetone pressure mm	Foreign gas	Foreign gas pressure mm	$1/Q$ (arb. units)
	$T=25$°C		
25	none		21
50	none		23.5
100	none		26
150	none		28
200	none		29
	$T=50$°C		
25	none		24
50	none		27.5
100	none		32
150	none		34
200	none		35
150	NO	5	167
150	NO	7	200
	$T=120$°C		
25	none		72
50	none		100
100	none		120
150	none		127
200	none		130
	$T=140$°C		
25	none		107
50	none		127
100	none		145
150	none		160
200	none		167
150	O_2	5	210
150	O_2	10	215
150	O_2	20	215
50	O_2	5	177
50	O_2	10	182
50	O_2	20	183
150	NO	7.5	208
150	NO	25	211
150	N_2	52.5	160
150	N_2	23.7	160
150	H_2	15.2	160
150	H_2	46.0	160
	$T=200$°C		
25	none		160
50	none		177
100	none		185
150	none		192
200	none		200
160	O_2	16	220
	$T=300$°C		
50	none		227
100	none		238
150	none		252
200	none		265

(One arbitrary unit = 15 absolute units.)

TABLE III. Effect of cobalt blue filter on the quenching effect of nitric oxide.

Temperature	Filter	$1/Q$ (with NO)	$1/Q$ (without NO)	$1/Q$ (with) $1/Q$ (without)
140	None	218	158	1.38
140	2-mm Cobalt	442	342	1.29
50	None	200	34	5.9
50	2-mm Cobalt	420	104	4.0

temperature, except when the response of the photo-multiplier tube is nonlinear. The effect of temperature on $1/Q$ is more uncertain, both because of the wavelength shift and because of the change in absorption coefficient with temperature. Absorption coefficients were determined carefully, several times at each temperature, for the light sources used (see Table IV below).

The important trends in the results may be seen in Table II.

The effects of foreign gases on the fluorescence efficiency of acetone may be summarized as follows:

(1) As oxygen is added at a given acetone pressure, $1/Q$ rises sharply and then levels off at a very nearly constant value. As the temperature increases, the variation in $1/Q$ becomes less and less until at 200°, $1/Q$ changes only between 2 and 3 percent as the oxygen pressure increases from 0 to 20 mm at 160-mm acetone pressure.

(2) The constant value of $1/Q$ as a function of oxygen pressure depends on the acetone pressure and tends to be higher at higher acetone pressures, but it is nearly independent of temperature.

(3) The effect of nitric oxide on $1/Q$ is similar to that of oxygen.

(4) It was determined, by insertion of a cobalt blue filter, that nitric oxide is more effective in quenching wavelengths longer than 4500A than in quenching shorter wavelengths. The data, which are not very quantitative, are shown in Table III.

(5) Increase in temperature has little effect on the limiting value of $1/Q$ at high pressures of nitric oxide.

(6) Nitrogen, in the few cases studied, caused no change in $1/Q$.

(7) Hydrogen, in the few cases studied, caused no change in $1/Q$.

In addition to the above facts, which were obtained during the course of this work, any theory of the fluorescence must account for the data of Kaskan and Duncan,[17] which show a logarithmic decay of fluorescence with a mean life of about 2×10^{-4} sec, together with a decrease in mean life with increase in acetone pressure.

A further point of interest may be noted. The calculation of fluorescent radiation demands an accurate knowledge of the amount of radiation absorbed. It was

[17] W. E. Kaskan and A. B. F. Duncan, J. Chem. Phys. 18, 427 (1950).

TABLE IV. Dependence of absorption coefficient on temperature[a].

Temperature °C	Quartz burner absorption coefficient	*AH-6* absorption coefficient
25	2.86	—
50	2.85	—
120	3.58	2.87
140	3.83	2.97
200	4.42	3.58
250	5.03	—
300	5.78	4.78

[a] The absorption coefficients given here are the values of k in the expression $I_t=I_0 10^{-kcd}$, where I_t is radiation transmitted, I_0 is the incident intensity, c is concentration in moles per liter, and d is distance in centimeters.

found that absorption coefficients for acetone increase with the increase in temperature. By pure coincidence, the absorption at constant pressure, but decreasing gas density, remains nearly constant above 50°. Table IV shows the dependence of absorption coefficient (k in $I_t=I_0 10^{-kcd}$, where I_t is radiation transmitted, I_0 is incident intensity, c is concentration in moles per liter, and d is distance) on temperature for the group of lines at 3130A as obtained with the Alpine burner and the combination of color filters used. The data should serve as a warning to those who assume absorption coefficients to be independent of temperature. Absorption coefficients can only be reproduced exactly with the same lamp-color filter combination.

DISCUSSION

It is possible either to give a perfectly generalized theory of the fluorescence based on all types of transition which could occur, or to specify the minimum number of steps which must be used in deriving an equation of the right form to fit the data. It is impossible, in the latter case, to prove that the mechanism is the only one which would satisfy the facts.

At least two upper states capable of fluorescent emission must be used to provide the necessary number of parameters in the equations for quenching. One of these states must be quenched by oxygen and by nitric oxide (both of which are paramagnetic gases) and also must either be destroyed, or rendered incapable of emission by increase in temperature. This state is the one responsible for the "structure" which has been observed in the fluorescence spectrum.[16] The other state seems to be unaffected by oxygen or by nitric oxide, and moreover, the emission from this state is either continuous or has so much overlapping structure that it appears to be continuous. This state is only moderately quenched by collision with other acetone molecules.

The primary quantum yield for photo-chemical dissociation of acetone at 3130A is quite high, even at room temperature, and approaches unity at temperatures slightly over 100°C.[18] However, much of this dissociation is prevented by the addition of a few mil-

[18] W. A. Noyes, Jr. and L. M. Dorfman, J. Chem. Phys. 16, 788 (1948).

limeters of iodine.[19] An appreciable fraction of the dissociation apparently does not result from a repulsive upper electronic state and must occur after a delay of 10^{-8} second, or greater, after the absorption act.

Fluorescence and dissociation must, therefore, be competing processes for the removal of one or the other, or probably both of the fluorescing states. In at least one case, therefore, the lifetime is probably determined by the rate of dissociation rather than by the rate of transition from upper to lower state. It is possible that the lifetime observed by Kaskan and Duncan of about 10^{-4} second[17] is that of only one of the states. In this event, the lifetime of the fluorescence in the presence of oxygen as well as at a high temperature might be quite different and probably much shorter.

The natures of the two states cannot be specified with any certainty. There is no conclusive evidence that one is "singlet" and the other "triplet" or indeed, that either of them is "triplet," although the long lifetime[17] is some sort of supporting evidence for such a conclusion.[20]

It would be possible to explain the data on the assumption that one of the states merely lies above some predissociation limit of an upper electronic state, and the other either lies below, or has a much slower rate of dissociation. Actually, it is an oversimplification to discuss only two states since many rotation and vibration levels might be involved for each one.

It is possible to specify a mechanism based on two states which will lead to equations for the quenching and for the lifetime of the right forms to fit the data. This mechanism is based on the following steps:

$$A+h\nu=A^* \tag{1}$$

$$A^*=D \tag{2}$$

$$A^*=A^{**} \tag{3}$$

$$A+A^*=A^{**}+A \tag{4}$$

$$A^*=A+h\nu' \tag{5}$$

$$A^{**}=A+h\nu'' \tag{6}$$

$$A^*=A \tag{7}$$

$$A^{**}+A=D+A \tag{8}$$

$$A^{**}+O_2=X \tag{9}$$

$$A^{**}+A=A^*+A \tag{10}$$

D=dissociation products; X=unknown, and Eq. (9) is written this way to indicate that O_2 quenches the fluorescence. (NO could be substituted for O_2 in the mechanism.)

It is possible to show that no single step in this mechanism can be omitted without causing disagreement with some aspect or other of the data, but there seems to be no reason to discuss this mechanism in great detail. Numerical values for the various rate constants can be specified so as to give a more or less quantitative numerical fit to the facts. Only one or two points in this connection will be made. The constant for reaction (2) must be of the order of magnitude of 10^7 sec^{-1} at 50°C, and it must have a small activation energy of 5 kcal or less.[18] The constant for reaction (5) must be about 10^5 sec^{-1} at 300°C, and that for reaction (6) must be about 5×10^3 sec^{-1} at 50°C. Reaction (10) is necessary to afford an explanation of the effect of pressure on lifetime, which was observed by Kaskan and Duncan.[17]

The absolute fluorescence efficiency predicted by this mechanism, and with the use of the constants mentioned, is between 10^{-2} and 10^{-3} at 50°C. This is of the correct order of magnitude. The values of $1/Q$, the quenching, are not very sensitive to the magnitudes of most of the constants, but the form of the equation derived on the assumption of the steady state for A^* and A^{**} is correct.

[19] E. Gorin, J. Chem. Phys. **7**, 256 (1939). J. N. Pitts, Jr. and F. E. Blacet, private communication.
[20] D. S. McClure, J. Chem. Phys. **17**, 905 (1949).

Transport Properties of Gases with a Square-Well Molecular Interaction Potential*

EUGENE M. HOLLERAN† AND HUGH M. HULBURT
Catholic University of America, Washington, D.C.

(Received October 26, 1950)

The kinetic theory cross-section integrals are calculated for the square-well molecular potential model. Parameters are determined for light gases from viscosity measurements and are used to reproduce viscosity data for pure gases and binary mixtures.

Comparison is made between these parameters and those found from compressibility data and other transport properties. Different sets of parameters are apparently required for each transport property in order to account for the experimental results. The thermal diffusion constant for this model is a function of temperature and one other parameter. Excellent reproduction of the neon isotope data is obtained, and predictions of the qualitative behavior of the thermal diffusion ratio are made.

INTRODUCTION

THE exact kinetic theory for a gas of spherically symmetrical molecules sufficiently dilute that triple collisions are unimportant was developed independently by Enskog and Chapman and is detailed in the book by Chapman and Cowling.[1] According to this theory the coefficients of the transport properties of such a gas can be expressed in terms of certain cross-section integrals, $H^{(l,k)}$, whose values depend ultimately on the shape of the intermolecular force field. Below are given the first approximations to the coefficients of viscosity, η; diffusion, D; thermal conductivity, λ; and the thermal diffusion constant, α.

For a binary mixture

$$\eta=\frac{3M_1M_2E_{12}[E_{11}E_{22}(U_1+U_2-2A_{12}+4/3)+2E_{12}(E_{11}A_{22}+E_{22}A_{11})]}{4A_{12}E_{11}E_{22}+12M_1M_2E_{12}(U_1E_{22}A_{11}+U_2E_{11}A_{22}+2E_{12}A_{11}A_{22})}, \tag{1}$$

where $M_1=m_1/m_1+m_2$ and similarly for M_2; m_1 and m_2 are the masses of the two types of molecules, m_2 being equal to or less than m_1;

$$A_{12}=\frac{2H_{12}^{(2,7)}}{15H_{12}^{(1,5)}}, \tag{2}$$

with similar relations for A_{11} and A_{22}. The subscripts 11, 22, and 12 differentiate quantities calculated for encounters between molecules which are both of type 1 or 2 or one of each. Unless otherwise specified the expressions for three such quantities differ only by obvious changes in subscripts.

$$E_{12}=\frac{J_{12}}{16M_1M_2H_{12}^{(1,5)}}, \quad E_{11}=\frac{J_{11}}{4H_{11}^{(1,5)}} \tag{3}$$

where

$$J_{12}=\left(\frac{2\mu kT}{\pi}\right)^{\frac{1}{2}} \quad \text{and} \quad J_{11}=\left(\frac{m_1kT}{\pi}\right)^{\frac{1}{2}} \tag{4}$$

where μ is the reduced mass, equal to m_1m_2/m_1+m_2.

$$U_1=\frac{n_1}{n_2}\left(\frac{2}{3}+\frac{m_1}{m_2}A_{12}\right) \tag{5}$$

where n_1 and n_2 are the number densities of the respective components. U_2 is the same except for an interchange of the subscripts 1 and 2.

For a pure gas Eq. (1) reduces to

$$\eta=E_{11}/4A_{11}. \tag{6}$$

For a binary mixture

$$D=\frac{3E_{12}}{2n(m_1+m_2)}, \tag{7}$$

where $n=n_1+n_2$.

For a pure gas Eq. (7) reduces to

$$D=3E_{11}/4\rho, \tag{8}$$

where ρ, the density, equals nm, m being the mass of the molecules. This represents the coefficient of self-diffusion which, of course, cannot be determined experimentally for a pure gas. However, Eq. (8) is often applied to mixtures of isotopes or any two molecular species, like carbon dioxide and nitrous oxide, whose masses, sizes, and shapes are similar enough.

For a pure gas

$$\lambda=5/2C_v\eta \tag{9}$$

where C_v is the constant volume heat capacity.

For a binary mixture

$$\alpha=\frac{5(C_{12}-1)(x_1S_1-x_2S_2)}{x_1^2Q_1+x_2^2Q_2+x_1x_2Q_{12}}, \tag{10}$$

where x_1 and x_2 are the mole fractions of the two gases,

* Taken in part from a dissertation submitted to the Catholic University of America in partial fulfillment of the requirements for the Ph.D. degree and carried out during the tenure of an American Chemical Society Predoctoral Fellowship, 1946–1948.

† Present address: St. John's College, Brooklyn, New York.

[1] S. Chapman and T. G. Cowling, *The Mathematical Theory of Non-Uniform Gases* (The Cambridge University Press, New York, 1939).

and

$$C_{12}=\frac{2H_{12}^{(1,7)}}{5H_{12}^{(1,5)}} \tag{11}$$

$$S_1=\frac{4M_1^2A_{11}E_{12}}{E_{11}}+M_2(3M-4M_1A_{12}), \tag{12}$$

M being M_1-M_2,

$$S_2=\frac{4M_2^2A_{22}E_{12}}{E_{22}}-M_1(3M+4M_2A_{12}) \tag{13}$$

$$Q_1=\frac{4M_1A_{11}E_{12}}{E_{11}}[6M_2^2+(5-4B_{12})M_1^2+8M_1M_2A_{12}] \tag{14}$$

with a similar relation for Q_2

$$Q_{12}=\frac{32M_1M_2A_{11}A_{22}E_{12}^2}{E_{11}E_{22}}+3M^2(5-4B_{12})+4M_1M_2A_{12}(11-4B_{12}) \tag{15}$$

$$B_{12}=\frac{5H_{12}^{(1,7)}-H_{12}^{(1,9)}}{5H_{12}^{(1,5)}}. \tag{16}$$

Equation (10) reduces to zero for a pure gas. For a mixture of isotopes the quantities involved in Eq. (10) are greatly simplified, and Jones[2] gives an even further approximation for this case which can be written as

$$\alpha=\frac{3.75M(C-1)(A+1)}{A(2A-B+2.75)}. \tag{17}$$

The quantities $H^{(l,k)}$ are determined by the following equations.

$$H_{12}^{(l,k)}=s_{12}^2\Omega_{12}^{(l,k)}, \tag{18}$$

where s_{12} is an arbitrary constant length, and

$$\Omega_{12}^{(l,k)}=\int_0^\infty e^{-\gamma^2}\sigma^2(\gamma)\gamma^k\Theta_{12}^{(l)}d\gamma, \tag{19}$$

where $\sigma(\gamma)$ is an arbitrary function of γ, and

$$\gamma=g(\mu/2kT)^{\frac{1}{2}} \tag{20}$$

in which g is the magnitude of the relative velocity of the two molecules at infinite separation;

$$\Theta_{12}^{(l)}=\int_0^\infty[1-P_l(\cos\theta_{12})]\beta d\beta \tag{21}$$

where

$$\beta=\frac{b}{s\sigma(\gamma)} \tag{22}$$

b being the closest distance to which the centers of the two molecules would approach if they experienced no deflection. The quantity θ is the angle of deflection of one molecule in the mutual force field, measured in the center of gravity coordinate system. If the intermolecular potential is known, θ can be calculated from the collision dynamics according to the expression

$$\theta_{12}=\pi-2\int_0^t\frac{dy}{[1-y^2-(2/\mu g^2)\Phi_{12}(r)]^{\frac{1}{2}}} \tag{23}$$

where $y=b/r$ and $\Phi_{12}(r)$ is the potential between the two molecules of types 1 and 2, r being the distance between the centers of the two molecules at any time. Using Φ_{11} or Φ_{12}, the potentials between two identical molecules, one obtains $H_{11}^{(l,k)}$ or $H_{22}^{(l,k)}$.

The integration limit, t, is the maximum value of y, i.e.,

$$t=b/r_{\min} \tag{24}$$

where $r_{\min}$ is the distance of closest approach of the two molecules. For some simple potential models, the value of $r_{\min}$ is obvious upon inspection; otherwise, t must be calculated as the smallest positive root of the equation

$$1-t^2-\frac{2\Phi(r_{\min})}{\mu g^2}=0. \tag{25}$$

These $\Omega^{(l,k)}$'s are the same as those used by Jones,[2] and the relations between them and the Ω's of Chapman and Cowling,[1] and the W's of Hirschfelder *et al.*[3] are as follows for $l=1$ or 2.

$$s^2\Omega^{(l,k)}=\frac{3}{4-l}\left[\frac{\mu}{2\pi kT}\right]^{\frac{1}{2}}\Omega^{(l)}\left(\frac{k-3}{2}\right) \tag{26}$$

$$\Omega^{(l,k)}=\frac{3}{4-l}W^{(l)}\left(\frac{k-3}{2}\right). \tag{27}$$

In practice a potential model is postulated for which Φ is a function of r and various parameters characteristic of the model. The $H^{(l,k)}$'s will then be functions of these parameters, and their values can be determined by fitting experimental data on the transport properties.

The $H^{(l,k)}$'s will also be functions of the temperature for all but the simplest potential models. They never depend on any other variables, the masses of the molecules included, so that for isotopes $H_{11}^{(l,k)}=H_{12}^{(l,k)}=H_{22}^{(l,k)}$ at a given temperature.

The potentials that have been investigated include the elastic sphere, the inverse power, the Sutherland, and the Lennard-Jones models. Of these the last three yield temperature dependent $H^{(l,k)}$'s and can account for most of the experimental data on viscosity, diffusion, and conductivity. Only the Lennard-Jones model, however, has any success in accounting for the experi-

[2] R. C. Jones, Phys. Rev. 59, 1019 (1941).

[3] Hirschfelder, Bird, and Spotz, J. Chem. Phys. 16, 968 (1948).

mental results on thermal diffusion. The intermolecular force for this model is given by the expression

$$F=\kappa/r^{\nu}-\kappa'/r^{\nu'} \tag{28}$$

where κ, κ', ν, ν' are constants. The mathematical labor involved in leaving all four parameters arbitrary is prohibitive, and ν and ν' are chosen from other considerations. The potential is then conveniently expressed in terms of the two parameters r_0, the value of r when $\Phi=0$, and ϵ, the minimum potential energy. Jones[2] and Hirschfelder *et al.*[3] have given the $\Omega^{(l,k)}$'s as functions of ϵ/kT for $s=r_0$ for the 9,5 and 13,7 models. The results have been compared by Grew[4,5] with experimental thermal diffusion data. The agreement is rather good, but still not entirely satisfactory.

The particular features of thermal diffusion, which make it especially useful in determining the intermolecular potential, are not hard to understand, at least in part. Equations (1), (6), (7), (8), and (9) for the other transport properties show a temperature dependence, exclusive of the $H^{(l,k)}$'s, which is already roughly correct. Thus many fairly crude models which give temperature dependent $H^{(l,k)}$'s can satisfactorily reproduce experimental data on these properties. On the other hand, Eqs. (10) and (17) show that the temperature variation of α comes entirely from the $H^{(l,k)}$'s. A further demand on the accuracy of the temperature variation of the $H^{(l,k)}$'s in these equations is due to the fact that they appear only in ratios. Naturally, the dependence of these ratios on the temperature or any other variable disappears whenever the dependence on that variable of the two $H^{(l,k)}$'s involved is the same. Thus, for example, α for the inverse power model is independent of the temperature even though the $H^{(l,k)}$'s are not. For other models the temperature dependences may largely cancel out.

In the same way α often becomes nearly independent of the size of the molecules. For many models, including that of Lennard-Jones, if s is chosen to be equal to one of the length parameters, the s^2 in Eq. (18) represents the entire dependence of the $H^{(l,k)}$'s on this parameter. Since s_{11}, s_{12}, and s_{22} are usually not very different, α will vary only slightly with this parameter in Eq. (10). For isotopes the dependence disappears completely.

In the present investigation we are interested in finding, for a relatively simple potential model, the effect of an additional length parameter such that even for isotopes the thermal diffusion constant will depend on the size of the molecules in addition to the temperature.

The only forms of the potential function, $\Phi(r)$, which can be integrated analytically through the first stage, Eq. (23), are $C_1+C_2/r+C_3/r^2$ and $C_1+C_2/r^2+C_3r^2$, where the C's are constants which may be zero. Only the simplest examples of these lead to results which can be integrated further without resort to numerical methods.

Although functions of the foregoing forms lead to the easiest mathematics they do not, in general, represent acceptable intermolecular potentials. However, a function which more or less closely approximates the actual intermolecular potential can be constructed of sections each of which is mathematically simple, preferably $\Phi(r)=$ a constant. If the number of sections is not large, the complications introduced by this approach are more than offset by the advantage of accomplishing the first integration analytically.

Thus we are led to the square-well model, defined subsequently. Integration of Eq. (23) gives θ as a function of g, a necessary and sufficient condition for temperature dependent $H^{(l,k)}$'s. The model has two length parameters, and it is the simplest that will give the isotope thermal diffusion constant as a function of temperature and one other parameter.

CALCULATIONS

The square-well molecular model is the spherically symmetrical potential defined as follows:

$$\begin{aligned}&\Phi(r)=\infty \quad \text{when} \quad 0\leqq r\leqq a\\ &\Phi(r)=-\epsilon \quad \text{when} \quad a\leqq r\leqq c\\ &\Phi(r)=0 \quad \text{when} \quad c<r\leqq\infty.\end{aligned}$$

For the calculation of θ, the angle of deflection, we distinguish three types of encounters:

I. When b lies between zero and some value, h, which is between a and c, collisions between the hard cores of the molecules occur.

II. When b lies between h and c, deflections occur without collisions between the cores.

III. When $b>c$, $\theta=0$.

For case I, $r_{\min}=a$, and in Eq. (23) the upper limit of integration, t, will be b/a according to Eq. (24). The integral must be divided into two ranges of y since $\Phi(b/y)=0$ for y from zero to b/c and $-\epsilon$ for y from b/c to t. Thus

$$\theta=\theta_1=\pi-2\int_0^{b/c}\frac{dy}{(1-y^2)^{\frac{1}{2}}}-2\int_{b/c}^{b/a}\frac{dy}{\left(1-y^2+\dfrac{\partial\epsilon}{\mu g^2}\right)^{\frac{1}{2}}}$$

$$\theta_1=2\left(\arccos\frac{Gb}{a}+\arcsin\frac{Gb}{c}-\arcsin\frac{b}{c}\right) \tag{29}$$

where $G=(\mu g^2/\mu g^2+2\epsilon)^{\frac{1}{2}}$.

For case II, Eq. (25) gives $t=1/G$, and dividing the integral into two ranges as before we obtain:

$$\theta=\theta_2=2\left(\arcsin\frac{Gb}{c}-\arcsin\frac{b}{c}\right). \tag{30}$$

For case III, $t=1$ since $r_{\min}=b$, and integration of Eq. (23) confirms the fact that $\theta=\theta_3=0$.

[4] K. E. Grew, Proc. Roy. Soc. (London) **A189**, 402 (1947).
[5] K. E. Grew, Proc. Phys. Soc. (London) **62A**, 655 (1949).

If we let $\sigma(\gamma)=1$, $s=c$, and $a/c=d$, we can write

$$\begin{aligned} &\text{for} \quad 0\leq\beta\leq d/G \quad \theta=\theta_1=\theta_2+2\arccos G\beta/d \\ &\text{for} \quad d/c\leq\beta\leq 1 \quad \theta=\theta_2=2(\arcsin G\beta-\arcsin\beta) \\ &\text{for} \quad 1<\beta<\infty \quad \theta=\theta_3=0. \end{aligned} \tag{31}$$

Both d and G range from zero to one. Whenever d is greater than G there are no encounters of type II. In that case $\theta=\theta_1$, for β from zero to one, and $\theta=\theta_3$ for β from one to infinity.

To obtain $\Theta^{(l)}$ the integrals of Eqs. (21) must be divided into ranges of the variable, β, as before, and we get

$$\theta^{(l)}=\int_0^{d/G}[1-P_l(\cos\theta_1)]\beta d\beta + \int_{d/G}^{1}[1-P_l(\cos\theta_2)]\beta d\beta. \tag{32}$$

The integral from one to infinity is always zero since $P_l(\cos\theta_3)=1$, and the integration thus need never be carried beyond the upper limit one. When d is greater than G the first integral in Eq. (32) goes from zero to one, and the second drops out. Since the only values of l we need are one and two, the following are the integrations that must be carried out to obtain $\Theta^{(l)}$ as functions of G and d:

$$\theta_{G<d}{}^{(1)}=\int_0^1(1-\cos\theta_1)\beta d\beta \tag{33a}$$

$$\theta_{G>d}{}^{(1)}=\int_0^{d/G}(1-\cos\theta_1)\beta d\beta \tag{33b}$$

$$+\int_{d/G}^{1}(1-\cos\theta_2)\beta d\beta \tag{33b}$$

$$\theta_{G<d}{}^{(2)}=\tfrac{3}{2}\int_0^1(1-\cos^2\theta_1)\beta d\beta \tag{33c}$$

$$\theta_{G>d}{}^{(2)}=\tfrac{3}{2}\int_0^{d/G}(1-\cos^2\theta_1)\beta d\beta + \tfrac{3}{2}\int_{d/G}^{1}(1-\cos^2\theta_2)\beta d\beta. \tag{33d}$$

Certain simple cases of the integration of Eqs. (33) are of interest. When $d=1$ the square-well model is reduced to an elastic sphere, and for this case we obtain $\Theta^{(l)}=\frac{1}{2}$, the usual elastic sphere value.

The case $G=1$ (or $\epsilon=0$) is also an elastic sphere, and integration of (33) gives $\Theta^{(l)}=d^2/2$. This difference is simply due to the unusual choice of s, and one still arrives at the correct elastic sphere $H^{(l,k)}$'s.

The case $G=0$ with finite d is the model with an infinitely deep potential well. This also leads to exactly the same results as the hard spheres.

The "softest" variation of the square-well model is obtained when the hard core is eliminated by letting $d=0$. For this case

$$\Theta^{(l)}=\frac{1}{2}-\frac{G^2}{6}-\frac{G}{4}+\frac{1}{6G}-\frac{1}{4G^3} +\frac{(1-G^4)(1-G^2)}{8G^4}\ln\frac{1+G}{1-G}. \tag{34}$$

The evaluation of this equation for certain values of G is included in Table I.

For the case $d=G$ we get

$$\Theta^{(l)}=\frac{1}{3}+\frac{G^2}{6}-\frac{G}{8}-\frac{1}{24G}+\frac{19}{24G^3}-\frac{5}{8G^5} +\frac{[1-G^2]^2[(1+G^2)^2+4]}{16G^3}\ln\frac{1+G}{1-G}. \tag{35}$$

This result has no special physical significance (the model "ducks" for *slow* collisions), but it is very useful as a check on the numerical integrations.

TABLE I. The quantities $\Theta^{(l)}(d, G)$ for the square-well model.

G \ d	$\Theta^{(1)}$ 0	0.4	0.6	0.8	$\Theta^{(2)}$ 0	0.4	0.6	0.8
0.0	0.3333	0.5000	0.5000	0.5000	0.4000	0.5000	0.5000	0.5000
0.2	0.3879	0.3565	0.4312	0.4735	0.5201	0.4044	0.4611	0.4871
0.4	0.2720	0.3058	0.3652	0.4456	0.4705	0.3942	0.4089	0.4693
0.5	0.2117	0.3478	0.3357	0.4305	0.4147	0.4922	0.3850	0.4575
0.6	0.1553	0.2982	0.3260	0.4140	0.3390	0.4658	0.3940	0.4429
0.7	0.1026	0.2305	0.3301	0.3960	0.2471	0.3752	0.4362	0.4253
0.8	0.0560	0.1659	0.2795	0.3809	0.1472	0.2602	0.3692	0.4156
0.86	0.0323	0.1322	0.2445	0.3748	0.0889	0.1914	0.3054	0.4186
0.88	0.0253	0.1221	0.2332	0.3681	0.0708	0.1698	0.2833	0.4090
0.90	0.0190	0.1127	0.2220	0.3606	0.0538	0.1494	0.2620	0.3959
0.92	0.0133	0.1040	0.2119	0.3522	0.0380	0.1304	0.2408	0.3805
0.94	0.0083	0.0962	0.2023	0.3436	0.0241	0.1132	0.2215	0.3639
0.96	0.0043	0.0895	0.1936	0.3341	0.0125	0.0984	0.2041	0.3458
1.00	0.0000	0.0800	0.1800	0.3200	0.0000	0.0800	0.1800	0.3200

The values for $G=1$ are $d^2/2$. When $d=1$, $\Theta^{(l)}=\frac{1}{2}$ for all G.

When $d=G=0$ we get $\Theta^{(1)}=\frac{1}{3}$ and $\Theta^{(2)}=\frac{2}{5}$. Since $G=0$, d finite, gives $\Theta^{(1)}=\frac{1}{2}$, we see that $\Theta^{(1)}$ is discontinuous at the point $d=G=0$. However, since the values of $\Theta^{(1)}$ for small G are unimportant in the integrations of Eq. (19), the behavior of this quantity near $G=0$ need not greatly concern us.

The integrations of Eqs. (33) can be performed analytically, for the general case also, but they then become so involved and yield such unwieldy results that numerical integration is more practical. However, this is not without its own difficulties, which arise when G is less than d from the variable limits on the integrals and from the erratic behavior of the integrands, as shown in Fig. 1.

To eliminate some of these difficulties Eqs. (33) were transformed so that the limits of integration were from zero to one for all integrals. Besides giving constant limits this has the effect of stretching both the two sections of the integrands, above and below the point $\beta=d/G$, over the whole range of integration, thus eliminating the discontinuity of slope at $\beta=d/G$ (see Fig. 1). To accomplish this the second terms in (33b) and (33d) are expressed as the integrals from zero to one, minus the integrals from zero to d/G. Then, in all the integrals with limits zero and d/G, the substitution $\beta=dp/G$ is made. This gives the same limits, zero and one, for all the integrals, but some of the integrations are to be performed with respect to p and some with respect to β. Since this difference is immaterial we can combine all the integrals in each equation under one integral sign, obtaining

$$\Theta_{G<d}^{(1)}=\int_0^1\left[1+\cos 2\left(\arcsin G\beta-\arcsin\beta-\arcsin\frac{G\beta}{d}\right)\right]\beta d\beta \tag{36a}$$

$$\Theta_{G>d}^{(1)}=\int_0^1\left[1-\cos 2(\arcsin G\beta-\arcsin\beta)+\frac{d^2}{G^2}\cos 2\left(\arcsin d\beta-\arcsin\frac{d\beta}{G}\right)\right.$$
$$\left.+\frac{d^2}{G^2}\cos 2\left(\arcsin d\beta-\arcsin\beta-\arcsin\frac{d\beta}{G}\right)\right]\beta d\beta \tag{36b}$$

$$\Theta_{G<d}^{(2)}=\tfrac{3}{2}\int_0^1\left[1-\cos^2 2\left(\arcsin G\beta-\arcsin\beta-\arcsin\frac{G\beta}{d}\right)\right]\beta d\beta \tag{36c}$$

$$\Theta_{G>d}^{(2)}=\tfrac{3}{2}\int_0^1\left[1-\cos^2 2(\arcsin G\beta-\arcsin\beta)+\frac{d^2}{G^2}\cos^2 2\left(\arcsin d\beta-\arcsin\frac{d\beta}{G}\right)\right.$$
$$\left.-\frac{d^2}{G^2}\cos^2 2\left(\arcsin d\beta-\arcsin\beta-\arcsin\frac{d\beta}{G}\right)\right]\beta d\beta. \tag{36d}$$

This transformation greatly reduced the number of different values of β for which the integrands had to be evaluated, but even so approximately 3500 cosines and arc sines had to be looked up and interpolated from the tables.[6,7]

The substitution $x=\beta^2$ was also made because it increases the accuracy of the quadratures by eliminating the maximum in the $\Theta^{(1)}$ integrands, and by moving the minimum in all the integrands farther from the $G=1$

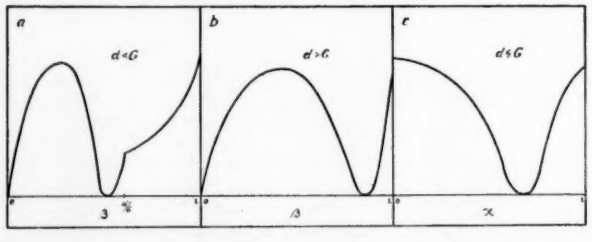

FIG. 1. Typical integrands for the $\Theta^{(1)}$ integrations are shown for the cases indicated. Use of transformations given in the text eliminate in (c) one bend of the curve and the discontinuity of slope at d/G.

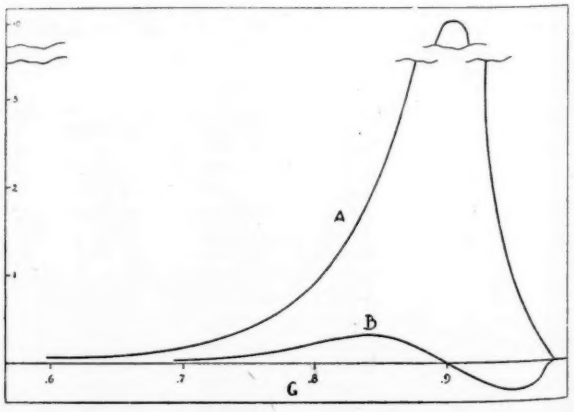

FIG. 2. Curves A and B are typical integrands for Eqs. (38) and (39), respectively.

[6] *Table of Cosine x*, Math. Tables Project (Columbia University Press, New York, 1945).

[7] *Table of Arc sin x*, Math. Tables Project (Columbia University Press, New York, 1945).

end (see Fig. 1). The final expressions so obtained were then integrated by the sixteen point Gaussian numerical integration formula[8] to give $\Theta^{(l)}(d, G)$ for the values of d and G given in Table I.

The values of $\Theta^{(1)}$ obtained by numerical integration were checked for the cases where $d=G$ and $d=0$ against the evaluation of Eqs. (34) and (35). In no case did the two results differ by more than one in the fourth decimal place after rounding.

Since we now have $\Theta^{(l)}$ as functions of G for given d's, we transform the variable of integration in Eq. (19) from γ to G. Defining $Q \equiv \epsilon/kT$, one finds from (20)

$$\gamma^2 = QG^2/(1-G^2). \tag{37}$$

When this substitution is made in (19) we obtain, assuming Q constant,

$$\Omega^{(l,k)} = Q^{(k+1)/2} \int_0^1 e^{-QG^2/(1-G^2)} \frac{G^k \Theta^{(l)} dG}{(1-G^2)^{(k+3)/2}}. \tag{38}$$

A typical integrand of Eq. (38) is shown in Fig. 2. The value of the integrand varies very rapidly with G, having a sharp maximum usually near $G=0.9$. For this reason the integrals are difficult to obtain accurately by direct numerical integration of Eq. (38). If, however, we write $K+[\Theta^{(l)}-K]$, where K is a constant, for $\Theta^{(l)}$ in (38), and integrate out the first term analytically we obtain the expression

$$\Omega^{(l,k)} = \frac{K}{2}\left(\frac{k-1}{2}\right)! + Q^{(k+1)/2} \int_0^1 e^{-QG^2/(1-G^2)} \frac{G^k(\Theta^{(l)}-K)dG}{(1-G^2)^{(k+3)/2}}. \tag{39}$$

A plot of the integrand in Eq. (39) is also shown in Fig. 2, in which K is taken equal to the value of Θ at $G=0.9$. The constant K can always be chosen so that the contribution to Ω from the numerically integrated second term of (39) is a small fraction of the value of Ω, thus increasing the accuracy of the results.

The best value of K to use is easily determined. It is the value, which we shall call K_0, that causes the second term of (39) to vanish. This will occur when

$$\int_0^1 e^{-QG^2/(1-G^2)} \frac{G^k \Theta^{(l)} dG}{(1-G^2)^{(k+3)/2}} = \int_0^1 e^{-QG^2/(1-G^2)} \frac{G^k K_0 dG}{(1-G^2)^{(k+3)/2}}. \tag{40}$$

Thus

$$K_0 = \frac{\displaystyle\int_0^1 e^{-QG^2/(1-G^2)} \frac{G^k \Theta^{(l)} dG}{(1-G^2)^{(k+3)/2}}}{\displaystyle\int_0^1 e^{-QG^2/(1-G^2)} \frac{G^k dG}{(1-G^2)^{(k+3)/2}}}. \tag{41}$$

We now obtain

$$\Omega^{(l,k)} = K_0/2(k-1/2)!. \tag{42}$$

Equation (42), for which K_0 was obtained from (41) by numerical integration of both numerator and denominator, is the equation that was used to find the values of the Ω's that are given in Table II. We may note that the denominator of (41) can be integrated exactly. If this is done, however, (42) reduces to (38) which, we have observed, is difficult to obtain accurately; but if the denominator of (41) is integrated numerically in the same manner as the numerator, the errors in both numerator and denominator, being in the same direction and of comparable magnitude, will largely cancel.

TABLE II. $\Omega^{(l,k)}$ for the square-well model.

d \ Q		0	0.2	0.4	0.6	0.8	1.0	1.2	2.0
0	1, 5	0.0000	0.0063	0.0159	0.0261	0.0360	0.0457	0.0549	0.0878
	1, 7	0.0000	0.0104	0.0274	0.0477	0.0687	0.0896	0.1104	0.1893
	1, 9	0.0000	0.0275	0.0716	0.1279	0.1902	0.2536	0.3175	0.5720
	2, 7	0.0000	0.0280	0.0770	0.1322	0.1871	0.2402	0.2913	0.4740
0.4	1, 5	0.0800	0.0921	0.1071	0.1221	0.1363	0.1497	0.1624	0.2051
	1, 7	0.2400	0.2622	0.2907	0.3221	0.3534	0.3839	0.4136	0.5233
	1, 9	0.9600	1.0228	1.1024	1.1934	1.2892	1.3841	1.4780	1.8416
	2, 7	0.2400	0.2840	0.3440	0.4104	0.4756	0.5380	0.5978	0.8085
0.6	1, 5	0.1800	0.1964	0.2141	0.2303	0.2444	0.2568	0.2677	0.2984
	1, 7	0.5400	0.5714	0.6079	0.6450	0.6800	0.7123	0.7423	0.8389
	1, 9	2.1600	2.2503	2.3579	2.4710	2.5847	2.6929	2.7960	3.1598
	2, 7	0.5400	0.5938	0.6661	0.7391	0.8064	0.8668	0.9211	1.0820
0.8	1, 5	0.3200	0.3357	0.3503	0.3610	0.3686	0.3744	0.3790	0.3915
	1, 7	0.9600	0.9902	1.0260	1.0561	1.0794	1.0975	1.1120	1.1498
	1, 9	3.8400	2.9235	4.0379	4.1443	4.2353	4.3091	4.3696	4.5295
	2, 7	0.9600	1.0150	1.0809	1.1350	1.1742	1.2019	1.2214	1.2569

For $Q=\infty$, and for $d=1$, $\Omega^{(l,k)} = \frac{1}{4}\left(\frac{k-1}{2}\right)!$.

[8] Lowan, Davis, Levenson, Bull. Am. Math. Soc. 48, 739 (1942).

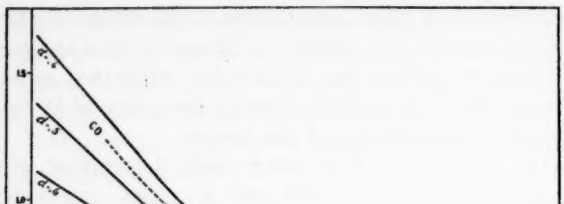

FIG. 3. Plot of X *vs* Y for the square-well model for the values of d indicated. The broken curves are X' *vs* Y' for the indicated gases in their best fit positions.

They cancel completely when $\Theta^{(l)}$ is a constant, since this will be a common factor in all the terms of the summation in the numerator, and K_0 will equal $\Theta^{(l)}$ no matter how crude the quadratures.

Simpson's rule was chosen as the most convenient for these integrations. For the values of Q which were used, most of the significant contributions to the integrals came for values of G between 0.8 and 1. The integrations were therefore performed using integrand values at intervals of G of 0.01 between 0.8 and 0.98, 0.005 above 0.98 when necessary, and 0.05 below 0.8 for as far as was necessary. Several test integrations using integrand values much closer together left the results unchanged for four decimal places. The values of $\Theta^{(l)}$ used were found or interpolated from Table I. The values of $\Omega^{(l,k)}(d, Q)$ thus obtained are given in Table II.

COMPARISON WITH EXPERIMENT

Viscosity

The most abundant experimental data on the temperature dependence of any of the transport properties is for the viscosity of pure gases. However, the results reported by different investigators, and even by the same investigator at different times, are often highly inconsistent. In making the original attempt at fitting experimental data it was therefore found necessary to use results reported at one time by one laboratory, since these are at least self consistent. The data of Johnston and co-workers[9,10] were chosen for this purpose because they are fairly recent and extensive, covering a considerable temperature range, 80° to 300°K, a region in which, as it turns out, it is most easy to fit the data unambiguously. Measurements are given for nine gases, including three noble gases which, being spherically symmetrical, should be especially susceptible to treatment by the Enskog-Chapman theory.

TABLE III. Parameters of the square-well model for various gases as found from viscosity.

	ϵ/k(°K)	a(A)	c(A)	d
N_2	80	3.36	7.00	0.480
CO	91	3.29	7.48	0.440
H_2	94	2.57	3.67	0.700
O_2	94	3.16	6.72	0.470
Ne	101	2.38	3.66	0.650
A	167	2.98	5.84	0.510
CH_4	174	3.35	6.57	0.510
He	232	1.90	2.64	0.720
Air	87	3.30	6.88	0.480

The following method was used to determine the square-well parameters for the various gases. From the theoretical values of $\Omega^{(2,7)}$ in Table II the quantity $X \equiv \ln(\Omega/d^2)$ was evaluated as a function of Q for various values of d and plotted against $Y \equiv -\ln Q$, as in Fig. 3. The experimental values of the coefficients of viscosity were used to make a plot of $X' \equiv \ln[T^{\frac{1}{2}}/(\eta \times 10^5)]$ versus $Y' \equiv \ln(T \times 10^{-2})$ for each gas, using the same scales as for the X, Y plot. Some of these curves are included in Fig. 3. Keeping the coordinate axes parallel, the X', Y' curve for each gas was then moved about over the X, Y plot until the position of best fit was found. The values of d, R_0, and R_1 in this position were noted, R_0 being the value of Y' corresponding to $Y=0$, and R_1 being the value of X' corresponding to $X=1$.

Upon substituting η from Eq. (6) in the expression for X' we find that

$$2 \ln a = R_1 + \tfrac{1}{2} \ln Nm - 36.4541 \qquad (43)$$

where N is Avogadro's number. From our definition of $Q \equiv \epsilon/kT$ we find

$$\ln(\epsilon/k \times 10^{-2}) = R_0. \qquad (44)$$

The values of a and ϵ/k were found for each gas from these equations, and the values of c were found as a/d. The precision with which d, R_0, and R_1 could be established from repeated attempts to fit the experimental and theoretical curves was such that the parameter a could be determined to three significant figures, and c and ϵ/k to two.

Better reproduction of the data, however, was obtained with the somewhat more exact values of c and ϵ/k given in Table III. It is possible that other combinations of values differing slightly in the third figures would do as well, so that these parameters must be considered to be determined unambiguously only to within about one percent.

For reproducing the data by Eq. (6), values of $\Omega_{11}^{(2,7)}$ were interpolated graphically to within about two percent using the parameters of Table III. The results are compared with the experimentally observed viscosities in Table IV. The experimental data have been rounded to two decimal places because it is only after such rounding that they are at all consistent. Except for hydrogen at the higher temperatures the agreement between theory and experiment is usually within two

[9] H. L. Johnston and E. R. Grilly, J. Phys. Chem. 46, 948 (1942).

[10] H. L. Johnston and K. E. McCloskey, J. Phys. Chem. 44, 1038 (1940).

percent and may thus be considered satisfactory. The agreement with the results of Trautz and co-workers[11] meets the more severe test since these data extent to a completely different temperature range from that used to determine the parameters.

A comparison of sorts can be made between viscosity parameters and those found for the square-well model by Hirschfelder, McClure, and Weeks[12] from compressibility data. This property does not permit the unambiguous determination of all three parameters, but if one is chosen arbitrarily the other two are determined. Similarly, for the hydrocarbons studied the viscosity data are only extensive enough to establish two of the parameters after one is chosen. In Table V are given the values of a and c that are required by both properties for the values of ϵ/k listed. The discrepancy is disappointing, but it still does not exclude the possibility that the correct viscosity parameters found from sufficient data would also fit the compressibility data.

An attempt was made to account for the viscosity of some binary gas mixtures with the use of Eq. (1). The Ω_{12}'s necessary for this were determined from Table II by assuming that for Φ_{12} the parameters a_{12} and c_{12} are the averages of those for the two pure gases, and that $\epsilon_{12}=(\epsilon_{11}\epsilon_{22})^{\frac{1}{2}}$. The predictions of Eq. (1) are compared with the observed values of Trautz and co-workers[11] in Table VI. The agreement is good for A–Ne and CO–N mixtures, but is unsatisfactory for He–A and He–Ne mixtures, for which the difference in masses of the two components is considerable. The He–A mixture is especially interesting since its viscosity is greater than that of either component.

The disagreement may be due to the assumed relation between Φ_{12} and the pure gas potentials. Somewhat better agreement can be obtained retaining this assumption and using an empirical equation of the form

$$\eta S=Z_1\eta_1+Z_2\eta_2+Z_{12}\eta_{12} \tag{45}$$

where $S=Z_1+Z_2+Z_{12}$ and Z_1/S is the fraction of all the collisions in the gas which are of the type 11, and similarly for Z_2 and Z_{12}; η_1 and η_2 are the viscosities of the pure components determined either experimentally or from Eq. (6), and η_{12} is found from Eq. (6) using Φ_{12} as above and the average m. Z_1 may be taken proportional to $x_1^2c_{11}^2/m_1^{\frac{1}{2}}$, with a similar expression for Z_2, and Z_{12} may be taken proportional to $x_1x_2\bar{c}^2/\bar{m}^{\frac{1}{2}}$, where $\bar{c}$ and $\bar{m}$ are the mean values. The results from Eq. (45) are included in Table VI. They are an improvement for those mixtures for which Eq. (1) does poorly.

Diffusion

Equation (7), for the diffusion coefficient of a mixture, makes no provision for the effect of the relative concentrations of the components, and is therefore of little use, since the diffusion coefficients of mixtures vary considerably with composition. Also, Eq. (9), though a good test of the general Enskog-Chapman theory, provides no additional information for our purpose.

Equation (8), for the self-diffusion coefficient, can be tested most conveniently by combining it with Eq. (6) giving

$$\rho D/\eta=3A_{11}. \tag{46}$$

Table VII gives some values of $\rho D/\eta$ for several gases as listed by Winn[13] and the corresponding values of $3A_{11}$ found by using the parameters of Table III. Aside from the possibility that Eq. (46) is too approximate, the discrepancies may be due to the use of the viscosity parameters. Although the data are not extensive enough to establish unambiguous parameters, other sets can easily be found that give the correct direction of temperature variation for hydrogen and exact results for the other gases. This need for different

TABLE IV. Reproduction of viscosity data of pure gases.

Gas	A		He		Ne		CH_4	
T	obs.	calc.	obs.	calc.	obs.	calc.	obs.	calc.
80	0.69	0.68	0.82	0.82	1.20	1.18	...	...
100	0.84	0.82	0.95	0.96	1.43	1.42	0.40	0.40
150	1.22	1.21	1.24	1.24	1.93	1.90	0.59	0.59
200	1.59	1.57	1.50	1.50	2.38	2.38	0.78	0.78
250	1.88	1.91	1.69	1.72	2.71	2.75	0.95	0.96
300	2.27	2.25	1.99	1.98	3.17	3.23	1.12	1.12
293	2.21	2.21	1.94	1.93	3.09	3.07	1.09	1.09
373	2.69	2.67	2.28	2.28	3.62	3.62	1.33	1.34
473	3.22	3.25	2.67	2.66	4.22	4.19	1.60	1.61
523	3.46	3.47	2.85	2.90	4.50	4.48	1.72	1.74
	H_2		CO		O_2		N_2	
80	...	...	0.53	0.52	...	...	...	...
100	0.42	0.42	0.67	0.66	0.77	0.78	0.70	0.72
150	0.56	0.55	0.98	0.96	1.13	1.16	1.01	1.04
200	0.68	0.68	1.27	1.28	1.48	1.49	1.30	1.30
250	0.79	0.78	1.54	1.52	1.79	1.80	1.55	1.57
300	0.90	0.88	1.78	1.77	2.07	2.07	1.79	1.81
300	0.89	0.88	1.78	1.77	2.06	2.07	1.78	1.81
400	1.09	1.04	2.18	2.15	2.57	2.55	2.19	2.18
500	1.26	1.19	2.55	2.53	3.02	2.97	2.56	2.54
550	1.38	1.27	2.71	2.73	3.22	3.17	2.73	2.72

The first column under each gas gives the observed experimental values in poise $\times 10^{-4}$, and the second column gives the results calculated from Eq. (6) using the square-well parameters in Table III. Above the broken lines, the observed values are those of Johnston and co-workers; below, they are those of Trautz and co-workers.

TABLE V. Viscosity and compressibility parameters.

Gas	ϵ/k	Comp. a	Comp. c	Visc. a	Visc. c
Ethane	244	3.54	5.84	3.81	8.71
Propane	347	4.42	6.47	4.21	8.77
n-butane	387	4.82	7.11	4.50	9.78
Ethene	222	3.35	5.61	3.73	8.48
Propene	339	4.32	6.31	4.02	8.93

[11] Landolt-Bornstein, *Physical Chemical Tables* (Julius Springer, Berlin, 1935), fifth edition, Vol. I, Suppl. 1, 2, 3.

[12] Hirschfelder, McClure, and Weeks, J. Chem. Phys. **10**, 201 (1942).

[13] E. B. Winn, Phys. Rev. **74**, 698 L (1948).

TABLE VI. Reproduction of viscosity data for mixtures.

T	38.2 percent He in A obs.	Eq. (1)	Eq. (45)	T	56.2 percent He in Ne obs.	Eq. (1)	Eq. (45)
293	2.29	2.22	2.25	293	2.70	2.64	2.70
373	2.74	2.68	2.71	373	3.17	3.11	3.17
473	3.25	3.21	3.25	473	3.70	3.62	3.70
523	3.49	3.45	3.49				
	60.9 percent A in Ne				39.7 percent CO in N_2		
293	2.50	2.48	2.47	300	1.78	1.79	1.78
373	2.99	2.99	2.97	400	2.18	2.18	2.18
473	3.53	3.54	3.54	500	2.56	2.56	2.56
523	3.79	3.79	3.79	550	2.72	2.72	2.72

parameters for different properties seems to be a general fault of the square-well model, arising also in considerations of compressibility and thermal diffusion data.

Thermal Diffusion

The function R_T is defined as α/α_h where α is the thermal diffusion constant found either experimentally or theoretically for a particular molecular model and α_h is the theoretical constant for hard spheres found by using viscosity diameters. Table VIII includes along with the quantities A, B, and C, R_T for isotopes as a function of Q and d, the α's having been found according to Eq. (17). The values of R_T plotted in Fig. 4 were taken or interpolated from Table VIII.

Stier[14] has measured the temperature variation of R_T for neon and argon isotopes. For neon he found that R_T varies from 0.39 to 0.82 as the temperature changes from 129° to 712°K, the experimental values agreeing within one percent with those predicted by the empirical equation

$$R_T=0.25\ln(T/26.6). \tag{47}$$

Similarly for argon, the experimental results are adequately represented by the equation

$$R_T=0.25\ln(T/86.9) \tag{48}$$

for temperatures in the range 129°–720°K, as R_T varies from 0.07 to 0.53.

It is immediately evident from Fig. 4 that the viscosity parameters cannot account for these experimental results since the d's found for these gases will not allow low enough values of R_T. However, it was found possible to reproduce the results for neon almost perfectly, as in Table IX, by using the "thermal diffusion parameters" $d=0.55$ and $\epsilon/k=120°$. Argon is not quite so tractable. The best parameter values, approximately 0.4 and 150°, give deviations up to 0.05 between experimental and calculated R_T's. The more exact Eq. (10) does no better. Using molecular weights of 40 and 36 for the argon isotopes, and 0.997 and 0.00307 for

TABLE VII. Experimental and theoretical values of $\rho D/\eta$.

Gas	T°C	$\rho D/\eta$	$3A_{11}$
H_2	20	1.370	1.23
	−188	1.32	1.32
	−253	1.28	1.37
Ne	20	1.275	1.23
A	22	1.31	1.29
CH_4	20	1.33	1.30
N_2	20	1.48	1.24

TABLE VIII. The quantities A, B, C, and R_T for the square-well model.

d \ Q	0.2	0.4	0.6	0.8	1.0	1.2	2.0
				A			
0	0.5870	0.6457	0.6751	0.6930	0.7008	0.7075	0.7197
0.4	0.4110	0.4281	0.4480	0.4651	0.4791	0.4908	0.5255
0.6	0.4031	0.4148	0.4278	0.4399	0.4501	0.4587	0.4861
0.8	0.4031	0.4114	0.4192	0.4247	0.4280	0.4297	0.4298
				B			
0	0.7778	0.8226	0.8475	0.8517	0.8508	0.8543	0.8531
0.4	0.6258	0.6556	0.6832	0.7011	0.7153	0.7266	0.7556
0.6	0.6178	0.6367	0.6548	0.6672	0.6765	0.6840	0.6935
0.8	0.6122	0.6235	0.6295	0.6303	0.6295	0.6282	0.6230
				C			
0	0.6603	0.6893	0.7310	0.7633	0.7842	0.8044	0.8624
0.4	1.1388	1.0857	1.0552	1.0371	1.0258	1.0187	1.0206
0.6	1.1637	1.1357	1.1203	1.1129	1.1095	1.1092	1.1245
0.8	1.1799	1.1716	1.1702	1.1714	1.1725	1.1736	1.1748
				R_T (Eq. (17))			
0	−1.230	−1.037	−0.8648	−0.7438	−0.6688	−0.6008	−0.4871
0.4	0.6817	0.4084	0.2539	0.1657	0.1121	0.0800	0.0828
0.6	0.8176	0.6628	0.5737	0.5255	0.4998	0.4909	0.5297
0.8	0.8963	0.8414	0.8209	0.8163	0.8148	0.8166	0.8205

For $Q=0$, and for $d=1$, $A=0.4$, $B=0.6$, $C=1.2$, and $R_T=1$.

[14] L. G. Stier, Phys. Rev. 62, 548 (1942).

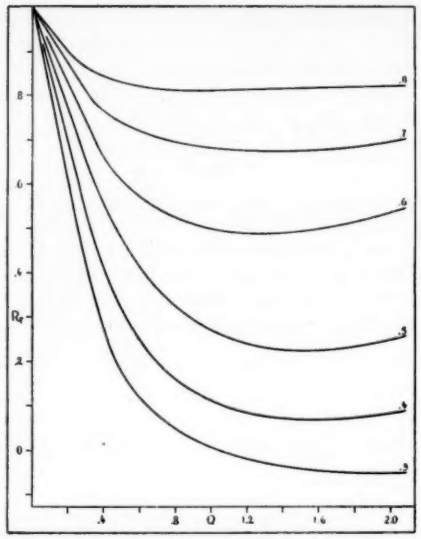

FIG. 4. R_T for isotopes from Eq. (17) is shown as a function of Q for the indicated values of d according to the square-well model.

their respective mole fractions, Eq. (10) leads to

$$R_T=\frac{3.952(C-1)(A+0.909)}{A(1.812A-B+2.467)}. \tag{49}$$

The results from this for $d=0.4$ differ by less than one percent from those of Eq. (17) given in Table VIII.

Using the isotope simplification of Eq. (10) Grew[5] obtained a fairly good correspondence between the 13,7 Lennard-Jones model predictions and experimental thermal diffusion data for several noble gas mixtures. The square-well model cannot duplicate this since it does not show the leveling off of R_T at about 0.63 at higher temperatures as required by the data. But by the same token the Lennard-Jones model fails to account for Stier's isotope data, especially for neon which has $R_T=0.82$ at 712°K.

TABLE IX. Reproduction of R_T data for neon isotopes.

T°K	129	200	300	400	500	600	712
Calc.	0.39	0.49	0.60	0.68	0.74	0.78	0.82
Obs.	0.39	0.50	0.60	0.68	0.73	0.78	0.82

The observed values were calculated from Eq. (47), and the calculated values were found from Eq. (17) using $d=0.55$, $\epsilon/k=120°$.

Neither the Lennard-Jones nor the square-well model can reproduce the constancy of R_T at 0.59 for the H_2-He mixture over the range 12° to 600°K. This may be a quantum effect. The longer range of quantum fields compared to classical will modify the temperature dependence of the $H^{(l,k)}$'s and could possibly give a temperature independent α.

Several general qualitative conclusions can be drawn from the behavior of R_T for the square-well model as shown in Fig. 4. R_T is always less than one, but when the temperature approaches zero or infinity R_T approaches one, that is, α approaches the value for hard spheres. This should be true for actual molecules, since at the extremes of temperature all important deflections involve collisions between the hard repulsive cores. The temperature at which the value of R_T is a minimum, and whether the minimum is positive or negative, depend on the exact form of the intermolecular potential. Since values of d for thermal diffusion are evidently less than those listed in Table III, it is probable that many gases will show negative R_T's. For these gases there will be two temperatures at which $R_T=0$.

The Infrared and Raman Spectra of SiF_4

E. A. JONES,* J. S. KIRBY-SMITH, P. J. H. WOLTZ, AND A. H. NIELSEN†
K-25 Research Laboratories, Carbide and Carbon Chemicals Division, Union Carbide and Carbon Corporation,‡ Oak Ridge, Tennessee
(Received September 15, 1950)

The infrared and Raman spectra of SiF_4 have been completely reexamined and extended. The Raman spectrum yields four lines at 268 cm^{-1}, 390 cm^{-1}, 800 cm^{-1}, and 1010 cm^{-1}, which have been assigned ν_2, ν_4, ν_1, and ν_3 respectively. In the infrared measurements, both prism and grating spectrometers were utilized. Several bands reported in earlier work have been ascribed to impurities and nine new bands have been observed and identified. The long-wave ν_4 at 391 cm^{-1} has been observed with a KRS-5 prism and its envelope determined. Bands involving ν_3 appear to have a *PR* spacing of about 12 cm^{-1} while those involving ν_4 appear to have a *PR* spacing of about 20 cm^{-1}.

I. INTRODUCTION

THE infrared spectrum of gaseous SiF_4 was measured in 1938 by Bailey, Hale, and Thompson[1] over the region 2–19μ. These authors report eleven bands and give their frequency assignments. In 1936 the Raman spectrum of liquid SiF_4 was examined by Yost, Lassettre, and Gross[2] who reported a line at 800 cm^{-1}. The existence of two additional lines at 268 cm^{-1} and 463 cm^{-1} was quoted by Yost[3] from some unpublished work by Best and Trampe.

During the past year, there has been occasion to reexamine the infrared spectrum of SiF_4 in this laboratory.[4] As it was not possible to make the measurements of Bailey, Hale, and Thompson agree completely with the new measurement on a very pure sample of SiF_4, it was concluded that a complete reinvestigation of both the infrared and Raman spectra would be of value. The infrared spectrum has, therefore, been reinvestigated from 2–19μ and extended to 38μ. Several of the regions of absorption have been further studied with a grating spectrometer. This paper is a report on these new measurements.

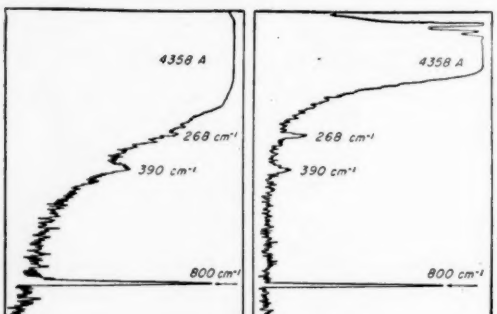

FIG. 1. Microphotometer traces of the Raman spectrum of SiF_4.

II. EXPERIMENTAL DETAILS

Raman

The Raman spectrum was photographed in a Lane-Wells spectrograph using tri-*X* Pan photographic film. The mercury 4358A line, filtered by a solution of Rhodamine 5 GDN extra and paranitrotoluene, was the exciting radiation. For plates of good contrast the exposures were about two hours at slit widths of 100μ. A comparison spectrum of iron, from which the frequency shifts were determined, was superposed on the film. For presentation purposes, traces of the films were made on a Leeds and Northrup microphotometer.

Infrared

A Perkin-Elmer infrared spectrometer equipped with NaCl, KBr, LiF, and KRS-5 prisms was used in the new measurements. Calibration of the prisms was effected by observing well-known infrared spectra and interpolating the frequencies from a graph. Several regions were examined in greater detail on the University of Tennessee prism-grating spectrograph[5] using a 3600 line-per-inch grating in several orders, and a Golay detector-amplifier system built by Eppley Laboratories. The grating instrument was calibrated with the 1μ-mercury line observed in several orders. Fluorothene absorption cells, 10 cm long and closed with

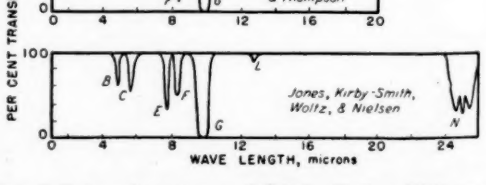

FIG. 2. Infrared spectrum of SiF_4 by Bailey, Hale, and Thompson, and the present work.

* Now at Vanderbilt University, Nashville, Tennessee.
† The University of Tennessee, Knoxville, Tennessee.
‡ This work is based on work performed for the AEC by Carbide and Carbon Chemicals Division, Union Carbide and Carbon Corporation at Oak Ridge, Tennessee.
[1] Bailey, Hale, and Thompson, Proc. Roy. Soc. (London) **A, 167**, 555 (1938).
[2] Yost, Lassettre, and Gross, J. Chem. Phys. **4**, 325 (1936).
[3] D. M. Yost, Proc. Indian Acad. Sci. **8A**, 333 (1938).
[4] Woltz, Jones, and Nielsen, Phys. Rev. **79**, 416 (1950).
[5] A. H. Nielsen, J. Tenn. Acad. Sci. **XXII**, No. 4, 241 (1947).

NaCl, KBr and KRS-5 windows, were used to contain the gas. Various pressures were used to observe the bands to best advantage.

III. EXPERIMENTAL RESULTS

Raman

In Fig. 1 are shown two microphotometer traces of exposures of the Raman spectrum of SiF_4 to bring out all the lines with good contrast. Four lines may be seen with frequency shifts of 268 cm^{-1}, 390 cm^{-1}, 800 cm^{-1}, and 1010 cm^{-1}. They are identified as the fundamental modes ν_2, ν_4, ν_1, and ν_3, respectively. The lines at 390 cm^{-1} and 1010 cm^{-1} have not previously been reported. No trace of a line at 463 cm^{-1} could be found. It is presumed that this line was caused by an impurity in the sample used in the earlier work because, in view of the exact agreement of the 268 cm^{-1} line with the present work, an error of 73 cm^{-1} in the 463 cm^{-1} line quoted by Yost is most unlikely.

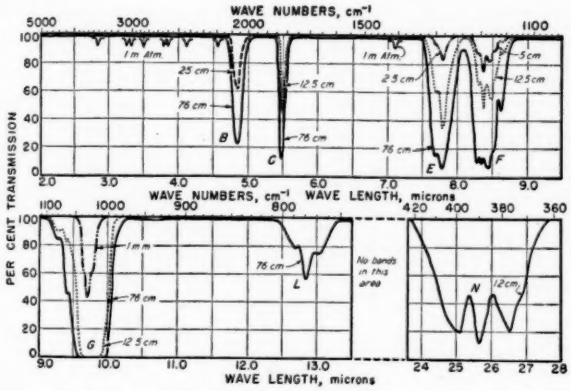

FIG. 3. Detailed prism spectrum of SiF_4.

Infrared

Figure 2 shows the observations of Bailey, Hale, and Thompson and the present work plotted to the same scale so that the differences may readily be seen. A number of new bands not listed by these authors have been discovered and bands *A*, *D*, *H*, *K*, and *M* in their work have been eliminated. The gas used in the present investigation was extensively purified which probably accounts for the elimination of these bands. The intensities of *E* and *F* have been reversed which is to be expected if an impurity overlapping *F* were removed. In addition, the low frequency fundamental ν_4, labeled *N* in Fig. 2, was discovered at 391 cm^{-1} in excellent agreement with the Raman line in the liquid at 390 cm^{-1}.

In Figure 3 is shown the complete prism spectrum with somewhat better resolving power than was available to Bailey and co-workers. The various gas pressures are listed for each region. It may be seen that regions *E*, *F*, and *G* are complicated by overlapping bands, and that no structure is apparent in regions *B* and *C*. For these reasons, it was considered of value to obtain records across these regions with the grating instrument.

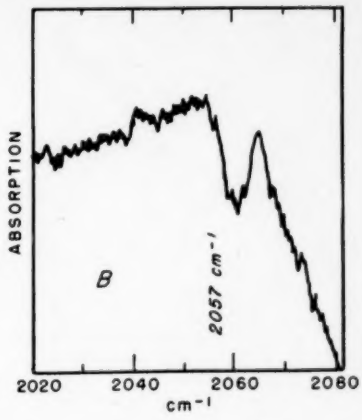

FIG. 4. Grating record of $2\nu_3$ (Region *B*).

Figure 4 shows the band *B* recorded with the grating. This band has *PQR* structure with its *Q* branch at about 2057 cm^{-1}. The *Q* branch is shaded in the direction of lower frequencies and overlaps the *P* branch strongly. The *R* branch is very narrow, showing strong convergence of the rotation lines. Separation of the *P* and *R* branches is found to be about 15 cm^{-1}.

In Fig. 5 are shown two grating records across the region *C* which lies near the edge of the 6.2μ-atmospheric water vapor band. The upper record was made with the cell in the beam, and the lower one with the cell out of the beam. The dotted curve is the resultant absorption caused by SiF_4. This band has *PQR* structure with the *Q* branch located at 1827 cm^{-1}. In this band the *Q* branch stands out from the *P* and *R* branches in contrast to the band shown in Fig. 4. The $P-R$ distance is about 12 cm^{-1}.

Grating records of regions *E* and *F* are shown in Fig. 6. The band *E* has much the same appearance as the one at *B*. It has *PQR* structure with the *Q* branch at 1294 cm^{-1} and a *PR* spacing of about 12 cm^{-1}. The *Q* branch shades toward low frequencies and strong convergence exists in the *R* branch. Region *F* appears to be composed of two overlapping *PQR* bands with *Q* branches at 1191 cm^{-1} and 1161 cm^{-1}. The *Q* branch of the band at 1191 cm^{-1} stands out strongly from the *P*

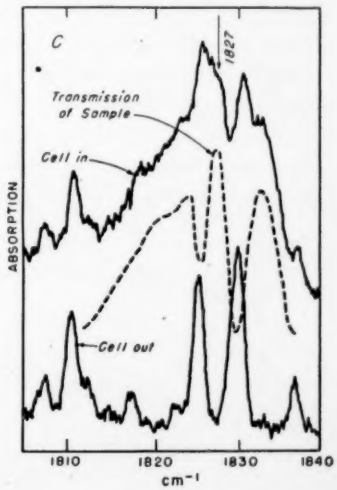

FIG. 5. Grating records showing the envelope of $\nu_1+\nu_3$ (Region *C*).

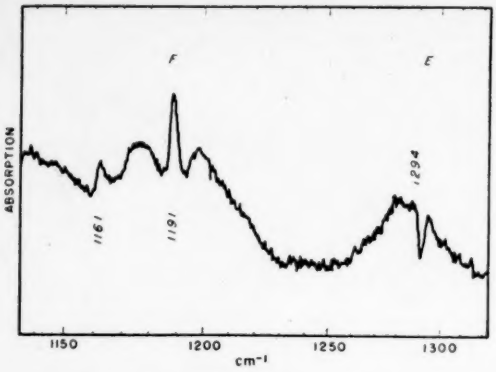

FIG. 6. Grating records of $\nu_2+\nu_3$, $\nu_1+\nu_4$ and $3\nu_4$ (Regions *E* and *F*).

and *R* branches as in *C*, Fig. 5. It shades, however, toward high frequencies. The *PR* distance is about 20 cm^{-1}. In the band at 1161 cm^{-1} the *Q* branch also shades toward high frequencies but does not stand out nearly as strongly. Neither of these bands appears to have as strong convergence of the rotation lines as either *B* or *E*. The *PR* spacing is probably about 20 cm^{-1}.

Figure 7 shows a grating record of region *G* observed with atmospheric pressure in a 10 cm cell in order to bring out the weak band with *Q* branch at 1065 cm^{-1}. The fundamental ν_3 is totally absorbed under these conditions. The *PR* separation appears to be about 20 cm^{-1}. The *Q* branch stands out strongly and shades toward low frequencies.

With less than 1 mm pressure of SiF_4 in a 10-cm cell the absorption *G* is shown in Fig. 8. This intense band is ν_3, and its envelope is very similar to *B* and *E* which is characterized by strong convergence of the *R* branch, and the shading of the *Q* branch toward low frequencies. The *Q* branch is located at about 1030 cm^{-1}, and the *PR* spacing is about 11 cm^{-1}.

A new band, ν_4, labeled *N* in Fig. 3, was discovered in extending the region of measurement. The curve shown is in percent absorption obtained with about 1-cm pressure in a 10-cm cell. This curve was obtained with a *KRS*-5 prism, and the cell was equipped with *KRS*-5 windows. The *Q* branch stands out from the *PR* branches and is located at 391 cm^{-1}. The *PR* spacing appears to be about 24 cm^{-1}. No strong convergence is apparent, and the envelope of this band resembles those of *C* and *F*.

A search for weak bands in SiF_4 was made using a LiF prism and a one-meter cell filled to atmospheric pressure. The relatively larger sample used in this search was not as pure as that used for the other measurements reported here. Instead of the bands *A*, *D*, *H*, *K*, and *M* of Bailey, *et al.*, which were eliminated, nine weak bands were discovered which were ascribed to SiF_4 with fair certainty. These bands are shown in Fig. 3 and listed in Table I, with an asterisk. Several other bands were also observed but were rejected as impurities for various reasons. The nine bands listed were retained largely because their envelopes resembled other more intense bands of SiF_4 and because it was possible to make reasonable assignments in terms of the new values of the fundamental frequencies given in Table I.

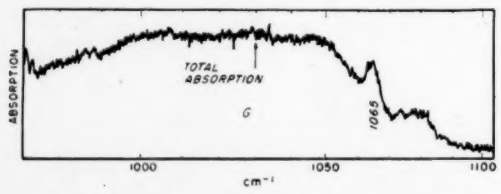

FIG. 7. Grating record showing the envelope of $\nu_2+2\nu_4$ (Region *G*).

IV. CONCLUSION

In Table I are given the collected frequencies, their relative intensities, and their assignments in the light of the new data. This assignment is compared with that of Bailey, Hale, and Thompson.

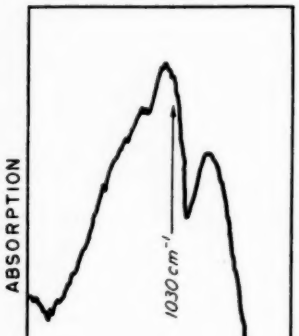

FIG. 8. Grating record showing the envelope of ν_3 (Region *G*).

The values of the fundamental frequencies given here differ from those quoted by Bailey and co-workers as two of their values 420 cm^{-1} and 260 cm^{-1} were obtained indirectly, whereas in the present work they were observed directly. The assignment is, however, the same. The bands at 2057, 1827, and 1294 cm^{-1} are shifted by a few cm^{-1}, but the assignment is the same. The band listed here as 1191 cm^{-1} is probably the one they give at 1202 cm^{-1} and is similarly identified with a slightly better fit. The bands at 1161 cm^{-1} and 1065 cm^{-1} have not previously been reported as they are both fairly weak. The most reasonable low combination which gives a frequency near 1161 cm^{-1} is $3\nu_4$ with a calculated frequency of 1173 cm^{-1}. For the band at 1065 cm^{-1}, the most reasonable identification appears to be $\nu_2+2\nu_4$ with a calculated frequency of 1050 cm^{-1}.

Two possible assignments for the band at 780 are apparent, $2\nu_4$ with a calculated frequency of 782 cm^{-1}, and $\nu_3-\nu_2$, as suggested by Bailey, Hale, and Thompson, with a calculated frequency of 763 cm^{-1}. An at-

TABLE I.

Observed frequency cm^{-1} Raman	Infrared	Designation in Figs. 2 and 3	Assignment Bailey, Hale, and Thompson	Assignment This work	Calculated frequency cm^{-1}	$\Delta\nu(PR)$ cm^{-1}	Intensity
268			ν_2	ν_2			
390	391	N	ν_4 (not obs.)	ν_4			s
	780	L	$\nu_3-\nu_2$	$2\nu_4$	782	24	m
800			ν_1	ν_1			
1010	1031	G	ν_3	ν_3		11	vs
	1065	G	Not obs.	$\nu_2+2\nu_4$	1050	20	w
	1161	F	Not obs.	$3\nu_4$	1173	20	w
	1191	F	$\nu_1+\nu_4$	$\nu_1+\nu_4$	1191	20	ms
	1294	E	$\nu_2+\nu_3$	$\nu_2+\nu_3$	1299	12	ms
	1404*		Not obs.	$\nu_3+\nu_4$	1422		vw
	1827	C	$\nu_1+\nu_3$	$\nu_1+\nu_3$	1831	12	ms
	2057	B	$2\nu_3$	$2\nu_3$	2062	15	ms
	2186*		Not obs.	$\nu_3+3\nu_4$	2204		vw
	2445*		Not obs.	$2\nu_3+\nu_4$	2453		vw
	2603*		Not obs.	$2\nu_2+2\nu_3$	2598		vw
	2627*		Not obs.	$2\nu_1+\nu_3$	2631		vw
	2854*		Not obs.	$\nu_1+2\nu_3$	2862		vw
	3033*		Not obs.	$3\nu_1-\nu_3-\nu_4$	3040		vw
	3065*		Not obs.	$3\nu_3$	3093		vw
	3612*		Not obs.	$2\nu_2+3\nu_3$	3629		vw

* The bands marked with an asterisk are weak and were observed in a one-meter cell with a sample of lower purity. They are, however, believed to be attributable to SiF_4.

tempt was made to determine the assignment by cooling the sample to the temperature of solid CO_2. If the band were a difference band, it should be considerably weakened at this low temperature. No apparent loss of intensity was noted and the band is, therefore, assigned to $2\nu_4$.

In molecules with spherical symmetry such as CH_4, SiH_4, and GeH_4, an interaction of the Coriolis type is possible between ν_2 and ν_4 which makes ν_2 active in the infrared if these frequencies are nearly degenerate.[6] Though ν_2 and ν_4 in SiF_4 only differ by 123 cm^{-1}, the degeneracy is not nearly as significant as it is in SiH_4 where both ν_2 and ν_4 are considerably higher frequencies. A search was nevertheless made for ν_2 utilizing a *KRS*-5 prism and a 10-cm cell at 2 atmos pressure of SiF_4. The band was not observed with this amount of gas.

Upon examination of all the observed bands, it appears that though they are all *PQR*-type bands they fall into two essentially different envelope types. In the first type, ν_3 occurs as an overtone or combination with either ν_1 or ν_2. The *PR* spacing is about 12 cm^{-1} for each band, and the *Q* branch shades off to low frequencies and loses its prominence by overlap with the *P* branch. In the second type, ν_4 occurs either as an overtone or combination with ν_1 or ν_2. The *PR* spacing is about 20 cm^{-1}, and the *Q* branch is very prominent.

V. ACKNOWLEDGMENT

The authors take pleasure in expressing their gratitude to Mr. A. V. Faloon and Mr. W. B. Kenna of the Physics Department for their careful sample preparations, and continued interest in the problem.

[6] Straley, Tindal, and Nielsen, Phys. Rev. **58**, 1002 (1940); Straley, Tindal, and Nielsen, Phys. Rev. **62**, 161 (1942); Tindal, Straley, and Nielsen, Phys. Rev. **62**, 151 (1942); J. S. Burgess, Phys. Rev. **76**, 302 (1949).

The Role of Hybridization and Resonance in Molecular Structure

JULES DUCHESNE
Department of Chemical Physics, University of Liège, Belgium
(Received November 23, 1950)

It is shown that hybridization of the end-atoms in multiple-bonded molecules, as well as in single-bonded ones, is necessary for the understanding of the chemical bond properties. Resonance effects seem to play a minor role, except for conjugated systems.

IN a recent paper[1] we have shown, from a comparative study of the behavior of the bond lengths in halogenated tetrahedral molecules, that the size of the halogen atoms depends to some extent upon hybridization, which itself varies according to the molecule in which the atom is involved. In the same way, resonance effects appeared less significant than was assumed before. The analysis was, however, limited to single-bonded systems.

The aim of this paper is to extend these views to multiple-bonded molecules and to try to clarify the question of the part played by resonance. Our interest will be especially concentrated on the molecules cyanogen chloride and chloroacetylene, which are very appropriate for this study and for which structural data of considerable accuracy are known.

Cyanogen chloride shows very peculiar bond properties as compared with methyl chloride. Indeed, the C—Cl bond distance and force constant are strikingly modified on passing from CH_3Cl to ClCN. The bond distance shortens from 1.786A to 1.630A,[2] and the force constant increases from 3.4×10^5 d/cm to about 5×10^5 d/cm.[3] These changes in the bond constants are qualitatively compatible with the fact that the carbon hybrid atomic orbitals are different ($sp^3\rightarrow sp$) and behave so as to give a shorter and stronger C—Cl bond in ClCN.[4] However, the contribution of this factor cannot explain a change of more than about 15 percent in the force constant, by analogy with the change due to the same factor for the CH bond on passing from CH_4 (5×10^5 dynes/cm) to HCN (5.7×10^5 d/cm).[4] Since, for the chlorine derivatives, the force constant change amounts to 45 percent, we have concluded earlier[4] that resonance between the covalent structure and the double-bonded structure $\bar{N}=C=Cl^+$ is inevitable.

In chlorocetylene, the C—Cl bond distance is 1.632A[5] and the stretching force constant is about 5×10^5 d/cm.[6] For the same reasons as for ClCN, it would appear necessary to invoke resonance with a double-bonded structure such as $H-\bar{C}=C=Cl^+$.[6]

It is to be pointed out that, while the assumption of such a structure seems to account for the behavior of the C—Cl bond in both compounds, we are faced with severe difficulties when we consider other bonds in the molecules. For ClCN, the resonance structure would reduce the CN bond order with respect to HCN, and the same is true for the CC bond order in ClCCH, with respect to C_2H_2. That means that we should expect to find weaker CN and CC bonds in ClCN and ClCCH, than in HCN and C_2H_2. Instead of that, very precise measurements[2,3,5] show a practical identity of these bond distances and force constants as follows:

	Bond distances (A)	Force constants (10^5 dynes/cm)
HCN	1.157 (CN)	~18 (CN)
ClCN	1.163 (CN)	~18 (CN)
C_2H_2	1.202 (CC)	15.6 (CC)
ClCCH	1.211 (CC)	>15 (CC)

Moreover, both halogenated molecules have almost exactly the same C—Cl bond characteristics; this is another fact which cannot be explained on resonance grounds. Indeed, this would necessarily imply the same amount of resonance in both compounds, despite the fact that they have different bonds. Even the existence of a positive stretch-stretch force constant does not invalidate these conclusions, since it has been shown[7] that factors other than resonance also provide a positive sign.

On the whole, the present analysis shows that the generally admitted hypothesis of resonance cannot be considered as a proper means of interpreting the bond characteristics of these triple-bonded molecules. We will now show that the idea, recently set forth by us,[1] of hybridization of the end-atoms—in this case a halogen atom—permits one to overcome these difficulties and must therefore take the place of the resonance concept. We shall assume that the chlorine atom in both compounds involves a hybrid atomic orbital as +bp in order to give a better overlapping with the sp orbital of the carbon atom than a pure p orbital. If this is so, the shortening of the C—Cl bond distance and

[1] J. Duchesne, Trans. Faraday Soc. **46**, 187 (1950).
[2] Dailey, Mays, and Townes, Phys. Rev. **76**, 136 (1949); W. Gordy, Revs. Modern Phys. **20**, 668 (1948); J. W. Simmons, Phys. Rev. **76**, 686 (1949).
[3] J. W. Linnett, Quarterly Rev. **1**, 73 (1947); J. Duchesne and A. Monfils, J. Chem. Phys. **17**, 586 (1949).
[4] J. Duchesne, V. Henri Mem. Vol., Desoer (Liège, 1947), p. 47.
[5] Westenberg, Goldstein, and Wilson, J. Chem. Phys. **17**, 1319 (1949).
[6] W. S. Richardson and J. H. Goldstein, J. Chem. Phys. **18**, 1314 (1950).
[7] J. Duchesne, Mémoires Soc. Roy. Sci. Liège, 429 (1943); Coulson, Duchesne, and Manneback, V. Henri Mem. Vol., Desoer (Liège, 1947), p. 33.

the strengthening of the C—Cl force constant in ClCN and ClCCH, with respect to CH_3Cl, needs more s in the Cl atom of the former compounds than in the latter. Recent theoretical work on the principle of maximum overlapping due to Mulliken, Rieke, Orloff, and Orloff,[8] and to Maccoll[9] allows us to arrive at a better understanding of what occurs. It has been accepted that the overlap integral measures the strength of the bond. Maccoll has computed this integral for the sp^3, sp^2, and sp hybrid orbits. For the CH bonds, he finds, respectively, the values 0.72, 0.74, and 0.76. We therefore see that a change as high as 15 percent in the CCl force constant on passing from CH_3Cl to ClCN (or ClCCH) may be explained by a corresponding change of 5.5 percent in the overlap integral. Of course, we cannot suppose that the carbon hydridization in CH and CCl behaves exactly in the same way with regard to the change of the overlap integral. It is even to be anticipated that the integral increases more rapidly when a chlorine atom rather than a hydrogen atom is bound, if the former is in an sp state. This would mean that a change of 15 percent in the force constant is a lower limit for CCl. In order to explain the remaining 30 percent of strengthening in C—Cl (this is now an upper limit) we would have to increase further the overlap integral about 10 percent in hybridizing Cl as well. This, of course, assumes that overlap integrals and force constants are proportional. However, if chlorine would behave as carbon in the sp^3 state, a tremendous amount of hybridization would be needed to obtain such an increase. Fortunately, calculations by Maccoll show that the change of the overlap integral in CH, in terms of the percentage of s character in carbon, is much more rapid when the proportion of s compared to p is small than thereafter, and the same occurs for C—C. We can therefore assume that chlorine in C—Cl follows the same law, and as all the C—Cl bonds involve a Cl atom which is not too far from a pure p state, we can conclude that a small amount of s character may be responsible for a change of 10 percent in the overlap integral. It is still impossible to evaluate the exact change, but it may be less than 2 percent.

The increase of the amount of hybridization through the series CH_3Cl, ClCN (ClCCH), which we must now accept as an experimental fact, may be understood on the basis of a new principle which we express as follows: "The hybridization of an atomic orbital of an atom bonded to a hybridized carbon atom changes with the amount of hybridization of carbon and tends to become equivalent."

This principle also accounts for the striking fact that the C—Cl force constant and bond distance are practically the same in ClCN and ClCCH. We are now in a position to ascertain that the concept of hybridization extended to end-atoms provides an adequate explanation for every characteristic of the chemical bonds in triple-bonded as well as in single-bonded systems. It is to be presumed that the structural properties of double-bonded molecules such as CO_2, COS, C_2Cl_4, will also find a logical explanation on the same grounds. It therefore appears that the field in which resonance continues to play a major role must now be considered as restricted to conjugated systems.

Our thanks are due to Professor C. A. Coulson, for helpful correspondence on this subject.

[8] Mulliken, Rieke, Orloff, and Orloff, J. Chem. Phys. **17**, 1248 (1949).

[9] A. Maccoll, Trans. Faraday Soc. **46**, 369 (1950).

Use of a Low Temperature Bolometer for Detecting a Beam of Free Radicals

C. A. REILLY
Department of Chemistry, Dalhousie University, Halifax, N. S., Canada

AND

B. S. RABINOVITCH
Department of Chemistry and Chemical Engineering, University of Washington, Seattle, Washington

(Received November 30, 1950)

It was suggested by Estermann[1] in 1946 that a beam of free radicals might be detectable through the energy released upon condensation on a metal strip bolometer. Such a detector has since been developed by us at the Gibbs Chemical Laboratory, Harvard University, in connection with some other work on molecular beams. Our initial attempts to detect a free radical beam using a platinum strip bolometer at room temperature were unsuccessful; but, by cooling the bolometer to a sufficiently low temperature, detection of a beam of methyl free radicals is believed to have been achieved. Some interesting observations and inferences on the behavior of these free radicals arise out of our experiments and are here noted.

The beam apparatus was a conventional one[1] consisting of a quartz oven, a source slit, a collimating slit, and a detector located in an observation chamber. The source slit, 0.1 mm wide by 8 mm high, was located about 5 mm from the end of the electrically heated oven through which azomethane was pumped at a high velocity. The collimating slit, 0.3 mm wide by 2 mm high was located 12 cm from the source slit.

The detector was located 8 cm from the collimating slit and consisted of two platinum strips 0.5 mm wide, 12 mm long, and about 3×10^{-4} mm thick mounted on platinum posts which were connected to shielded leads of platinum.* The all-platinum circuit was found necessary to avoid disturbances due to thermoelectric effects. Junctions to copper leads were made outside the apparatus and these were well lagged and shielded. The posts carrying the strips passed through a mild steel block (for shielding purposes) but were electrically insulated from it by Bakelite bushings. These detecting elements were located in a well milled in the front of the block. A metal cover for the well with slots at the proper location with respect to the strips was screwed in place. This detector assembly was attached to the bottom plug of a liquid nitrogen container (a brass tube) by means of a thin-walled (~0.03 cm) brass tube 1.3 cm in diameter by 2.5 cm long screwed to it. The large mass of the housing (~85 g) and the relatively small conductivity of its brass supporting tube helped to minimize at the detector the effects of small temperature fluctuations due to boiling in the liquid nitrogen container. Surrounding the housing was a thermal radiation shield of thin-walled copper with slots at the appropriate locations. This was also screwed to the base of the liquid nitrogen container. Using this cooling arrangement the platinum strips could be cooled to −180°C.

TABLE I. Detection of a beam of azomethane and of methyl free radicals.

Approx. oven temp.	Bridge current	Strip temp.	Galvo. defl.	Remarks
25°C	10 mA	−175°C	0.3 cm	No beam
25	10	−175	11	Beam of azomethane only
25	15	−160	3	
25	20	−110	Erratic but small.	
450	15	−160	6	Beam of free radicals plus decomposition products
600	15	−160	6.5	
750	10	−175	6	
750	20	−110	6	
750	25	+10	Erratic but small.	
800	15	−160	8	
600	10	−175	0.5	No beam

The detecting elements were connected as two arms of a Wheatstone bridge, the current in which caused appreciable heating of the strips. Thus, by varying this current the operating temperature of the strips could be easily adjusted to any value between −180°C and about +100°C. This operating temperature was calculated from the measured resistance of the strips.

When a beam, interrupted at intervals of several seconds by a shutter, was allowed to fall on one of the strips and to condense there, its heating effect caused an unbalance in the bridge. This unbalance was measured by means of a sensitive galvanometer the deflection of which was taken as a measure of the beam intensity. The data in Table I show a typical behavior of the detecting system under two different sets of conditions: Oven at room temperature, i.e., no free radicals present; and oven heated, i.e., free radicals presumed to be present, along with other azomethane decomposition products.

These data show a striking difference in the dependence of galvanometer deflection on strip temperature with the oven cold and with it hot. With the cold oven, the galvanometer deflection falls off rapidly as the strip temperature is raised above −175°C, becoming negligible before −110°C is reached; with the hot oven, the galvanometer deflection remains approximately constant up to −110°C. and then falls off, becoming negligible only at some temperature between

[1] I. Estermann, Revs. Modern Phys. 18, 300 (1946).
* Strips were mounted for us by Baird Associates, Inc., University Road, Cambridge, Massachusetts.

−110°C and +10°C. Separate experiments have shown that nitrogen and ethane, the chief secondary products from the azomethane pyrolysis as carried out in these experiments, were not detectable at any temperature using this scheme. Chemical analysis has shown that other products were much too small in amount to account for the observed effects. Hence it is concluded that some intermediate product of the pyrolysis was being detected, and there can be little doubt from other work on azomethane[2] that this intermediate was the methyl free radical.

The probable nature of the detection of CH_3 radicals in these experiments is of interest. The energy required for detection is most likely to come from the following sources: (1) Adsorption of CH_3 on the metal surface with release of the heat of adsorption, and/or (2) recombination of CH_3 radicals on the surface of the strip to form C_2H_6. The sensitivity of the detector as determined from the radiation absorbed from a standardized incandescent bulb was about 10^{-8} w per cm galvanometer deflection when using a bridge current of 10 mA. Assuming a nominal heat of adsorption of 10 kcal per M, the number of CH_3 radicals needed to produce an observed deflection of 6 cm would correspond to a beam intensity of 4×10^{13} particles per sec per cm^2. This compares with a maximum possible intensity for our beam geometry of about 10^{14} particles per sec per cm^2.[3] However, assuming a cross section per free radical of 10^{-15} cm^2, the time required to build up a monolayer would be of the order of a minute at these intensities. In this case, a decrease in galvanometer deflection would have been observed after the beam had been impinging on the surface for a minute or more. No such decrease was observed even after many minutes of operation, and thus it is unlikely that adsorption alone was the mechanism of detection. Now, if recombination of CH_3 radicals to form C_2H_6 takes place with the release of 85 kcal of energy per M,[4] the beam intensity required to produce a galvanometer deflection of 6 cm would have been only about 5×10^{12} radicals per sec per cm^2. The time required to build up a monolayer, and thus to reach a maximum heating effect if the radicals were immobile on the surface, would then have been several minutes. However, a maximum galvanometer deflection was reached within a few seconds (the period of the galvanometer) after turning on the beam, and, furthermore, there was no residual deflection after turning it off. This behavior indicates that the CH_3 radicals must have recombined within a second or so after striking the detector. Thus, it appears necessary to assume a relatively high mobility and rapid reaction of the CH_3 radicals on the metal surface even at the low temperatures employed in these experiments.

Since no galvanometer deflection was produced at a strip temperature above +10°C, it is evident that, in this case, methyl free radicals were neither recombining nor permanently adsorbing on the surface of the strip. This explains the failure of our initial attempts to find them using a detector at room temperature.

We wish to thank Professor G. B. Kistiakowsky for suggesting this study and for many valuable discussions. The awards of a Royal Society of Canada Fellowship to one of us (B.S.R.) and of a Monsanto Fellowship to the other (C.A.R.) are gratefully acknowledged.

[2] H. A. Taylor and F. P. Jahn, J. Chem. Phys. **7**, 470 (1939); F. P. Jahn and H. A. Taylor, *ibid.* **7**, 474 (1939), O. K. Rice and H. Gershinowitz, *ibid.* **3**, 479 (1935).

[3] R. G. J. Fraser, *Molecular Beams* (Methnen and Company, London, 1937), p. 6.

[4] F. W. R. Steacie, *Atomic and Free Radical Reactions* (Reinhold Publishing Corporation, New York, 1946), p. 79.

Letters to the Editor

THIS section will accept reports of new work, provided these are terse and contain few figures, and especially few half-tone cuts. The Editorial Board will not hold itself responsible for opinions expressed by the correspondents. Contributions to this section should not exceed 600 words in length and must reach the office of the Managing Editor not later than the 15th of the month preceding that of the issue in which the letter is to appear. No proof will be sent to the authors. The usual publication charge ($8.00 per page) will not be made and no reprints will be furnished free.

A Mechanism of Formation of Nitric Oxide in Glow Discharges

R. W. NICHOLLS
Department of Physics, University of Western Ontario, London, Ontario, Canada
December 7, 1950

IN an experimental and theoretical investigation of mechanisms of excitation of the triplet bands of nitrogen, at present being carried out here, the well-known excitation of accompanying nitric oxide band systems in nitrogen contaminated with molecular oxygen has also received attention from a theoretical and experimental point of view. In view of the interest in these band systems particularly in terrestrial astrophysics[1] it is the purpose of this note to point out energy resonances existing in a simple mechanism of formation of nitric oxide in such discharges.

It is suggested that in a glow discharge plasma in oxygen contaminated nitrogen, molecules in vibrational levels of the $B^3\Pi_g$ state (amongst others) may be depopulated by collisions with oxygen ground-state molecules ($X^3\Sigma_g^-$) with the formation of two nitric oxide molecules, one in its ground state ($X^2\Pi$) and the other in any of the vibrational levels of the excited states A, B, C, D, or E.[2] This mechanism may be represented by the equation

$$N_2(B^3\Pi_g)+O_2(X^3\Sigma_g^-)\rightarrow NO(X^2\Pi)+NO\begin{cases}A^2\Sigma^+\\B^2\Pi\\C^2\Sigma\\D^2\Sigma^+\\E^2\Sigma^+\end{cases}.$$

Such a nonradiative depopulation of $N_2(B^3\Pi_g)$ and the consequent formation of NO (excited) would cause a diminution in the intensity of bands of the first positive system with the consequent appearance of bands of the NO systems. This reaction, involving as it does, redistribution both of particles and excitation, is very difficult to analyse by quantum mechanics.[3] However, as has been observed in the quantum-mechanical treatment of similar more simple processes[3] and as may be expected by more general considerations, energy resonance between the systems on either side of the equation is a major criterion in deciding the probability of this mechanism. Accordingly energies appropriate to all the possibilities of vibrational excitation of each side of the equation have been calculated. That is, the difference between energy of excitation of any vibrational level, and the sum of the dissociation energies of the molecules when in the ground state, was calculated for each vibrational possibility for each side of the equation. Comparison between these is shown in Fig. 1 where some quite strong energy resonances are observed.

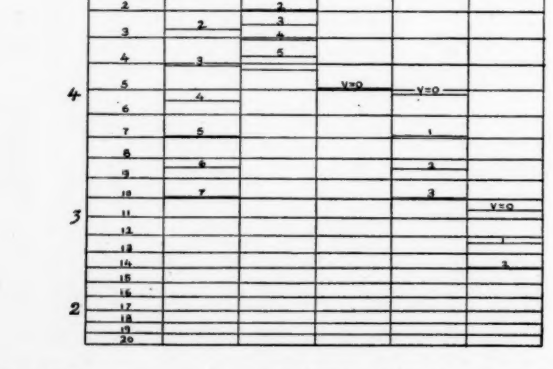

FIG. 1. Energy resonances between $N_2(B^3\Pi_g)$ and NO (A, B, C, D, E).

If an empirical resonance criterion of a few hundredths of an electron volt energy difference be accepted as indicating the probability of the reaction then Table I summarizes the expected vibrational sequences of the first positive system which will be weakened by the appearance of the indicated vibrational sequences of the nitric oxide systems.

TABLE I. Vibrational levels of $N_2(B^3\Pi)$ and NO ($A^3\Sigma$, $B^3\Pi$, $C^3\Sigma$, $D^3\Sigma$, $E^3\Sigma$) which are in near energy resonance.

N_2	NO				
$B^3\Pi$	$A^3\Sigma$	$B^3\Pi$	$C^3\Sigma$	$D^3\Sigma$	$E^3\Sigma$
0	0				
2		2			
3		4			
4	3				
5			0		
7	5			1	
10	7			3	
12					1
14					2

Spectrograms of plates exposed to discharges run in N_2/O_2 mixtures confirm qualitatively the general scope of the above prediction. The appearance of sequences of NO bands other than those specifically quoted above is readily explained by re-excitation of the NO molecules formed in the discharge and less stringent resonance conditions than the arbitrary one above.

Quantitative measurements made on the dependence of the intensity of nitric oxide bands on those of the first positive, to compare with a kinetic analysis which has been made of this mechanism will be the real test of this mechanism. Work has been started here upon such measurements, but in view of the current interest in the spectra of these molecules it has been thought worthwhile to draw attention at this stage to the close energy resonances there existing.

[1] *The Emission Spectra of the Night Sky and Aurorae* (The Physical Society, London, 1948).
[2] A. G. Gaydon, Proc. Phys. Soc. (London) **56**, 95, 160 (1944). M. W. Feast, Can. J. Research **A28**, 488 (1950).
[3] Mott and Massey, *The Theory of Atomic Collisions* (1949), second edition.

Dipole Moment and Electric Quadrupole Effects in HNCO and HNCS

J. N. SHOOLERY,* R. G. SHULMAN,† AND DON M. YOST
California Institute of Technology,‡ Pasadena, California
November 24, 1950

INTERACTION of the electric quadrupole moment of the nitrogen nucleus with the molecular electric fields of isocyanic and isothiocyanic acids results in a hyperfine splitting of the rotational transitions. The quadrupole coupling constant, eQq, for each of these molecules has been determined from the splitting of the $0_{0,0}-1_{0,1}$ transition of HNCO at 21,981.7[1] Mc and the $1_{1,1}-2_{1,2}$ transition of HNCS at 23,499.5 Mc.[2]

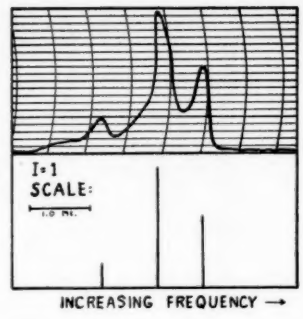

FIG. 1. Hyperfine structure of $0_{0,0}-1_{0,1}$ transition of HNCO. The two lower frequency lines are separated by 0.90 Mc and the two higher frequency lines by 0.60 Mc.

A standard Stark modulation microwave spectroscope with a lock-in detector and recording meter was used for these measurements. Recording meter traces were compared with the theoretical patterns in order to determine the sign of eQq. Accurate frequency measurements were made on an oscilloscope. To resolve lines 0.35 Mc apart it was necessary to reduce the pressure to 10^{-4} mm, the temperature to $-78°$C, and the Klystron cavity sweep rate to 2 cycles per second. Frequencies were reproducible to within 0.02 Mc with HNCO and 0.05 Mc with HNCS.

Figures 1 and 2 compare the observed hyperfine structure of HNCO and HNCS with the theoretical patterns expected on the basis of eQq equal to $+2.00\pm0.05$ Mc for HNCO and $+1.2\pm0.2$ Mc for HNCS.

TABLE I. N^{14} nuclear quadrupole coupling in cyanides and isocyanates.

Molecule	eQq (mc/sec)
HCN	−4.58[a]
CH_3CN	−4.67[b]
ClCN	−3.67[c]
BrCN	−3.83[c]
ICN	−3.80[c]
HNCS	+1.2[d]
HNCO	+2.00[d]

[a] Simmons, Anderson, and Gordy, Phys. Rev. **77**, 77 (1950).
[b] Kisliuk and Townes, J. Res. Nat. Bur. Stand. **44**, 611 (1950).
[c] Smith, Ring, Smith, and Gordy, Phys. Rev. **74**, 310 (1948) and Townes, Holden, and Merritt, Phys. Rev. **74**, 1113 (1948).
[d] Present work.

Values of eQq for various compounds containing carbon to nitrogen multiple bonds are given in Table I.

It is interesting to note that compounds in which the nitrogen atom is on the end of the molecule, as in the cyanides, lead to coupling constants of the order of −4 Mc/sec. Isocyanic and isothiocyanic acids, on the other hand, possess small positive coupling constants. The similarity of these values in the two molecules and the difference between these and the $-C\equiv N$ values listed above lead to two qualitative conclusions. (1) Bonds to nitrogen in isocyanic acid are similar to those in isothiocyanic acid, and (2) these bonds are in both cases quite dissimilar to the $-C\equiv N$ bond which would be found if the molecules were HOCN and HSCN. Therefore, the alternative structures HNCO and HNCS are indicated.

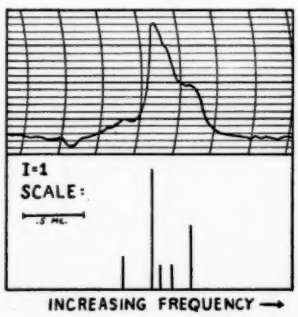

FIG. 2. Hyperfine structure of $1_{1,1}-2_{1,2}$ transition of HNCS. The two large peaks are separated by 0.35 Mc. The frequency of the small peak could not be measured on the oscilloscope.

TABLE II. Dipole moment of HNCO and DNCO.

State of molecule	Freq. of $0_{0,0}-1_{0,1}$ transition in Mc/sec.	Dipole moment in Debye units
HNCO: ground state	21,981.7	1.592±0.015
High frequency bending vibration	21,993.0	1.760±0.015
Low frequency bending vibration	22,017.3	1.620±0.015
DNCO: ground state	20,394.7	1.619±0.015

More quantitative calculations of the coupling constants to be expected were made, following the theory of Townes and Dailey.[3] Calculated values correctly predicted in each case the sign of eQq, but they were only roughly in agreement with the observed magnitudes.

Beard and Dailey[2] have shown from the measured moments of inertia that HNCS is a reasonable structure but HSCN is not. Also, an investigation of the hydrogen stretching frequencies of HNCO and HNCS reported in an earlier paper[1] established that both of these molecules have the proton bonded to the same atom. All of this evidence leads us to the conclusion that the structures are similar and are HNCO and HNCS.

The slight asymmetry of HNCO should result in two, low frequency, nondegenerate vibrations. Two absorption lines, corresponding to molecules in each of these excited vibrational states, were observed. Dependence of intensities upon temperature confirmed the assignment as excited vibrational states; however, the intensity measurements were not sufficiently reproducible to allow a determination of the vibrational frequencies.

Stark splittings were measured as a function of the applied electric field for the $0_{0,0}-1_{0,1}$ transition of $HN^{14}C^{12}O^{16}$ and $DN^{14}C^{12}O^{16}$ in the ground vibrational states, and for $HN^{14}C^{12}O^{16}$ in the excited vibrational states. Since HNCO is very nearly linear, the theory of the Stark effect in linear molecules was applied in each case and the component of the dipole moment along the principal axis of least moment of inertia was calculated. These values are given in Table II. No satisfactory explanation has been found for the large difference in the change of dipole moment in the two excited vibrational states.

This work was supported in part by a grant from the Research Corporation, to whom we wish to express our gratitude. We wish also to thank Professors H. V. Neher and W. H. Pickering and Mr. Bart Locanthi for valuable assistance in electronics problems.

* General Electric Swope Fellow, 1950–1951.
† Present address: Hughes Aircraft Company, Culver City, California.
‡ Contribution from the Gates and Crellin Laboratories of Chemistry.
[1] Jones, Shoolery, Shulman, and Yost, J. Chem. Phys. **18**, 990 (1950).
[2] C. I. Beard and B. P. Dailey, MITRLE Tech. Report No. 112 (1949).
[3] C. H. Townes and B. P. Dailey, J. Chem. Phys. **17**, 782 (1949).

Kinetics of Gas Adsorption as a Method of Area Determination

GEORGE JURA AND RICHARD E. POWELL
Department of Chemistry and Chemical Engineering, University of California, Berkeley, California
December 12, 1950

TO date, the methods of surface area determination of solids by the adsorption of gases have been based upon appropriate theoretical treatment of the equilibrium measurements.[1,2] Provided there is a significant change in the rate of adsorption when a monolayer is adsorbed, a measurement of gas adsorption kinetics will lead to an independent determination of the surface area of a solid. It appears that no detailed experimental study of adsorption in the multilayer region has been published. We wish to report here the observations on two systems for which the specific rate of

adsorption decreases sharply with the completion of a monolayer. The values of surface area so computed are in good agreement with those previously computed by the BET and HJ theories.

In order to keep the theoretical treatment as general as possible, we assume only that (1) the rate-determining step in adsorption involves a single molecule, so that the rate of adsorption is proportional to the first power of the pressure, and (2) the adsorbed molecules are in equilibrium over the entire extent of surface. These assumptions specifically exclude those cases in which diffusion is rate-controlling.

From the first assumption, the rate of adsorption, R_f, is proportional to the pressure, P, and to some function, $F(V)$, of the volume, V, of the gas adsorbed:

$$R_f = k_f P F(V). \tag{1}$$

The rate of desorption, R_b, is proportional to some function, $G(V)$, of the volume adsorbed:

$$R_b = k_b G(V). \tag{2}$$

At equilibrium, we can evaluate $k_b G(V)$ from the requirement that there the net rate is zero:

$$0 = k_f P_V F(V) - k_b G(V) \tag{3}$$

where P_V is the equilibrium pressure at adsorption V. By our second assumption, this evaluation of the desorption rate applies during the adsorption process. The net rate, R, is then

$$R = k_f (P - P_V) F(V). \tag{4}$$

In a constant-volume system Eq. (4) becomes

$$-\mathrm{d}P/\mathrm{d}t = k(P - P_V)F(V). \tag{5}$$

The dependence of the rate on the surface coverage, which is the object of our investigation, is contained in the function $F(V)$. Accordingly we make a plot of $-(\mathrm{d}P/\mathrm{d}t)/(P-P_V)$ *versus* V. The instantaneous rate, $\mathrm{d}P/\mathrm{d}t$, is evaluated from the adsorption data by numerical differentiation. P_V is obtained from the isotherm, even an approximate isotherm being adequate for the purpose of this computation.

When the amount adsorbed is less than a monolayer, $F(V)$ will in general be a falling function of V. In the case of an ideal localized monolayer (Langmuir adsorption) $F(V)$ will be a linear function of V, becoming zero at $V = V_m$.

Figures 1 and 2 respectively present data for the adsorption kinetics of NH_3 on a silica-alumina cracking catalyst at 0°C, and of H_2O at 25°C on anatase treated with aluminum oxide. The data

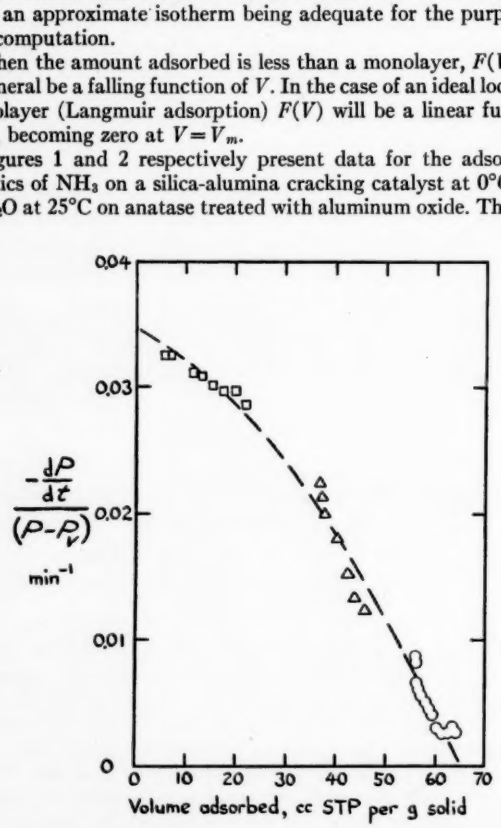

FIG. 1. Adsorption of NH_3 on a cracking catalyst.

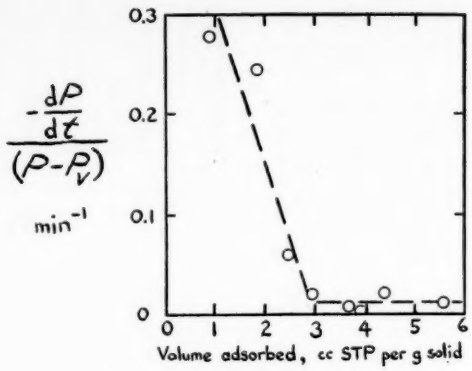

FIG. 2. Adsorption of H_2O on anatase.

were originally taken incidentally to the determination of the isotherms. The specific adsorption rate for both systems is seen to drop markedly as V increases to V_m. The rate when V is greater than V_m is small and appears to be independent of V. Extrapolation of the rates to zero gives V_m for these samples. The areas so obtained are 290 $m^2\,g^{-1}$ for the cracking catalyst and 8.6 $m^2\,g^{-1}$ for the anatase. The specific surface area of the catalyst is 370 $m^2\,g^{-1}$, as determined by nitrogen adsorption at 77.9°K. The area of the anatase varied from 8.9 $m^2\,g^{-1}$ by the absolute method to 11.8 $m^2\,g^{-1}$ by the application of the BET theory to water adsorption.[2] Values for the area computed from the kinetic data are at most 20 percent lower than those computed from equilibrium data. A discrepancy of this magnitude is no greater than that between one and another of the older methods.

[1] Brunauer, Emmett, and Teller, J. Am. Chem. Soc. **60**, 309 (1938).
[2] W. D. Harkins and G. Jura, J. Am. Chem. Soc. **66**, 1366 (1944).

The Fundamental Vibrations and Crystal Structure of H_2S and D_2S

J. B. LOHMAN, F. P. REDING, AND D. F. HORNIG
Metcalf Research Laboratory, Brown University, Providence, Rhode Island*
December 1, 1950

IN a recent note Allen, Cross, and King[1] have published a complete quadratic expression for the vibrational energy of the H_2S molecule. Two of the three fundamental frequencies in their expression differ by more than 50 cm^{-1} from the commonly accepted values[2] and indicate the almost complete absence of P branches in the bands of the antisymmetric stretching vibration, ν_σ, and the bending mode, ν_δ.

We should like to report that the spectrum of crystalline H_2S at 68°K is in agreement with their expression and cannot be recon-

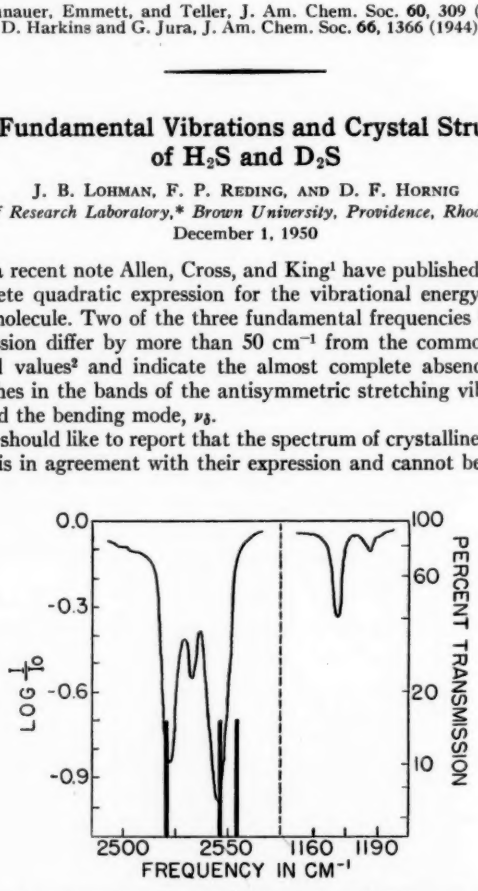

FIG. 1. Infrared spectrum of crystalline H_2S at 68°K. Raman spectrum is indicated by vertical lines.

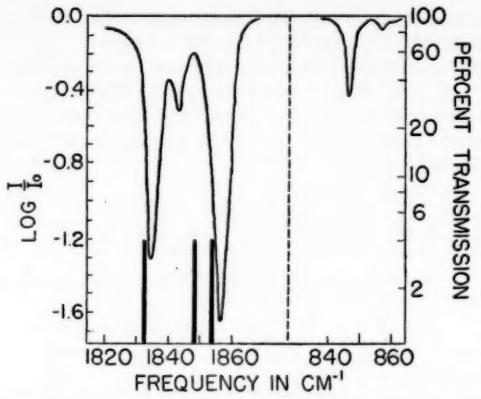

FIG. 2. Infrared spectrum of crystalline D_2S at 68°K. Raman spectrum is indicated by vertical lines.

ciled with the older frequency assignment. Furthermore, the spectrum of crystalline D_2S shows that the situation in D_2S parallels that in H_2S closely and that the current assignment of fundamental frequencies[2] must be revised in the same way.

The infrared spectra of H_2S and D_2S at 68°K in the vicinity of the fundamental frequencies are shown in Figs. 1 and 2. The extreme sharpness of the vibrational lines when they are not complicated by rotational structure is apparent,[3] average widths at half the maximum absorption coefficient being 6 cm^{-1} and 4 cm^{-1} in H_2S and D_2S, respectively. The Raman frequencies[4] are included as vertical solid lines for comparison.

It has been reported that H_2S has a face-centered cubic lattice[5] similar to that of CO_2 and contains four molecules in a unit cell. This structure is certainly incorrect when the hydrogen is considered since it requires that H_2S be linear. Further, the presence of four distinct components arising from the two stretching vibrations and of two components from the bending vibration eliminates the CO_2 structure. In this structure the symmetric stretch is inactive and only one component of the antisymmetric stretch and two components of the bend may appear in the infrared spectrum.

The fact that all four of the components arising from the two stretching vibrations occur in the range 2523–2554 cm^{-1} indicates that the separation of the two fundamentals in the gas must be less than 31 cm^{-1}. Since there is no question about assignment of ν_π to 2611 cm^{-1}, we would conclude that ν_σ must lie at a frequency lower than 2640 cm^{-1}, in agreement with the first reference which gives 2625 cm^{-1} as its value. More detailed arguments regarding crystalline coupling strengthen this conclusion and will be reported in a fuller account of our work. However, they lead to the assignment given in Table I.

The mean value of the two components of the bending frequency is 1178 cm^{-1}. In all previously observed cases of hydrogen bonding in simple molecules,[6] as well as on theoretical grounds, stretching frequencies decrease but bending frequencies increase. Hence, one might conclude that 1178 cm^{-1} should constitute an upper limit to the frequency of ν_δ. This is not quite in agreement with Allen, Cross, and King who give 1183 cm^{-1} for this frequency; however, it disagrees completely with the value 1290 cm^{-1} which Herzberg regards as most reliable.

Extension of these arguments in a straightforward way leads to the approximate fundamental frequencies for gaseous D_2S which are given in Table I. They are believed to be reliable to better than 10 cm^{-1}. The values of ν_σ and ν_δ obtained here for D_2S are both of the order of 100 cm^{-1} lower than those cited by Herzberg.

TABLE I. Fundamental frequencies of crystalline and gaseous H_2S and D_2S (cm^{-1}).

	H_2S			D_2S		
	Crystal		Gas[b]	Crystal		Gas
	Infrared	Raman[a]		Infra-red	Raman[a]	
ν_σ	—	2554	2626	1854	1853	1900
	2544	2546		—	1848	
ν_π	2532	—	2611	1842	—	1892[a]
	2523	2521		1834	1832	
ν_δ	1171	—	1183	846	—	855
	1186	—		857	—	

[a] See reference 4.
[b] See reference 2.

* This work was supported by the ONR under contract N6ori-88, Task Order I.

[1] Allen, Cross, and King, J. Chem. Phys. **18**, 1412 (1950).
[2] See G. Herzberg, *Infra-Red and Raman Spectrum of Polyatomic Molecules* (D. Van Nostrand Company, Inc., New York, 1945), p. 283.
[3] D. F. Hornig, J. Chem. Phys. **16**, 1063 (1948).
[4] G. M. Murphy and J. E. Vance, J. Chem. Phys. **6**, 426 (1938).
[5] G. Natta, Rend. accad. naz. Lincei **11**, 679, 749 (1930).
[6] D. F. Hornig, Trans. Faraday Soc. (to be published).

Critical Limits of Metastability in Binary Systems

HOWARD REISS AND LAWRENCE FRIEDMAN
Department of Chemistry, Boston University, Boston, Massachusetts
December 11, 1950

THE kinetics of phase transitions in binary systems has recently been treated.[1,2] In this note an effort will be made to compare the theoretical deductions contained in that treatment with available experimental information.

Using the older quasi-thermodynamic approach[3] it could be shown that the rate I^* at which fragments of a new phase were formed could be expressed as

$$I^* = Ce^{-\omega_0/kT},$$

where k is the Boltzmann constant, T, the absolute temperature, and ω_0, the reversible work required in the formation of a critical binary embryo. C is an unknown coefficient. As the original phase grows more metastable I^* increases slowly, until a point is reached where it suddenly increases from a very small, almost zero, value to an almost infinite value for a very small increment of metastability. This point defines the critical limit of metastability.

The sudden change is due to a sudden change in the exponential factor. C, though unknown through the older theory, has been assumed to change only slightly. Nevertheless, an assumed constant value for C must be available if the critical limit is to be determined through use of (1).

It had previously been possible to compute C for a one-component system. Workers in the field then assumed that the value of C computed for either pure component of the binary mixture at the same temperature and pressure could be used in (1), applied to binary systems. In this way Volmer and Flood[4] conducted experiments on the condensation of gaseous mixtures and found critical limits which agreed well with calculations based on (1) and the above assumption concerning the value of C.

With the completion of the work referred to as reference 1, it became possible to calculate C for binary systems [see Eq. (86) of

TABLE I.[a]

Mole % benzene	Surface tension (dynes/cm²)
0	28.59
20	28.63
40	28.67
50	28.69
60	28.75
80	28.80
100	28.94
Temp = 18°C	

[a] ICT, Vol. IV, p. 473.

TABLE II.

$p_{tol}=p_{tol}^{\circ}$	p_{ben}	C	$\exp(-\omega_0/kT)$
	1.50	2.43×10^{29}	2×10^{-87}
*	3.05	4.44×10^{28}	1.59×10^{-30}
	3.15		$10^{-29.5}$
	3.30		10^{-28}
	3.40		$10^{-27.2}$
	3.70		10^{-27}
	4.00	3.56×10^{29}	1.26×10^{-22}

reference 1]. These calculations are extremely laborious, consuming much time.

We have computed C for the binary system, benzene-toluene vapor, in order to test, theoretically, the assumptions which have been made concerning it, and which appear to be experimentally justifiable.

Benzene and toluene were chosen because they form a system ideally fitted to the equations developed in reference 1. The liquid solution, besides being thermodynamically ideal, possesses a surface tension which is virtually independent of composition at 180°C. This is illustrated in Table I, in which the surface tension is listed as a function of the mole percent of benzene in the solution.

At 18°C, the temperature for which the following calculations have been carried out, the vapor pressures of pure toluene and pure benzene are[5]

$$p_{tol}^{\circ}=26.7\times10^{3}\text{ dynes/cm}^2,$$
$$p_{ben}^{\circ}=90.7\times10^{3}\text{ dynes/cm}^2.$$

The relative constancy of C was first examined in its dependence upon supersaturation. Some results are shown in Tables II and III where C and $\exp(-\omega_0/kT)$ are listed as functions of p_{ben}, the partial pressure of benzene in the vapor mixture, for two values of p_{tol}, i.e. $p_{tol}=p_{tol}^{\circ}$ in Table II, and $p_{tol}=0.5p_{tol}^{\circ}$ in Table III.

In both tables the critical pressures are starred. It will be noted that in Table II, C remains in the neighborhood of 10^{28} while $\exp(-\omega_0/kT)$ varies from 10^{-87} to 10^{-22}. In Table III, C remains at

TABLE III.

$p_{tol}=0.5p_{tol}^{\circ}$	p_{ben}	C	$\exp(-\omega_0/kT)$
	1.50	8.29×10^{27}	10^{-155}
	4.00	6.54×10^{28}	$10^{-30.8}$
	4.03		$10^{-30.8}$
*	4.04	6.28×10^{28}	10^{-28}
	4.20		$10^{-24.3}$
	4.65		$10^{-22.4}$
	5.00		$10^{-20.8}$
	6.00		10^{-17}

about 10^{28} while $\exp(-\omega_0/kT)$ passes from 10^{-155} to 10^{-28}. Obviously, C is relatively constant and independent of supersaturation.

The error introduced in (5) by using the C for a one component system was examined next. Three critical compositions were selected and the values of C were computed for these using the binary theory. For each of these three cases the values of C were computed for pure toluene and pure benzene at the pressure

$$p=p_{tol}+p_{ben}$$

where p_{tol} and p_{ben} are the partial pressures in the corresponding critical mixture. The results are shown in Table IV. It is seen that for all practical purposes the value of C for either pure component

TABLE IV.

p_{ben}	p_{tol}	p, dynes/cm²	$C_{mixture}$	C_{ben}	C_{tol}
$3p_{ben}^{\circ}$	$1p_{tol}^{\circ}$	303×10^{3}	4.44×10^{28}	2.80×10^{27}	3.77×10^{27}
$3.4p_{ben}^{\circ}$	$0.75p_{tol}^{\circ}$	328×10^{3}	3.60×10^{27}	3.39×10^{27}	4.41×10^{27}
$4.04p_{ben}^{\circ}$	$0.50p_{tol}^{\circ}$	375×10^{3}	6.28×10^{28}	4.29×10^{27}	5.76×10^{27}

may be used in place of the binary value, when the tremendous variation of $\exp(-\omega_0/kT)$ is taken into account.

If this is generally possible (and it now seems probable in view of the existence of both experimental and theoretical checks), it constitutes a great advantage since the evaluation of C for a one component system is very much less laborious than its evaluation for a binary system.

[1] Reiss, J. Chem. Phys. 18, 840 (1950).
[2] Reiss, J. Chem. Phys. 18, 996 (1950).
[3] Volmer, Z. physik Chemie 119, 277 (1926).
[4] Volmer, *Kenetik der Phasenbildung* (Edwards Brothers, Inc., Ann Arbor, 1945), p. 155.
[5] Lange, *Handbook of Chemistry* (Handbook Publishers, Inc. Sandusky, Ohio, 1941), 4th Edition, pp. 1241, 1249.

The Effect of Gegen Ions on the Light Scattering by Solutions of Colloidal Electrolytes

TODD M. DOSCHER AND KAROL J. MYSELS
Department of Chemistry, University of Southern California, Los Angeles, California
December 18, 1950

THE determination of particle weight by light scattering is well established in theory and practice for macromolecular nonelectrolytes. In recent years, applications to colloidal electrolytes led to the development of theory taking into account the effect of the electric charge and consequent presence of gegen ions. Hermans[1] by considering light scattering as an interference phenomenon has derived in detail the necessary equations. The same result may be obtained more simply yet and generally enough to include the effect of neutral salts by an extension of the fluctuation theory of light scattering to include the requirement of electroneutrality, which, Hermans[1] has shown is valid except at most extreme dilutions.

The basic Einstein equation[2] may be written:

$$H\frac{c}{T}=N_2\frac{d\ln f_2}{dc_2}, \tag{I}$$

where N_2 is the concentration of colloid in moles per liter; c_2 its concentration in grams per liter; and f_2 its activity. Assuming unit activity coefficients, the activity of the solute is equal to:

$$f_2=n_m\times n_i^{p}, \tag{II}$$

where n_m is the molar concentration of the colloidal ion; n_i, the concentration of oppositely charged simple ions; and p, the number of the latter associated with one charged colloidal ion, i.e., the charge of the colloidal ion if the gegen ions are univalent. Differentiating (II) and substituting in (I), together with the relation $c_2/M_2=n_2$ gives:

$$H\frac{c}{T}=\frac{1}{M_2}\left(1+p\frac{n_2dn_i}{n_idn_2}\right). \tag{III}$$

However, in order to maintain electrical neutrality, $(dn_i/dn_2)=p$; therefore:

$$H\frac{c}{T}=\frac{1}{M_2}\left(1+p^2\frac{n_2}{n_i}\right). \tag{IV}$$

If the colloidal electrolyte is pure, i.e., no neutral salt is present so that $n_1/n_2=p$, this general expression (IV) reduces to

$$H\frac{c}{T}=\frac{1}{M_2}(1+p) \tag{V}$$

which is the same as Hermans'[1] result.

As the concentration of neutral salt increases $H(c/T)$ decreases from $(1+p)/M_2$ to $1/M_2$ so that light scattering, like other colligative properties, can be used to determine directly the size of colloidal electrolytes provided swamping electrolytes are present and their effect taken into account. Taking this effect into account precisely is not simple because of interactions between all scattering species,[3] but as a first approximation the effects may be considered additive.

In the case of association colloids having a critical micelle concentration, the simple ions present at this cmc act as a swamping electrolyte so that the simple extrapolation of $H(c/T)$ to the cmc as was done for example by Debye[4] should give as a first approximation, the correct value for the size of the micelle.

As the concentration of an association colloid increases $H(c/T)$ must decrease since M_2 can only increase and p/M_2 decrease.

[1] J. J. Hermans, Rec. Tran. Chim. des Pays-Bar **68**, 859 (1948).
[2] A. Einstein, Ann. Physik. **33**, 1275 (1910).
[3] H. C. Brinkman and J. J. Hermans, J. Chem. Phys. **17**, 574 (1949).
[4] P. Debye, J. Phys. Colloid Chem. **53**, 1 (1949).

Ionic Transport in Liquid Silicates

J. O'M. Bockris, J. A. Kitchener, and A. E. Davies
Department of Inorganic and Physical Chemistry, Imperial College, London, England
November 29, 1950

SOME uncertainty exists concerning the presence of semiconduction in the electric conduction of liquid silicates. This may be resolved only by measurements of the applicability of Faraday's Laws to the electric transport processes in the melt. Such measurements are considered to be difficult at 800°C in liquid salts.[1]

A method has been devised in these laboratories whereby the oxygen evolved at the anode during electrolysis of lithium silicate is measured. The silicate is heated under vacuum in a molybdenum cell with a carbon anode and an alumina anode compartment. Oxygen liberated during electrolysis attacks the carbon giving a mixture of CO and CO_2, which is adsorbed on charcoal cooled in liquid air and subsequently analyzed.

In the case of a silicate in which the metallic component is not too small, the most likely anodic reaction is

$$SiO_4^{4-} - 4e \rightarrow SiO_2 + O_2.$$

The results in Table I have been obtained for the system $Li_2O:SiO_2$.

Table I.

Composition $Li_2O:SiO_2$	Temp. °C	Faradays passed	O_2 obtained g equiv.
40:60	1300	0.0172	0.0164
45:55	1305	0.0243	0.0251
45:55	1305	0.0321	0.0325
20:80	1335	0.0286	0.0273
20:80	1335	0.0363	0.0380

These results show that within the experimental error of ∓5 percent the conduction is wholly ionic.

A systematic examination of electric transport in various binary liquids silicates is in progress.

The authors wish to acknowledge with thanks the financial support of this work by the British Iron and Steel Research Association.

[1] Drossbach, *Electrochemie Geschmolzener* (Salze, Berlin, 1938).

Oxidation Kinetics of Nickel and Cobalt

Walter J. Moore and James K. Lee
The Catholic University of America, Washington, D. C.
December 18, 1950

THE first part of an investigation of the kinetics of the formation of oxide films on nickel and cobalt foils has recently been completed, a study of the oxidation at temperatures high enough that the parabolic rate law is followed, and at pressures high enough that the rate constants are virtually independent of pressure. The results are summarized in Fig. 1, in the form of plots of log$k$ *vs* $1/T$, where k is defined by the rate law $dy/dt = k/y$, y being the oxide-film thickness at time t. The measurements were made with cobalt-free nickel foil (99.8 percent Ni), and cobalt foil of 99.1 percent purity. The oxygen pressure was 10 cm and the temperatures ranged from 400° to 900°C for nickel, and from 500° to 800°C for cobalt. A volumetric method that has been described elsewhere[1] was employed to follow the rate of oxygen uptake.

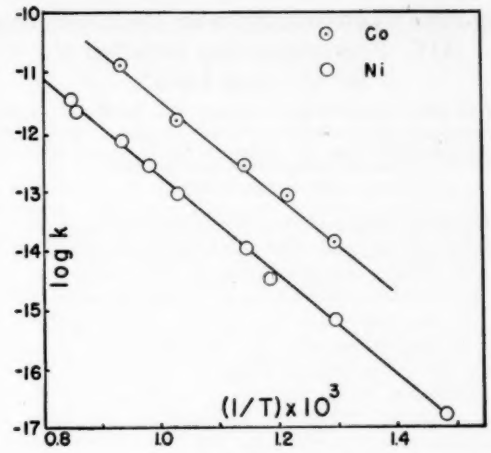

Fig. 1. Plot of log$k$ *vs* $1/T$.

The rate constants can be expressed as follows:[2]

$$\text{nickel } k = 3.09\times10^{-5}\exp(-38400/RT) \text{ cm}^2 \text{ sec}^{-1},$$
$$\text{cobalt } k = 7.60\times10^{-4}\exp(-38400/RT) \text{ cm}^2 \text{ sec}^{-1}.$$

It may be noted that although the cobalt rate constant is about 25 times that for nickel, the activation energies are nearly the same, so that the difference in rates is due to the pre-exponential or "entropy" factors.

An expression similar to one given by Mott[3] relates k to the cationic diffusion coefficient D and the fraction f of vacant sites at the oxide-oxygen interface: $k = 2Df$. The vacant cation sites ($\square_c$) are formed as oxygen is adsorbed:

$$2M^{+2} + 1/2O_2 = 2M^{+3} + O = +\square_c.$$

As long as the oxide surface is completely covered with adsorbed oxide ions, which is the situation in the pressure-independent range of reaction, the concentration of vacancies at the surface should be determined only by the number of available surface adsorption sites. If this number is independent of temperature the activation energy for D should be equal to that for k. This may be the case in the oxidation of copper to cuprous oxide.[4] It is likely that nickel and cobalt behave in the same way. The observed rate constants therefore suggest that the activation energies for cationic diffusion, via a vacancy mechanism, are the same in cobalt oxide (CoO) and in nickel oxide (NiO), but that CoO contains about 25 times more vacancies. A possible explanation of such a temperature-independent difference in the vacancy concentrations would be that only a small fraction of the oxide surface ("active centers") is effective in the dissociation and ionization of oxygen molecules, and this fraction is 25 times greater for CoO than for NiO.

The adsorption theory of Volkenshtein,[5] however, emphasizes the possibility that the number of active surface sites may be itself a function of the temperature. It should be possible to check this hypothesis by independent measurements of the diffusion coefficients in metal oxides and the parabolic oxidation rates.

This work has been done under Contract NOrd 10260. The assistance of The Frederick Gardiner Cottrell fund of the Research Corporation is also gratefully acknowledged.

[1] W. J. Moore and J. K. Lee, Trans. Faraday Soc. (to be published).
[2] The value given here for nickel differs somewhat from one previously reported from this laboratory [J. Chem. Phys. **18**, 231 (1950)]. The present value is considerably more reliable.
[3] N. F. Mott, Trans. Faraday Soc. **35**, 1175 (1939).
[4] G. W. Castellan and W. J. Moore, J. Chem. Phys. **17**, 41 (1949).
[5] F. F. Volkenshtein, Zhurr. Fiz. Khim. **23**, 917 (1949).

Carrier-Free Radioisotopes from Cyclotron Targets XIV. Preparation and Isolation of $Bi^{204, 206}$ from Lead*

JEANNE D. GILE, WARREN M. GARRISON, AND JOSEPH G. HAMILTON
Crocker Laboratory, Radiation Laboratory, and Divisions of Medical Physics, Experimental Medicine, and Radiology; University of California, Berkeley and San Francisco, California
December 4, 1950

THE present paper reports a carrier-free procedure used in isolating radio-bismuth from a lead target which had been bombarded with 19-Mev deuterons in the 60-inch cyclotron at Crocker Laboratory. Deuteron bombardment of lead produces $Bi^{204,206}$ by the nuclear reactions:[1,2] $Pb^{204}(d, 2n)Bi^{204}$, $Pb^{206}(d, 2n)Bi^{206}$. Other possible concurrent reactions include: formation of radio-lead isotopes by $(d-p)$ reaction, radioisotopes of Tl by $(n-p)$ reaction, and radioisotopes of Hg by $(n-a)$ reaction. The short-lived thallium activities, $Tl^{206,207,208}$, had decayed out prior to the chemical separation reported here. The long-lived Tl^{204} and Hg^{203} were not detected. The target was spectrographically-pure[3] lead foil ($\frac{1}{8}$-inch thick) clamped to a water-cooled aluminum target plate. It was bombarded with 19-Mev deuterons for a total of 20 μa-hr at a maximum beam intensity of 5 μa. Higher bombardment intensities would have melted the target. After bombardment, the foil (approximately 1 g) was dissolved in a minimum volume of 16N nitric acid and the resultant solution was evaporated to dryness. The lead nitrate containing the carrier-free $Bi^{204,206}$ was dissolved in excess 10 percent sodium hydroxide to give a clear "solution" of sodium plumbate and radiocolloidal[4] $Bi^{204,206}$. This solution, after dilution with an equal volume of water, was drawn through two consecutive Whatman No. 50 filter papers which retained over 98 percent of the carrier-free $Bi^{204,206}$ as absorbed radiocolloid. The filters were washed with five percent sodium hydroxide until lead could not be detected in the filtrate, followed by distilled water to remove sodium hydroxide. Less than one percent of bismuth activity was removed from the filter paper during the washing. The $Bi^{204,206}$ was removed from the filter paper with a minimum amount of 6N hydrochloric acid which, after a reduction in volume by evaporation, was neutralized with sodium hydroxide to give an isotonic saline solution for biological investigation.

The decay curve was followed for 30 days and showed two periods: 12-hour Bi^{204} and 6.4-day Bi^{206}. Forty hours after bombardment, the activity contained only 6.4-day Bi^{206}. The lead absorption curve showed the 1.1-Mev gamma-ray and the softer component (approximately 0.4 Mev) previously reported.[2] The aluminum absorption curve had an end-point of approximately 300 mg, a somewhat lower value than that given in reference 2. The activity was further identified by chemical separation using bismuth, lead, thallium and mercury carriers. Over 99 percent of the added tracer activity was recovered in the bismuth fraction.

We are grateful to Professor G. T. Seaborg for helpful suggestions and Mr. T. Putnam, Mr. G. B. Rossi, and the crew of the 60-inch cyclotron for bombardments.

* This document is based on work performed under Contract No. W-7405-eng-48-A for the AEC.
[1] G. T. Seaborg and I. Perlman, Revs. Modern Phys. **20**, 185 (1948).
[2] Templeton, Howland, and Perlman, Phys. Rev. **72**, 766 (1947).
[3] Bismuth was not detected by spectrographic analysis.
[4] O. Hahn, *Applied Radiochemistry* (Cornell University Press, Ithaca, New York, 1936).

On the Origin of Low Frequency Raman Lines in Organic Crystals

S. C. SIRKAR
Indian Association for the Cultivation of Science, Calcutta, India
December 6, 1950

IT has been pointed out recently by Fruhling[1] that, on the basis of the nature of polarization of the four lines of frequency shifts, 35, 63, 69, and 105 cm^{-1}, observed in the case of single crystal of benzene at 0°C, these lines can be assigned to rotatory oscillations of the benzene molecule about its three axes, as suggested earlier by Kastler and Rousset[2] and also by Bhagavantam.[3] It has further been assumed by Fruhling that the intermolecular forces act essentially between nearest hydrogen atoms and he has derived on this assumption the value 4×10^2 d/cm for the force constant between two such hydrogen atoms belonging to two neighboring molecules.

It has, however, to be pointed out that this assumption made in calculating the force constant is not correct, because the hydrogen atoms are not free, and in the type of oscillation postulated by Fruhling there would be either a deformation or a stretching of the C−H bond and this would make the frequency many times larger than what is actually observed. On the other hand, if we calculate the force constant f on the assumption that a benzene molecule of radius r executes rotatory oscillations about one of its axes and a force of restitution fx acts at each end of the molecule where x/r is the angular displacement of the molecule from its mean position the calculated value of f is found to be about 30 times larger than that reported by Fruhling. For instance, taking the Raman line at 100 cm^{-1} the value of the restoring couple β for a rotation of one radian of the molecule is obtained from the relation

$$\beta=4\pi^2\nu^2I. \tag{1}$$

Assuming the value of I to be 130×10^{-40} g-cm^2, we find

$$\beta=4.4\times10^{-12}.$$

But

$$\beta=2fr^2, \tag{2}$$

fr being the restoring force at each end of the molecule. The value of f obtained from (1) and (2) is about 1.1×10^4 d/cm.

Again, if it is assumed that two benzene molecules execute a linear oscillation against each other with a force constant f' giving rise to the polarized line at 65 cm^{-1} the value of f' is found to be about 1×10^4 d/cm.

The force constant is thus much stronger than Van der Waal forces and is many times larger than that reported by Fruhling.[1] This large value of the force constant suggests that the benzene molecules in the crystal are present in the form of small groups of molecules in which the single molecules are associated with each other through virtual bonds. Such a hypothesis was put forward long ago by the present writer[4] and is supported by the results of further investigations carried out in this laboratory recently.[5,6]

[1] A. Fruhling, J. Chem. Phys. **18**, 1119 (1950).
[2] A. Kastler and A. Rousset, J. phys. radium **2**, 49 (1941).
[3] S. Bhagavantam, Proc. Indian Acad. Sci. **13A**, 543 (1941).
[4] S. C. Sirkar, Indian J. Phys. **10**, 109 (1936); *ibid.* **10**, 189 (1936); *ibid.* **11**, 55 (1937).
[5] A. K. Ray, Indian J. Phys. **24**, 111 (1950).
[6] S. C. Sirkar and A. K. Ray, Indian J. Phys. **24**, 189 (1950).

Erratum: On the Stability of Gas Bubbles in Liquid-Gas Solutions

[J. Chem. Phys. **18**, 1505 (1950)]
P. S. EPSTEIN AND M. S. PLESSET
California Institute of Technology, Pasadena, California

THE cuts of Figs. 3 and 4 were interchanged so that the labeling below them is incorrect.

Remarks on the Calculating Rates of Some Radical Reactions

M. SZWARC
Chemistry Department, The University of Manchester, Manchester, England
November 24, 1950

THE determination of the concentration of radicals or atoms participating in many chemical reactions presents formidable technical difficulties. Without these data we are unable to calculate the rate constants of elementary reactions involving

radicals. However, we can determine the relative rate constants for two competing elementary reactions in which the same radical or atom participates. The following two examples illustrate a method which is well known and often applied.

Example I.—

$$R+\chi_1 \rightarrow \text{Products (1)} \cdots k_1,$$
$$R+\chi_2 \rightarrow \text{Products (2)} \cdots k_2.$$

R denotes a radical or atom, χ_1 and χ_2, two molecules present in the system and reacting with the species R. The ratio of rate constants k_1/k_2 is given by the expression:

$$k_1/k_2=(d \text{ Products (1)}/dt)\cdot[\chi_2]/(d \text{ Products (2)}/dt)\cdot[\chi_1].$$

This expression is still valid even if the concentration of R varies during the experiment.

Example II.—

$$R+\chi \rightarrow \text{Products (1)} \cdots k_1,$$
$$R+R \rightarrow \text{Products (2)} \cdots k_2,$$

where R and χ have the previous meaning.

The relationship between k_1 and k_2 is usually given in the form

$$k_1/k_2^{\frac{1}{2}}=(d \text{ Products (1)}/dt)/(d \text{ Products (2)}/dt)^{\frac{1}{2}}\cdot[\chi].$$

This expression is strictly correct only if the concentration of R remains stationary during the whole time of the experiment. If the concentration of R varies, however, such as in the case of photochemical experiments when the intensity of light fluctuates, or in experiments in which high proportions of products are formed then a correction must be introduced.

Let us consider a case in which the concentration of 1χ remains constant for all practical purposes, while the concentration of R varies. The amount of Products (1) formed in such an experiment is given by

$$\int_0^t k_1\cdot[R]\cdot[\chi]\cdot dt=k_1\cdot\langle[R]\rangle_{Av}\cdot[\chi]\cdot t,$$

where $\langle[R]\rangle_{Av}$ denotes the average concentration of R and is given by

$$\langle[R]\rangle_{Av}=\frac{1}{t}\int_0^t[R]\cdot dt.$$

The amount of Products (2) formed in the same experiment is given by

$$\int_0^t k_2[R]^2dt=k_2\langle[R]^2\rangle_{Av}\cdot t$$

where $\langle[R]^2\rangle_{Av}$ denotes the mean of square of R concentration, and is given by

$$\langle[R]^2\rangle_{Av}=\frac{1}{t}\int_0^t[R]^2dt.$$

Thus we obtain

$$k_1/k_2^{\frac{1}{2}}=\{(d \text{ Products (1)}/dt)/(d \text{ Products (2)}/dt)^{\frac{1}{2}}\cdot[\chi]\}\cdot(\langle[R]^2\rangle)^{\frac{1}{2}}/\langle[R]\rangle.$$

It is known that $(\langle[R]^2\rangle_{Av})^{\frac{1}{2}}\geq\langle[R]\rangle_{Av}$, and therefore the correction factor $(\langle[R]^2\rangle_{Av})^{\frac{1}{2}}/\langle[R]\rangle_{Av}$ is always greater or equal to 1. The minimum value of 1 is obtained if the concentration of R remains strictly constant during the experiment, otherwise the correction factor increases with increasing variation in R. The latter point bears some importance in the problems of estimating the value of $E_1-\frac{1}{2}E_2$ (E_1 and E_2 denoting activation energies of reactions (1) and (2)). In many cases the extent to which the reaction is allowed to proceed is greater at higher temperatures than at lower temperatures. By neglecting this correction factor the estimated energy E_1 becomes slightly lower than its true value. This might be the case in the determination of the activation energy for the reaction,

$$CH_3+C_6H_5\cdot CH_3\rightarrow CH_4+C_6H_5\cdot CH_2,$$

which was evaluated by Szwarc and Roberts[1] at about 12 kcal/M. The introduction of the correction factor mentioned above might make the estimated value still higher.

[1] M. Szwarc and J. I. Roberts, Trans. Faraday Soc. **46**, 625 (1950).

Carbon-14 Isotope Effect in an Inorganic Equilibrium

D. R. Stranks and G. M. Harris
Chemistry Department, University of Melbourne, Melbourne, Australia
December 11, 1950

Recently, attention has been directed to the isotope effect of C^{14} in relation to C^{12} in reaction rate studies. Quantitative experimental work[1,2] has indicated that the ratios of the corresponding specific rate constants in various reactions may deviate from unity by as much as 40 percent. Theoretical calculations[3,4] have qualitatively confirmed the magnitude of the observed effects.

The previously reported isotopic exchange reaction between carbonato-tetrammine cobaltic ion and carbonate ion[5] offers an alternative experimental approach to the investigation of C^{14} isotope effect. The reaction is

$$\{Co(NH_3)_4C^{12}O_3\}^+ + C^{14}O_3^= \rightleftarrows \{Co(NH_3)_4C^{14}O_3\}^+ + C^{12}O_3^=.$$

Its equilibrium constant may be written

$$K=\frac{[\{Co(NH_3)_4C^{14}O_3\}^+]}{[\{Co(NH_3)_4C^{12}O_3\}^+]}\Big/\frac{[C^{14}O_3^=]}{[C^{12}O_3^=]}.$$

Since the C^{14} is present only in tracer quantity, specific activity measurement of $BaCO_3$ samples derived from the two reactant types after isotopic equilibration enables direct determination of the concentration ratios required to evaluate K. Deviation of this constant from unity is an indication of the extent of isotope effect.

Aqueous solutions of carbonato-tetrammine cobaltic nitrate and C^{14}-labelled sodium carbonate/bicarbonate were mixed to give a solution 0.03376 molar in the complex and 0.01469 molar in carbonate radical (i.e. a molar ratio of reactants of 2.300). Previous kinetic runs at 20.30°C and pH's of ~10 and ~9 (adjusted by means of the carbonate/bicarbonate ratio) showed the exchange half-times to be 400 and 270 minutes respectively in two experiments. Thus, beginning after more than seven half-times of exchange (i.e. reaction within one percent of equilibrium), samples were taken for determination of C^{14} content of each component. Uncomplexed carbonate was precipitated as barium carbonate, washed, and counted on aluminium pans according to standard radiochemical procedure. The carbonato complex was prepared for isotopic assay by complete decomposition in vacuum with CO_2-free H_2SO_4, absorption of the evolved CO_2 in carbonate-free NaOH, and precipitation of barium carbonate samples as before. Radioactivity determinations were made with an end-window type Geiger-counter assembly, and any required coincidence corrections were applied. Self-absorption corrections were avoided by contriving that all barium carbonate samples were very close to the same size. All countings were of sufficient duration to insure that the random error was within one percent. Table I summarizes the results.

Table I.

	Duration of exchange (hours)	Specific activity of $BaCO_3$ samples (c/mg/min) From uncomplexed carbonate	From carbonato complex	2.300 × activity of carbonato complex (c/mg/min)	Total activity recovered (c/mg/min)
Expt. 1 ($pH\cong10$)	50.3	338	300	690	1028
	67.5	336	298	686	1022
	Mean:	337	299	688	1025
	(Initial activity)	1033	none	none	1033
Expt. 2 ($pH\cong9$)	48	323	289	664	987
	72	329	290	667	996
	72	321	288	662	983
	Mean:	324	289	664	988
	(Initial activity)	1003	none	none	1003

It is seen that satisfactorily complete recovery of activity is indicated in all measurements. The values of the equilibrium constants calculated for the two experiments agree well within experimental error; i.e. for expt. 1, $K=299/337=0.886$, and for expt. 2, $K=289/324=0.892$. Thus a deviation from unity of some 11 percent exists in the exchange equilibrium constant. The interpretation of this in terms of specific reaction rates necessitates a knowledge of the exact mechanism of the exchange, a report on which is to be published soon.

[1] P. E. Yankwich and M. Calvin, J. Chem. Phys. **17**, 109 (1949).
[2] W. H. Stevens and R. W. Attree, Can. J. Research **B27**, 807 (1949); J. Chem. Phys. **18**, 574 (1950).
[3] J. Bigeleisen, Science **110**, 14 (1949); J. Chem. Phys. **17**, 675 (1949).
[4] K. S. Pitzer, J. Chem. Phys. **17**, 1341 (1949).
[5] G. M. Harris, J. Chem. Phys. **18**, 764 (1950).

The Decomposition of Excited Ethylene*

B. deB. Darwent
Division of Chemistry, National Research Council, Ottawa, Canada
December 18, 1950

THE data given by LeRoy and Steacie[1] together with some results obtained in this laboratory indicate the possibility that excited ethylene molecules, which may be[2] vibrationally excited triplets, decompose on the wall. This conclusion is of interest since it is usually assumed that excited particles tend to loose their energy when they strike the wall.

The following sequence of reactions,

$$C_2H_4+Hg(^3P_1)\rightarrow C_2H_4^*+Hg(^1S_0) \quad (1)$$

$$C_2H_4^*+C_2H_4\rightarrow 2C_2H_4 \quad (2)$$

$$C_2H_4^*\rightarrow C_2H_2+H_2 \quad (3)$$

was proposed[1] to account for the characteristics of the reaction between $Hg(^3P_1)$ atoms and ethylene. In the region of complete quenching, it may easily be shown, if the above mechanism is correct, that

$$\frac{1}{R_3}=\frac{1}{I_a}+\frac{k_2}{k_3 I_a}[C_2H_4]$$

and so a plot of the reciprocal of the rate of production of H_2 (or C_2H_2) against pressure should be a straight line. However, when the data of LeRoy and Steacie was plotted on this basis, a curved, instead of a straight line resulted, indicating that the rate decreased with increasing pressure more rapidly than would be expected from the above relationship. This deviation from linearity has been confirmed by further experiments in this laboratory. However, a reasonably straight line is obtained when $1/R_3$ is plotted against p^2. For this to hold, it is necessary either for reaction (2) to occur by a three-body process:

$$C_2H_4^*+2C_2H_4\rightarrow 3C_2H_4 \quad (2^1)$$

or for the decomposition (3) to take place on the wall:

$$C_2H_4^* \xrightarrow{\text{wall}} C_2H_2+H_2 \quad (3^1)$$

since the relationship between $1/R_3$ and p^2 requires the ratio of deactivation to reaction to vary as the square of the pressure. It has been possible to decide between these two alternatives by investigating the effect of varying concentrations of mercury vapor on R_3 at constant ethylene pressure. Because of the very high absorption coefficient of mercury for $\lambda 2537$, it is possible to alter the mercury concentration within quite wide limits without affecting significantly the fraction of the incident resonance line that is absorbed in the 10-cm cell. Reaction (2^1) should not be influenced by change in the mercury concentration. However, reaction (3^1) is sensitive to the [Hg] since the effect of a low [Hg] is to spread the absorption zone away from the incident window of the cell. This lengthens the path through which $C_2H_4^*$ must diffuse, and so increases the probability of deactivation before it can attain the wall. It has been found that when the partial pressure of mercury was reduced from 12.0×10^{-4} mm to 4.0×10^{-4} mm, R_3 decreased from 5.8 to 3.5×10^3 mm·min^{-1}. This reduction of about 40 percent in the rate is significant and is taken as strong indication that reaction (3^1) and not (2^1) is responsible for the relationship found between the reciprocal rate and the square of the pressure.

The data in its present state does not permit any reliable estimate to be made of the average natural life of $C_2H_4^*$, but we may assign an approximate lower limit. If the excited molecules are in thermal equilibrium, their velocities will be about 5×10^4 cm sec^{-1}, and if we assume that they travel an average distance of about 0.5 cm before striking the wall, they must exist for about 10^{-5} sec without decomposing. Since 10 percent of homogeneous decomposition would probably have been detected, we may then assume that the average natural life is at least 10^{-4} sec. LeRoy and Steacie[1] estimated τ_3 to be about 2×10^{-7} sec but it may be shown that the basis of their estimate is unsound.

The results mentioned above, together with some new data on the reaction of $Hg(^3P_1)$ atoms with ethylene, will be presented in greater detail in a forthcoming publication.

* Contribution from the National Research Council.
[1] D. J. LeRoy and E. W. R. Steacie, J. Chem. Phys. **9**, 829–39 (1941).
[2] K. J. Laidler, J. Chem. Phys. **10**, 43–50 (1942).

Application of the Mass Law to Adsorption of Divalent Ions on Hydrous Ferric Oxide

M. H. Kurbatov, G. B. Wood, and J. D. Kurbatov
The Ohio State University, Columbus, Ohio
November 22, 1950

IN the past, adsorption of ions on hydrous oxides has been treated by means of various isotherms with qualitative descriptions of the influence of other factors on these isotherms. For the first time a hydrous oxide has been considered as an ion exchanger and the factors such as pH and anion concentration quantitatively related to adsorbate and adsorbent quantities by a mass law expression. This was made possible by studies of the adsorption of Sr, Ba, Ra, and Co ions on hydrous ferric oxide from very dilute solutions (10^{-9} gram atom per ml), in the region of the isotherms where Henry's law applies. This region of the isotherms permits the evaluation of the influence of a single variable on adsorption.

It has been found that the adsorption of divalent ions reaches an equilibrium. Therefore it is postulated that it may be represented by a chemical equation the equilibrium constant for which is

$$K_1=\frac{M(Ad\cdot S)_x\cdot(NH_4^+)^z\cdot(H_3O^+)^{(x-z)/2}}{(M)(HAd\cdot S)^x\cdot(NH_3)^z\cdot(OH^-)^{(x-z)/2}} \quad (1)$$

In this expression M is the divalent cation and $HAd\cdot S$ is the hydrous ferric oxide which is assumed to have replacable hydrogen atoms and S molecules of water and/or ammonia attached. $M(Ad\cdot S)_x$ is the adsorbent with M ions adsorbed. Ammonium chloride was present in these experiments. Since the product of $[(NH_4^+)/(NH_3)]^z$ and $[(H_3O^+)/(OH^-)]^{(x-z)/2}$ is directly proportional to $(H_3O^+)^z$,

$$K_2=\frac{M(Ad\cdot S)_x\cdot(H_3O^+)^z}{(M)(HAd\cdot S)^x}. \quad (2)$$

When $HAd\cdot S$ is large as compared to $M(Ad\cdot S)_x$ the total gram atoms of iron in the adsorbent can be used as a measure of $HAd\cdot S$ and the quantity of M adsorbed, as a measure of $M(Ad\cdot S)_x$. If the fraction of adsorbed ion, M, is y then $1-y$, the fraction unadsorbed represents the concentration of M in solution, for studies at constant volume. So Eq. (2) can be written

$$K_3=\frac{y}{1-y}\frac{(H_3O^+)^z}{(\text{gram atoms of iron})^z}. \quad (3)$$

If the quantity of adsorbent is held constant and the pH varied or pH held constant and adsorbent quantity varied a plot of $\log(y/1-y)$ *vs* pH or $\log$(gram atoms of iron) should give straight lines of equal slope, x. This has been verified experimentally. If

both *pH* and quantity of adsorbent are constant while the total quantity of *M* ion is varied, the ratio $(y/1-y)$ would be constant. This is the region in which Henry's law applies.

Equation (1) does not represent the observed decreased adsorption of divalent cation with increased ammonium chloride concentration at constant *pH*. However, if it is postulated that the adsorbent has replacable anions the influence of ammonium chloride may be represented as

$$M+xHAd\cdot S\cdot Cl_w^-+(x+w)OH^-\rightleftharpoons M(Ad\cdot S\cdot OH_w^-)_x+wCl^-+xH_2O. \quad (4)$$

The equilibrium constant for Eq. (4) can be reduced, for constant *pH*, to

$$K_4=\frac{y}{1-y}\frac{(Cl^-)^w}{(HAd\cdot S\cdot Cl_w^-)^x}. \quad (5)$$

If the quantity of $HAd\cdot S\cdot Cl_w^-$ is determined by the (Cl^-) in solution a plot of $\log(y/1-y)$ *vs* $\log(Cl^-)$ should give a straight line. This has been verified experimentally, and the results will be published.

It is a pleasure to express appreciation to Professor Edward Mack, Jr., for his interest in and support of this work. The grant-in-aid received from the Graduate School of The Ohio State University is greatly appreciated by the authors.

Suggested Structures of Water in Inert Gas Hydrates

W. F. Claussen
Illinois State Water Survey, Urbana, Illinois
September 26, 1950

GAS hydrates, such as methane hydrate, have been known for many years,[1] but even today their exact structure is not known. The concept that these hydrates arise from the packing of the hydrating molecules into void spaces in an ice-like lattice has been generally considered. However, ordinary ice does not possess void spaces believed to be large enough to accommodate even the smaller of these hydrating molecules. M. v. Stackelberg[2] has studied the structure of gas hydrates by means of x-rays, one conclusion of this work being that all crystals were in the cubic class. The structure proposed by v. Stackelberg is different from that proposed here, a criticism of the former being that some of the bond angles between water molecules appear to be around 60 degrees, much smaller than the tetrahedral angle, which is considered to be a relatively strain free angle and which is present between water molecules in the ordinary ice lattice.

The study in this laboratory of possible ice-like hydrate structures by means of molecular models two years ago revealed the desirability of fitting a regular pentagonal dodecahedral water structure (Fig. 1) into some kind of a crystalline lattice because (1) this structure would give a large enough space for the smaller hydrating molecules, (2) the water molecules in this structure would be in about the same energy state as those of ordinary ice since the pentagonal angle (108°) is very close to the tetrahedral angle (109½°), and (3) the number of water molecules belonging to a single hole would be 5, close to the hydrating number for the smaller inert gases. In the figure, each ball represents one water molecule, or each ball may represent an oxygen molecule with each stick being a hydrogen bond. It was apparent, after a little study, that the *regular* pentagonal dodecahedron would not pack in any kind of a crystalline lattice.

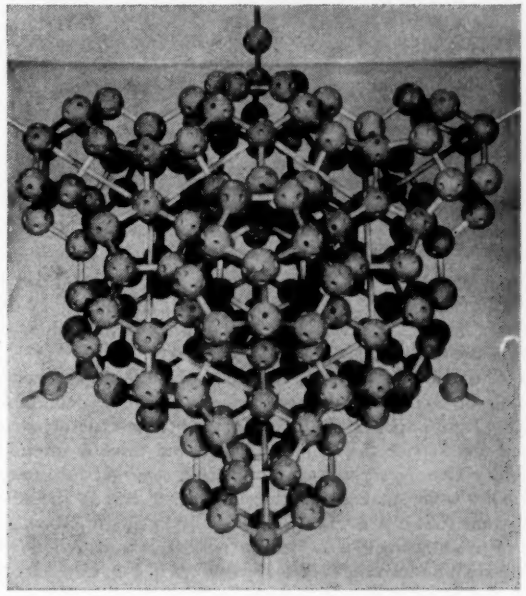

FIG. 2. Pentagonal dodecahedral-diamond lattice.

A manner of packing these dodecahedra was recently discovered, which consisted of, first, slightly deforming the regular dodecahedron so that the angles around two opposite molecules were exactly tetrahedral, then superimposing these two tetrahedral points on pairs of carbon atoms in a diamond type lattice. The amazing result was the packing to form a cubic cell (Fig. 2). The longer sticks in this model pass through dodecahedra and are

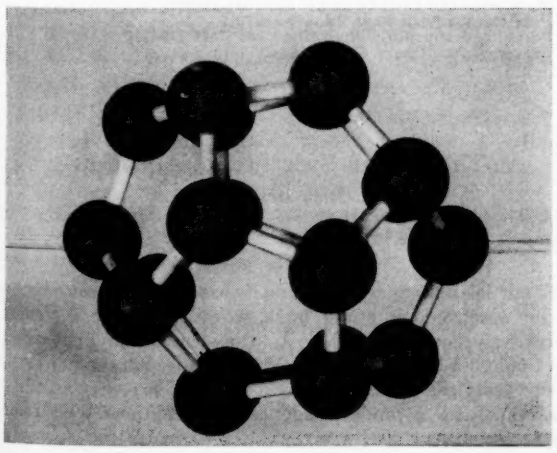

FIG. 1. Pentagonal dodecahedron.

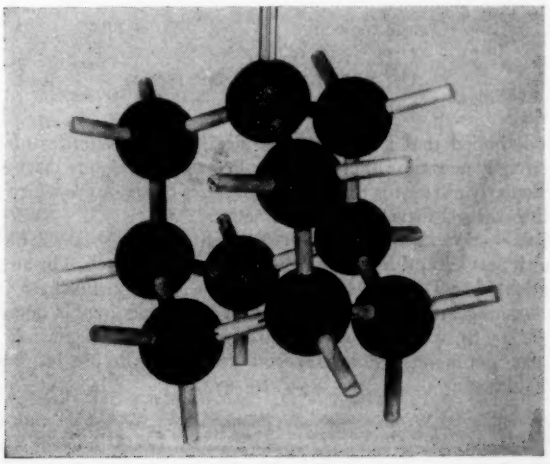

FIG. 3. Diamond lattice.

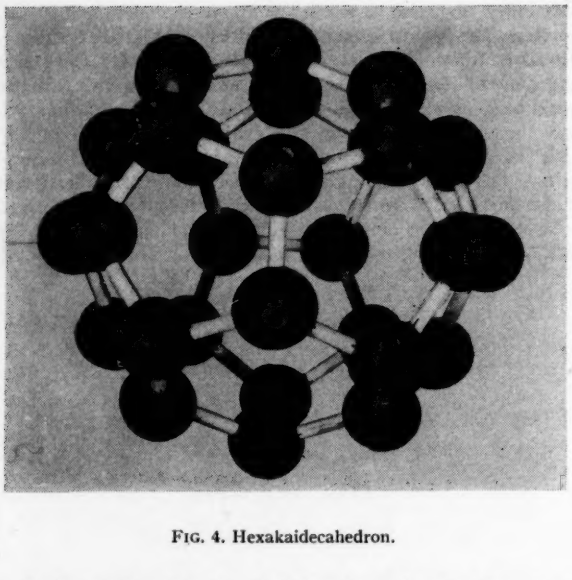

FIG. 4. Hexakaidecahedron.

attached at each end to tetrahedral water molecules; they do not represent bonds; however they are directly comparable to the bonds in the diamond lattice (Fig. 3).

Out of this diamond-pentagonal dodecahedral lattice has come a new hole or void, a hexakaidecahedron (16 hedron) containing 4 hexagonal and 12 pentagonal faces (Fig. 4). This structure contains a larger void space than the dodecahedron, thereby offering the possibility that large hydrating molecules can get into only the large holes while smaller molecules might get into all the holes. It is apparent that one might expect two hydrating numbers on the basis of this structure, in agreement with the known facts.

Some data on the unit cubic cell as shown in Fig. 2 are as follows:

Total number of balls (water molecules) in model		242
Number of molecules in unit cell		136
Number of pentagonal dodecahedra		12
Number of hexakaidecahedra		8
Hypothetical hydrating numbers		
For large molecules	136/8	17
For small molecules	136/20	$5\frac{2}{3}$

Examples of the small and large molecule hydrates are as follows:

Small molecules

CH_4 7.18 H_2O [3]	SO_2 6.1 H_2O [2]
C_2H_6 8.25 H_2O [3]	Cl_2 5.9 H_2O [2]
C_2H_6 5.8 H_2O [2]	Br_2 7.9 H_2O [2]

Large molecules

C_3H_8 17.95 H_2O [3]
CH_3I 17 H_2O [2]
C_2H_5Cl 16 H_2O [2]

It is hoped that in a future publication the properties of this apparently new type of crystal may be more completely discussed, particularly as regards the density, the sizes of molecules which can go into the void spaces, and symmetry.

This work was made possible by grants from the U. S. Public Health Service and from the Office of Naval Research. The author is indebted to Drs. A. M. Busweil and W. H. Rodebush for their encouraging interest and their helpful comments in this development. Dr. Buswell aided considerably in the first application of the regular pentagonal dodecahedron to the structure of water molecules.

[1] Summary by W. Schroeder, *Die Beschichte der Gashydrate*, Stuttgart (1926).
[2] M. v. Stackelberg, Naturwiss. **36**, 327, 359 (1949).
[3] W. M. Deaton and E. M. Frost, *Gas Hydrates and Their Relation to the Operation of Natural Gas Pipe Lines*, U. S. Bur. Mines Monograph 8, (1949), p. 27.

A Reply to Fu Regarding the New Method of Estimating the Surface Area of Powder

MASATAKA MIZUSHIMA
Physics Department, Faculty of Science, Tokyo University, Tokyo, Japan
August 23, 1950

SOME remarks on my note[1] regarding a method of estimation of the surface area of powder have been published by Fu.[2] His letter is, unfortunately, full of elementary misunderstandings. Here I will show again that my method is correct.

(1) Fu says that my equation is obtained by equating the change of free energy of the adsorbate to the change of the available surface energy of the adsorbent. I cannot understand how my procedure can be so interpreted. I have equated two expressions for the free energy change during one thermodynamic process, which is a common procedure of thermodynamic theories. These expressions cannot be attributed to adsorbate or adsorbent, just as we cannot attribute a handclapping to a right or left hand. The equation of free energy change, $\Delta G = kT\int_1^n \ln[p_0/p(\nu)]d\nu$, in my process (4) may have confused him. This process may be divided into two parts; take a fraction of gas containing $d\nu$ molecules, compress it to pressure $p(\nu)$, and then condense it on the surface of the adsorbent. The free energy change in the former process is $kT\ln[p_0/p(\nu)]d\nu$, while that in the latter is zero, since we assumed the adsorption is *reversible*. Thus our equation expresses the change of the free energy of the system as a whole.

(2) My Eq. (4) is certainly not suitable, which is the only point which needs revision in my paper. It would be better to put $\sigma_{SA}-\sigma_{LS}=46.5$ erg/cm^2 instead of (4). Bartell and Merrill[3] measured this value by the contact angle of solid and two liquids, while the expression $\sigma_{LA}\cos\theta$ may be adopted for the case of contact angle of solid, liquid, and air system. But this is only a question of expression and has no effect on the confirmation of my theory.

(3) I compared the data of Carver on Pyrex glass[4] with that of Bartell and Merrill on silica.[3] Fu says that these two matters are quite different, but I wonder if they are so different that we cannot compare them at all. Even lead glass and silica are not so different in surface characteristics (contact angle) according to Bartell and Merrill's experiment itself.[3]

(4) Fu says that the change of surface free energy is not $a(\sigma_{SL}-\sigma_{SA})$ but $a(\sigma_{SL}+\sigma_{LA}-\sigma_{SA})$, because a liquid surface has been created. As the reply to this remark I would say, "please take any textbook of college physics and learn the definition of interfacial tension σ_{SL}".

(5) Fu says that Carver's data[4] is not reliable. Since I am a theoretical physicist, I cannot judge how reliable it is. But I think we may naturally put confidence in published papers, although there may be exceptional cases, as Fu's letter.

[1] M. Mizushima, J. Chem. Phys. **17**, 1357 (1949).
[2] Ying Fu, J. Chem. Phys. **18**, 899 (1950).
[3] Bartell and Merrill, J. Phys. Chem. **36**, 1178 (1932).
[4] Carver, J. Am. Chem. Soc. **45**, 63 (1932).

The Raman Spectrum of Allene-d_4

R. C. LORD AND J. OCAMPO*
Spectroscopy Laboratory and Department of Chemistry, Massachusetts Institute of Technology, Cambridge, Massachusetts
December 18, 1950

IN our laboratory cyclopropane-d_6 has recently been prepared for spectroscopic study by a series of syntheses[1] yielding, successively, methyl acetylene-d_4, propylene-d_6, allyl chloride-d_5, and 1-chloro-3-bromopropane-d_6. It was noticed in the synthesis of methyl acetylene-d_4 that a small amount (<5 percent) of allene-d_4 was formed as a by-product under certain conditions. We therefore prepared sufficient methyl acetylene-d_4 to enable the isolation of 2–3 cc of liquid allene-d_4. The methyl acetylene-d_4 was removed from the allene-d_4 by means of ammoniacal silver solution.

TABLE I.

Allene				Allene-d_4			
$\Delta\tilde{\nu}$	I	$\Delta\tilde{\nu}$	I	$\Delta\tilde{\nu}$	I	$\Delta\tilde{\nu}$	I
356	3	1421	2	315	2b	1151	2
707	3b	1440	9 pol	436	0	1203	1
848	5b	1646	1	615	0?	1228	8 pol
865	0	1694	1	667	5b	1587	3
920	2	1960	0	847	2	2070	2b
991	3	2043	0	874	10 pol	2120	3b
1076	10 pol	2861	3	933	3	2152	3
1226	1	2996	10 pol	987	3	2195	10 pol
1296	2	3067	8b	1053	2b	2304	5b
1351	1						

In Table I are given the Raman spectra of allene and allene-d_4 studied in the liquid state at about -60°C. The columns labeled $\Delta\tilde{\nu}$ give the Raman shifts in cm^{-1} and those labeled "I" the visually estimated relative intensities. The low temperature system of Lord and Nielsen[2] was used, and polarization measurements were carried out by the single-exposure method employed by them in the study of diborane-d_6.[3] Detailed discussion of these spectra will be given later when the infrared results are reported. We wish here to point out that the product rule for the totally symmetrical frequencies is satisfied for either the D_{2h} or the D_{2d} structure:

$$\nu_{obs}=(1076\cdot 1439\cdot 2994)/(874\cdot 1228\cdot 2195)$$
$$=1.968 \text{ (theoretical}=2.00).$$

However there is evidence against the D_{2h} structure in the rather considerable number of near-coincidences between infrared and Raman frequencies. We have found, for example, infrared vapor bands at 349 cm^{-1} in allene and 307 in allene-d_4. These frequencies disagree with the values 356 and 315 in Table I by more than the usual experimental error, but the differences can readily be attributed to the change in state. This point will be investigated with the help of the infrared spectra of the liquids in the near future.

Acknowledgment is made of support of this work by the Office of Naval Research under Contract N5ori-07810, Project designation NR-019-103. Dr. E. R. Lippincott gave valuable help in photographing the Raman spectra.

* Present address: Department of Chemistry, Columbia University, New York City. This note is based on a thesis submitted by J. Ocampo to the Massachusetts Institute of Technology in partial fulfillment of the requirements for the degree of Bachelor of Science.

[1] A. W. Baker and R. C. Lord (to be published).
[2] R. C. Lord and E. Nielsen, J. Opt. Soc. Am. **40**, 655 (1950).
[3] R. C. Lord and E. Nielsen, J. Chem. Phys. (to be published).

The Decomposition of Radicals Produced by Mercury Photo-Sensitization

A. F. TROTMAN-DICKENSON
University of Manchester, Manchester, England
November 21, 1950

IN two recent papers[1] studies of the thermal decomposition of the organic radicals produced by mercury photo-sensitization of methyl alcohol and dimethyl ether have been described. The decompositions were studied over a range of temperature and the proportion of radicals disappearing by decomposition and by dimerization was found. The activation energies of the decompositions were found by plotting the function

$$\log\frac{\text{rate of production of decomposition products}}{(\text{rate of production of dimer})^{\frac{1}{2}}} \text{ vs } 1/T$$

which gives $E_{\text{decomposition}}-\frac{1}{2}E_{\text{dimerization}}$. The authors expressed their results in arbitrary units depending upon the dimensions of the apparatus; however the tacit assumption was made that the reactions effectively took place in some volume which was independent of temperature. I have recalculated the results in terms of molecules, cc, and sec, making the assumption that the reactions take place uniformly throughout the illuminated cell, and found the values of $k_1/k_2^{\frac{1}{2}}$ where k_1 is the rate constant of the decomposition reaction and k_2 that of the dimerization (for dimethyl ether the mean of the values at 28 mm and 110 mm was taken). Now

$$k_1/k_2^{\frac{1}{2}}=A\exp(-E_1/RT)/\{P_2Z_2\exp(-E_2/RT)\}^{\frac{1}{2}},$$

where the symbols have the usual significance. $E_1-\frac{1}{2}E_2$ has been determined experimentally and Z_2 has been calculated assuming a collision diameter of 5 Å for the radicals. The value of the steric or P factors is unknown. For the combination of methyl radicals values of approximately unity and 10^{-4} have been suggested;[2,3] the value of unity is a maximum. Taking these two values we get:

	$E_1-\frac{1}{2}E_2$ (kcal)	A (when $P=1$)	A (when $P=10^{-4}$)
Dimethyl ether	19	1.7×10^{10}	1.7×10^{8}
Methyl alcohol	29	1.5×10^{10}	1.5×10^{8}

The value of E_2 has no effect upon these conclusions. The maximum values of the frequency factors of the unimolecular decompositions lie far below that of $10^{12}-10^{13}$ normally found for simple bond fission. Unless the experimental activation energies are at least 4–5 kcal too low this discrepancy is real.

The experiments were carried out in circulating systems so that the mercury atom concentration in the cell would be the equilibrium pressure at room temperature, say, 25°C. Then 95 percent of the mercury resonance radiation would be absorbed in the first 3 mm of the cell.[4] If the effective reaction volume is one-fiftieth of the volume of the cell then the values of A given should be multiplied by 7; they will still be well below the expected magnitude.

If for a methoxymethyl radical $E_1-\frac{1}{2}E_2=19$ kcal and $A=1.7\times10^{10}$ sec^{-1}, then at 500°K the half-life of the radical is 4×10^{-3} sec. From the usual formula based on the kinetic theory of gases the mean distance which such a radical will diffuse through 100 mm of dimethyl ether vapor is approximately 0.5 mm. Therefore diffusion will probably have little influence upon the effective reaction volume or its temperature dependence. As the ratio of the rate constants $k_1/k_2^{\frac{1}{2}}$ is dependent upon the square root of the effective reaction volume, this ratio will be still less influenced.

The matter is of importance and should be investigated further because the method is one of the very few by which knowledge about the thermal stability of free radicals can be obtained. The abnormally low frequency factor is of great interest. A falling-off of the rate due to the very low concentration of the reactant, which has been observed in some unimolecular decompositions, is unlikely to appear here because of the great similarity between the radicals and the parent molecules which are present in high concentration. Finally, this is an extreme example of the importance of a knowledge of the effective reaction volumes occurring in photo-chemical processes.

[1] R. A. Marcus, B. deB. Darwent, and E. W. R. Steacie, J. Chem. Phys. **16**, 987 (1948); M. K. Phibbs and B. deB. Darwent, J. Chem. Phys. **18**, 495 (1950).
[2] R. Gomer, J. Chem. Phys. **18**, 998 (1950).
[3] Unpublished results of D. M. Miller quoted by A. F. Trotman-Dickenson and E. W. R. Steacie, J. Chem. Phys. **18**, 1097 (1950).
[4] H. W. Melville and J. C. Robb, Proc. Roy. Soc. (London) **196A**, 466 (1950).

Liquid-Vapor Transition Region and Physical Adsorption According to van der Waals' Equation*

TERRELL L. HILL
Naval Medical Research Institute, Bethesda, Maryland
December 13, 1950

VARIOUS applications of van der Waals' equation have been published recently.[1–6] Tolman[3] (liquid-vapor transition region) and Barrer and Robins[6] (physical adsorption) use different approaches but both assume that only the *local* density at a point of the fluid effects the properties of the fluid at the point. Hence both treatments give a discontinuous jump in density in the transition region, which seems physically unsatisfactory. More

rigorous and formal discussions[7–9] do not seem amenable to numerical applications at present.

The present method, suggested by and in some ways a refinement of the work of Barrer and Robins, makes use of the actual statistical-molecular foundation[1] of van der Waals' equation and applies to both problems mentioned. There is a continuous transition region and the adsorption isotherm reduces to an earlier equation[10–12] as a limiting approximation, as it should (failure to do this is a serious fault of the treatment of Barrer and Robins; also, the liquid-vapor transition is not taken care of as a limiting case).

The chemical potential μ of a uniform van der Waals fluid is given by

$$\begin{aligned} \nu &= \ln[\theta/(1-\theta)] + [\theta/(1-\theta)] - \alpha\theta \\ \theta &= Nb/V = b/v \\ \alpha &= 2a/bkT \\ \nu &= [\mu - \mu^0(T) - kT\ln(kT/b)]/kT \end{aligned} \tag{1}$$

where $-\alpha\theta$ is the contribution owing to the potential energy of interaction of a given molecule with the rest of the fluid.[1,13] In calculating this potential energy the van der Waals theory assumes a radial distribution function of unity outside of $r=r^*$ and zero inside, the potential of intermolecular force being

$$\begin{aligned} u(r) &= -\epsilon(r^*/r)^6 \quad r \geqslant r^* \\ &= +\infty \qquad\quad r < r^* \end{aligned} \tag{2}$$

so that

$$b = 2\pi r^{*3}/3, \quad a = \epsilon b. \tag{3}$$

In the more complicated problems of interest here, we assume that nonpotential energy contributions to μ are determined only by the local density[14] but we take into account nonlocal contributions (as in the uniform fluid) in the integration giving the potential energy analog of $-\alpha\theta$ at a point. Let the z axis be normal to planes of uniform density. Then for the liquid-vapor problem

$$\begin{aligned} \nu &= \nu_{\text{Gas}} = \nu_{\text{Liquid}} = \text{constant} \\ &= \ln\{\theta(s)/[1-\theta(s)]\} + \{\theta(s)/[1-\theta(s)]\} + \Phi(s) \end{aligned} \tag{4}$$

$$\Phi = \frac{1}{bkT}\int_0^{2\pi}\int_0^{\pi}\int_{r^*}^{\infty} u(r')\theta(z+z')r'^2 \sin\theta' dr' d\theta' d\varphi'$$

$$= -\frac{3\alpha}{8}\left[\int_{-\infty}^{-1} \theta(s+t)t^{-4}dt + \int_{-1}^{+1} \theta(s+t)dt + \int_{+1}^{+\infty} \theta(s+t)t^{-4}dt\right] \tag{5}$$

where $s=z/r^*$ and $\nu=\nu(T)$ is independent of s and is determined by the usual bulk equilibrium conditions $\nu_G(\theta_G{}^0, T) = \nu_L(\theta_L{}^0, T)$ and $p_G(\theta_G{}^0, T) = p_L(\theta_L{}^0, T)$, using Eq. (1) and van der Waals' equation of state. This also determines $\theta_G{}^0$ and $\theta_L{}^0$. For the adsorption problem, the solid occupying the region $z \leqslant 0$,

$$\begin{aligned} \nu &= \nu_G = \text{constant} \\ &= \ln\{\theta(s)/[1-\theta(s)]\} + \{\theta(s)/[1-\theta(s)]\} + \Phi_1(s) + \Phi_2(s) \end{aligned} \tag{6}$$

where $\nu_G(\theta_G, T)$ is given by Eq. (1), θ_G being the limiting gas density far from the surface $(0 \leqslant \theta_G \leqslant \theta_G{}^0)$. $\Phi_1 kT$ is the potential energy of interaction of a molecule at z with all other gas molecules $(z>0)$, and is given by

$$\Phi_1 = -\frac{3\alpha}{8}\left[\int_{-s}^{-1} \theta(s+t)t^{-4}dt + \int_{-1}^{+1} \theta(s+t)dt + \int_{+1}^{+\infty} \theta(s+t)t^{-4}dt\right] \quad (s \geqslant 1) \tag{7a}$$

$$= -\frac{3\alpha}{8}\left[\int_{-s}^{+1} \theta(s+t)dt + \int_{+1}^{+\infty} \theta(s+t)t^{-4}dt\right] \quad (0 \leqslant s \leqslant 1). \tag{7b}$$

$\Phi_2 kT$ is the interaction energy of a molecule at z with the solid, which we take here as[10a]

$$\begin{aligned} \Phi_2 &= -(\epsilon_1 r_1{}^6 \pi\rho_1/6r^{*3}kT)s^{-3} \quad (s \geqslant r_1/r^*) \\ &= +\infty \quad (s < r_1/r^*). \end{aligned} \tag{8}$$

In Eq. (7a), Barrer and Robins have in effect replaced $\theta(s+t)$ by $\theta(s)$ and also the limit on the first integral $-s$ by $-\infty$.

The method can be extended easily to solutions, liquid-liquid interfaces, and adsorption from a mixture of gases. Also, the van der Waals' model can be replaced by more satisfactory models of the liquid state.

Details and applications will be published later. But for illustration, Fig. 1 shows the liquid-vapor transition at $T/T_c = \frac{1}{2}$, obtained

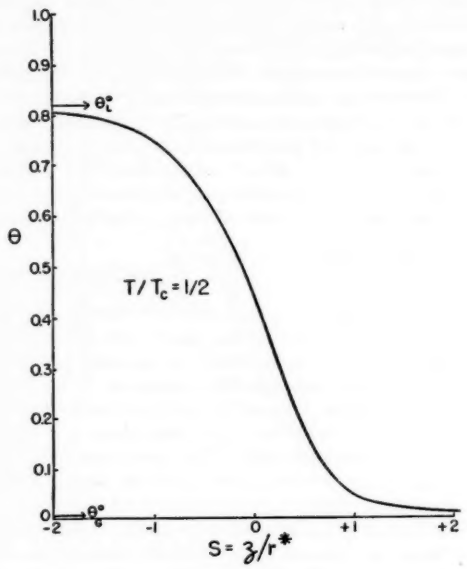

FIG. 1. Liquid-vapor transition, $T/T_c = \frac{1}{2}$. $\nu = -5.01$.

by successive approximations (using a step function $\theta_G{}^0 \to \theta_L{}^0$ at $z=0$ as a first approximation to $\theta(z)$ in order to compute Φ for use in Eq. (4) to obtain a second approximation to $\theta(z)$, etc.). Convergence is rapid. At this temperature the transition region occupies only about three molecular diameters.

* The opinions contained herein are the writer's and are not necessarily those of the Navy Department.

[1] T. L. Hill, J. Chem. Ed. **25**, 347 (1948).
[2] F. T. Wall, J. Chem. Phys. **16**, 508 (1948).
[3] R. C. Tolman, J. Chem. Phys. **17**, 118, 333 (1949).
[4] F. T. Wall and G. S. Stent, J. Chem. Phys. **17**, 1112 (1949).
[5] J. W. Drenan and T. L. Hill, J. Phys. and Coll. Chem. **54**, 1132 (1950).
[6] R. M. Barrer and A. B. Robins, preliminary paper given at the Dundee conference on adsorption, July, 1950, as summarized in Office of Naval Research, London, Technical Report ONRL-84-50 by G. J. Szasz.
[7] A. Wheeler, paper given at American Chemical Society meeting in Atlantic City, September, 1949.
[8] S. Ono, J. Chem. Phys. **18**, 397 (1950).
[9] J. G. Kirkwood and F. P. Buff, J. Chem. Phys. **17**, 338 (1949).
[10] T. L. Hill, J. Chem. Phys. **17**, 590, 668 (1949).
[11] G. Halsey, J. Chem. Phys. **16**, 931 (1948).
[12] J. Frenkel, *Kinetic Theory of Liquids* (Oxford University Press, London, 1946), p. 409.
[13] The potential energy of the entire fluid is $-\alpha\theta NkT/2$.
[14] By using other free volume models of a liquid it might be possible to improve this assumption.